DESIGN AND SYNTHESIS OF CATIONIC AMPHIPHILES

By Brandon Findlay

A Thesis submitted to the Faculty of Graduate Studies of the
University of Manitoba
in partial fulfillment of the degree of

DOCTOR OF PHILOSOPHY

Department of Chemistry
University of Manitoba
Winnipeg, Manitoba, Canada

For Lisa, who has always given the right amount of encouragement.

Abstract

Cationic antimicrobial peptides (CAMPs) are produced by plants, animals and bacteria to protect their host against antagonistic microbes. The antitheses of selective antibiotics, these peptides are drawn by electrostatic and hydrophobic interactions to targets as diverse as the bacterial membrane, nucleic acids and serum proteins. This lack of specificity is their greatest strength, as mutations to single genes rarely lead to bacterial resistance. Resistance may be conferred by large scale alterations in cell envelope composition, which generally reduces bacterial fitness in the absence of peptide.

Clinical applications of natural CAMPs are limited, as the peptides are toxic to mammalian cells and rapidly inactivated *in vivo* by serum albumin and proteases. Faced with these challenges we have prepared a number of CAMP analogues, with the goal of creating lead compounds for further development of antibacterial therapeutics. Much of our work has focused on ultrashort lipopeptides and lipopeptoids, which have properties similar to natural CAMPs and extremely abbreviated sequences. The simple structure of these scaffolds allows rapid creation of CAMP analogues in a brief period of time, allowing us to rapidly explore the structural requirements for CAMP activity. The balance of this work focuses on imparting CAMP-like behaviour to known antibiotics, in order to expand their spectrum of susceptible bacteria and combat the development of drug-resistant bacteria. In particular, the aminoglycosides neomycin and tobramycin have been fused to phenolic disinfectants such as triclosan and biclotymol, in order to improve their diffusion across the bacterial envelope and activity against Gram-negative bacteria.

Acknowledgements

For every man with his head in the clouds there are a dozen on the ground supporting him. This work could not have happened without the help of those dozen and more, for which I am incredibly grateful. Special thanks go to my supervisor, Dr. Frank Schweizer, for his guidance and kind mentoring. While I was excited by the latest idea he was level headed, directing my energies towards the long term and forever working to make sure I had the resources needed to succeed. His actions were strengthened by the advice of my examining committee, Drs. Gaik-Lean Chee, Joe O'Neil, John Sorensen and George G. Zhanel, to whom I am indebted.

I would like to thank our collaborators over the years, who have contributed their expertise to this work. Nancy Liang and Dr. George G. Zhanel, for their work with bacterial and hemolytic testing; Ka-Yee (Grace) Choi and Dr. Neeloffer Mookherjee, for their work measuring induced cytokine production; and Dr. Gilbert Arthur, for his work with cancer cell lines. I was fortunate enough to mentor three undergraduate students over the course of my studies, and would like to thank Paul Szelemej, Riley Hartmann and Ben Eisner for the enthusiasm they brought to the lab and the contributions they made to research in the Schweizer group. My thanks go to Dr. Kirk Marat for his assistance with NMR experiments, to Drs. Wayne Buchanon and Tom Ward for their assistance with the equipment of the MCAL, and to Dr. Erika Lattová and Emy Komatsu for HRMS analysis.

My labmates have been ever tolerant as my workspace encroached on theirs, for which they have my thanks. I have learned much from members of the Schweizer lab past and present, and they have made these studies enjoyable and worthwhile. Likewise, over the past

years I have turned to faculty, postdocs and students from throughout the department and have always been glad of their support.

I would like to thank the Manitoba Health Research Council and the University of Manitoba for their generous support, as well as the Faculties of Graduate Studies and Science, and the families and friends of Hugh J. Anderson and Ernst and Ingrid Bock, who have helped establish graduate scholarships in department of chemistry. And I would like to thank my family and friends, especially my wife, Lisa Freeman. I could not have done this without you.

Table of Contents

List of Figures

List of Tables

List of Abbreviations

Boc	tert-butyl carbonyl
Boc_2O	Di-tert-butyl dicarbonate
BSA	Bovine Serum Albumin
CAMP	Cationic Antimicrobial Peptide
$CDCl_3$	Deuterated Chloroform
COSY	Correlation Spectroscopy
D_2O	Deuterium Oxide
DCM	Dichloromethane
DIPEA	Diisopropylethylamine
DMF	N,N-Dimethylformamide
ESI	Electrospray Ionization
ELISA	Enzyme Linked Immunosorbent Assay

Et_2O	Diethyl Ether
EtOAc	Ethyl Acetate
Fmoc	9-Fluorenylmethoxycarbonyl
Gly	Glycine
Har	Homoarginine
HDP	Host-Defence Peptide
HSQC	Heteronuclear Single Quantum Coherence
IL-1β	Interleukin 1-Beta
IL-8	Interleukin 8
J	NMR Coupling Constant (in hertz)
LDH	Lactate Dehydrogenase
Lys	Lysine
MALDI	Matrix Assisted Laser Desorption Ionization
MeOD	Deuterated Methanol
MeOH	Methanol
MIC	Minimum Inhibitory Concentration
MRSA	Methicillin-Resistant *Staphylococcus aureus*
NMR	Nuclear Magnetic Resonance
OMe	methoxy
ppm	Parts Per Million
PyBop hexafluorophosphate	Benzotriazol-1-yl Oxytripyrrolidinophosphonium
RBC	Red Blood Cell
SPPS	Solid Phase Peptide Synthesis
TBDMS	tert-Butyldimethylsilyl

TBTU	O-(1H-Benzotriazole-1-yl)-N,N,N’,N’-Tetramethyluronium tetrafluoroborate
TC	Tissue Culture
TEA	Triethylamine
TFA	Trifluoroacetic Acid
THF	Tetrahydrofuran
TLR	Toll-Like Receptor
Tosyl	Toluene Sulfonyl
Ts	Toluene Sulfonyl
TNFα	Tumor Necrosis Factor Alpha

Chapter 1: Thesis Objectives

By Brandon Findlay

This thesis has been compiled according to the "Sandwich Thesis" format. Where noted this thesis includes published results from my graduate research, edited from their original form for consistency and clarity as well as on the recommendations of my advising and examining committees. These edits include reformatting of the references to a consistent style, alteration of the text to correct typos and clarify ambiguous statements, and other modifications as deemed appropriate. Of special note, the text of Chapter 2 has been updated from its original form to both include a new section on the immunomodulatory properties of antimicrobial peptides, and to reflect research conducted in the period 2010–2013, between when the chapter was originally published as a review in the journal Antimicrobial Agents and Chemotherapy and when it was included in this thesis.

At the beginning of my graduate studies many of the physical properties which impart antimicrobial peptides with antibacterial and anticancer properties were known. The cationic charge imparted by basic amino acid residues draws the peptides to negatively charged bacterial membranes, allowing free interaction between the bulky hydrophobic residues and membrane phospholipids. These interactions disrupt the delicate bilayer structure, leading to pore formation and potentially membrane depolarization (1). Peptides with smaller hydrophobic domains were more likely to translocate into the cell, and subsequently disrupt internal processes such as DNA and protein synthesis (2).

As discussed in the introduction (Chapter 2), numerous artificial scaffolds had replicated these findings (3-5), and so the goal of my thesis was to do more than simply produce a new

amphiphilic scaffold with antibacterial activity. I sought to address several fundamental drawbacks in CAMPs, which were conserved across both natural and synthetic scaffolds. The most apparent of these was a significant toxicity towards mammalian cells, driven by the same hydrophobic interactions that resulted in the bactericidal effect (6). Reducing the size of the hydrophobic domain reduced this toxicity, but almost eliminated bactericidal activity.

Overly large hydrophobic domains were also detrimental *in vivo*, as they led to strong interactions with the hydrophobic pocket of serum albumin (7). *In vitro* this binding was found to all but eliminate antimicrobial activity, as the bound peptides are no longer free to interact with bacterial membranes. As a final concern, CAMPs are also susceptible to proteolytic cleavage, with overexpression of exogenous proteases imparting some *Bacillus anthracis* strains with high-level resistance to the human host defence peptide LL-37 (8).

As described in Chapters 3 and 4, on beginning my studies I sought to create cationic amphiphiles without the previously mentioned limitations, by either reducing interactions with mammalian membranes and bovine serum albumin or by taking advantage of protease-resistant scaffolds. I began by creating new ultrashort lipopeptides and lipopeptoids (explained in further detail in Chapters 3 and 4, respectively), establishing a model system for determining the effect of the hydrophobic domain on CAMP activity in the presence and absence of hydrophobic serum proteins. The lipopeptoids also had the advantage of inherent protease resistance, and with the aid of Dr. Zhanel we described the first direct comparison of lipopeptides and analogous lipopeptoids, demonstrating that the two scaffolds had functionally equivalent antimicrobial activity. This confirmed that lipopeptoids have the potential to replace lipopeptides as the next generation of ultrashort CAMP analogues.

Chapter 5 covers the next phase of this research, as we turned to the immunomodulatory properties of our CAMP mimics, evaluating their activity on macrophage-like THP-1 cells with the assistance of Dr. Neeloffer Mookherjee. Human CAMPs like LL-37 do not act primarily through direct bacterial killing, and instead modulate the immune response to a bacterial infection (9). *In vitro* the THP-1 cells replicate this behaviour, and we found cytokine production with both LL-37 and several lipopeptide and lipopeptoid sequences. Production of chemokines Groα and IL-8 was linked to both peptide/peptoid sequence and the length of the lipid tail, and was independent of the previously assessed antimicrobial activity.

Also interested in imparting AMP-like behaviour in known antibiotics, Chapter 6 details my experiments with e aminoglycoside antibiotic neomycin B, as it was linked to a number of phenolic disinfectants. The resulting amphiphilic species demonstrate activity against neomycin-susceptible bacteria, but had improved activity against a neomycin-resistant MRSA strain and two strains of *Pseudomonas aeruginosa.* Unlike work with previously reported amphiphilic aminoglycosides, this increase in activity is not linked to a large increase in toxicity towards mammalian erythrocytes. Unfortunately, activity against phenolic-susceptible bacteria was not observed, and it appears that attaching a linker to the phenol of these hydrophobic compounds eliminated their antibacterial action.

The next generation of amphiphilic aminoglycoside design therefore sought to combine a number of bivalent phenolic disinfectants with the more clinically relevant aminoglycoside tobramycin, forming the unpublished research that is Chapter 7. Attaching a linker to these compounds left one phenol free to interact with small cations, and should allow retention of the phenols activity. Unfortunately, creating mono-alkylated bisphenols and biphenols proved synthetically challenging, limiting amphiphile production to biclotymol and biphenol derivatives.

While further research is required to develop the compounds outlined in this thesis into CAMPs which do not suffer from the drawbacks described above, with this body of work we have made significant progress. We have demonstrated equivalence between antibacterial lipopeptides and lipopeptoids, allowing much of the previous research on CAMP sequences to be used in future antimicrobial peptoid discovery. The ultrashort lipopeptides and lipopeptoids we have characterized are the shortest known immunomodulatory peptides by amino acid sequence, with similar activity to LL-37 but less than a quarter the molar weight. And the work with aminoglycoside hybrids has increased our access to aminoglycoside scaffolds, and may lead to the development of a new generation of aminoglycoside antibiotics.

Chapter 2: Cationic Amphiphiles, a New Generation of Antimicrobials Inspired by the Natural Antimicrobial Peptide Scaffold

By Brandon Findlay, George G. Zhanel and Frank Schweizer. First Published in Antimicrobial Agents and Chemotherapy, 54, 2010, 4049-58. Reproduced with permission.

2.1 Authorship Consideration

Brandon Findlay conducted a literature search and prepared the initial draft of the paper, on the advice of Frank Schweizer. Frank Schweizer and George G. Zhanel then suggested modifications, which were incorporated by Brandon Findlay to create the final form, provided here. Frank Schweizer was corresponding author.

2.2 Abstract

Naturally occurring cationic antimicrobial peptides (AMPs) and their mimics form a diverse class of antibacterial agents currently validated in pre-clinical and clinical settings for the treatment of infections caused by antimicrobial-resistant bacteria. Numerous studies with linear, cyclic and diastereomeric AMPs have strongly supported the hypothesis that their physicochemical properties, rather than any specific amino acid sequence are responsible for their microbiological activities. It is generally believed that the amphiphilic topology is essential for insertion into and disruption of the cytoplasmic membrane. In particular, the ability to rapidly kill bacteria and the relative difficulty with which bacteria develop resistance make AMPs and their mimics attractive targets for drug development. However, the therapeutic use of naturally occurring AMPs is hampered by the high manufacturing costs, poor pharmacokinetic properties and both low bacteriological efficacy and high toxicity in animal models. In order to overcome these problems, a variety of novel and structurally diverse cationic amphiphiles that

mimic the amphiphilic topology of AMPs have recently appeared. Many of these compounds exhibit superior pharmacokinetic properties and reduced in vitro toxicity while retaining potent antibacterial activity against resistant and non-resistant bacteria. In summary, cationic amphiphiles promise to provide a new and rich source of diverse antibacterial lead structures in the years to come.

2.3 **Current Research in Natural Antimicrobial Peptides (AMPs)**

The past twenty years have been a time of discovery for AMPs, with over 1200 peptides in five structural classes cataloged in the antimicrobial peptide database (1). In the interest of brevity, only peptides that adopt an amphiphilic α-helical structure in their target membrane will be discussed in this review, as these most directly lead to an understanding of both AMPs and their mimics. These AMPs are between ten and fifty residues long and contain a mixture of both cationic and hydrophobic amino acids, distributed to distinct regions or faces of the α-helix (2). While the pathways and thermodynamics of AMP binding are currently being investigated (3-6), they will not be discussed in detail; rather the focus is on the effects of sequence1specific modifications.

2.3.1 Stable Amphiphilic Helices Lead to Hemolysis

The secondary structure of many AMPs is highly dependent on their environment, modulating their activity. Folding into a stable α-helix separates the positive and hydrophobic amino acids, resulting in an overall amphiphilic structure. Association with negatively charged phospholipids may induce this folding and studies using circular dichroism (CD) have demonstrated that many AMPs are structured in their target membranes, but may be

disordered in simple buffered solutions (5). Selectively disrupting the α-helix by replacing key amino acids with their D enantiomers suggested that some pre-folded AMPs are capable of inserting into neutral membranes, leading to hemolysis (2). This conclusion has been reaffirmed by work on V_{681}, which forms stable α-helical conformations in both aqueous and lipid environments (7). Disrupting the hydrophobic region of V_{681} via insertion of a polar lysine residue on the hydrophobic face was found to destabilize the α-helix in aqueous buffer, leading to a variant with over thirty times less hemolytic activity and unaltered antimicrobial activity (Tables

Table 2.1, see section 1.17). The reverse transition has also been observed with the AMP RTA3, which contains a polar amino acid on the peptide's hydrophobic face (8). Substituting this residue to create RTA-R5L strengthened both the amphiphilic α-helix and the hemolytic effect. Disrupting the helix of V_{681} via D-amino acid substitutions created the less hemolytic peptides $V13V_D$ and $V13K_D$, which retained the antimicrobial activity of V_{681} (9).

Other researchers have taken advantage of peptoid residues to disrupt helical AMPs. Peptoids share the same structure as the amino acids they are derived from, with the exception that the side chain has been moved from the alpha carbon to the amide nitrogen. In one study, replacing three leucine and isoleucine residues in the hydrophobic region of melittin with peptoids such as N_f (Figure 2.1) resulted in twofold reduced antibacterial activity, but concomitantly increased the minimum hemolytic concentration (MHC) from 0.78 μM to greater than 100 μM (Tables

Table 2.1) (10). It should be noted, however, that the peptoid residues also altered the hydrophobic moment.

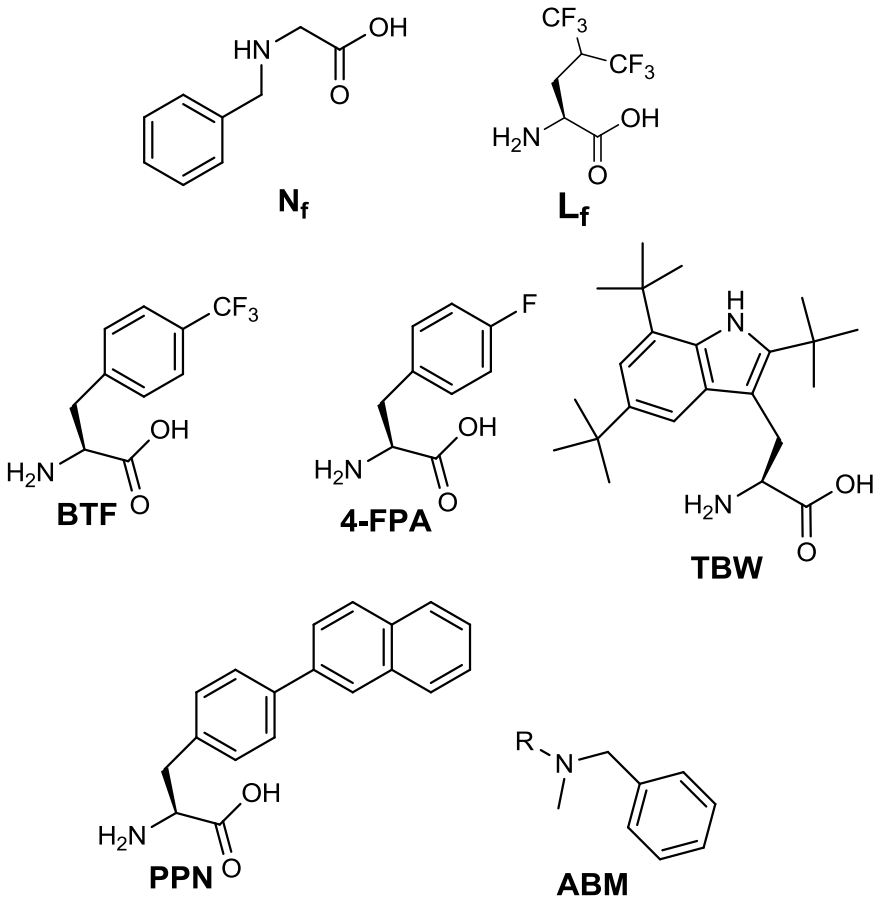

Figure 2.1. Non-proteogenic amino acids used in AMP research. Peptoid N_f was used to reduce the hemolytic nature of melittin, while fluorinated leucine (L_f), can be used to increase the hydrophobic nature of some AMPs.

The remaining non-proteogenic amino acids have all been used in short cationic AMP studies. BTF and 4-FPA increase the activity of small amphiphilic peptides by increasing peptide hydrophobicity, while TBW both increased activity and allowed Arg-TBW-Arg peptides to pierce

biofilms. PPN was the most active hydrophobic substituent in a study on trypsin-resistant tripeptides and ABM conferred trypsin resistance when attached to the C-Terminus.

2.3.2 Peptide Hydrophobicity and Charge: Twin Windows of Activity

Because AMPs interact nonspecifically with their target membranes through charge and hydrophobic interactions, varying a peptide's physical parameters occurs via optimization of the amino acid sequence. Positive charge is required for initial attraction to negatively charged bacterial membranes, whereas hydrophobic bulk guides insertion into, and disruption of, the membrane itself (2). Increasing hydrophobicity may increase antimicrobial activity, albeit often alongside an increase in hemolytic activity. For example, replacing two leucine residues with the more hydrophobic hexafluoro-leucine (L_f) residues (Figure 2.1) in buforin II 10 enhanced antibacterial activity, without significantly impacting the hemolytic activity (Table 2.2) (11). Similar experiments with an initially highly active antimicrobial peptide, magainin 2, created analogues with increased hemolytic activity and unaltered antibacterial activity, suggesting a window of effective hydrophobicity (12). Varying the hydrophobicity of V_{681} through amino acid substitutions revealed a similar window of activity (13). Peptides which are not significantly hydrophobic are both non-hemolytic and non-antimicrobial, and peptides with most of their hydrophilic amino acids replaced with more hydrophobic residues are highly hemolytic (Table 2.2). The significantly hydrophobic peptides self-associate, which may account for their reduced antimicrobial activity (7, 14).

Increasing the positive charge of an AMP by adding arginine, lysine or histidine residues to the peptide sequence can also increase antibacterial activity. The increased charge raises electrostatic interactions between AMPs and the negatively charged bacterial membranes,

without affecting interactions with the zwitterionic lipids found in mammalian membranes (15, 16). Systematically increasing the positive charge of V_{681}-V13K revealed a threshold, past which hemolytic activity dramatically increases, with no significant change to activity against bacteria as shown with V_{681}-V13K/T15K/T19K in Table 2.2 (17). As many oligocationic molecules are cell penetrating it may be that highly charged AMPs, drawn by the negative membrane potential inside the cell, are inserting into mammalian cells (18). In a second example of this effect, dimerizing a well known cell penetrating peptide, penetratin, created an AMP with similar antimicrobial activity but eight-fold increased hemolytic activity (Table 2.2). The two peptides had near identical CD spectra, but only dual-penetratin was found to lyse artificial liposomes (bacterial membrane mimics) composed of phosphatidyl ethanolamine and phosphatidyl glycerol, indicating that despite similar conformations the longer dual-penetratin had a different spectrum of activity (81).

2.4 **The Development of Short Cationic AMPs**

Unfortunately, the high costs associated with the synthesis of lengthy natural antimicrobial peptides combined with their poor pharmacokinetic properties limits their utility as pharmaceutical agents (19). Studies into the efficacy of peptides ten residues or less have been conducted, leading to the discovery of several highly effective short, cationic antimicrobial peptides (SCAMPs) which rely on the activity of a few key amino acids.

In one study of the AMP Bac2A (RLARIVVIRVAR-NH_2), every possible mono-substituted derivative was created; that is, every derivative that varied from Bac2A via the substitution of a single amino acid (20). Four amino acids were found to generally increase activity: cysteine, lysine, arginine and tryptophan. Cysteine substitutions were proposed to result in Bac2A dimers

via disulphide bridge formation, while the other residues increased either the hydrophobicity or the charge of Bac2A. Further substitutions determined that arginine and lysine substitutions were most effective when complemented with tryptophan substitutions, as tryptophan appeared to act as a hydrophobic moiety, balancing the cationic charge provided by either lysine or arginine. This result was reconfirmed in a more recent *in silico* analysis of over 100, 000 nonameric peptides by Hancock and Cherkasov, which showed a strong preference for tryptophan residues in the top 50% of sequences as organized by predicted activity, with the top three sequences all containing different combinations of the following residues: five tryptophan, one lysine, and three arginine (21). It is interesting that tryptophan was favoured over the more hydrophobic amino acids leucine, isoleucine and valine (22), possibly due to membrane perturbation resulting from the size of the indole ring. The *in silico* approach was chosen to mitigate the large investment required to prepare and test such a large number of peptides, though it should be noted that PCR based methods of direct testing have been developed (23).

Further reducing the length of AMPs demonstrated that simple arginine tryptophan (RW) repeats are capable of antimicrobial activity (24), despite their inability to form an α-helix (Table 2.3). The shortest active sequence is the amidated peptide RWR and both antimicrobial activity and to a lesser extent hemolytic activity increase with the number of RW repeats (24). Esterification or amidation of the negatively charged C-terminal carboxylic acid moiety (25) and attachment of discrete RW units to a molecular scaffold (Figure 2.2) (26, 27) are strategies which have been used to increase antimicrobial activity against both actively growing and biofilm-bound bacteria, without impacting the MHC (Table 2.3).

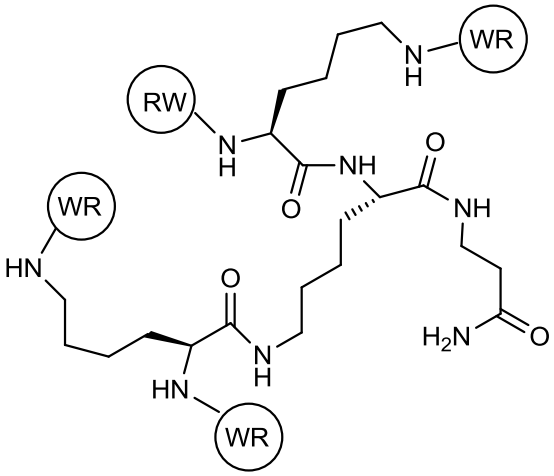

Figure 2.2. Structure of RW_{4D}. A multivalent antimicrobial peptide, with arginine-tryptophan repeats. Amino acids are attached at the N-terminus and are denoted by their single letter abbreviations.

2.5 **Increasing Activity**

The short sequence of short cationic AMPs allows for facile incorporation of non-proteogenic amino acids, expanding the range of hydrophobicity beyond what can be obtained by leucine and tryptophan. One study using the fluorine containing amino acid analogues BTF and 4-FPA (Figure 2.1) found that raising the hydrophobicity of phenylalanine residues by replacing hydrogen atoms with fluorine atoms increased activity to roughly that of peptide sequences with tryptophan. The most active peptides in this series contained two residues of BTF, the most heavily fluorinated and hydrophobic residue (28). All the synthesized chains were reported to be non-hemolytic at 250 μg/mL though no hemolysis data was provided.

Attempts to increase the steric bulk of the hydrophobic group have met with similar success. In one example, a short Arg-X-Arg peptide with X equal to t-butylated tryptophan

(TBW, Figure 2.1), is highly active, and unlike many conventional antibiotics is able to penetrate biofilms. As a result, this peptide is active against *Staphylococcus epidermidis*, a well described biofilm producer associated with device-related infections (29, 30). Similar Arg-X-Arg molecules were created during research into protease susceptibility; the most active derivative contained a bulky para-phenyl naphthalene substitution (PPN) as the variable component (31). In an interesting exception to the general rule on stereochemistry in AMPs, the activity of peptide Arg-TBW-Arg varied as the chirality of each alpha carbon was altered (32). The strongest activity was observed in the all D and all L variants, which were also the most hydrophobic as measured by HPLC retention times. The least biologically active and least retained peptides were D-D-L and L-L-D, with NMR studies suggesting that the long chains of the arginine residues were shielding the TBW group, leading to a largely hydrophilic rather than amphiphilic conformation.

2.6 **Reducing Protease Degradation**

A significant drawback to AMPs is their protease susceptibility. This limits their oral bioavailability and also provides bacteria with a convenient route towards peptide inactivation, by potentially over-expressing an endogenous peptidase (19, 33). Attempts to create protease-resistant AMPs have traditionally focused on the incorporation of D-amino acids, with some success. Complete substitution creates enantiomers which behave similarly to their L-amino acid counterparts, while diastereomeric sequences tend to be slightly less active against bacteria, though beneficial reductions in hemolytic activity have been observed (34, 35). Any loss of *in vitro* activity appears to be balanced by reduced susceptibility to *in vivo* degradation; one peptide sequence ($LKL_DLKK_DLL_DK_DKLLK_DLL\text{-}NH_2$) is known to be effective against Gram-negative infections in mice, but only as a diastereomer (36).

An emerging method of conveying protease resistance is the incorporation of bulky side chains, which prevent the peptide from entering the peptidase active site (31). Combinatorial studies of a number of RWR analogues led to the discovery of molecules resistant to both trypsin and chymotrypsin at pH 8.6, via the attachment of disubstituted amides such as ABM (Figure 2.1) to the C-terminus (31, 37).

2.7 **Lipopeptides**

Adding hydrophobic lipid tails to natural peptides increases bactericidal and fungicidal activity, likely by increasing association with the cell membrane. This effect has been observed with both naturally occurring AMPs (38) and short cationic AMPs (39), and may be used to impart antibacterial activity in otherwise inactive lysine/leucine sequences (39) (

Table 2.4). The shortest cationic lipopeptides resemble antimicrobial surfactants (40), and are effective against fungi, Gram-positive and Gram-negative bacteria, with moderate hemolytic activity in the more active variants such as C16-LysLysLys (41, 42) (

Table 2.4). Studies have shown that membrane depolarization and calcein dye leakage correlate to activity, suggesting either pore formation or cell lysis is the mode of action (38, 39, 43). This correlation can be easily observed with histidine rich lipopeptides (

Table 2.4), as these peptides depolarize cells primarily at a reduced pH, which corresponds to a large increase in antimicrobial activity (43).

As with the short cationic AMPs, the cationic, amphiphilic topology is more influential than the specific peptide sequence when considering lipopeptide antimicrobial activity. For instance, diastereomeric tetra-lipopeptides and tetra β-amino acid lipopeptides exhibit similar

antibacterial activities when compared to the standard L-amino acid derived lipopeptides *in vitro* (44), with the diastereomeric lipopeptides effective against topical *Aspergillus fumigatus* infections in a mouse model (45).

2.8 **Introduction: Antimicrobial Peptides Target the Membrane**

The rise in antibiotic resistance among pathogenic bacteria and the declining rate of novel drug discovery is a common concern in medicine (46), driving research into new antibacterial classes and novel drugs in order to maintain the existing ability to treat infectious diseases, especially those caused by multi-drug resistant (MDR) organisms (47, 48).

While the enzymatic inhibitors from which are derived many of our strongest antibiotics are highly effective in the microbial world, higher order organisms do not appear to rely entirely on such selective inhibitors (49). These organisms instead produce a number of broad range antimicrobial peptides (AMPs), which do not target any single molecule or process but instead associate with cellular membranes, resulting in depolarization, lysis and cell death through a disruption of the membrane topology. A subset of these peptides is able to translocate into the cell and disrupt cellular processes such as protein and DNA synthesis (50). AMPs play a key role in the human immune system, and mutations affecting their production and expression have been linked to diseases like cystic fibrosis and Crohn's disease (51, 52).

Membrane targeting offers advantages over standard methods of drug design and antibiotic activity due to the wide variety of active structures and a reduced development of resistance mechanisms (52). Nevertheless, potential cytotoxicity to the host cells remains a major unsolved challenge. Mutants resistant to AMPs have been developed in the laboratory (53), however, such mutants may be hyper-susceptible to conventional antibiotics as well as

demonstrating reduced growth compared to wild type strains (54). These results are in line with natural AMP resistance mechanisms, which as a rule significantly reduce the virulence of the expressing bacterial strain (55). The lack of a specific cellular targ{{}}et is another significant advantage of AMPs, as activity towards Gram-positive and Gram-negative bacteria, fungi and viruses has been reported (16, 56-59). The development of AMPs as pharmaceutical agents shows great promise, with a variety of natural and synthetic compounds currently in development (58). However, natural AMPs often suffer from a variety of pharmacokinetic shortcomings including poor bioavailability, low metabolic stability and formulations difficulties due to their size and the high number of amide bonds, which has driven research towards the creation of partially and wholly synthetic analogues. This review will examine recent research on AMPs and their mimics in an attempt to elucidate the underlying pharmacophore shared between them and highlight the current challenges in AMP-based drug design.

2.9 **Oligo Acyl-Lysine Chains (OAKs)**

Oligo Acyl-Lysine (OAK) chains represent a novel derivatization of the antimicrobial peptide backbone, linking lysine residues together with alkyl chains (Figure 2.3). As an extensive review of these molecules was recently published (60), they will not be covered in detail. OAKs that display high selectivity for bacterial cells over RBCs do not strongly absorb in some circular dichroism studies, suggesting that they do not adopt a rigid conformation in aqueous buffer or phosphatidylcholine/phosphatidylglycerol membranes (61). OAKs that do appear to adopt stable conformations in aqueous buffer, such as OAK B (Figure 2.3), form visible aggregates and are hemolytic (HD_{50} = 4.1 μM) (62), with ability to aggregate tied to the length of the acyl linkers. OAKs with chains that are twelve carbons long appear to fold upon themselves, creating a

hydrophobic loop which absorbs circularly polarized light. When several loops come together they then form a hydrophobic core, creating a stable, rigid superstructure. Shorter OAKs such as OAK A lack linkers long enough to form stable folds, and do not display similar aggregation or hemolysis (<10% hemolysis at 100 μM) (61).

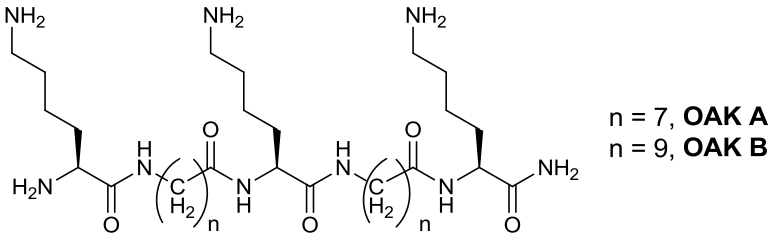

Figure 2.3. Two representative OAK molecules, based on the same scaffold. With a spacer equal to seven methylene units, OAK A is unable to form stable aggregates in aqueous buffer and is non-hemolytic, while the slightly longer acyl chains in OAK B allow aggregation and lead to hemolysis.

2.10 **Synthetic Mimics of AMPs**

Work by the Gellman group has shown that the pharmacophore of AMPs can be mimicked by amphiphilic β-amide copolymers (63). Though no well-defined secondary structure was possible, these polymers selectively lysed Gram-positive and Gram-negative cells over mammalian cells, confirming the potential of wholly synthetic AMP mimics (63). Early synthetic mimics of AMPs began with an attempt to mimic the amphiphilic nature of the protein α-helix without the use of natural amino acids (64). Initial structures, exemplified by AMP mimetic A in Figure 2.4, were equally active against both Gram-negative and Gram-positive bacteria and human erythrocytes (65). Reducing the flexibility of the molecule by establishing an extended hydrogen bonding system (shown in synthetic AMP mimetic B), had little effect on the hemolytic

activity, but significantly increased activity against representative bacterial strains *Escherichia coli* and *Bacillus subtilis* (66). Dye leakage assays, a common method of assessing cell lysis (67), confirmed disruption of the target membranes, suggesting a lytic or pore-forming effect resulting in enhanced permeability of the bacterial membrane is the mode of action.

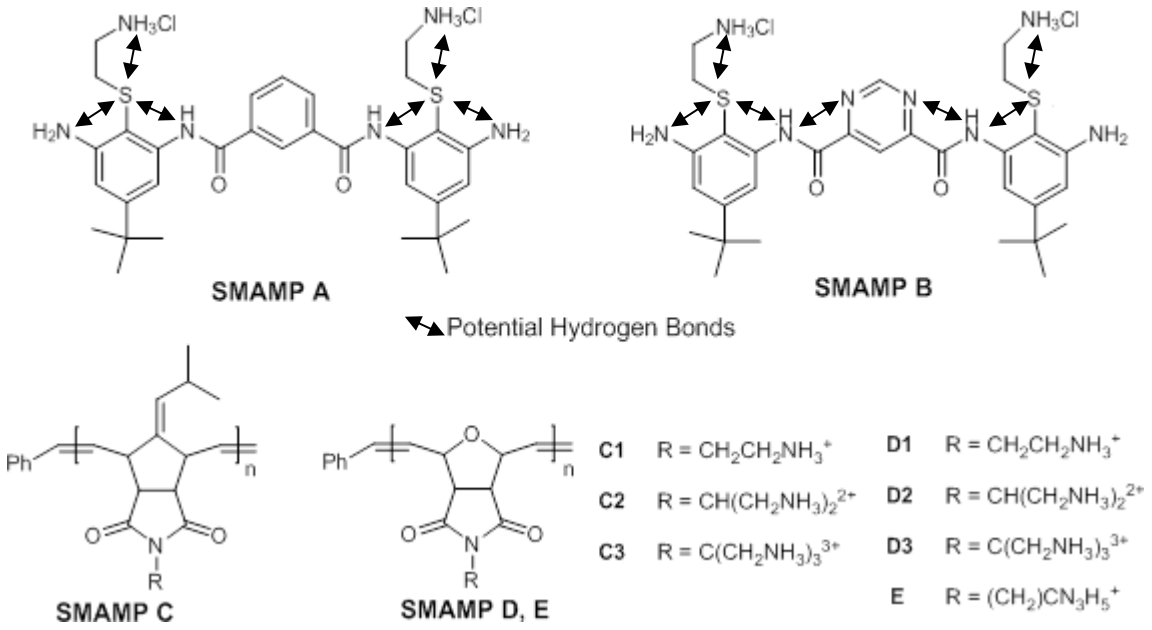

Figure 2.4. Initial design of AMP mimetics and more advanced analogues. AMP mimetic A displayed roughly equivalent activity between Gram-positive and Gram-negative bacteria and red blood cells. AMP mimetic B contains an extended hydrogen bonding network, as shown with dashed lines, and had significantly increased activity against representative Gram-positive and Gram-negative bacteria, with hemolytic activity similar to SMAMP A. Later research using mimetics C, D and E probed the effect of charge on activity. The R groups of both the C and D series are the same, with the molecules varying only in their respective backbones, shown on the left. The AMP mimetic E has a unique guanidyl derived R group, but shares the same backbone as the D series. All compounds were prepared via polymeric techniques, with subunits linked by alkene groups and M_n = 3 kDa. Counterions are 2,2,2-trifluoroacetate.

2.11 **Charge-based Selectivity**

As with the short cationic AMPs and lipopeptides, the net molecular charge is an important component to mimic AMP selectivity. Varying the number of amine functional groups in two AMP mimetics series, shown in Figure 2.4, was found to modulate both hemolytic and antibacterial activity (Table 2.5) (68, 69). Hemolysis in the AMP mimetic C series decreased roughly 700-fold by an increase of +1 to +2 charges per residue, but no significant effect was observed with the relatively non-hemolytic D series. Instead, increased charge lead to a 16-fold decrease of the MIC against the *Staphylococcus aureus*. Dye leakage assays with liposomes designed to mimic mammalian, Gram-negative and Gram-positive cells found that leakage only partially correlated with activity, suggesting several modes of action (68). Further work indicated that a guanidine function was more effective in conferring selectivity to AMP mimetic E (68). The resulting AMP analog did not appear to cause calcein dye leakage, but some AMPs and AMP mimetics associate with both negatively charged bacterial polysaccharides and with DNA and may therefore act internally (70, 71)

2.12 **Incorporating the Pharmacophore of AMPs into Known Drugs**

In the last two years a novel class of oligocationic amphiphiles; the aminoglycoside antibiotics-derived amphiphiles (AADAs) have emerged (Figure 2.5) (72-78). The most potent compound, AADA F, exhibits strong Gram-positive coccal activity against methicillin-resistant *Staphylococcus epidermidis* (MRSE) [MIC 0.5 μg/mL] and methicillin-resistant *Staphylococcus aureus* (MRSA) [MIC 1 μg/mL] and reduced activity against the Gram-negative *E. coli* (three strains, MIC = 16-32 μg/mL) (74). The AADAs A-J are believed to mimic the physicochemical and

amphiphilic properties of AMPs, by combining the cationic nature of aminoglycosides with hydrophobic side groups. The side groups are attached to auxiliary hydroxides via an amide bond, as in AADAs A-D, or either carbamate or ether linkages, as in AADAs E-H. Click chemistry has also been used, to connect short hydrophobic peptide sequences to the aminoglycosides and test the potential for peptides to modulate activity (73). The AADAs may retain the RNA-binding properties of aminoglycoside antibiotics and a dual warhead function has been hypothesized (72). Whether the conversion of highly cationic aminoglycosides into cationic amphiphiles results in synergistic effects between these two modes of action is unclear, but combination studies using AADA A with other antibiotics does show an enhancement over either agent alone (78).

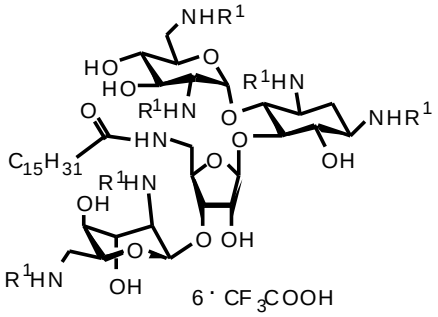

AADA A: R^1 = H x TFA
AADA B: R^1 = C(NH)NH_2 x TFA

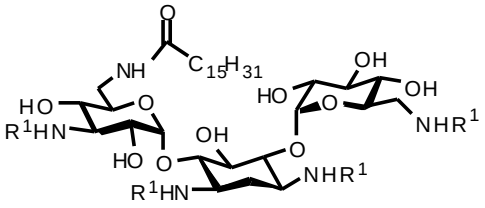

AADA C: R^1 = H x TFA
AADA D: R^1 = C(NH)NH_2 x TFA

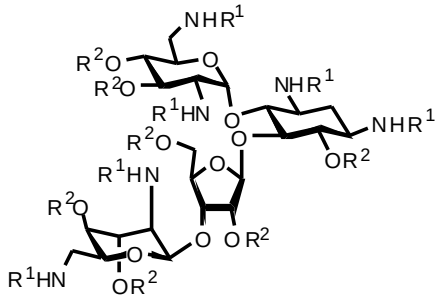

AADA E: R^1 = H x TFA; R^2 = $CH_2C_6H_5$
AADA F: R^1 = H x TFA; R^2 = C(O)NHC_6H_5

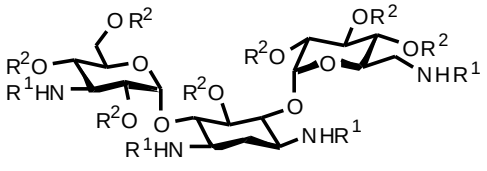

AADA G: R^1 = H x TFA; R^2 = $CH_2C_6H_5$
AADA H: R^1 = H x TFA; R^2 = C(O)NHC_6H_5

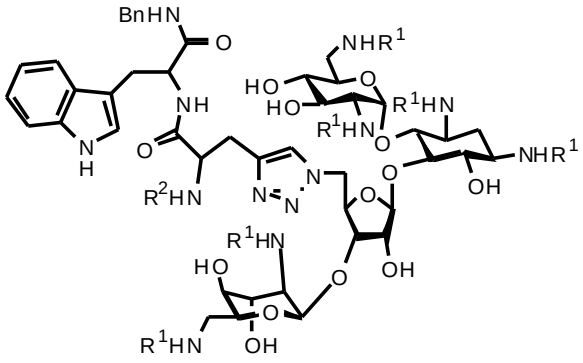

AADA I: R^1 = H x TFA; R^2 = Fmoc;

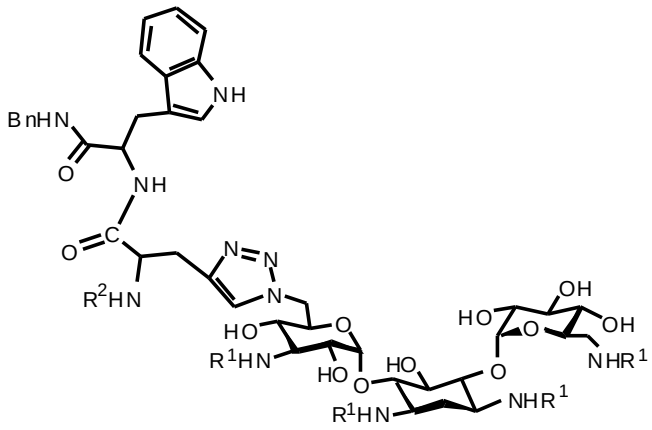

AADA J: R^1 = H x TFA; R^2 = Fmoc;

Figure 2.5. Structures of aminoglycoside antibiotics-derived amphiphiles (AADAs) that exhibit potent antibacterial activity.

2.13 **Combining Information from Multiple Antimicrobial Classes**

As the interaction between bacterial membranes and AMPs and their mimics is based primarily on non-specific interactions such as hydrophobicity and electrostatics, it is not surprising that a large variety of sequences and structures have been found effective in the search for novel therapeutics. It is the common trends which unite these compounds that are most interesting, as they aid research towards ever more active and selective compounds (*vide infra*), and provide information towards the underlying role each molecule plays.

Notably, every molecule discussed has the ability to form an amphiphilic structure in the target membrane, either as a result of spatial separation of charges and hydrophobic region or by folding into secondary structure. In several instances, such as with the natural AMPs RTA and V_{681} and the synthetic OAKs, the presence of a stable amphiphilic structure in aqueous buffer is linked to a large increase in hemolytic activity (7, 8, 14). This relationship is especially important when one considers the lipopeptides, as their long hydrophobic tails may promote separation from the aqueous solution into micelles and other aggregates (38).

At least two distinct modes of action are visible in the compounds discussed in this review. The first results in enhanced permeability, disruption or perforation of the membrane, and is exemplified by melittin, the lipopeptides and others (10, 41, 54). This perturbation is observed via dye leakage assays and depolarization studies, which indicate free transfer of small molecules through the lipid bilayer (67). In the second method of activity, characterized by AMPs buforin and plectasin and the AMP mimetic E1(68, 79), the membrane does not appear to be perturbed, and antibacterial activity results from interactions with an unknown target(s), likely negatively charged molecules such as nucleic acids and LPS (4, 45, 70, 80). These alternative AMP interactions may interfere with processes such as DNA replication, protein folding and cell wall synthesis/cell division and septum formation (81). Modification of the AMP

or AMP mimic may switch between these modes of action; as observed when lipid tails are added to the N-terminus of magainin or in the modification of AMP mimetics D1 to E, and so it is likely that the balance between the polar and hydrophobic nature of AMPs determines which mode of action will result (38, 68). Indeed, it has been suggested that cationic antimicrobial peptides are "dirty drugs" in that they potentially have many targets owing to their amphiphilic nature and cationic charge (33).

An initial concern involving AMPs was their poor bioavailability, which can result from non-specific reactions with either serum or protein containing media or from the digestive action of proteases. However, *in vivo* studies with short cationic AMPs and lipopeptides containing D-amino acids have found increased specificity for the bacterial membrane and resilience towards mammalian proteases (36, 82). The more synthetic molecules such as the OAKs and AMP mimetics were in part conceived to circumvent proteolysis, and have also shown good *in vivo* activity (83, 84).

2.14 **In Vivo Studies with AMP-mimetics**

Only a limited number of *in vivo and toxicology* studies have been performed with cationic amphiphile-based AMP mimetics (61, 62, 82, 83). In one example, mortality was reduced in an *E*. *coli* mice model when O-acyl lysine compounds, such as those shown in Figure 2.3, were injected several hours after *intra peritoneal* infection with *E. coli*. While antimicrobial peptides were degraded by plasma proteases, a three hour preincubation in either mouse or human plasma had little effect on OAK activity. *In vivo* toxicology tests with these OAKs after a single intraperitoneal administration to neutropenic mice revealed no signs of adverse effects at dosages of 10 mg/kg body weight (61). Similarly encouraging *in vivo* results have also been

obtained with lipopeptides and AMP mimetics. A lipopeptide tetramer markedly increased the survival rate of *Aspergillus fumigatus* infected mice with tolerated doses of up to 10 /kg body weight (82). Finally, Arylamide AMP mimetics have been tested using a mouse thigh burden infection model, where colony forming unit (CFU) reductions comparable to 30mg/kg of vancomycin were observed (83).

2.15 **Immunomodulatory Properties of Cationic Amphiphiles**

Recent analysis of *in vivo* concentrations of human antimicrobial peptides such as LL-37 has shown that in the absence of injury or bacterial infection they are expressed at concentrations well below that required for the observed antimicrobial effect *in vitro* (85-88). Instead of acting to prevent bacterial infection, these peptides appear to assist in coordinating the innate immune system, inducing cytokine production in nearby macrophages and other white blood cells (85). During an infection the concentration of AMPs increases dramatically (86), and the resulting cascade results in recruitment of white blood cells to the site of infection (88). At such high concentrations the peptides may demonstrate a direct killing effect, but their roles in promoting wound healing and inactivating pro-inflammatory particles such as lipopolysaccharide are of equal if not greater importance.

Attempts to create immunomodulatory agents based on the AMP scaffold have met with some success, especially with analogues based directly on the human AMP LL-37 (89, 90). These agents are able to exert anti-infective behaviour in a mouse model despite lacking any direct antimicrobial activity *in vitro.* Design of wholly *de novo* agents has been more problematic, though series of SMAMPs were found to induce production of the chemoattractant murine KC (91). Antibacterial activity does not appear to be a prerequisite for

immunomodulatory activity, though as this is a new sub-field of AMP discovery it may be some time before we fully understand the relationship between the two biological functionalities.

2.16 **Concluding Remarks**

Research into the activity and design of antimicrobial peptides (AMPs) and their mimics has produced several antimicrobial compounds with potent antibacterial activity and elucidated trends of increasing activity and specificity. Applications for this work are numerous, including antimicrobial surfaces (92, 93) and conjugates in targeted therapy (94, 95). It is expected that interest in AMPs will grow in the coming years, opening up new avenues in both antimicrobial drug design.

2.17 **Acknowledgments**

This work was supported by the Natural Sciences and Engineering Research Council of Canada (NSERC), the Canadian Institutes of Health Research (CIHR) and the Manitoba Health Research Council (MHRC).

2.18 **Tables**

Table 2.1. Antimicrobial peptide activity compared with alpha-helical stability

Name	Sequence[a]	MIC Gram -[b]	MIC Gram +[b]	MHC[c]	Ref.
Melittin[d]	GIGAVLKVLTTGLPALISWIKRKRQQ-NH_2	2μM (EC)	0.5μM (SA)	0.78μM	(10)
Melittin Peptoid F	GIGAVN_fKVLTTGN_fPALISWN_fKRKRQQ-NH_2	4μM (EC)	2μM (SA)	>100μM	(10)
RTA	RPAFRKAAFRVMRACV-NH_2	4μM (PA)	N/P[e]	>1300μM	(8)
RTA-F4W, R5L[d]	RPAWLKAAFRVMRACV-NH_2	4μM (PA)	N/P[e]	~7μM	
V681[d]	Ac-KWKSFLKTFKSAVKTVLHTALKAISS-NH_2	2.1μM (EC)	N/P[e]	5.2μM	(7)
V_{681}-V13K	Ac-KWKSFLKTFKSAKKTVLHTALKAISS-NH_2	0.89μM (EC)	N/P[e]	>88.6μM	(7)
V_{681}-V13V_D	Ac-KWKSFLKTFKSAV$_D$KTVLHTALKAISS-NH_2	1.1μM (EC)	N/P[e]	22.2μM	(9)
D-V_{681}-V13K	Ac-$K_DW_DS_DF_DL_DK_DT_DF_DK_DS_DA_DK_DK_DT_DV_DL_DH_DT_DA_DL_DK_DA_DI_DS_DS_D$-NH2	1.1μM (EC)	N/P[e]	>88.6μM	(9)

[a]Amino acids are denoted by their one letter abbreviations. [b]EC = *Escherichia coli*, PA = *Pseudomonas aeruginosa,* BS = *Bacillus subtilis*, SA = *Staphylococcus aureus,* All values are in μM unless otherwise noted. [c]Minimal hemolytic concentration. [d]Shading indicates peptides with high hemolytic activity, which also adopt stable alpha-helical structures in aqueous buffer.[e]N/P = Not performed.

Table 2.2. The effect of charge and hydrophobicity on the activity of selected antimicrobial peptide series.

Name	Sequence[a]	MIC Gram -[b]	MIC Gram +[b]	MHC[c]	Ref.
Buforin II 10	FPVGRVHRLLRK-H	>173μM (EC)	>173μM (BS)	>270μM (HC_{50})[d]	(12)
Buforin II 10 – L9L_f, L10L_f	FPVGRVHRL_fL_fRK-H	23μM (EC)	5.9μM (BS)	>235μM (HC_{50})[d]	(12)
Magainin 2	GIGKFLHAAKKFAKAFVAEIMNS-NH_2	1.0μM (EC)	1.0μM (BS)	70.6μM (HC_{50})[d]	(12)
Magainin 2- L6L_f, I20L_f 2	GIGKFL_fHAAKKFAKAFVAEL_fMNS-NH_2	0.92μM (EC)	0.92μM (BS)	7.4μM (HC_{50})[d]	(12)
Magainin 2- L6L_f, A9L_f, A13L_f, I20L_f	GIGKFL_fHAL_fKKFL_fKAFL_fAEL_fMNS-NH_2	13μM (EC)	3.3μM (BS)	3.6μM (HC_{50})[d]	(12)
Penetratin	RQIKIWFQNRRMKWKK-NH_2	2μM (EC)	1μM (SA)	>200μM	(57)
Dual-Penetratin	$(RQIKIWFQNRRMKWKK)_2$K-NH_2	2μM (EC)	1μM (SA)	25μM	(57)
V_{681}- L6A, L21A	Ac-KWKSFAKTFKSAKKTVLHTAAKAISS-NH_2	168μM (PA)	N/P[e]	336μM	(13)

V_{681}-A12L, A20L, A23L	Ac-KWSFLKTFKSLKKTVLHTLLKLISS-NH_2	168μM (PA)	N/P[e]	1.3μM	(13)
V_{681}-V13K, T15K, T19K	Ac-KWKSFLKTFKSALysLysLysVLHKALKAISS-NH_2	2.8μM (EC)	11μM (BS)	<2.8μM	(7)
D-V681-V13K	Ac-$K_DW_DS_DF_DL_DK_DT_DF_DK_DS_DA_DK_DK_DT_DV_DL_DH_DT_DA_DL_DK_DA_DI_DS_DS_D$-$NH_2$	5.3μM (PA)	N/P[e]	88.6μM	(9)

[a]Amino acids are denoted by their one letter abbreviations. [b]EC = *E. coli*, PA = *P. aeruginosa,* BS = *B. subtilis*, SA = *S. aureus,* all values are in μM unless otherwise noted. [c]Minimal hemolytic concentration. [d] concentration for 50% hemolysis of blood cells. [e]N/P = Not performed.

Table 2.3. Antibacterial and hemolytic activity of several arginine tryptophan (RW) based short cationic antimicrobial peptides.

Name	Sequence[a]	MIC Gram -[b]	MIC Gram +[b]	MHC[c]	Ref.

WRW-amide	WRW-NH_2	>436μM (EC)	218μM (SA)	>500μg/mL	(25)
WRW-ester	WRW-OBz	140μM (EC)	9μM (SA)	>500μg/mL	(25)
$(RW)_3$	RWRWRW-NH_2	16μM (EC)	8.0μM (SA)	210μM (HC_{50})[d]	(24)
$(RW)_4$	RWRWRWRW-NH_2	9.6μM (EC)	5.1μM (SA)	100μM (HC_{50})[d]	(26)
$(RW)_5$	RWRWRWRWRW-NH_2	6.2μM (EC)	3.6μM (SA)	76μM (HC_{50})[d]	(26)
RW_{4D}	see Fig. 2	2.4μM (EC)	8.7μM (SA)	760μM (HC_{50})[d]	(26)

[a]Amino acids are denoted by their one letter abbreviations. [b]EC = *E. coli*, PA = *P. aeruginosa,* SA = *S. aureus,* All values are in μM unless otherwise noted. [c]Minimal hemolytic concentration. [d] concentration for 50% hemolysis of red blood cells. [e]N/P = Not performed.

Table 2.4. Antifungal and antibacterial activity of selected (lipo)peptides.

Name	Sequence[a]	MIC[b] Bacterial[c] (*E. coli*)	MIC Fungi[d] (*Aspergillus fumigatus*)	MHC[e]	Ref.
Magainin 2-F12W	GIGKFLHSAKKWGKAFVGEIMNS-NH_2	N/P[f]	>50μM	N/S[g]	(38)

UA-Magainin 2-F12W	$CH_3(CH_2)_9CO$- GIGKFLHSAKKWGKAFVGEIMNS-NH_2	N/P[f]	6.25μM	N/S[g]	(38)
$(L_D)_6K_6$	$L_DKKL_DL_DL_DKKL_DL_DKKL_D$-$NH_2$	>50μM	50μM	N/H at 25μM[h]	(39)
DDA-$(L_D)_6K_6$ (pH 7.4)	$CH_3(CH_2)_{10}CO$- $L_DKKL_DL_DL_DKKL_DL_DKKL_D$ –NH_2	25μM[i]	6.25μM	N/H at 25μM[h]	(39)
C16-LysLysLys	$CH_3(CH_2)_{14}CO$-LysLysLys-NH_2	1.56μM	3.1μM	100μM (HD_{50})[j]	(41)
DDA-$(L_D)_6H_6$ (pH 7.4)	$CH_3(CH_2)_{10}CO$-$L_DHHL_DL_DHHL_DL_DHHL_D$-NH_2	>100μM	>100μM	N/H at 50μM[h]	(43)
DDA-$(L_D)_6H_6$ (pH 5.5)	$CH_3(CH_2)_{10}CO$- $L_DHHL_DL_DHHL_DL_DHHL_D$ -NH_2	>100μM	6.2μM	N/P[f]	(43)

[a]The amino acids are denoted by their one letter abbreviations. [b]All values are in μM unless otherwise noted. [c]*Escherichia coli*. [d]*Aspergillus fumigatus*. [e]Minimal hemolytic concentration. [f]N/P = Not performed. [g]N/S: The compounds were described as either non-hemolytic or weakly hemolytic at the bacterial MIC, but no data was provided. [h]N/H: Not hemolytic. [i]Two strains tested. [j]Concentration for 50% hemolysis of red blood cells.

Table 2.5. Activity of polymeric synthetic mimics of antimicrobial peptides.

SMAMP	MIC_{90}[a] *E. coli*	MIC_{90}[a] *S. aureus*	HC_{50}[b]	Ref.
C1	25	50	1	(69)
C2	6	50	700	(69)
C3	25	25	500	(69)
D1	>400	>200	>2150	(69)
D2	200	25	1400	(69)
D3	200	15	1200	(69)
E	6	12	1500	(68)

[a] Minimal inhibitory concentration required to inhibit bacterial growth by 90%. [b] concentration required for 50% hemolysis of red blood cells. All values are in μg/mL

2.19 **References**

1. Wang G, Li X, Wang Z. APD2: The updated antimicrobial peptide database and its application in peptide design. Nucleic Acids Res. 2009 Jan;37(Database issue):D933-7.

2. Dathe M, Wieprecht T. Structural features of helical antimicrobial peptides: Their potential to modulate activity on model membranes and biological cells. Biochim Biophys Acta. 1999 Dec 15;1462(1-2):71-87.

3. van den Bogaart G, Guzman JV, Mika JT, Poolman B. On the mechanism of pore formation by melittin. J Biol Chem. 2008 Dec 5;283(49):33854-7.

4. Bhunia A, Ramamoorthy A, Bhattacharjya S. Helical hairpin structure of a potent antimicrobial peptide MSI-594 in lipopolysaccharide micelles by NMR spectroscopy. Chem Eur J. 2009 Jan 29;15(9):2036-40.

5. Klocek G, Schulthess T, Shai Y, Seelig J. Thermodynamics of melittin binding to lipid bilayers. Aggregation/Pore formation. Biochemistry. 2009 Jan 27;48(12):2586-96.

6. Melo MN, Ferre R, Castanho MA. Antimicrobial peptides: Linking partition, activity and high membrane-bound concentrations. Nat Rev Microbiol. 2009 Mar;7(3):245-50.

7. Chen Y, Mant CT, Farmer SW, Hancock RE, Vasil ML, Hodges RS. Rational design of alpha-helical antimicrobial peptides with enhanced activities and specificity/therapeutic index. J Biol Chem. 2005 Apr 1;280(13):12316-29.

8. Hawrani A, Howe RA, Walsh TR, Dempsey CE. Origin of low mammalian cell toxicity in a class of highly active antimicrobial amphipathic helical peptides. J Biol Chem. 2008 Jul 4;283(27):18636-45.

9. Chen Y, Vasil AI, Rehaume L, Mant CT, Burns JL, Vasil ML, et al. Comparison of biophysical and biologic properties of alpha-helical enantiomeric antimicrobial peptides. Chem Biol Drug Des. 2006 Feb;67(2):162-73.

10. Zhu WL, Song YM, Park Y, Park KH, Yang ST, Kim JI, et al. Substitution of the leucine zipper sequence in melittin with peptoid residues affects self-association, cell selectivity, and mode of action. Biochim Biophys Acta. 2007 Jun;1768(6):1506-17.

11. Naarmann N, Bilgicer B, Meng H, Kumar K, Steinem C. Fluorinated interfaces drive self-association of transmembrane alpha helices in lipid bilayers. Angew Chem Int Ed Engl. 2006 Apr 10;45(16):2588-91.

12. Meng H, Kumar K. Antimicrobial activity and protease stability of peptides containing fluorinated amino acids. J Am Chem Soc. 2007 Dec 19;129(50):15615-22.

13. Chen Y, Guarnieri MT, Vasil AI, Vasil ML, Mant CT, Hodges RS. Role of peptide hydrophobicity in the mechanism of action of alpha-helical antimicrobial peptides. Antimicrob Agents Chemother. 2007 Apr;51(4):1398-406.

14. Sarig H, Rotem S, Ziserman L, Danino D, Mor A. Impact of self-assembly properties on antibacterial activity of short acyl-lysine oligomers. Antimicrob Agents Chemother. 2008 Dec;52(12):4308-14.

15. Matsuzaki K. Control of cell selectivity of antimicrobial peptides. Biochim Biophys Acta, Biomembr. 2008;1788(8):1687-92.

16. Zhu WL, Lan H, Park IS, Kim JI, Jin HZ, Hahm KS, et al. Design and mechanism of action of a novel bacteria-selective antimicrobial peptide from the cell-penetrating peptide pep-1. Biochem Biophys Res Commun. 2006 Oct 20;349(2):769-74.

17. Jiang Z, Vasil AI, Hale JD, Hancock RE, Vasil ML, Hodges RS. Effects of net charge and the number of positively charged residues on the biological activity of amphipathic alpha-helical cationic antimicrobial peptides. Biopolymers. 2008;90(3):369-83.

18. Stewart KM, Horton KL, Kelley SO. Cell-penetrating peptides as delivery vehicles for biology and medicine. Org Biomol Chem. 2008 Jul 7;6(13):2242-55.

19. Marr AK, Gooderham WJ, Hancock RE. Antibacterial peptides for therapeutic use: Obstacles and realistic outlook. Curr Opin Pharmacol. 2006 Oct;6(5):468-72.

20. Hilpert K, Volkmer-Engert R, Walter T, Hancock RE. High-throughput generation of small antibacterial peptides with improved activity. Nat Biotechnol. 2005 Aug;23(8):1008-12.

21. Fjell CD, Jenssen H, Hilpert K, Cheung WA, Pante N, Hancock RE, et al. Identification of novel antibacterial peptides by chemoinformatics and machine learning. J Med Chem. 2009 Apr 9;52(7):2006-15.

22. Kyte J, Doolittle RF. A simple method for displaying the hydropathic character of a protein. J Mol Biol. 1982 May 5;157(1):105-32.

23. Guralp SA, Murgha YE, Rouillard JM, Gulari E. From design to screening: A new antimicrobial peptide discovery pipeline. PLoS One. 2013;8(3):e59305.

24. Liu Z, Brady A, Young A, Rasimick B, Chen K, Zhou C, et al. Antimicrob Agents Chemother. 2007;51(2):597-603.

25. Strøm MB, Haug BE, Skar ML, Stensen W, Stiberg T, Svendsen JS. The pharmacophore of short cationic antibacterial peptides. J Med Chem. 2003;46(9):1567.

26. Liu Z, Young AW, Hu P, Rice AJ, Zhou C, Zhang Y, et al. Tuning the membrane selectivity of antimicrobial peptides by using multivalent design. ChemBioChem. 2007;8(17):2063-5.

27. Chen X, Zhang M, Zhou C, Kallenbach NR, Ren D. Control of bacterial persister cells by Trp/Arg-containing antimicrobial peptides. Appl Environ Microbiol. 2011 Jul;77(14):4878-85.

28. Giménez D, Andreu C, Olmo Md, Varea T, Diaz D, Asensio G. The introduction of fluorine atoms or trifluoromethyl groups in short cationic peptides enhances their antimicrobial activity. Bioorg Med Chem. 2006 10/15;14(20):6971-8.

29. Haug BE, Stensen W, Kalaaji M, Rekdal O, Svendsen JS. Synthetic antimicrobial peptidomimetics with therapeutic potential. J Med Chem. 2008 Jul 24;51(14):4306-14.

30. Flemming K, Klingenberg C, Cavanagh JP, Sletteng M, Stensen W, Svendsen JS, et al. High in vitro antimicrobial activity of synthetic antimicrobial peptidomimetics against staphylococcal biofilms. J Antimicrob Chemother. 2009 Jan;63(1):136-45.

31. Svenson J, Stensen W, Brandsdal BO, Haug BE, Monrad J, Svendsen JS. Antimicrobial peptides with stability toward tryptic degradation. Biochemistry. 2008 Mar 25;47(12):3777-88.

32. Isaksson J, Brandsdal BO, Engqvist M, Flaten GE, Svendsen JS, Stensen W. A synthetic antimicrobial peptidomimetic (LTX 109): Stereochemical impact on membrane disruption. J Med Chem. 2011 Aug 25;54(16):5786-95.

33. Peschel A, Sahl HG. The co-evolution of host cationic antimicrobial peptides and microbial resistance. Nat Rev Microbiol. 2006 Jul;4(7):529-36.

34. Shai Y, Oren Z. From "carpet" mechanism to de-novo designed diastereomeric cell-selective antimicrobial peptides. Peptides. 2001 Oct;22(10):1629-41.

35. Papo N, Shai Y. Effect of drastic sequence alteration and D-amino acid incorporation on the membrane binding behavior of lytic peptides. Biochemistry. 2004 Jun 1;43(21):6393-403.

36. Braunstein A, Papo N, Shai Y. In vitro activity and potency of an intravenously injected antimicrobial peptide and its DL amino acid analog in mice infected with bacteria. Antimicrob Agents Chemother. 2004 Aug;48(8):3127-9.

37. Karstad R, Isaksen G, Brandsdal BO, Svendsen JS, Svenson J. Unnatural amino acid side chains as S1, S1', and S2' probes yield cationic antimicrobial peptides with stability toward chymotryptic degradation. J Med Chem. 2010 Aug 12;53(15):5558-66.

38. Avrahami D, Shai Y. Conjugation of a magainin analogue with lipophilic acids controls hydrophobicity, solution assembly, and cell selectivity. Biochemistry (N Y). 2002 02/01;41(7):2254-63.

39. Malina A, Shai Y. Conjugation of fatty acids with different lengths modulates the antibacterial and antifungal activity of a cationic biologically inactive peptide. Biochem J. 2005 Sep 15;390(Pt 3):695-702.

40. Mitra RN, Shome A, Paul P, Das PK. Antimicrobial activity, biocompatibility and hydrogelation ability of dipeptide-based amphiphiles. Org Biomol Chem. 2009 Jan 7;7(1):94-102.

41. Makovitzki A, Baram J, Shai Y. Antimicrobial lipopolypeptides composed of palmitoyl di- and tricationic peptides: In vitro and in vivo activities, self-assembly to nanostructures, and a plausible mode of action. Biochemistry. 2008 Oct 7;47(40):10630-6.

42. Mangoni ML, Shai Y. Short native antimicrobial peptides and engineered ultrashort lipopeptides: Similarities and differences in cell specificities and modes of action. Cell Mol Life Sci. 2011 Jul;68(13):2267-80.

43. Makovitzki A, Shai Y. pH-dependent antifungal lipopeptides and their plausible mode of action. Biochemistry (N Y). 2005 07/01;44(28):9775-84.

44. Serrano GN, Zhanel GG, Schweizer F. Antibacterial activity of ultrashort cationic lipo-{beta}-peptides. Antimicrob Agents Chemother. 2009 Feb 23;53(5):2215-7.

45. Jadhav V, Maiti S, Dasgupta A, Das PK, Dias RS, Miguel MG, et al. Effect of the head-group geometry of amino acid-based cationic surfactants on interaction with plasmid DNA. Biomacromolecules. 2008 07/01;9(7):1852-9.

46. Song J. What's new on the antimicrobial horizon? Int J Antimicrob Agents. 2008 12;32(Supplement 4):S207-13.

47. Mulvey MR, Simor AE. Antimicrobial resistance in hospitals: How concerned should we be? CMAJ. 2009 Feb 17;180(4):408-15.

48. Otter JA, French GL. Nosocomial transmission of community-associated meticillin-resistant staphylococcus aureus: An emerging threat. Lancet Infect Dis. 2006 12;6(12):753-5.

49. Hancock RE, Scott MG. The role of antimicrobial peptides in animal defenses. Proc Natl Acad Sci U S A. 2000 Aug 1;97(16):8856-61.

50. Jenssen H, Hamill P, Hancock RE. Peptide antimicrobial agents. Clin Microbiol Rev. 2006 Jul;19(3):491-511.

51. Wehkamp J, Stange EF. A new look at crohn's disease: Breakdown of the mucosal antibacterial defense. Ann N Y Acad Sci. 2006 Aug;1072:321-31.

52. Zasloff M. Antimicrobial peptides in health and disease. N Engl J Med. 2002 Oct 10;347(15):1199-200.

53. Perron GG, Zasloff M, Bell G. Experimental evolution of resistance to an antimicrobial peptide. Proc Biol Sci. 2006 Jan 22;273(1583):251-6.

54. Yang L, Gordon VD, Trinkle DR, Schmidt NW, Davis MA, DeVries C, et al. Mechanism of a prototypical synthetic membrane-active antimicrobial: Efficient hole-punching via interaction

with negative intrinsic curvature lipids. Proc Natl Acad Sci U S A. 2008 Dec 30;105(52):20595-600.

55. Koprivnjak T, Peschel A. Bacterial resistance mechanisms against host defense peptides. Cell Mol Life Sci. 2011 Jul;68(13):2243-54.

56. Hoskin DW, Ramamoorthy A. Studies on anticancer activities of antimicrobial peptides. Biochim Biophys Acta. 2008 Feb;1778(2):357-75.

57. Zhu WL, Shin SY. Antimicrobial and cytolytic activities and plausible mode of bactericidal action of the cell penetrating peptide penetratin and its lys-linked two-stranded peptide. Chem Biol Drug Des. 2009 Feb;73(2):209-15.

58. Hancock RE, Sahl HG. Antimicrobial and host-defense peptides as new anti-infective therapeutic strategies. Nat Biotechnol. 2006 Dec;24(12):1551-7.

59. Ge Y, MacDonald DL, Holroyd KJ, Thornsberry C, Wexler H, Zasloff M. In vitro antibacterial properties of pexiganan, an analog of magainin. Antimicrob Agents Chemother. 1999 Apr;43(4):782-8.

60. Rotem S, Mor A. Antimicrobial peptide mimics for improved therapeutic properties. Biochim Biophys Acta. 2008 Nov 5;1788(8):1582-92.

61. Radzishevsky IS, Rotem S, Bourdetsky D, Navon-Venezia S, Carmeli Y, Mor A. Improved antimicrobial peptides based on acyl-lysine oligomers. Nat Biotechnol. 2007 Jun;25(6):657-9.

62. Radzishevsky IS, Kovachi T, Porat Y, Ziserman L, Zaknoon F, Danino D, et al. Structure-activity relationships of antibacterial acyl-lysine oligomers. Chem Biol. 2008 Apr;15(4):354-62.

63. Mowery BP, Lee SE, Kissounko DA, Epand RF, Epand RM, Weisblum B, et al. Mimicry of antimicrobial host-defense peptides by random copolymers. J Am Chem Soc. 2007 Dec 19;129(50):15474-6.

64. Scott RW, DeGrado WF, Tew GN. De novo designed synthetic mimics of antimicrobial peptides. Curr Opin Biotechnol. 2008 Dec;19(6):620-7.

65. Tew GN, Liu D, Chen B, Doerksen RJ, Kaplan J, Carroll PJ, et al. De novo design of biomimetic antimicrobial polymers. Proc Natl Acad Sci U S A. 2002 Apr 16;99(8):5110-4.

66. Tang H, Doerksen RJ, Jones TV, Klein ML, Tew GN. Biomimetic facially amphiphilic antibacterial oligomers with conformationally stiff backbones. Chem Biol. 2006 Apr;13(4):427-35.

67. Chongsiriwatana NP, Barron AE. Comparing bacterial membrane interactions of antimicrobial peptides and their mimics. Methods Mol Biol. 2010;618:171-82.

68. Gabriel GJ, Madkour AE, Dabkowski JM, Nelson CF, Nusslein K, Tew GN. Synthetic mimic of antimicrobial peptide with nonmembrane-disrupting antibacterial properties. Biomacromolecules. 2008 Nov;9(11):2980-3.

69. Al-Badri ZM, Som A, Lyon S, Nelson CF, Nusslein K, Tew GN. Investigating the effect of increasing charge density on the hemolytic activity of synthetic antimicrobial polymers. Biomacromolecules. 2008 Oct;9(10):2805-10.

70. Beckloff N, Laube D, Castro T, Furgang D, Park S, Perlin D, et al. Activity of an antimicrobial peptide mimetic against planktonic and biofilm cultures of oral pathogens. Antimicrob Agents Chemother. 2007 Nov;51(11):4125-32.

71. Brogden KA. Antimicrobial peptides: Pore formers or metabolic inhibitors in bacteria? Nat Rev Microbiol. 2005 Mar;3(3):238-50.

72. Bera S, Zhanel GG, Schweizer F. Design, synthesis, and antibacterial activities of neomycin-lipid conjugates: Polycationic lipids with potent gram-positive activity. J Med Chem. 2008 Oct 9;51(19):6160-4.

73. Bera S, Zhanel GG, Schweizer F. Evaluation of amphiphilic aminoglycoside-peptide triazole conjugates as antibacterial agents. Bioorg Med Chem Lett. 2010 May 15;20(10):3031-5.

74. Bera S, Zhanel GG, Schweizer F. Antibacterial activities of aminoglycoside antibiotics-derived cationic amphiphiles. polyol-modified neomycin B-, kanamycin A-, amikacin-, and neamine-based amphiphiles with potent broad spectrum antibacterial activity. J Med Chem. 2010 Apr 7;53(9):3626-31.

75. Bera S, Zhanel GG, Schweizer F. Antibacterial activity of guanidinylated neomycin B- and kanamycin A-derived amphiphilic lipid conjugates. J Antimicrob Chemother. 2010 Mar 23(6):1224-7.

76. Baussanne I, Bussiere A, Halder S, Ganem-Elbaz C, Ouberai M, Riou M, et al. Synthesis and antimicrobial evaluation of amphiphilic neamine derivatives. J Med Chem. 2010 Jan 14;53(1):119-27.

77. Zhang J, Chiang FI, Wu L, Czyryca PG, Li D, Chang CW. Surprising alteration of antibacterial activity of 5"-modified neomycin against resistant bacteria. J Med Chem. 2008 Dec 11;51(23):7563-73.

78. Zhang J, Keller K, Takemoto JY, Bensaci M, Litke A, Czyryca PG, et al. Synthesis and combinational antibacterial study of 5''-modified neomycin. J Antibiot (Tokyo). 2009 Oct;62(10):539-44.

79. Park CB, Kim HS, Kim SC. Mechanism of action of the antimicrobial peptide buforin II: Buforin II kills microorganisms by penetrating the cell membrane and inhibiting cellular functions. Biochem Biophys Res Commun. 1998 Mar 6;244(1):253-7.

80. Giuliani A, Pirri G, Rinaldi AC. Antimicrobial peptides: The LPS connection. Methods Mol Biol. 2010;618:137-54.

81. Hale JD, Hancock RE. Alternative mechanisms of action of cationic antimicrobial peptides on bacteria. Expert Rev Anti Infect Ther. 2007 Dec;5(6):951-9.

82. Vallon-Eberhard A, Makovitzki A, Beauvais A, Latge JP, Jung S, Shai Y. Efficient clearance of aspergillus fumigatus in murine lungs by an ultrashort antimicrobial lipopeptide, palmitoyl-lys-ala-DAla-lys. Antimicrob Agents Chemother. 2008 Sep;52(9):3118-26.

83. Choi S, Isaacs A, Clements D, Liu D, Kim H, Scott RW, et al. De novo design and in vivo activity of conformationally restrained antimicrobial arylamide foldamers. Proc Natl Acad Sci U S A. 2009 Apr 28;106(17):6968-73.

84. Rotem S, Radzishevsky IS, Bourdetsky D, Navon-Venezia S, Carmeli Y, Mor A. Analogous oligo-acyl-lysines with distinct antibacterial mechanisms. FASEB J. 2008 Aug;22(8):2652-61.

85. De Y, Chen Q, Schmidt AP, Anderson GM, Wang JM, Wooters J, et al. LL-37, the neutrophil granule- and epithelial cell-derived cathelicidin, utilizes formyl peptide receptor-like 1 (FPRL1) as a receptor to chemoattract human peripheral blood neutrophils, monocytes, and T cells. J Exp Med. 2000 Oct 2;192(7):1069-74.

86. Heilborn JD, Nilsson MF, Kratz G, Weber G, Sorensen O, Borregaard N, et al. The cathelicidin anti-microbial peptide LL-37 is involved in re-epithelialization of human skin wounds and is lacking in chronic ulcer epithelium. J Invest Dermatol. 2003 Mar;120(3):379-89.

87. Mookherjee N, Brown KL, Bowdish DM, Doria S, Falsafi R, Hokamp K, et al. Modulation of the TLR-mediated inflammatory response by the endogenous human host defense peptide LL-37. J Immunol. 2006 Feb 15;176(4):2455-64.

88. Nijnik A, Hancock RE. The roles of cathelicidin LL-37 in immune defences and novel clinical applications. Curr Opin Hematol. 2009 Jan;16(1):41-7.

89. Nijnik A, Madera L, Ma S, Waldbrook M, Elliott MR, Easton DM, et al. Synthetic cationic peptide IDR-1002 provides protection against bacterial infections through chemokine induction and enhanced leukocyte recruitment. J Immunol. 2010 Mar 1;184(5):2539-50.

90. Yeung AT, Gellatly SL, Hancock RE. Multifunctional cationic host defence peptides and their clinical applications. Cell Mol Life Sci. 2011 Jul;68(13):2161-76.

91. Thaker HD, Som A, Ayaz F, Lui D, Pan W, Scott RW, et al. Synthetic mimics of antimicrobial peptides with immunomodulatory responses. J Am Chem Soc. 2012 Jul 11;134(27):11088-91.

92. Willcox MD, Hume EB, Aliwarga Y, Kumar N, Cole N. A novel cationic-peptide coating for the prevention of microbial colonization on contact lenses. J Appl Microbiol. 2008 Dec;105(6):1817-25.

93. Madkour AE, Dabkowski JM, Nusslein K, Tew GN. Fast disinfecting antimicrobial surfaces. Langmuir. 2009 Jan 20;25(2):1060-7.

94. Hansel W, Leuschner C, Enright F. Conjugates of lytic peptides and LHRH or betaCG target and cause necrosis of prostate cancers and metastases. Mol Cell Endocrinol. 2007 Apr 15;269(1-2):26-33.

95. Ellerby HM, Bredesen DE, Fujimura S, John V. Hunter-killer peptide (HKP) for targeted therapy. J Med Chem. 2008 Oct 9;51(19):5887-92.

Chapter 3: Investigating the Antimicrobial Peptide 'Window of Activity' Using Cationic Lipopeptides with Hydrocarbon and Fluorinated Tails

By Brandon Findlay, George G. Zhanel and Frank Schweizer.

First Published in the International Journal of Antimicrobial Agents, 40, 2012, 36-42.

Reproduced with permission.

3.1 Authorship Considerations

Brandon Findlay was responsible for designing, synthesizing and characterizing the peptides, on the advice of Frank Schweizer. The biological activity of the peptides was then assessed by Nancy Laing under the supervision of George G. Zhanel (NL did not have a role in experimental design and declined authorship). The preliminary draft of the paper was written by Brandon Findlay, annotated by Frank Schweizer and George G. Zhanel, and then rendered into its final form by Brandon Findlay. Frank Schweizer was the corresponding author.

3.2 Abstract

To probe the effect of fluorination on antimicrobial peptide–membrane interactions, 24 cationic lipopeptides were created. The collection of lipopeptides was built from two different peptide sequences, LysGlyLys and LysLysLys, with a variety of different lipids selected to probe the effectiveness both of hydrocarbon and fluorinated tails. The antimicrobial activity of each peptide was tested against a mixture of pathogenic and reference bacterial strains, with the strongly membrane-lytic cationic disinfectant benzalkonium chloride used as a positive control. Non-specific interactions with hydrophobic proteins were assessed by repeating antimicrobial

testing in the presence of the model hydrophobic binding protein bovine serum albumin (BSA), and the toxicity of the lipopeptides was assessed by measuring lysis of ovine erythrocytes. Peptide sequence had a moderate effect on activity, with the most active peptide (C16-LysGlyLys) inhibiting the growth of two Staphylococcus epidermidis strains at ≤0.25 μg/mL. Tail composition was less important than the overall hydrophobicity, with the most active fluorinated tails equivalent to moderately active hydrocarbon tails. The activity of all peptides was significantly reduced by the presence of BSA, and hemolysis was closely correlated with antimicrobial activity.

3.3 **Introduction**

Over the last few decades, the emergence of drug-resistant bacteria has reduced the efficacy of current antibiotics, relegating first-line treatments to the sidelines (1). With a reduction in industry investment, the drug pipeline has not kept pace with bacterial evolution, leading many health experts to declare an urgent need for new antibacterials and novel antibiotic scaffolds (2).

One promising avenue of research involves the cationic antimicrobial peptides (CAMPs), used throughout the plant and animal kingdoms to defend against invasive bacteria and viruses (3). Unlike most antibiotics, CAMPs do not appear to act on any single molecular target. Instead they associate with a large number of anionic, hydrophobic structures such as DNA, folding proteins and the bacterial membrane (4). This promiscuity is the CAMPs' greatest strength and weakness. Effective resistance mechanisms are rare and are difficult for bacteria to develop in vitro without reducing fitness in the absence of CAMPs (5-7). Unfortunately, the same tendency for non-specific interactions may lead to significant eukaryotic cell toxicity, limiting therapeutic

use of AMPs to topical applications (8, 9). The development and widespread application of CAMPs is further complicated by their long length, as the peptides are impractical to produce synthetically at industrial scales. In vivo production of the 15–30-residue sequences is more cost effective but requires the development of sophisticated production and purification methodology to limit bacterial toxicity (10, 11).

Attempts to circumvent the high cost of CAMP production led to the ultrashort lipopeptides, analogues with brief amino acid sequences and a lipid tail (12). In lipopeptides, the necessary cationic charge is provided by two or more basic residues, while the tail provides a strong hydrophobic domain. As with natural CAMPs, large hydrophobic domains increase interactions with bacterial and eukaryotic membranes, leading to depolarisation and lysis of the cell (13, 14), while smaller domains allow amphiphiles to pass through the membrane and interact with internal targets such as DNA (4). Larger hydrophobic domains also increase binding to hydrophobic proteins such as bovine serum albumin (BSA), and so the activity of many natural CAMPs and derivatives is sharply decreased in environments similar to human serum (15).

Examining the current literature, we observed that most CAMPs used only carbon–hydrogen bonds in their hydrophobic domains (16-18). Molecules with carbon–fluorine (CF) bonds are both hydrophobic and lipophobic and as a result may associate primarily with other CF-containing materials. Amphiphiles heavy with CF bonds might therefore prefer to self-associate, reducing the effect of their hydrophobic character while in solution and potentially creating areas of high peptide concentration within the membrane. Because the initial interactions between CAMPs and bacterial membranes involve electrostatic interactions between the cationic moieties and the anionic bacterial phospholipids (3), self-association of

fluorinated CAMPs is unlikely to alter insertion into bacterial membranes. In contrast, initial CAMP interactions with the zwitterionic eukaryotic membrane are dominated by hydrophobic interaction effects. Fluorinated CAMPs could thus show significantly reduced toxicity without a similar reduction in their antimicrobial activity, greatly widening the therapeutic window. As interactions with BSA are also largely driven by hydrophobic effects (15), these compounds might even retain their antibacterial activity in the presence of BSA.

Starting with the known lipopeptides C16-LysLysLys and C16-LysGlyLys (13), a series of analogues of various tail lengths was prepared to investigate this hypothesis (Table 3.1, see section 3.7). Hydrophobic tails were constructed both of saturated hydrocarbons and fluorocarbons, with a larger selection of hydrocarbons to investigate the difference in tail type from both a length and mass standpoint.

3.4 **Results**

3.4.1 Lipopeptide Synthesis

Twenty-four amphiphilic lipopeptides were synthesised on solid phase (Table 3.1). A variety of hydrocarbon and fluorocarbon lipid tails were used to create strong hydrophobic domains, while the amino acid sequences LysLysLys and LysGlyLys were used to provide a cationic charge at physiological pH through protonation of the lysine R group. As amides containing fully fluorinated carbon tails were found to be unstable, hydrolysing at room temperature to highly acidic carboxylic acids, fluorinated tails with ethylene spacers between the carboxylic acid and CF bonds were used instead. The two peptides with hydrophilic tails (C16OH-LysGlyLys and C16OH-LysLysLys) were produced without issue.

3.4.2 Antimicrobial Activity

Using the cationic disinfectant benzalkonium chloride (BAC) as a positive control (19), the activity of the cationic lipopeptides was assessed against a selection of Gram-positive and Gram-negative bacteria (Table 3.2 and Table 3.3). The best antimicrobial activity obtained was that of C16-LysGlyLys against the MSSE and MRSE strains. Inhibiting bacterial growth at ≤0.25 μg/mL, this peptide was more active than even F11-LysGlyLys, despite the long fluorinated tail. Lipopeptide C16-LysGlyLys was also the strongest compound overall, with no other agent displaying greater activity against any of the bacterial strains tested. The activity of all peptides was stronger against Gram-positive bacteria, with MIC values ranging from ≤0.25 μg/mL to 32 μg/mL for peptides with C16 and C20 tails versus 16–512 μg/mL for the same peptides against Gram-negative bacteria. Activity against *S. pneumoniae* was an exception to this grouping, displaying significantly less susceptibility to the lipopeptides than other Gram-negative species, although the activity of BAC was not diminished. Peptides with shorter hydrocarbon tails or with tails containing hydroxyl groups were significantly less active against all species, with all peptides with tails shorter than nine carbons exhibiting low or undetectable antimicrobial activity.

Antimicrobial activity of the longest fluorinated compounds was moderate against Gram-positive bacteria (32 μg/mL for F11-LysGlyLys) and weaker against Gram-negative bacteria (64 μg/mL to >512 μg/mL). Activity of the other fluorinated tails reduced as the lipids became shorter, with the compounds F7-LysGlyLys and F7-LysLysLys broadly inactive against the strains tested.

3.4.3 Bovine Serum Albumin Testing

Addition of 4% BSA to the testing mixture reduced the apparent antimicrobial activity of BAC from 2 μg/mL to 16 μg/mL against most Gram-positive bacteria and from 32 μg/mL to 256 μg/mL for nearly all of the Gram-negative strains surveyed (Table 3.4 and Table 3.5). The lipopeptides were even more susceptible, with the activity of C16-LysGlyLys lowered to 256–512 μg/mL, a reduction of up to a 1000-fold over the activities observed in the absence of BSA. Other lipopeptides with both hydrocarbon and fluorinated tails were similarly inhibited, with the exception of C11-LysGlyLys that suffered only two- to four-fold reduction in activity.

3.4.4 Haemolytic Testing

BAC lysed ca. 70% of the erythrocytes tested at 100 μg/mL, greater than any of the lipopeptides (Table 3.2 and Table 3.3). The most haemolytic peptides were those with the longer tails, with C16-LysGlyLys and C20-LysLysLys lysing 63% and 62% of red blood cells at 100 μg/mL, respectively. Peptides with shorter hydrocarbon tails and C20-LysGlyLys were significantly less haemolytic, with all peptides with tails 11 carbons and shorter displaying negligible toxicity. Peptides with longer fluorinated tails were more haemolytic on a per molar basis, but due to their increased weight had toxicities between that of their C14 and C16 analogues on a per mass basis (17% hemolysis for F11-LysGlyLys vs. 6% for C14-LysGlyLys and 63% for C16-LysGlyLys, all at 100 μg/mL). The compounds with hydroxylated lipid tails (C16OH-LysGlyLys and C16OH-LysLysLys) were not appreciably haemolytic.

3.5 **Discussion**

3.5.1 Lipopeptide Design

While it was our intention to compare fully fluorinated lipid chains with their hydrocarbon analogues, the high acidity of the fully fluorinated precursors limited us to compounds with ethylene spacers between the carboxylic acid functional group and fluorocarbon tail. As these were significantly rarer, commercial availability of the carboxylic acids was limited to tails that were no more than 11 carbons in length. Because F11-LysGlyLys and F11-LysLysLys were roughly equivalent in weight to the previously investigated lipopeptides C16-LysGlyLys and C16-LysLysLys (13, 20), testing of these longer hydrocarbon tails was performed to allow comparison of the antimicrobial activity and toxicity of fluorinated tails on both a molar and weight basis. Previous work with these reference compounds had shown that long hydrocarbon tails were significantly haemolytic, and so to limit the hydrophobic effect of the lipid tail while retaining its length and membrane-disruptive properties, two analogues were created, C16OH-LysGlyLys and C16OH-LysLysLys. Both have a hydroxyl moiety at the end of their lipid tail, and the resulting hydration shell was meant to impose a relatively large energetic penalty to hydrophobic interactions between membrane phospholipids and the hydrocarbon tail.

3.5.2 Antimicrobial Activity

The ability of the lipopeptides to inhibit the growth of Gram-positive and Gram-negative bacteria strongly correlated with the length of the peptides' lipid tail, with compounds containing hydrocarbon tails displaying a 'window of activity' similar to that reported during research of many other CAMPs (21). CAMPs that lack sufficient hydrophobicity, such as C7-

LysGlyLys, are unable to effectively insert into the bacterial membrane, disrupt the membrane after insertion or interfere with intracellular processes. Those that have overly large hydrophobic domains, such as C20-LysGlyLys, may aggregate and precipitate from the solution, increasing their apparent MICs. While we had only a small set of fluorinated peptides to work with, they appear to behave similarly to standard hydrocarbon tails, although in our case the most active peptide bore the largest commercially available tail. While we did not observe an eventual decrease in activity as the tail became longer and more hydrophobic, such an effect can be inferred from the haemolytic behaviour of the fluorinated peptides (*vide infra*).

Comparing the activity of the LysGlyLys and LysLysLys series reveals an interesting contradiction. Previous research has found that the LysLysLys sequence is more active than its LysGlyLys counterpart when linked to a palmitic tail, likely due to increased interactions with the negatively charged bacterial membrane (13). However, in our hands almost every compound in the LysLysLys series was found to be two- to four-fold weaker than its counterpart in the LysGlyLys series, including the previously reported C16-LysGlyLys and C16-LysLysLys (13). Why a third charge would result in reduced activity is not well understood but may stem from a combination of increased flexibility in the core of the LysGlyLys series and steric interactions between the hydration shell of the central lysine in the LysLysLys series and the bacterial membrane. Both charges in LysGlyLys are able to rotate easily to the same face of the peptide, whereas in the LysLysLys series the central charge commonly sits opposite the others, with steric interactions between the R-group and carbonyl groups in the backbone impeding easy rotation to place all three charges together (22, 23). The position of the central lysine out of the plane of the other two may reduce the depth of lipopeptide insertion into the membrane, reducing the lipopeptide's disruptive ability.

The 'best-in-class' nature of C16-LysGlyLys, the most active peptide against every tested bacterial strain, matches what is currently known about CAMPs. The antimicrobial behaviour of CAMPs is not dependent on inhibition of any specific enzyme or process and instead depends on the physicochemical properties of the amphiphiles themselves (3, 21). In the absence of specific resistance mechanisms, the compound with the best balance of hydrophobicity and charge is best able to inhibit all bacteria (7), with the specific sequence or stereochemistry of the compound a secondary concern. Slight deviations from the optimum, as seen by the lipopeptides C20-LysGlyLys, C16-LysLysLys and C20-LysLysLys, led to a reduction in activity, while larger deviations create compounds with little or no activity. The general difference in activity between prokaryotic and eukaryotic cells can be explained by their different bilayer compositions. The presence of eukaryotic cholesterol in particular instils resistance to membrane perturbation (24).

3.5.3 Strain-specific Activities

However, not all bacteria were equally susceptible to the action of the lipopeptides or BAC. Gram-positive bacteria in general were far more susceptible, with the previously mentioned weakness shown by both strains of *S. epidermidis* to C16-LysGlyLys (MIC ≤ 0.25 μg/mL), and MICs between 4 μg/mL and 16 μg/mL for most of the other Gram-positive bacteria. Gram-negative bacteria were in general more resistant, although the *E. coli* strains tested were a notable exception. MICs ranged from 16 μg/mL to 128 μg/mL for C16-LysGlyLys, and it appears the combination of inner and outer bacterial membranes with an intervening peptidoglycan layer offers significant protection against CAMPs.

Results with BAC followed the same trends observed for the lipopeptides, from good activity against the Gram-positive bacteria (MICs of 2–4 μg/mL) to moderate activity against the Gram-negative bacteria (MICs of 16–64 μg/mL). With the exception of the activity of C16-LysGlyLys against MRSE and MSSE, BAC was more active than all lipopeptides tested. Notably, the activity of BAC against *S. pneumoniae* was similar to the activity against the other Gram-positive bacteria tested, while the most active lipopeptides in this series were significantly weaker in relation to their activity against other Gram-positive bacteria such as MRSA (MIC = 128 μg/mL vs. 4 μg/mL for C16-LysGlyLys and MIC = 128 μg/mL vs. 16 μg/mL for C16-LysLysLys). This discrepancy may stem from an uncharacterised resistance element (7).

A distinction should be made between the ATCC reference strains in the current study and the clinically relevant bacteria obtained from the CANWARD and CAN-ICU surveillance studies (25, 26). Strains found in the clinical surveillance studies have only recently been transferred from the hospital environment to the laboratory setting and are significantly more resistant to the effects of antibiotics (26). However, the two types of bacteria showed little intraspecies variance in their susceptibility to the lipopeptides, suggesting little overlap between resistance to classical antibiotics and CAMPs.

3.5.4 Activity in the Presence of Bovine Serum Albumin

Much of the observed antibacterial activity in CAMPs is thought to lie with non-specific interactions (e.g. protein, membrane binding) driven by hydrophobicity. Adding a small amount of BSA to the testing mix interferes with these interactions and may significantly reduce the observed antibacterial activity of CAMPs (15). When our earlier antimicrobial testing was repeated with 4% BSA in the standard Muller–Hinton broth, the activity of BAC was decreased

roughly eight-fold, but it retained moderate activity against Gram-positive bacteria (Table 3.4 and Table 3.5). The lipopeptides were far more susceptible and were almost completely inactivated. The peptide least affected (C11-LysGlyLys) was at best moderately active under normal testing conditions but retained weak activity against *S. epidermidis* and *E. faecalis*. The hydrocarbon tail appears to be too short for strong interactions with either bacterial membranes or hydrophobic proteins, allowing C11-LysGlyLys to achieve low activity under all conditions. Lengthening the tail created C14-LysGlyLys, a compound with far more activity under normal testing conditions that is almost completely inhibited by the addition of BSA. High quantities of hydrophobicity appear to be counterproductive, despite the high antimicrobial activity in initial surveys.

Knowing BSA inactivation depends on hydrophobic interactions, we attempted to circumvent binding by adding a hydrogen bond donor to the end of the lipid tail. In water this group could form a large hydration shell, imposing an energetic penalty to membrane insertion and potentially weakening interactions with BSA and eukaryotic membranes. Unfortunately, both C16OH-LysGlyLys and C16OH-LysLysLys, which contained polar hydroxy groups on their lipid tails, were inactive in the presence of BSA and only weakly active when it was absent. While it may be possible to increase CAMP specificity by adding hydrogen bond donors or acceptors to the lipid tail, groups with far smaller hydration shells will be required.

3.5.5 Haemolytic Activity

Commensurate with its strong antimicrobial activity, the positive control BAC was the most haemolytic agent studied (Table 3.2 and Table 3.3). Haemolytic activity in the current compounds also closely mirrors antimicrobial activity, with the increased hydrophobicity

instilled by the longer tails leading to more effective non-specific interactions against the membranes both of erythrocytes and bacteria. This trend did not hold for C20-LysGlyLys, likely due to a high level of aggregation reducing the effective lipopeptide concentration. Replacing the central glycine residue for a third lysine slightly counteracted the effect of increased hydrophobicity, perhaps due to either reduced interactions with the zwitterionic eukaryotic membrane or by imposing a slight energy penalty to membrane insertion. This second possibility is supported by the moderate reduction in antimicrobial activity observed between C16-LysGlyLys and C16-LysLysLys.

Because of the large number of CF bonds, we were particularly interested in the haemolytic ability of the fluorinated lipopeptides, supposing that they would display both hydrophobic and lipophobic behaviour, limiting their non-electrostatic membrane interactions. Unfortunately, while the fluorinated lipopeptides were far less haemolytic than the most active hydrocarbon lipopeptides, they were also less antimicrobial. With the moderate haemolytic results observed (17% hemolysis at 100 μg/mL of F11-LysGlyLys), it appears likely that longer fluorinated tails would have similar toxicity profiles, suggesting that the fluorination effect has little influence on the relationship between antimicrobial activity and eukaryotic toxicity.

3.6 **Conclusions**

In total, 24 lipopeptides were prepared, representing a mixture of fluorinated and non-fluorinated lipids tails between 7 and 20 carbons long. Compared with a well known cationic amphiphile, BAC, these compounds displayed good to poor activity against a mixture of reference and clinically relevant bacteria. Gram-positive bacteria were in general more susceptible to inhibition both by the positive control and our lipopeptides, while our agents

displayed at best only moderate activity (128 μg/mL) against Gram-negative bacteria, with the noticeable exception of all three *E. coli* strains. One of our agents (C16-LysGlyLys) was more active than BAC against *S. epidermidis* (≤0.25 μg/mL vs. 2 μg/mL), although in general the positive control was more effective. Peptides with CF bonds displayed stronger antimicrobial activity than their non-fluorinated analogues on a molar basis, but were less active by weight. Both types of lipopeptides and BAC displayed significant toxicity, and even those with fluorinated tails lysed red blood cells at concentrations only slightly above their MICs. Agents that did not display high levels of hemolysis were broadly ineffective against bacterial cells, with MICs ≥ 512 μg/mL.

In our hands, a moderate sequence-specific effect was observed, with the LysGlyLys series more active than or equal to the LysLysLys series in nearly all cases. This is in contrast to previously reported results (13), even when comparing identical lipopeptide structures and when testing against the same reference strain (C16-LysGlyLys and C16-LysLysLys against *E. coli* ATCC 25922). The few exceptions to this trend involved peptides with high levels of hydrophobicity such as C20-LysGlyLys versus C20-LysLysLys, where the additional charge of the LysLysLys lipopeptide may enhance water solubility and reduce peptide aggregation.

Efficacy of all active CAMPs tested was significantly reduced in the presence of BSA, except for C11-LysGlyLys. Moderately active against Gram-positive bacteria in the absence of BSA, C11-LysGlyLys retained most of this activity once BSA was added (256–512 μg/mL). The moderate hydrophobicity of this lipopeptide appears to prevent strong hydrophobic interactions both with the cellular membrane and with BSA, suggesting that instilling moderate amphiphilic character into already active antimicrobial agents may be an effective future strategy.

3.7 **Acknowledgments**

The authors are indebted to N. Liang for aid in haemolytic and microbial testing and to L.K. Freeman for helpful discussions. This research was supported by the Canadian Institutes of Health Research (CIHR), Manitoba Health Research Council (MHRC), the Natural Sciences and Engineering Research Council of Canada (NSERC) and the Canadian Foundation for Innovation (CFI).

3.8 **Tables**

Table 3.1. Lipopeptides under consideration.

Compound Designation	Sequence	Molecular Mass[a]
BenzAlk	$C_6H_5CH_2N(CH_3)_2RCl$; R = C_8H_{17} – $C_{18}H_{37}$	283.88 – 424.15 g/mol
C7-LysGlyLys	$CH_3(CH_2)_5CO$-LysGlyLys-NH_2	670.64 g/mol
C9-LysGlyLys	$CH_3(CH_2)_7CO$-LysGlyLys-NH_2	682.70 g/mol
C9B-LysGlyLys	$(CH_3)_2(CH_2)_7CO$-LysGlyLys-NH_2	712.72 g/mol
C11-LysGlyLys	$CH_3(CH_2)_9CO$-LysGlyLys-NH_2	726.75 g/mol
C14-LysGlyLys	$CH_3(CH_2)_{12}CO$-LysGlyLys-NH_2	768.83 g/mol
C16-LysGlyLys	$CH_3(CH_2)_{14}CO$-LysGlyLys-NH_2	796.82 g/mol
C20-LysGlyLys	$CH_3(CH_2)_{18}CO$-LysGlyLys-NH_2	852.99 g/mol
C16OH-LysGlyLys	$CH_2OH(CH_2)_{14}CO$-LysGlyLys-NH_2	812.88 g/mol
F7-LysGlyLys	$CF_3(CF_2)_3(CH_2)_2CO$-LysGlyLys-NH_2	832.56 g/mol
F9-LysGlyLys	$CF_3(CF_2)_5(CH_2)_2CO$-LysGlyLys-NH_2	932.57 g/mol
F9B-LysGlyLys	$(CF_3)_2(CF_2)_5(CH_2)_2CO$-LysGlyLys-$NH_2$	982.57 g/mol
F11-LysGlyLys	$CF_3(CF_2)_7(CH_2)_2CO$-LysGlyLys-NH_2	1032.59 g/mol
C7-LysLysLys	$CH_3(CH_2)_5CO$-LysLysLys-NH_2	855.79 g/mol
C9-LysLysLys	$CH_3(CH_2)_7CO$-LysLysLys-NH_2	883.84 g/mol

C9B-LysLysLys	$(CH_3)_2(CH_2)_7CO$-LysLysLys-NH_2	897.87 g/mol
C11-LysLysLys	$CH_3(CH_2)_9CO$-LysLysLys-NH_2	911.89 g/mol
C14-LysLysLys	$CH_3(CH_2)_{12}CO$-LysLysLys-NH_2	953.97 g/mol
C16-LysLysLys	$CH_3(CH_2)_{14}CO$-LysLysLys-NH_2	982.03 g/mol
C20-LysLysLys	$CH_3(CH_2)_{18}CO$-LysLysLys-NH_2	1038.13 g/mol
C16OH-LysLysLys	$CH_2OH(CH_2)_{14}CO$-LysLysLys-NH_2	996.09 g/mol
F7-LysLysLys	$CF_3(CF_2)_3(CH_2)_2CO$-LysLysLys-NH_2	1017.70 g/mol
F9-LysLysLys	$CF_3(CF_2)_5(CH_2)_2CO$-LysLysLys-NH_2	1117.72 g/mol
F9B-LysLysLys	$(CF_3)_2(CF_2)_5(CH_2)_2CO$-LysLysLys-$NH_2$	1167.72 g/mol
F11-LysLysLys	$CF_3(CF_2)_7(CH_2)_2CO$-LysLysLys-NH_2	1217.73 g/mol

[a] Molecular mass of the lipopeptides includes either two (LysGlyLys) or three (LysLysLys) equivalents of trifluoroacetic acid.

Table 3.2. Antimicrobial testing of LysGlyLys lipopeptides.[a]

Compound **Organism**	BenzAlk	C7-LysGlyLys	C9-LysGlyLys	C9B-LysGlyLys	C11-LysGlyLys	C14-LysGlyLys	C16-LysGlyLys	C20-LysGlyLys	C16OH-LysGlyLys	F7-LysGlyLys	F9-LysGlyLys	F9B-LysGlyLys	F11-LysGlyLys
***S. aureus*[b]**	2	>512	>512	>512	256	16	8	8	128	>512	256	128	32
MRSA[c]	2	>512	>512	>512	256	32	4	8	128	>512	256	128	32

MSSE[d]	2	>512	>512	512	64	16	≤0.25	8	128	>512	128	64	32
MRSE[e]	2	>512	>512	512	64	16	≤0.25	8	128	>512	128	128	32
E. faecalis[f]	4	>512	>512	512	256	64	16	16	256	>512	256	128	32
E. faecium[g]	4	>512	>512	>512	128	64	16	8	128	>512	256	128	32
S. pneumoniae[h]	4	>512	256	512	256	256	128	128	512	512	512	512	128
E. coli[i]	16	>512	>512	>512	512	128	16	256	256	>512	512	256	64
E. coli[j]	32	>512	>512	>512	512	128	16	256	128	>512	512	256	64
E. coli[k]	32	>512	>512	>512	512	128	16	256	128	>512	512	512	64
P. aeruginosa[l]	64	>512	>512	>512	512	256	64	256	512	>512	>512	256	256
P. aeruginosa[m]	64	>512	>512	>512	512	256	128	256	512	>512	>512	256	128
S. maltophilia[n]	32	>512	>512	>512	>512	512	128	256	512	>512	>512	512	>512
A. baumannii[o]	32	>512	>512	>512	>512	256	128	256	512	>512	>512	512	512
K. pneumoniae[p]	16	>512	>512	>512	>512	>512	128	256	128	>512	>512	512	512
Hemolysis[q]	69.96	0.82	0.63	0.82	1.80	5.74	63.30	25.40	0.84	0.72	0.96	2.16	16.70

[a] MIC_{90}, reported in µg/mL. [b] ATCC 29213. [c] ATCC 33592. [d] 81388 CANWARD 2008. [e] CAN-ICU 61589. [f] ATCC 29212. [g] ATCC 27270. [h] ATCC 49619. [i] ATCC 25922. [j] CAN-ICU 61714. [k] CAN-ICU 63074. [l] ATCC 27853. [m] CAN-ICU 62308. [n] CAN-ICU 62584. [o] CAN-ICU 63169. [p] ATCC 13883. [q] Percent hemolysis at 100µg/mL of compound.

Table 3.3. Antimicrobial testing of LysLysLys lipopeptides. [a]

Compound **Organism**	BenzAlk	C7-LysLysLys	C9-LysLysLys	C9B-LysLysLys	C11-LysLysLys	C14-LysLysLys	C16-LysLysLys	C20-LysLysLys	C16OH-LysLysLys	F7-LysLysLys	F9-LysLysLys	F9B-LysLysLys	F11-LysLysLys
***S. aureus*[b]**	2	512	>512	>512	512	64	16	8	256	>512	256	128	32
MRSA[c]	2	512	>512	>512	>512	64	16	16	256	>512	512	128	64
MSSE[d]	2	512	512	512	256	32	16	8	128	>512	128	64	16
MRSE[e]	2	>512	128	512	256	32	8	8	128	>512	128	16	16
***E. faecalis*[f]**	4	>512	512	512	>512	128	32	16	512	>512	128	128	64
***E. faecium*[g]**	4	>512	>512	>512	512	64	16	8	512	>512	512	128	32
***S. pneumoniae*[h]**	4	512	512	>512	512	256	128	128	512	>512	>512	512	128
***E. coli*[i]**	16	512	>512	>512	>512	256	32	64	512	>512	>512	512	128
***E. coli*[j]**	32	512	>512	>512	>512	256	32	64	>512	>512	>512	>512	128
***E. coli*[k]**	32	512	>512	>512	>512	256	32	64	512	>512	>512	512	128
***P. aeruginosa*[l]**	64	>512	>512	>512	>512	512	128	256	>512	>512	>512	>512	512
***P. aeruginosa*[m]**	64	>512	>512	>512	>512	512	256	128	>512	>512	>512	>512	256

S. maltophilia[n]	32	>512	>512	>512	>512	>512	512	128	>512	>512	>512	>512	>512
A. baumannii[o]	32	>512	>512	>512	>512	>512	256	64	>512	>512	>512	>512	>512
K. pneumoniae[p]	16	>512	>512	>512	>512	>512	128	32	>512	>512	>512	>512	512
Hemolysis	69.96	1.44	1.18	0.82	1.10	0.52	4.39	62.26	0.92	0.99	0.75	1.38	1.67

[a] MIC_{90}, reported in μg/mL. [b] ATCC 29213. [c] ATCC 33592. [d] 81388 CANWARD 2008. [e] CAN-ICU 61589. [f] ATCC 29212. [g] ATCC 27270. [h] ATCC 49619. [i] ATCC 25922. [j] CAN-ICU 61714. [k] CAN-ICU 63074. [l] ATCC 27853. [m] CAN-ICU 62308. [n] CAN-ICU 62584. [o] CAN-ICU 63169. [p] ATCC 13883. [q] Percent hemolysis at 100μg/mL of compound.

Table 3.4. Antimicrobial testing of LysGlyLys lipopeptides in the presence of 4% bovine serum albumin. [a]

Compound **Organism**	BenzAlk	C7-LysGlyLys	C9-LysGlyLys	C9B-LysGlyLys	C11-LysGlyLys	C14-LysGlyLys	C16-LysGlyLys	C20-LysGlyLys	C16OH-LysGlyLys	F7-LysGlyLys	F9-LysGlyLys	F9B-LysGlyLys	F11-LysGlyLys
S. aureus[b]	16	>512	>512	>512	>512	512	256	512	512	>512	512	256	256
MRSA[c]	16	>512	>512	>512	>512	512	256	512	512	>512	512	512	512
MSSE[d]	32	>512	>512	>512	256	512	256	256	512	>512	512	256	256
MRSE[e]	64	>512	>512	>512	256	512	256	512	512	>512	512	256	512
E. faecalis[f]	32	>512	>512	>512	256	512	512	512	>512	>512	512	512	512
E. faecium[g]	64	>512	>512	>512	512	512	256	512	512	>512	512	512	512

S.pneumoniae[h]	16	>512	512	512	256	>512	512	512	>512	>512	512	512	512
E. coli[i]	256	>512	>512	>512	512	512	256	>512	>512	>512	512	512	512
E. coli[j]	256	>512	>512	>512	>512	512	256	>512	>512	>512	>512	512	512
E. coli[k]	256	>512	>512	>512	>512	512	512	>512	>512	>512	>512	512	512
P. aeruginosa[l]	512	>512	>512	>512	>512	>512	512	>512	>512	>512	>512	>512	>512
P. aeruginosa[m]	512	>512	>512	>512	>512	512	512	>512	>512	>512	>512	>512	>512
S. maltophilia[n]	256	>512	>512	>512	>512	>512	512	>512	>512	>512	>512	>512	>512
A. baumannii[o]	256	>512	>512	>512	>512	>512	512	>512	>512	>512	>512	>512	>512
K. pneumoniae[p]	128	>512	>512	>512	>512	>512	512	>512	>512	>512	>512	512	>512

[a] MIC_{90}, reported in µg/mL. [b] ATCC 29213. [c] ATCC 33592. [d] 81388 CANWARD 2008. [e] CAN-ICU 61589. [f] ATCC 29212. [g] ATCC 27270. [h] ATCC 49619. [i] ATCC 25922. [j] CAN-ICU 61714. [k] CAN-ICU 63074. [l] ATCC 27853. [m] CAN-ICU 62308. [n] CAN-ICU 62584. [o] CAN-ICU 63169. [p] ATCC 13883.

Table 3.5. Antimicrobial testing of LysLysLys lipopeptides in the presence of 4% bovine serum albumin. [a]

Compound **Organism**	BenzAlk	C7-LysLysLys	C9-LysLysLys	C9B-LysLysLys	C11-LysLysLys	C14-LysLysLys	C16-LysLysLys	C20-LysLysLys	C16OH-LysLysLys	F7-LysLysLys	F9-LysLysLys	F9B-LysLysLys	F11-LysLysLys
S. aureus[b]	16	>512	>512	>512	>512	512	512	512	512	>512	>512	256	512
MRSA[c]	32	>512	>512	>512	>512	512	512	512	512	>512	>512	512	512
MSSE[d]	128	>512	>512	>512	>512	512	512	512	512	>512	>512	256	128

MRSE[e]	128	>512	>512	>512	>512	512	512	512	256	>512	>512	256	128
E. faecalis[f]	32	>512	>512	>512	>512	>512	512	512	512	>512	>512	>512	512
E. faecium[g]	32	>512	>512	>512	>512	512	512	512	512	>512	>512	512	512
S.pneumoniae[h]	16	512	512	512	512	>512	512	512	>512	>512	>512	>512	512
E. coli[i]	256	>512	>512	>512	>512	>512	512	>512	512	>512	>512	>512	512
E. coli[j]	256	>512	>512	>512	>512	>512	512	>512	>512	>512	>512	>512	512
E. coli[k]	256	>512	>512	>512	>512	>512	512	>512	>512	>512	>512	>512	512
P. aeruginosa[l]	512	>512	>512	>512	>512	>512	>512	>512	>512	>512	>512	>512	>512
P. aeruginosa[m]	512	>512	>512	>512	>512	>512	>512	>512	>512	>512	>512	>512	>512
S. maltophilia[n]	256	>512	>512	>512	>512	>512	>512	>512	>512	>512	>512	>512	>512
A. baumannii[o]	256	>512	>512	>512	>512	>512	>512	>512	>512	>512	>512	>512	>512
K. pneumoniae[p]	256	>512	>512	>512	>512	>512	>512	>512	>512	>512	>512	>512	512

[a] MIC_{90}, reported in µg/mL. [b] ATCC 29213. [c] ATCC 33592. [d] 81388 CANWARD 2008. [e] CAN-ICU 61589. [f] ATCC 29212. [g] ATCC 27270. [h] ATCC 49619. [i] ATCC 25922. [j] CAN-ICU 61714. [k] CAN-ICU 63074. [l] ATCC 27853. [m] CAN-ICU 62308. [n] CAN-ICU 62584. [o] CAN-ICU 63169. [p] ATCC 13883.

3.9 **Supporting Information**

Characterization data for new compounds, detailed experimental methods and other supporting information can be found in Chapter 10 of this thesis.

3.10 **References**

1. Arias CA, Murray BE. Antibiotic-resistant bugs in the 21st century--a clinical super-challenge. N Engl J Med. 2009 Jan 29;360(5):439-43.

2. Mulvey MR, Simor AE. Antimicrobial resistance in hospitals: How concerned should we be? CMAJ. 2009 Feb 17;180(4):408-15.

3. Hancock RE, Sahl HG. Antimicrobial and host-defense peptides as new anti-infective therapeutic strategies. Nat Biotechnol. 2006 Dec;24(12):1551-7.

4. Hale JD, Hancock RE. Alternative mechanisms of action of cationic antimicrobial peptides on bacteria. Expert Rev Anti Infect Ther. 2007 Dec;5(6):951-9.

5. Ge Y, MacDonald DL, Holroyd KJ, Thornsberry C, Wexler H, Zasloff M. In vitro antibacterial properties of pexiganan, an analog of magainin. Antimicrob Agents Chemother. 1999 Apr;43(4):782-8.

6. Perron GG, Zasloff M, Bell G. Experimental evolution of resistance to an antimicrobial peptide. Proc Biol Sci. 2006 Jan 22;273(1583):251-6.

7. Koprivnjak T, Peschel A. Bacterial resistance mechanisms against host defense peptides. Cell Mol Life Sci. 2011 Jul;68(13):2243-54.

8. Lipsky BA, Holroyd KJ, Zasloff M. Topical versus systemic antimicrobial therapy for treating mildly infected diabetic foot ulcers: A randomized, controlled, double-blinded, multicenter trial of pexiganan cream. Clin Infect Dis. 2008 Dec 15;47(12):1537-45.

9. Yeung AT, Gellatly SL, Hancock RE. Multifunctional cationic host defence peptides and their clinical applications. Cell Mol Life Sci. 2011 Jul;68(13):2161-76.

10. Marr AK, Gooderham WJ, Hancock RE. Antibacterial peptides for therapeutic use: Obstacles and realistic outlook. Curr Opin Pharmacol. 2006 Oct;6(5):468-72.

11. Wang H, Meng XL, Xu JP, Wang J, Wang H, Ma CW. Production, purification, and characterization of the cecropin from plutella xylostella, pxCECA1, using an intein-induced self-cleavable system in escherichia coli. Appl Microbiol Biotechnol. 2012 Jan 19.

12. Mangoni ML, Shai Y. Short native antimicrobial peptides and engineered ultrashort lipopeptides: Similarities and differences in cell specificities and modes of action. Cell Mol Life Sci. 2011 Jul;68(13):2267-80.

13. Makovitzki A, Baram J, Shai Y. Antimicrobial lipopolypeptides composed of palmitoyl di- and tricationic peptides: In vitro and in vivo activities, self-assembly to nanostructures, and a plausible mode of action. Biochemistry. 2008 Oct 7;47(40):10630-6.

14. Malina A, Shai Y. Conjugation of fatty acids with different lengths modulates the antibacterial and antifungal activity of a cationic biologically inactive peptide. Biochem J. 2005 Sep 15;390(Pt 3):695-702.

15. Svenson J, Brandsdal BO, Stensen W, Svendsen JS. Albumin binding of short cationic antimicrobial micropeptides and its influence on the in vitro bactericidal effect. J Med Chem. 2007 Jul 12;50(14):3334-9.

16. Meng H, Kumar K. Antimicrobial activity and protease stability of peptides containing fluorinated amino acids. J Am Chem Soc. 2007 Dec 19;129(50):15615-22.

17. Gottler LM, Lee HY, Shelburne CE, Ramamoorthy A, Marsh EN. Using fluorous amino acids to modulate the biological activity of an antimicrobial peptide. Chembiochem. 2008 Feb 15;9(3):370-3.

18. Giménez D, Andreu C, Olmo Md, Varea T, Diaz D, Asensio G. The introduction of fluorine atoms or trifluoromethyl groups in short cationic peptides enhances their antimicrobial activity. Bioorg Med Chem. 2006 10/15;14(20):6971-8.

19. McDonnell G, Russell AD. Antiseptics and disinfectants: Activity, action, and resistance. Clin Microbiol Rev. 1999 Jan;12(1):147-79.

20. Serrano GN, Zhanel GG, Schweizer F. Antibacterial activity of ultrashort cationic lipo-{beta}-peptides. Antimicrob Agents Chemother. 2009 Feb 23;53(5):2215-7.

21. Findlay B, Zhanel GG, Schweizer F. Cationic amphiphiles, a new generation of antimicrobials inspired by the natural antimicrobial peptide scaffold. Antimicrob Agents Chemother. 2010 Oct;54(10):4049-58.

22. Mowery BP, Lee SE, Kissounko DA, Epand RF, Epand RM, Weisblum B, et al. Mimicry of antimicrobial host-defense peptides by random copolymers. J Am Chem Soc. 2007 Dec 19;129(50):15474-6.

23. Kleywegt GJ, Jones TA. Phi/psi-chology: Ramachandran revisited. Structure. 1996 Dec 15;4(12):1395-400.

24. Dathe M, Schumann M, Wieprecht T, Winkler A, Beyermann M, Krause E, et al. Peptide helicity and membrane surface charge modulate the balance of electrostatic and hydrophobic interactions with lipid bilayers and biological membranes. Biochemistry. 1996 Sep 24;35(38):12612-22.

25. Zhanel GG, Adam HJ, Low DE, Blondeau J, Decorby M, Karlowsky JA, et al. Antimicrobial susceptibility of 15,644 pathogens from canadian hospitals: Results of the CANWARD 2007-2009 study. Diagn Microbiol Infect Dis. 2011 Mar;69(3):291-306.

26. Zhanel GG, DeCorby M, Laing N, Weshnoweski B, Vashisht R, Tailor F, et al. Antimicrobial-resistant pathogens in intensive care units in canada: Results of the canadian national intensive care unit (CAN-ICU) study, 2005-2006. Antimicrob Agents Chemother. 2008 Apr;52(4):1430-7.

Chapter 4: Guanidinylation and Tail Effects in Cationic Antimicrobial Lipopeptoids

By Brandon Findlay, Paul Szelemej, George G. Zhanel and Frank Schweizer. First published in PLOS ONE, 2012, e41141. Reproduced with permission.

4.1 Authorship Considerations

Paul Szlemej, on the advice of Brandon Findlay and Frank Schweizer, synthesized and characterized the peptoid C16-LysLysLys. Brandon Findlay was responsible for designing, synthesizing and characterizing the remaining peptoids, on the advice of Frank Schweizer. The biological activity of the peptoids was then assessed by Nancy Laing under the supervision of George G. Zhanel (NL did not have a role in experimental design and declined authorship). The preliminary draft of the paper was written by Brandon Findlay, annotated by Frank Schweizer and George G. Zhanel, and then rendered into its final form by Brandon Findlay. Frank Schweizer was the corresponding author.

4.2 Abstract

Background: Cationic antimicrobial peptides (CAMPs) are attractive scaffolds for the next generation of antimicrobial compounds, due to their broad spectrum of activity against multi-drug resistant bacteria and the reduced fitness of CAMP-insensitive mutants. Unfortunately, they are limited by poor *in vivo* performance, including ready cleavage by endogenous serum proteases.

Methodology/Principal Findings: To explore the potential for peptoid residues to replace well studied CAMP scaffolds we have produced a series of antimicrobial lipopeptoids, with sequences similar to previously reported lipopeptides. The activity of the peptoids was assessed against a panel of clinically relevant and laboratory reference bacteria, and the potential for non-specific binding was determined through hemolytic testing and repeating the antimicrobial testing in the presence of added bovine serum albumin (BSA). The most active peptoids displayed good to moderate activity against most of the Gram-positive strains tested and moderate to limited activity against the Gram-negatives. Antimicrobial activity was positively correlated with toxicity towards eukaryotic cells, but was almost completely eliminated by adding BSA.

Conclusion/Significance: The lipopeptoids had similar activities to the previously reported lipopeptides, confirming their potential to act as replacement, proteolytically stable scaffolds for CAMPs.

4.3 **Introduction**

Bacteria resistant to our current front-line therapeutics have been found sealed in permafrost, predating both the current antibiotic age and human society in general, proving antibiotic resistance mechanisms are ancient (1, 2). Dispersed throughout the pangenome at low population levels, the widespread use of antibiotics in recent times has selected for these bacteria and their resistance mechanisms, allowing them to displace their more susceptible brethren or confer their advantage to more pathogenic strains via lateral gene transfer (3).

Widespread use of antimicrobials will therefore inevitably lead to correspondingly pervasive bacterial resistance, as genes coding for resistance to the next generation of

antibiotics are already present throughout nature (1). However, the low prevalence of resistance mechanisms in pathogenic bacteria prior to the development of commercial antibiotics may offer a means of remaining one step ahead of infectious disease. In the absence of antibiotic selective pressure, resistance mechanisms are unlikely to enhance fitness, as each superfluous drug-inactivating enzyme or efflux pump requires resources which could have been used for growth and replication of the host cell (4). In antibiotic-free, nutrient-poor environments non-resistant bacteria can use this edge to outcompete strains expressing resistance elements and form the dominant bacterial population. Developing antimicrobials with energy intensive or mal-adaptive resistant mechanisms may allow researchers to accentuate this fitness penalty, preventing significant levels of resistance from persisting in the absence of antibiotic use.

Cationic antimicrobial peptides (CAMPs) have demonstrated this fitness gap (5), and their persistent activity in otherwise drug resistant strains has drawn interest (6-8). Counter to the "magic bullet" ideal of classical antibiotics, CAMPs interfere with a large number of targets, including negatively charged DNA and RNA, hydrophobic chaperone proteins, and the negatively charged bacterial membrane (8). Because cell death does not result from a single interaction or pathway and is derived from the physicochemical properties of the CAMP instead of specific structural features, it can be difficult for bacteria to develop widespread CAMP resistance. While several cases of *in vitro* resistance development have been reported (5, 7, 9), resistance may lead to reduced fitness in the absence of CAMPs, due to large scale alteration of the lipid bilayer composition (5). This is consistent with studies on resistance mechanisms in nature, which often reduce bacterial pathogenicity (9).

The key to CAMP activity is the spatial separation of opposing hydrophobic and cationic domains, which allows the CAMPs to effectively insert themselves into the negatively charged bacterial membrane, among other targets (6). This structural plasticity allows semi-synthetic analogues as small as three residues in length to exert antimicrobial activity, but also leads to high levels of toxicity and tight binding to hydrophobic proteins such as serum albumin (10, 11). Modifying the hydrophobic domain of the CAMPs appears to have the greatest effect on these nonspecific interactions, and linking lipid tails to short peptide sequences allows convenient analogue synthesis and rapid elucidation of optimal physicochemical properties (12). However, the inherent protease susceptibility of CAMPs may limit their use as therapeutics, as it offers a convenient handle for resistance development (11). Modified amino acid residues like peptoids are cleavage resistant, and have been recently used in the construction of a number of CAMP derivatives (13, 14). Peptoid residues are structurally similar to amino acids, but have the R-group transferred from the α-carbon to the amide nitrogen. Lacking the ability to form backbone hydrogen bonds, peptoids do not form standard peptide secondary structures but are able to mimic CAMP activity when composed of amphiphilic residues (13). Having constructed a series of ultrashort antimicrobial lipopeptides (15), we set out to prepare a series of ultrashort amphiphilic peptoids to better understand the effect of the modified backbone.

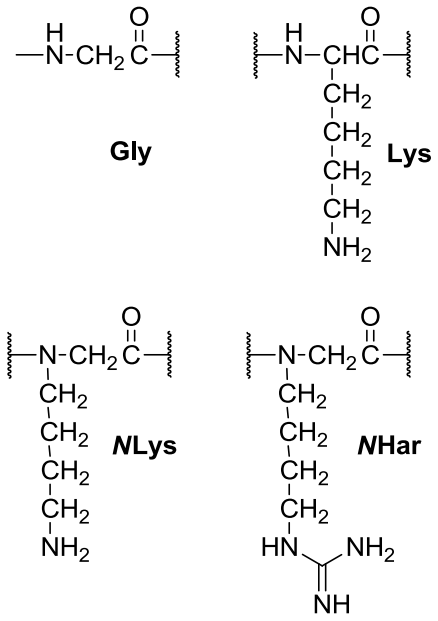

Figure 4.1. Peptoid residues with comparison amino acids. Lipid tails were attached at the N-terminus while all peptoids were amidated at their C-terminus.

4.4 **Results**

Nineteen lipopeptoids were prepared according to previously published procedures, with a mixture of different sequences and lipid tails (Table 4.1, see section 4.7). Initial synthesis of the lysine analogue containing peptoids was conducted on solid phase, with derivatization to the homoarginine-containing sequences completed in solution.

4.4.1 Antimicrobial Activity

The cationic disinfectant cetyltrimethylammonium chloride (CTAC, cetrimide) was used as a positive control, and displayed strong activity against Gram-positive bacteria (MIC 0.5 – 2

μg/mL), and moderate to limited activity against Gram-negative bacteria (MIC 16 – 128 μg/mL). *P. aeruginosa* was the least susceptible strain, in line with previous studies (16).

Activity of the lipopeptoids could be similarly divided, though the overall activity was lower. Activity of most peptoids was good to limited against Gram-positive bacteria (MIC 8 – 64 μg/mL) and moderate to weak against Gram-negative strains (MIC 16 – 512 μg/mL), with the exception of C11-*N*LysGly*N*Lys and C11-*N*Lys*N*Lys*N*Lys, which were broadly inactive. Activity against *S. pneumoniae* was significantly reduced relative to other Gram-positive bacteria, while all three *E. coli* strains were quite susceptible to peptoids with hydrophobic tails sixteen carbons in length. The three peptoids with fluorinated lipid tails were at best moderately active against Gram-positive bacteria, slightly less effective than their C14 analogues on a mass basis.

4.4.2 Antimicrobial Activity in the Presence of BSA

The addition of 4% BSA significantly reduced the activity of CTAC, raising activity against Gram-positive bacteria roughly sixteen fold (MIC 8 – 128 μg/mL) while all but eliminating activity against Gram-negative bacteria (MIC ≥512 μg/mL).

The lipopeptoids under investigation were similarly inhibited, with those based on the *N*LysGly*N*Lys and *N*HarGly*N*Har scaffolds demonstrating only weak activity (MIC 256 - >512 μg/mL) against Gram-positive bacteria when BSA was added to the testing solutions. The *N*Lys*N*Lys*N*Lys and *N*Har*N*Har*N*Har series fared somewhat better, and C20-*N*Lys*N*Lys*N*Lys was able to inhibit some Gram-positive strains at a high concentration (MIC 128 μg/mL, *S. epidermidis*).

4.4.3 Hemolytic Testing

The positive control CTAC was highly hemolytic, lysing 77% of the ovine erythrocytes at only 100 μg/mL. Hemolytic activity of the peptoids was proportional to their antimicrobial activity, though the most hemolytic peptoids, C20-*N*HarGly*N*Har and C20-*N*Har*N*Har*N*Har, were only slightly less toxic than CTAC (72% hemolysis at 100 μg/mL).

4.5 Discussion

4.5.1 Lipopeptoid Design

To allow ready comparison with our previous work the peptoid sequences were modeled after LysGlyLys and LysLysLys tripeptides (15), with the tails chosen for their previously demonstrated activity and selectivity (Table 4.1, Figure 4.1). Of note, one of our previously tested fluorinated tails was included, to test the effect of a hydrophobic and lipophobic moiety on peptoid toxicity and antimicrobial activity. Interested in the interplay between peptoid basicity and toxicity we also reacted nine of the ten initial lipopeptoids with a commercially available guanidylating reagent to create the homo-arginine peptoid analogues NHarGlyNHar and *N*Har*N*Har*N*Har (Figure 4.1). As the bacterial membrane is negatively charged, the stronger cationic character could potentially enhance antimicrobial activity.

4.5.2 Antimicrobial Activity

With the cationic disinfectant CTAC as a positive control the antimicrobial activity of the lipopeptoids was assessed against a panel of clinically relevant bacteria (Table 4.2 and Table 4.3). Several common reference laboratory bacterial strains were included as well, as quality

control and for comparison to scaffolds from other research groups. CTAC was selected as it is a potent disinfectant (16), and unsurprisingly demonstrated good activity against the Gram-positive bacteria (0.5 – 2 μg/mL) and moderate to limited activity against the Gram-negative strains (16 to 128 μg/mL) in our panel.

While the most active of our lipopeptoids were unable to match the high activity of CTAC, several displayed comparable activity against Gram-negative bacteria. In particular, both C16-NLysGlyNLys and C16-*N*HarGly*N*Har inhibited all three strains of *E. coli* tested at 16 μg/mL, despite their molecular mass being over twice that of CTAC (MIC 16 – 32 μg/mL).

The increased basicity of the NHarGlyNHar and NHarNHarNHar peptoid series appeared to convey a moderate increase in antimicrobial activity, though the effect varied depending on the lipid tail. When the *N*Lys analogue already demonstrated good activity, as in the case of C16-*N*Lys*N*Lys*N*Lys, the *N*Har variant had little change in Gram-positive activity but demonstrated improved activity against Gram-negative strains (MIC decrease two-fold for all tested strains) (Table 4.3). The greatest improvement was observed in peptoids which were already weakly active, such as C14-*N*LysGly*N*Lys and C14-*N*Lys*N*Lys*N*Lys. In these agents a two to four-fold improvement in MIC was observed against nearly every bacterial strain tested, though the activity always remained at or below that observed with C16-*N*Lys*N*Lys*N*Lys.

When the *N*Lys variant of the peptoid was broadly inactive, increasing basicity resulted in similar improvements to the antimicrobial activity, but only against Gram-positive bacteria. As both C11-*N*LysGly*N*Lys and C11-*N*Lys*N*Lys*N*Lys were inactive against most of the Gram-negative strains in our panels it is reasonable to assume that any improvement in activity remains beyond the limits of testing. Against expectations, increasing the basicity of even the most active peptoids did not increase their antimicrobial activity below 8 μg/mL. It is possible

that there is a minimum concentration for peptoid activity or that peptoid activity is self-limiting due to aggregation or an unknown mechanism.

4.5.3 Activity in the Presence of Bovine Serum Albumin

All CAMP analogues interact through non-specific interactions driven by their balance of hydrophobicity and charge, and the addition of hydrophobic proteins such as BSA is well known to cause a significant reduction in antimicrobial activity (10). The positive control CTAC was no exception, with an approximately sixteen-fold reduction in activity against Gram-positive bacteria when 4% BSA was added to the mixture (Table 4.4 and Table 4.5). Activity against Gram-negative bacteria, which are already naturally resilient to lysis because of their inner and outer cell membranes, was almost entirely eliminated.

Unfortunately, the peptoids were similarly limited. In the presence of BSA we observed nearly complete inhibition of both the *N*LysGly*N*Lys and *N*HarGly*N*Har series, with the most active peptoid, F11-*N*LysGly*N*Lys, demonstrating only limited activity against several Gram-positive bacteria (MIC 128 – 256 µg/mL) (Table 4.4). In a strange twist, the activity of C20-*N*HarGly*N*Har against *S. pneumoniae* actually appeared to increase in the presence of BSA, from 256 µg/mL to 64 µg/mL. As this appears out of line with the results against other bacterial strains we are hesitant to draw significant conclusions in the absence of further testing.

Increasing the number of positive charges on the peptoids appeared to mitigate the inhibitory effect of BSA, with C20-*N*Lys*N*Lys*N*Lys, F11-*N*Lys*N*Lys*N*Lys and C20-*N*Har*N*Har*N*Har all demonstrating limited activity against *S. aureus* and *S. epidermidis* (MIC 128 – 256 µg/mL) (Table 4.5). Because the antimicrobial activity of these peptoids was similar to their *N*LysGly*N*Lys and *N*HarGly*N*Har analogues it seems unlikely that the reduction in protein binding is a product of

increased solubility, though it may stem from the particular conformation adopted by these peptoids. NMR analysis of all of the peptoids showed the presence of distinct rotameric states about the amide moieties, with restricted peptoid conformations in solution past 80 °C (supplementary material). The central glycine residue in the *N*LysGly*N*Lys and *N*HarGly*N*Har peptoids allows them to freely rotate through their central core, and may aid in binding to the rigid BSA structure. In comparison, the *N*Lys*N*Lys*N*Lys and *N*Har*N*Har*N*Har scaffolds are restricted throughout, and may prevent some of the conformations from effectively binding to BSA. Increasing the peptoid basicity by altering residues from *N*Lys to *N*Har did not appear to reduce BSA binding, and may in fact have reduced selectivity for the bacterial membrane.

4.5.4 Hemolytic Activity

Toxicity is a major concern with CAMPs, as their reliance on non-specific interactions often leads to disruption of zwitterionic mammalian membranes (8). True to its strong antimicrobial activity, CTAC caused a high degree (77%) of lysis at 100 µg/mL, only slightly above its effective concentrations against Gram-negative bacteria (Table 4.2 and Table 4.3). The most toxic peptoids were also those with the strongest antimicrobial activity, though none were able to match the toxicity of CTAC. Seven of the eight peptoids with C16 or C20 tails lysed over 55% of the erythrocytes, with C20-*N*HarGly*N*Har reaching 72%. Peptoids with homoarginine moieties were in general more toxic than their lysine analogue counterparts, despite potential repulsion with the zwitterionic eukaryotic membrane. This counter-intuitive increase is most visible with the peptoids C14-*N*LysGly*N*Lys and C14-*N*HarGly*N*Har (2.9% vs 55.4% hemolysis at 100 µg/mL), and matches the corresponding increase in antimicrobial activity observed with these peptoids, as well as published work on longer lipopeptide sequences (12).

4.5.5 Comparison to Previously Reported Lipopeptides

While the exact values may differ, antimicrobial activity between these lipopeptoids and their closest lipopeptide analogues follow similar trends, with both types of CAMPs having similar windows of activity and toxicity (15). This reinforces the view that the primary activity of these CAMPs is determined by their physicochemical properties, not their specific structure, and suggests that previous research into lipopeptides can be directly applied to the development of new lipopeptoids.

However, the two scaffolds were not identical. Unlike the results obtained with the lipopeptide C16-LysGlyLys (15), no single lipopeptoid was significantly more effective than the others against Gram-positive bacteria. Following from the previous conclusions about the balance of physical characteristics required for antimicrobial activity, this suggests that none of the peptoids in this study have the perfect balance of hydrophobicity and cationic charge required to inhibit the growth of Gram-positive bacteria, with two or more of our compounds equally distant from the optimal lipopeptoid tail length. This is readily apparent with the peptoids C16-*N*Har*N*Har*N*Har and C20-*N*Har*N*Har*N*Har, which have nearly identical activity against each of the Gram-positive bacteria in our survey (Table 4.3).

Activity against Gram-negative bacteria by contrast showed a preference for just a few peptoid sequences, with both C16-*N*LysGly*N*Lys and C16-*N*HarGly*N*Har significantly more active than the peptoids with closely related tails (Table 4.2). The balance of lipopeptoid hydrophobicity and charge optimal for activity against Gram-positive bacteria appears to be different from that which is optimal against Gram-negative bacteria, suggesting that there is a mild structural interaction with the exterior of the two types of bacteria.

Interestingly, both sets of compounds were significantly less active against the Gram-positive bacteria *S. pneumoniae*, with activities more consistent with those displayed against Gram-negative strains. In the context of the lipopeptides we previously attempted to rationalize this resistance as the result of an unexplored resistance mechanism, and can now eliminate the possibility that *S. pneumoniae* is expressing an endogenous protease, as the peptoid backbone is not susceptible proteolytic cleavage (13). As both benzalknonium chloride and CTAC are able to maintain strong activity against *S. pneumoniae* a large scale alteration to the lipid bilayer also appears unlikely, suggesting that the poor lipopeptide and lipopeptoid activity against *S. pneumoniae* results from localization of the agents away from the bacterial membrane perhaps via electrophilic, extracellular polymers such as teichuronic acid (9). As benzalkonium chloride and CTAC contain quaternary amines they are extremely poor nucleophiles, unlikely to engage in hydrogen bonding.

4.6 **Conclusions**

Nineteen new lipopeptoids have been prepared, with a variety of sequences and lipid tails. The antimicrobial activity of these compounds was assessed against a panel of clinically relevant and laboratory reference bacterial strains, including several drug-resistant species. Compared to the cationic disinfectant CTAC the most active peptoids were less able to inhibit the growth of Gram-positive bacteria, but were more active against Gram-negative strains on a molar basis. Activity of all compounds in the presence of BSA was sharply reduced, though several peptoids retained limited activity against the Gram-positive bacteria *S. aureus* and *S. epidermidis* (MIC 128 – 256 μg/mL) (Table 4.4 and Table 4.5).

Toxicity towards eukaryotic cells was found to correlate to antimicrobial activity, with the most active antimicrobials significantly hemolytic as well. This correlation was not observed in the weakly active peptoids however, with C14-*N*LysGly*N*Lys and C14-*N*Lys*N*Lys*N*Lys able to inhibit Gram-positive bacteria without significant hemolytic activity (MIC 16 – 64 μg/mL, <5% hemolysis at 100μg/mL). Increasing the basicity of the compounds by replacing the lysine mimetic chains with homoarginine chains increased the activity of most of the peptoids tested, but in several cases resulted in a sharp increase in the hemolytic activity. Overall, the lipopeptoids produced were found to have antimicrobial activity similar to that of previously reported lipopeptides (15), with the potential to avoid proteolysis by both human serum proteins and endogenously expressed bacterial proteases.

4.7 **Acknowledgements**

We thank N. Liang for her assistance with antimicrobial and hemolytic testing and L.K. Freeman for helpful discussions.

4.8 **Tables**

Table 4.1. Lipopeptoids under consideration.[a]

Compound Designation	Sequence	Molecular Mass
CTAC	$N(CH_3)_3(CH_2)_{16}Cl$	320.00 g/mol
C11-*N*LysGly*N*Lys	$CH_3(CH_2)_9CO\text{-}N((CH_2)_4NH_2)CH_2CO\text{-}NCH_2CO\text{-}N((CH_2)_4NH_2)CH_2CO\text{-}NH_2$	726.75 g/mol
C14-*N*LysGly*N*Lys	$CH_3(CH_2)_{12}CO\text{-}N((CH_2)_4NH_2)CH_2CO\text{-}NCH_2CO\text{-}N((CH_2)_4NH_2)CH_2CO\text{-}NH_2$	768.83 g/mol
C16-*N*LysGly*N*Lys	$CH_3(CH_2)_{14}CO\text{-}N((CH_2)_4NH_2)CH_2CO\text{-}NCH_2CO\text{-}N([CH_2]_4NH_2)CH_2CO\text{-}NH_2$	796.88 g/mol
C20-*N*LysGly*N*Lys	$CH_3(CH_2)_{18}CO\text{-}N((CH_2)_4NH_2)CH_2CO\text{-}NCH_2CO\text{-}N([CH_2]_4NH_2)CH_2CO\text{-}NH_2$	852.99 g/mol
F11-*N*LysGly*N*Lys	$CF_3(CF_2)_7CH_2CH_2CO\text{-}N((CH_2)_4NH_2)CH_2CO\text{-}NCH_2CO\text{-}N((CH_2)_4NH_2)CH_2CO\text{-}NH_2$	1032.59 g/mol
C11-*N*HarGly*N*Har	$CH_3(CH_2)_9CO\text{-}N((CH_2)_4NHCN_2H_3)CH_2CO\text{-}NCH_2CO\text{-}N((CH_2)_4NHC\ N_2H_3)CH_2CO\text{-}NH_2$	810.83 g/mol
C14-*N*HarGly*N*Har	$CH_3(CH_2)_{12}CO\text{-}N((CH_2)_4NHCN_2H_3)CH_2CO\text{-}NCH_2CO\text{-}N((CH_2)_4NHCN_2H_3)CH_2CO\text{-}NH_2$	852.99 g/mol
C16-*N*HarGly*N*Har	$CH_3(CH_2)_{14}CO\text{-}N((CH_2)_4NHCN_2H_3)CH_2CO\text{-}NCH_2CO\text{-}N((CH_2)_4NHCN_2H_3)CH_2CO\text{-}NH_2$	880.96 g/mol
C20-*N*HarGly*N*Har	$CH_3(CH_2)_{18}CO\text{-}N((CH_2)_4NHCN_2H_3)CH_2CO\text{-}NCH_2CO\text{-}N((CH_2)_4NHCN_2H_3)CH_2CO\text{-}NH_2$	937.07 g/mol
F11-*N*HarGly*N*Har	$CF_3(CF_2)_7CH_2CH_2CO\text{-}N((CH_2)_4NHCN_2H_3)CH_2CO\text{-}NCH_2CO\text{-}N((CH_2)_4NHCN_2H_3)CH_2CO\text{-}NH_2$	1116.67 g/mol
C11-*N*Lys*N*Lys*N*Lys	$CH_3(CH_2)_9CO\text{-}N((CH_2)_4NH_2)CH_2CO\text{-}N((CH_2)_4NH_2)CH_2CO\text{-}N((CH_2)_4NH_2)CH_2CO\text{-}NH_2$	1038.51 g/mol
C14-*N*Lys*N*Lys*N*Lys	$CH_3(CH_2)_{12}CO\text{-}N((CH_2)_4NH_2)CH_2CO\text{-}N((CH_2)_4NH_2)CH_2CO\text{-}N((CH_2)_4NH_2)CH_2CO\text{-}NH_2$	1080.09 g/mol
C16-*N*Lys*N*Lys*N*Lys	$CH_3(CH_2)_{14}CO\text{-}N((CH_2)_4NH_2)CH_2CO\text{-}N((CH_2)_4NH_2)CH_2CO\text{-}N((CH_2)_4NH_2)CH_2CO\text{-}NH_2$	1108.15 g/mol

C20-*N*Lys*N*Lys*N*Lys	$CH_3(CH_2)_{18}CO\text{-}N((CH_2)_4NH_2)CH_2CO\text{-}N((CH_2)_4NH_2)CH_2CO\text{-}N((CH_2)_4NH_2)CH_2CO\text{-}NH_2$	1164.25 g/mol
F11-*N*Lys*N*Lys*N*Lys	$CF_3(CF_2)_7CH_2CH_2CO$ - $N((CH_2)_4NH_2)CH_2CO\text{-}N((CH_2)_4NH_2)CH_2CO\text{-}N((CH_2)_4NH_2)CH_2CO\text{-}NH_2$	1343.85 g/mol
C11-*N*Har*N*Har*N*Har	$CH_3(CH_2)_9CO\text{-}N((CH_2)_4NHCN_2H_3)CH_2CO\text{-}N((CH_2)_4NHCN_2H_3)CH_2CO\text{-}N((CH_2)_4NHCN_2H_3)CH_2CO\text{-}NH_2$	911.89 g/mol
C14-*N*Har*N*Har*N*Har	$CH_3(CH_2)_{12}CO\text{-}N((CH_2)_4NHCN_2H_3)CH_2CO\text{-}N((CH_2)_4NHCN_2H_3)CH_2CO\text{-}N((CH_2)_4NHCN_2H_3)CH_2CO\text{-}NH_2$	953.97 g/mol
C16-*N*Har*N*Har*N*Har	$CH_3(CH_2)_{14}CO\text{-}N((CH_2)_4NHCN_2H_3)CH_2CO\text{-}N((CH_2)_4NHCN_2H_3)CH_2CO\text{-}N((CH_2)_4NHCN_2H_3)CH_2CO\text{-}NH_2$	982.03 g/mol
C20-*N*Har*N*Har*N*Har	$CH_3(CH_2)_{18}CO\text{-}N((CH_2)_4NHCN_2H_3)CH_2CO\text{-}N((CH_2)_4NHCN_2H_3)CH_2CO\text{-}N((CH_2)_4NHCN_2H_3)CH_2CO\text{-}NH_2$	1038.13 g/mol

[a] Lipopeptoid masses include either two equivalents (*N*LysGly*N*Lys) or three equivalents (*N*Lys*N*Lys*N*lys) of trifluoroacetic acid.

Table 4.2. Antimicrobial testing of NLysGlyNLys based lipopeptoids.[a]

Compound **Organism**	CTAC	C11-*N*LysGlyNLys	C14-*N*LysGlyNLys	C16-*N*LysGlyNLys	C20-*N*LysGly*N*Lys	F11-*N*LysGly*N*Lys	C11-*N*HarGly*N*Har	C14-*N*HarGly*N*Har	C16-*N*HarGly*N*Har	C20-*N*HarGly*N*Har	F11-*N*HarGly*N*Har
S. aureus[b]	1	512	32	8	8	32	128	16	8	16	32
MRSA[c]	1	512	32	16	16	64	128	16	8	16	64
MSSE[d]	0.5	256	16	8	8	32	128	8	8	8	64
MRSE[e]	2	256	32	16	8	32	128	16	16	8	64
E. faecalis[f]	1	512	64	16	16	64	256	32	16	16	64
E. faecium[g]	0.5	512	64	16	16	64	256	32	16	16	32
S. pneumoniae[h]	2	512	256	128	128	256	512	128	128	256	256
E. coli[i]	16	>512	128	16	256	512	512	32	16	256	64
E. coli[j]	32	>512	128	16	256	512	512	64	16	256	128
E. coli[k]	16	>512	128	16	128	512	512	64	16	256	128
P. aeruginosa[l]	128	>512	256	64	256	512	>512	64	64	512	256
P. aeruginosa[m]	64	>512	512	128	256	512	512	128	64	256	256
S.	32	>512	512	128	128	>512	>512	256	64	256	>512

maltophilia[n]											
A. baumannii[o]	32	>512	256	128	128	>512	512	512	128	128	512
K. pneumoniae[p]	16	>512	256	64	128	>512	512	256	64	128	512
Hemolysis[q]	77.05	1.34	2.90	56.03	33.51	4.84	1.49	55.44	61.06	71.87	7.45

[a] MIC, reported in µg/mL. [b] ATCC 29213. [c] ATCC 33592. [d] 81388 CANWARD 2008. [e] CAN-ICU 61589. [f] ATCC 29212. [g] ATCC 27270. [h] ATCC 49619. [i] ATCC 25922. [j] CAN-ICU 61714. [k] CAN-ICU 63074. [l] ATCC 27853. [m] CAN-ICU 62308. [n] CAN-ICU 62584. [o] CAN-ICU 63169. [p] ATCC 13883. [q] Percent hemolysis at 100µg/mL of compound.

Table 4.3. Antimicrobial testing of NLysNLysNLys based lipopeptoids.[a]

Compound **Organism**	CTAC	C11-*N*Lys*N*Lys*N*Lys	C14-*N*Lys*N*Lys*N*Lys	C16-*N*Lys*N*Lys*N*Lys	C20-*N*Lys*N*Lys*N*Lys	F11-*N*Lys*N*Lys*N*Lys	C11-*N*Har*N*Har*N*Har	C14-*N*Har*N*Har*N*Har	C16-*N*Har*N*Har*N*Har	C20-*N*Har*N*Har*N*Har
S. aureus[b]	1	512	32	16	16	32	128	16	8	8
MRSA[c]	1	512	64	32	16	32	128	16	16	16
MSSE[d]	0.5	512	32	8	8	32	64	8	8	8
MRSE[e]	2	512	16	8	8	32	256	16	8	8
E. faecalis[f]	1	512	64	32	16	64	512	32	16	16
E. faecium[g]	0.5	256	64	32	16	64	256	16	16	8
S. pneumoniae[h]	2	>512	128	128	64	128	512	64	64	64
E. coli[i]	16	>512	128	32	32	64	>512	64	16	64
E. coli[j]	32	>512	128	64	32	64	>512	64	32	64
E. coli[k]	16	>512	128	64	32	128	>512	64	32	32
P. aeruginosa[l]	128	>512	512	128	128	128	>512	256	64	128
P. aeruginosa[m]	64	>512	512	128	64	256	>512	128	64	128
S.	32	>512	>512	256	64	>512	>512	256	128	64

maltophilia[n]										
A. baumannii[o]	32	>512	512	256	64	>512	>512	256	128	64
K. pneumoniae[p]	16	>512	512	128	64	>512	>512	256	256	64
Hemolysis	77.05	0.67	2.19	67.69	68.29	8.13	0.71	20.34	0.67	71.50

[a] MIC, reported in µg/mL. [b] ATCC 29213. [c] ATCC 33592. [d] 81388 CANWARD 2008. [e] CAN-ICU 61589. [f] ATCC 29212. [g] ATCC 27270. [h] ATCC 49619. [i] ATCC 25922. [j] CAN-ICU 61714. [k] CAN-ICU 63074. [l] ATCC 27853. [m] CAN-ICU 62308. [n] CAN-ICU 62584. [o] CAN-ICU 63169. [p] ATCC 13883. [q] Percent hemolysis at 100µg/mL of compound.

Table 4.4. Antimicrobial testing of NLysGlyNLys based lipopeptoids in the presence of 4% bovine serum albumin.[a]

Compound **Organism**	CTAC	C11-*N*LysGly*NL*ys	C14-*N*LysGly*NL*ys	C16-*N*LysGly*NL*ys	C20-*N*LysGly*NL*ys	F11-*N*LysGly*NL*ys	C11-*N*HarGly*N*Har	C14-*N*HarGly*N*Har	C16-*N*HarGly*N*Har	C20-*N*HarGly*N*Har	F11-*N*HarGly*N*Har
S. aureus[b]	32	>512	512	512	512	256	512	512	512	512	512
MRSA[c]	32	>512	512	512	512	256	512	512	512	512	512
MSSE[d]	16	512	512	512	256	128	256	512	512	256	512
MRSE[e]	128	512	512	512	512	256	512	512	512	256	512
E. faecalis[f]	32	>512	>512	512	512	256	>512	512	512	512	512
E. faecium[g]	64	>512	512	512	512	256	512	512	512	256	256
S. pneumoniae[h]	8	512	>512	512	512	512	>512	512	512	64	512
E. coli[i]	512	>512	>512	512	>512	512	512	512	512	512	>512
E. coli[j]	512	>512	>512	512	>512	512	>512	>512	512	>512	512
E. coli[k]	512	>512	>512	512	>512	>512	>512	>512	512	512	>512
P. aeruginosa[l]	>512	>512	>512	>512	>512	>512	>512	>512	>512	>512	>512
P. aeruginosa[m]	512	>512	>512	>512	>512	>512	512	>512	>512	>512	>512
S. maltophilia[n]	512	>512	>512	>512	>512	>512	>512	>512	>512	>512	>512
A. baumannii[o]	512	>512	>512	>512	>512	>512	>512	>512	>512	>512	>512

***K. pneumoniae*[p]**	512	>512	>512	>512	>512	>512	512	>512	512	512	>512

[a] MIC, reported in µg/mL. [b] ATCC 29213. [c] ATCC 33592. [d] 81388 CANWARD 2008. [e] CAN-ICU 61589. [f] ATCC 29212. [g] ATCC 27270. [h] ATCC 49619. [i] ATCC 25922. [j] CAN-ICU 61714. [k] CAN-ICU 63074. [l] ATCC 27853. [m] CAN-ICU 62308. [n] CAN-ICU 62584. [o] CAN-ICU 63169. [p] ATCC 13883.

Table 4.5. Antimicrobial testing of NLysNLysNLys based lipopeptoids in the presence of 4% bovine serum albumin.[a]

Compound **Organism**	CTAC	C11-*N*Lys*N*Lys*N*Lys	C14-*N*Lys*N*Lys*N*Lys	C16-*N*Lys*N*Lys*N*Lys	C20-*N*Lys*N*Lys*N*Lys	F11-*N*Lys*N*Lys*N*Lys	C11-*N*Har*N*Har*N*Har	C14-*N*Har*N*Har*N*Har	C16-*N*Har*N*Har*N*Har	C20-*N*Har*N*Har*N*Har
S. aureus[b]	32	>512	512	512	128	128	512	256	512	256
MRSA[c]	32	>512	512	>512	256	256	512	512	512	256
MSSE[d]	16	512	512	512	128	128	512	512	256	256
MRSE[e]	128	512	512	512	128	256	512	256	512	256
E. faecalis[f]	32	>512	512	>512	256	512	>512	512	512	512
E. faecium[g]	64	512	512	>512	256	256	512	256	512	128
S. pneumoniae[h]	8	>512	>512	512	512	512	>512	256	>256	256
E. coli[i]	512	>512	>512	>512	256	256	>512	512	512	512
E. coli[j]	512	>512	>512	>512	256	256	>512	512	512	512
E. coli[k]	512	>512	>512	>512	256	512	>512	512	>512	512
P. aeruginosa[l]	>512	>512	>512	>512	512	512	>512	>512	>512	512
P. aeruginosa[m]	512	>512	512	>512	512	512	>512	512	>512	>512
S.	512	>512	>512	>512	512	>512	>512	>512	>512	>512

maltophilia[n]										
A. baumannii[o]	512	>512	>512	>512	512	>512	>512	>512	>512	>512
K. pneumoniae[p]	512	>512	>512	>512	256	>512	>512	512	>512	>512

[a] MIC, reported in µg/mL. [b] ATCC 29213. [c] ATCC 33592. [d] 81388 CANWARD 2008. [e] CAN-ICU 61589. [f] ATCC 29212. [g] ATCC 27270. [h] ATCC 49619. [i] ATCC 25922. [j] CAN-ICU 61714. [k] CAN-ICU 63074. [l] ATCC 27853. [m] CAN-ICU 62308. [n] CAN-ICU 62584. [o] CAN-ICU 63169. [p] ATCC 13883.

4.9 **Supporting Information**

Characterization data for new compounds, detailed experimental methods and other supporting information can be found in Chapter 11 of this thesis.

4.10 **References**

1. D'Costa VM, King CE, Kalan L, Morar M, Sung WW, Schwarz C, et al. Antibiotic resistance is ancient. Nature. 2011 Aug 31;477(7365):457-61.

2. Wright GD, Poinar H. Antibiotic resistance is ancient: Implications for drug discovery. Trends Microbiol. 2012 Jan 25.

3. McDaniel LD, Young E, Delaney J, Ruhnau F, Ritchie KB, Paul JH. High frequency of horizontal gene transfer in the oceans. Science. 2010 Oct 1;330(6000):50.

4. Andersson DI, Hughes D. Antibiotic resistance and its cost: Is it possible to reverse resistance? Nat Rev Microbiol. 2010 Apr;8(4):260-71.

5. Yang L, Gordon VD, Trinkle DR, Schmidt NW, Davis MA, DeVries C, et al. Mechanism of a prototypical synthetic membrane-active antimicrobial: Efficient hole-punching via interaction with negative intrinsic curvature lipids. Proc Natl Acad Sci U S A. 2008 Dec 30;105(52):20595-600.

6. Findlay B, Zhanel GG, Schweizer F. Cationic amphiphiles, a new generation of antimicrobials inspired by the natural antimicrobial peptide scaffold. Antimicrob Agents Chemother. 2010 Oct;54(10):4049-58.

7. Perron GG, Zasloff M, Bell G. Experimental evolution of resistance to an antimicrobial peptide. Proc Biol Sci. 2006 Jan 22;273(1583):251-6.

8. Yeung AT, Gellatly SL, Hancock RE. Multifunctional cationic host defence peptides and their clinical applications. Cell Mol Life Sci. 2011 Jul;68(13):2161-76.

9. Koprivnjak T, Peschel A. Bacterial resistance mechanisms against host defense peptides. Cell Mol Life Sci. 2011 Jul;68(13):2243-54.

10. Svenson J, Brandsdal BO, Stensen W, Svendsen JS. Albumin binding of short cationic antimicrobial micropeptides and its influence on the in vitro bactericidal effect. J Med Chem. 2007 Jul 12;50(14):3334-9.

11. Svenson J, Stensen W, Brandsdal BO, Haug BE, Monrad J, Svendsen JS. Antimicrobial peptides with stability toward tryptic degradation. Biochemistry. 2008 Mar 25;47(12):3777-88.

12. Makovitzki A, Shai Y. pH-dependent antifungal lipopeptides and their plausible mode of action. Biochemistry (N Y). 2005 07/01;44(28):9775-84.

13. Chongsiriwatana NP, Miller TM, Wetzler M, Vakulenko S, Karlsson AJ, Palecek SP, et al. Short alkylated peptoid mimics of antimicrobial lipopeptides. Antimicrob Agents Chemother. 2011 Jan;55(1):417-20.

14. Chongsiriwatana NP, Barron AE. Comparing bacterial membrane interactions of antimicrobial peptides and their mimics. Methods Mol Biol. 2010;618:171-82.

15. Findlay B, Zhanel GG, Schweizer F. Investigating the antimicrobial peptide “Window of activity” using cationic lipopeptides with hydrocarbon and fluorinated tails. Int J Antimicrob Agents. 2012 In press.;40(1):36--42.

16. Maris P. Resistance of 700 gram-negative bacterial strains to antiseptics and antibiotics. Ann Rech Vet. 1991;22(1):11-23.

Chapter 5: Ultrashort Cationic Lipopeptides and Lipopeptoids Selectively Induce Cytokine Production in Blood-Derived Mononuclear Immune Cells.

By Brandon Findlay, Neeloffer Mookherjee and Frank Schweizer. First published in PLOS ONE, 2013, e54280. Reproduced with permission.

5.1 Authorship Considerations

Brandon Findlay was responsible for selecting peptides and peptoids for a preliminary immunomodulatory screen, on the advice of Frank Schweizer. These compounds were tested for cytotoxicity towards THP-1 macrophage-like cells, as well as their ability to induce production of the cytokines Groα and IL-8 in these same cells. After interpreting these intial results, Brandon Findlay designed, synthesized and characterized a second series of peptides/peptoids, on the advice of Frank Schweizer. This screen included previously prepared compounds, which if possible were obtained from previously prepared stock—not resynthesized. These compounds were submitted to the same biological studies as prior, as well as tests to determine the ability of the amphiphiles to induce production of the cytokines TNF-α and IL-1β. Following this testing Neeloffer Mookherjee prepared the biological methods section of the paper, with Brandon Findlay writing the remainder on the advice of Frank Schweizer and Neeloffer Mookherjee. Neeloffer Mookherjee and Frank Schweizer then annotated this version, and Brandon Findlay prepared the final version reproduced here. Frank Schweizer is the corresponding author.

5.2 **Abstract**

A series of ultrashort lipopeptides and lipopeptoids were tested for their ability to induce cytokine production in macrophages. Fourteen compounds were found to strongly induce production of chemokines Groα and IL-8, with a structural bias that was absent from previous antibacterial activity investigations. Compounds based on LysGlyLys and *N*LysGly*N*Lys sequences did not induce cytokine production, whereas those based on LysLysLys and *N*Lys*N*Lys*N*Lys were active only when linked to a lipid tail at least sixteen carbons long. Three lipopeptides induced high levels of IL-8 production, above that of equivalent concentrations of cathelicidin LL-37, while no compound induced production of the pro-inflammatory cytokine TNF-α at or below 100 μM. Two compounds, peptoids C16OH-*N*Lys*N*Lys*N*Lys and C16OH-*N*Har*N*Har*N*Har, were selective for IL-8 production and did not induce TNF-α or IL-1β. These compounds may prove beneficial for in vivo treatment of infectious disease, with improved bioavailability over LL-37 due to their protease-resistant scaffold.

5.3 **Introduction**

It is well established that the prevalence of antibiotic resistance is rising in pathogenic bacteria, in part due to selective pressure from human antibiotic use and from the use of antibiotics as growth promoters in livestock (1, 2). Efforts to develop new antibiotics and antibiotic scaffolds have met with mixed success, due to reduced industry investment and a number of complications arising from high-throughput screening of bacterial targets (3). The urgent need for new antibiotics has driven research into new scaffolds and unconventional modes of action, with the field of cationic antimicrobial peptides (CAMPs) of particular interest (4). First isolated from amphibians like *Xenopus laevis* (5), CAMPs are a rich class of structurally diverse antimicrobials found throughout the plant and animal kingdoms. Unlike classical

antibiotics, which derive their activity through inhibition of specific enzymes or processes, CAMPs largely interact with the cell through non-specific interactions driven by a mix of electrostatic and hydrophobic effects (6). Early researchers were particularly interested in the effect of CAMPs on bacterial and mammalian membranes, as many compounds were found to form membrane pores at sufficiently high concentrations and it was thought that a membrane-specific mode of action had reduced potential for resistance development (7, 8).

These initial investigations into pore formation eventually led to a more nuanced view of CAMPs (9). Examining CAMPs with high levels of antibacterial activity and low mammalian toxicity revealed that at their minimal inhibitory concentration (MIC) they were interfering with either internal cellular processes or membrane proteins, not predominantly with the bacterial membrane (4, 10). As efforts to optimize the more membrane-active peptides have been stymied by these peptides' ability to disrupt or lyse eukaryotic cells at concentrations generally only slightly above that of bacterial membranes (11), much of the research in recent years has focused on understanding the interaction between CAMPs and their non-membrane targets (4, 12, 13).

The human cathelicidin LL-37 has been a subject of particular interest, due to its widespread expression in human immune and epithelial cells. First discovered through its LPS binding ability (14), LL-37 is strongly antibacterial *in vitro* but has little direct antibacterial activity under physiological conditions (15). Instead, LL-37 appears to exert its antibacterial effect through modulation of the immune system (16, 17). Consistent with this, altered LL-37 expression has been linked to both auto-immune disorders and increased susceptibility to bacterial infection (18). LL-37 promotes wound healing (18), recruits leukocytes to the site of infection by acting as a direct chemoattractant or by inducing chemokine production, activates local dendritic cells and T-cells for clearing of invasive bacteria, and exhibits selective anti-

inflammatory effects (17). Modification of another immunomodulatory peptide, the bovine bactenacin, created IDR1, which has protective effects in a mouse infection model, despite lacking direct antibacterial activity (4, 19). Further library screening of bactenacin derivatives led to the more active IDR-1002 (20), while a proprietary compound, the pentapeptide IMX942, is currently entering phase 2 clinical trials (21).

To date, research into the immunomodulatory properties of CAMPs has focused on analogues of natural host defence peptides (HDPs), paring down the length of the peptide to reduce production costs while retaining a modified subsection for receptor binding (19). As natural immunomodulators like LL-37 act in part through low-affinity binding to chemotaxis receptor FPRL1 and to several intracellular receptors (22, 23), we hypothesized that compounds which mimic the physicochemical properties but not the sequence of HDPs may demonstrate improved activity, while allowing for incorporation of a protease-resistant scaffold. Protease resistance was desirable, as bacterial resistance to LL-37 can be readily conferred by metalloprotease secretion, increasing virulence (24). Recent reports confirmed this early hypothesis (25), demonstrating that protease-resistant synthetic mimics of antibacterial peptides based on a cationic arylether scaffold cause immunomodulatory responses.

Previous work by us and others has shown that for ultrashort lipopeptides and lipopeptoids only three amino acid residues and a hydrophobic lipid tail are required for efficient killing of a wide variety of bacteria *in vitro*.(26-28) Antibacterial activity was related to both peptidic sequence and length of the hydrophobic tail, with our most active lipopeptides and lipopeptoids unfortunately demonstrating significant toxicity towards mammalian red blood cells at slightly above their effective antibacterial concentrations. In lipopeptides this toxicity could be sharply reduced by adding a polar hydroxyl group to the terminus of the lipid tail (27), but these amphiphiles had little antibacterial activity.

With their large lipid tail ultrashort lipopeptides bear little similarity to known HDPs, and have shorter peptide sequences than the innate defence regulator peptides currently in clinical development. Like LL-37, *in vitro* they disrupt the bacterial membrane (26, 29), and we hypothesized that they could also modulate the immune system. As achiral molecules the lipopeptoids are further from the structure of current innate defence regulator peptides, but their naturally protease-resistant backbone offers several key advantages (*vide supra*) (30). The purpose of this study was to assess the ability of a series of ultrashort lipopeptides and lipopeptoids to induce production of chemokines Groα and IL-8 in human macrophage-like THP-1 cells. Macrophage-like THP-1 cells elicit cellular responses similar to peripheral blood-derived mononuclear cells in the presence of host defence peptides (31, 32), while Groα and IL-8 play a critical role in leukocyte recruitment to the site of infections, enhancing bacterial clearance (33). We further screened active compounds for the production of pro-inflammatory cytokines TNF-α and IL-1β. Compounds which selectively induce chemokine production without inducing pro-inflammatory cytokine TNF-α may be useful in antibacterial therapy.

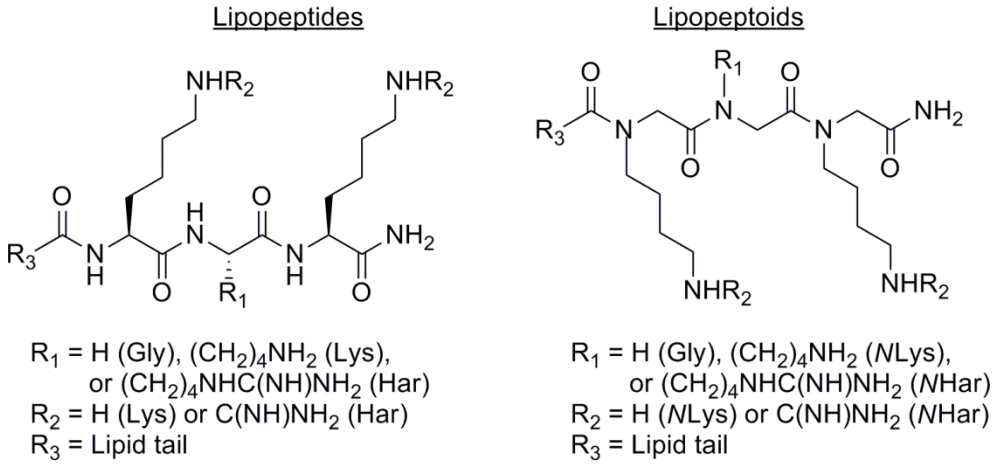

Figure 5.1. Structures for the cationic amphiphiles used in this study. Har = homoarginine; *N*Lys = lysine peptoid; *N*Har = homoarginine peptoid.

5.4 **Results and Discussion**

To display antibacterial activity lipopeptides and lipopeptoids require an overall cationic charge and long lipid tail, for attraction to the negatively charged bacterial outer membrane and insertion into the hydrophobic membrane core (26). Our compound synthesis was biased towards these properties (Supplementary Materials), with LysGlyLys- or LysLysLys- based amphiphiles (*N*LysGly*N*Lys and *N*Lys*N*Lys*N*Lys for the lipopeptoids) and lipid tails eleven to twenty carbons in length (Figure 5.1, Table 5.1, see section 5.7). Aware of the potential cytotoxicity of amphiphiles with large hydrophobic tails, a terminal hydroxy group was added to the C16 tails to disturb the classic amphiphilic nature of lipopeptides **6** and **10** and lipopeptoids **17** and **20**. Increasing the strength of the cationic charge has been found to improve antibacterial activity (28), and so each of the LysLysLys and *N*Lys*N*Lys*N*Lys compounds was mirrored by a homoarginine analogue (Har or *N*Har), to determine if immunomodulatory properties would be similarly enhanced. Amphiphile selection was roughly divided between lipopeptides and lipopeptoids, to assess the impact of chirality and conformation on activity.

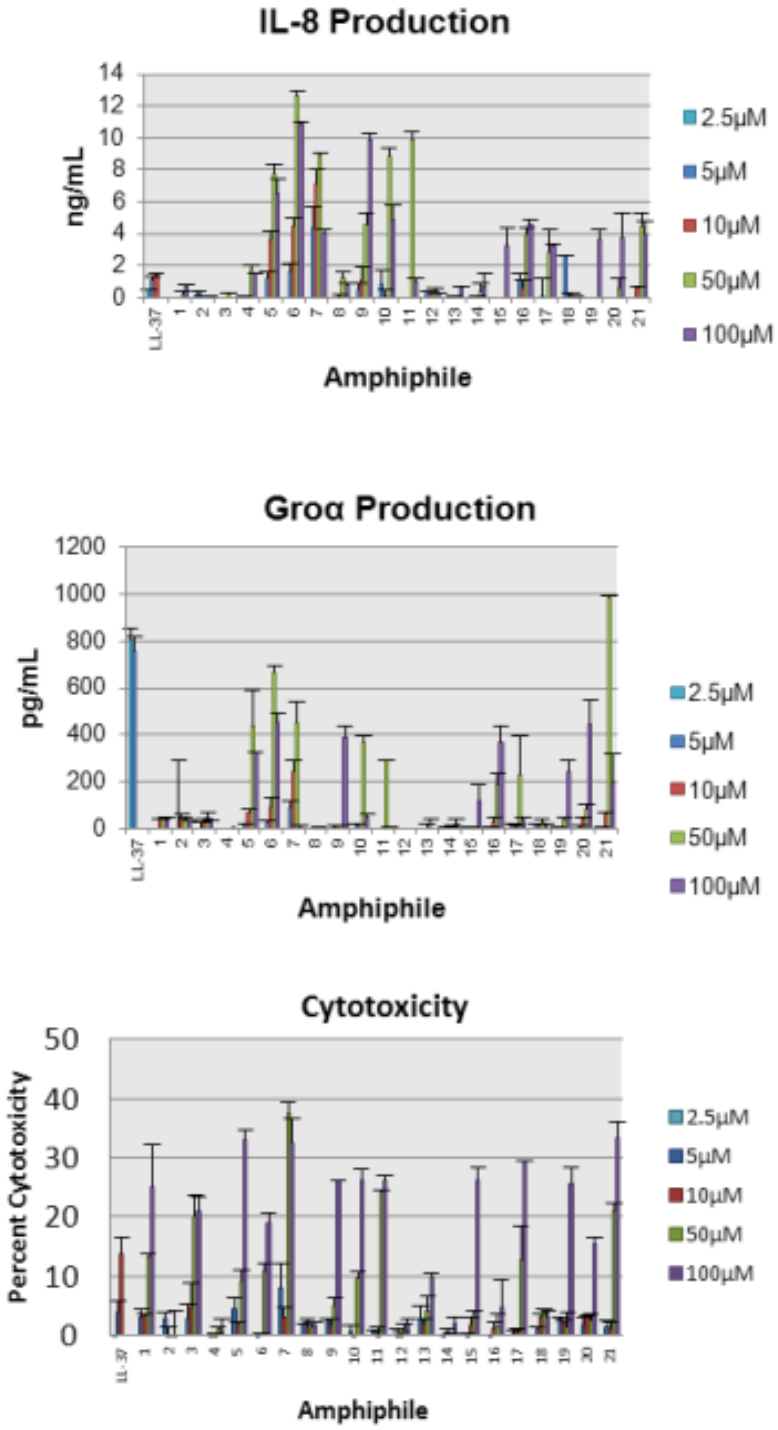

Figure 5.2. Cytokine production and LDH release by human macrophage-like THP-1 cells following incubation with amphiphiles 1-21. A) IL-8 production. TC supernatants were monitored for IL-8 production by ELISA, and results were recorded in pg/mL. B) Groα

production, in pg/mL. Inset: Expanded values for amphiphiles 5–7 and 21 at 5 μM and 10 μM. C) Cytotoxicity following incubation with amphiphiles 1-21. TC supernatants were monitored for LDH release as a measure of cellular toxicity, and results shown represent percent cytotoxicity over un-stimulated cells. All studies were performed in two independent biological replicates with two technical replicates each, with the data here presented as the mean plus standard error of the mean (sem) and with LL-37 data included as a positive control.

Prior to testing, human monocytic THP-1 cells were differentiated to plastic-adherent macrophage-like THP-1 cells as previously described (31). The cells were rested for twenty-four hours, then exposed to the amphiphiles of interest for twenty-four hours. Cell-free TC supernatants were monitored for the production of chemokines Groα and IL-8 by ELISA as previously described (31, 34). The constitutive background level of chemokine Groα was 6.6 ± 1.8 pg/ml, and that of IL-8 was 1.7 ± 0.16 ng/ml. Encouragingly, the majority of compounds were strong inducers of both IL-8 and Groα and increased chemokine levels above background (Figure 5.2). The lipopeptides (**1–11)** were more active than their corresponding lipopeptoids (**12–21)**, despite little difference in cytotoxic behaviour. The three amphiphiles with a LysLysLys peptide sequence and lipid tail at least sixteen carbons in length, **5–7**, were especially strong inducers of IL-8, increasing the concentration to 5-8 ng/mL ($p<0.05$) above control at 10 μM of lipopeptide, and up to 13 ng/mL ($p<0.01$) above control at 50 μM (Figure 5.2). These amphiphiles compared favourably to LL-37 (1.3 ng/mL of IL-8 above control at 10 μM), despite their brief peptide sequence. This activity was not shared by the LysGlyLys lipopeptides **2** and **3**, which failed to significantly increase IL-8 production at any of the concentrations tested. Guanidinylation did not improve IL-8 production at low lipopeptide concentrations, though amphiphiles **10–11** did induce up to 10 ng/mL ($p<0.05$) of IL-8 at 50 μM, suggesting a minimum

lipopeptide concentration is required for IL-8 production. All lipopeptides with lipid tails shorter than sixteen carbons were unable to induce either IL-8 or Groα at concentrations up to 100 μM (Figure 5.2, Supplementary material).

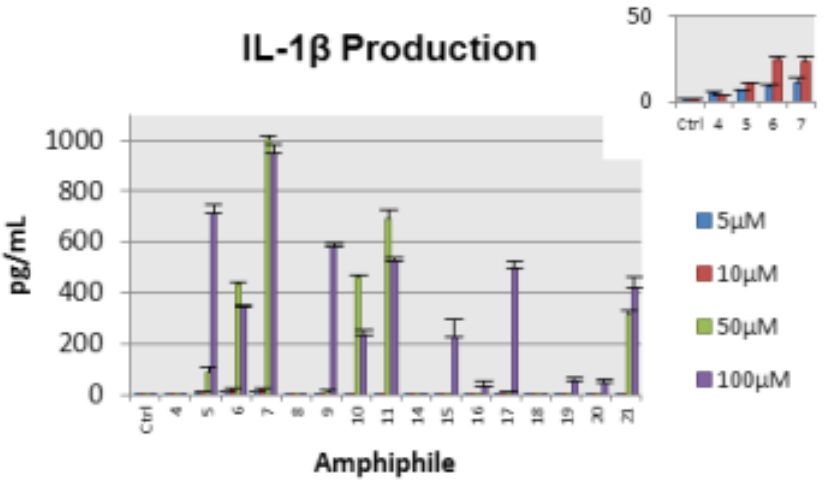

Figure 5.3. IL-1β production. Human macrophage-like THP-1 cells were exposed to amphiphiles 4–11 and 14–21, for twenty-four hours. TC supernatants were monitored for IL-1β by ELISA, with results shown in pg/mL. Studies were performed in two independent biological replicates with two technical replicate each, with the data here presented as the mean plus sem. Inset: Expanded results for the negative control and amphiphiles 4–7 at 5 μM and 10 μM.

The lipopeptides were less effective at inducing Groα production, though 50μM of amphiphile **6** compared favourably to 2.5μM of LL-37 (670 pg/mL vs 800 pg/mL, respectively). Lipopeptoid **21** was the strongest inducer of Groα among our amphiphiles, causing 996 ± 4 pg/mL ($p=0.003$) of Groα production at 50 μM (Figure 5.2). This peptoid is composed of a twenty carbon lipid tail and *N*Har*N*Har*N*Har sequence, and along with most of the lipopeptoids tested induced 6 ± 0.8 ng/mL ($p<0.05$) of IL-8 at 50 and 100 μM amphiphile concentrations. The

high level of Groα production at 50 μM did not extend from similar productions at lower concentrations, with peptoids **15–17** significantly weaker than amphiphiles **5–7** at 5 μM and 10 μM. Similar to the results with the lipopeptides, only lipopeptoids based on the *N*Lys*N*Lys*N*Lys sequence (**14–21**) were able to induce IL-8 or Groα production; *N*LysGly*N*Lys peptoids **12** and **13** were inactive.

Chemokine production by the lipopeptides and lipopeptoids was largely unaffected by disrupting the hydrophobic nature of the lipid tail with a terminal alcohol moiety. Little difference was observed between C16-LysLysLys (**5**) and C16OH-LysLysLys (**6**) at low concentrations, and amphiphile **6** led to the highest IL-8 production (12.5 ± 0.5 ng/ml, p=0.006) at high amphiphile concentration (50μM). This is in contrast to antibacterial activity, which has been found to be sharply reduced by the presence of a terminal alcohol function (27). As the antimicrobial activity of lipopeptides is mediated through non-specific membrane interactions (26), this discrepancy suggests that chemokine induction by our compounds is independent of membrane binding.

This is further supported by the lack of activity of amphiphiles **1–3** in contrast to **5–7**. At a concentration of 50 μM, C16-LysGlyLys (**1**) induced 0.2 ng/mL production of IL-8 above control values, while C16-LysLysLys (**5**) increased IL-8 production to 7.7 ± 0.6 ng/mL, p=0.02 (Figure 5.2), despite comparable antibacterial activities against both Gram-negative and Gram-positive bacteria (27). The significant loss in cytokine production observed between low concentrations of lipopeptides containing LysLysLys and HarHarHar sequences (compounds **5–7** and **9–11,** respectively) also suggests a sequence specific effect, though with the lipopeptoids this difference was not observed.

In contrast, cytotoxicity of the amphiphiles was independent of the peptidic sequence and correlated well with previously published antimicrobial activities and with lipid tail length

(Figure 5.2, Supplementary material) (27, 28). At high concentrations the amphiphiles appear able to disrupt the cellular membrane of macrophage-like cells, as cytotoxicity was evaluated through the release of the cytosol-localized protein lactate dehydrogenase (LDH). Our amphiphiles were broadly non-toxic at 5 μM and 10 μM, though the majority caused greater than 15% cytotoxicity at 100 μM; with amphiphiles **3**, **7**, **11** and **21** equally toxic at 50 μM.

Encouraged by the ability of our amphiphiles to induce chemokines Groα and IL-8, we examined the effect of the active amphiphiles on production of pro-inflammatory cytokines IL-1β and TNF-α. Binding of microbial lipopeptides Pam_3CSK_4 and MALP-2 to TLRs strongly induces the production of pro-inflammatory cytokines TNF-α and IL-1β, among others (35). Both of these bacterial lipopeptides have multiple lipid tails (three and two, respectively), but synthetic analogues with only a single lipid tail have recently been produced (36), suggesting that the activity of amphiphiles **1-21** may stem from binding to TLRs (37). Pro-inflammatory cytokines help combat infection, but inappropriate or amplified induction of these cytokines – especially TNF-α – leads to chronic inflammatory disorders such as rheumatoid arthritis, inflammatory bowel disease and psoriasis (38), reducing the utility of inflammatory compounds in infectious disease therapy.

In contrast to the previously published non-proteogenic immunomodulators (25), none of our compounds induced TNF-α production at any of the concentrations tested (Supplementary material), suggesting that the immunomodulatory activity of our compounds is not mediated by engagement of innate immune receptors such as TLRs. However, low concentrations of **5–7** (10 μM) were able to induce up to 25 pg/mL ($p<0.06$) of IL-1β (Figure 5.3). Moving from 10 μM to 50 μM of **7** increased the observed IL-1β concentration over forty-fold ($p=0.01$), suggesting a threshold peptide concentration was required for strong induction of IL-1β. It was previously demonstrated that the natural HDP LL-37, but not synthetic peptide IDR-1,

acts synergistically with IL-1β to induce the chemokine IL-8 (31). Induction of IL-1β may contribute in part to the high induction of IL-8 observed with our lipopeptides, as the spike in IL-1β production occurs over the same concentration as the increase in IL-8 production by amphiphiles **9–11** and **21.**

5.5 **Conclusion**

We have shown that ultrashort lipopeptides and lipopeptoids are able to induce selective cytokine production in human macrophages, despite little structural similarity to any known host defence peptide or CAMP. A lipid tail at least sixteen carbons long was required for activity, though the immunomodulatory effect of these compounds does not appear to be related to their effects on the bacterial membrane. Compounds with no appreciable antibacterial activity (MIC ≥ 128 μg/mL) were able to strongly induce the production of chemokines IL-8 and Groα at sub-cytotoxic concentrations, though the strongest inducer of Groα, C20-*N*Har*N*Har*N*Har (**21**), also has moderate antibacterial activity *in vitro* (MIC ≤ 16 μg/mL, Gram-positive strains) (28).

The LysLysLys series of peptides induced the greatest IL-8 production, even above that of LL-37. However, these compounds also caused a moderate amount of IL-1β production at the same concentration (10 μM, 25 pg/mL). Lipopeptoids were in general less active, though the peptoid C20-*N*Har*N*Har*N*Har was the strongest inducer of Groα, and a moderate inducer of IL-8. High concentrations of amphiphiles can result in IL-1β production, which may be synergistic in inducing the chemokine IL-8 (31, 39). None of the compounds induced TNF-α at any concentration tested, suggesting that cytokine production is not mediated by binding to TLR1:TLR2 or TLR6:TLR2 heterodimers (35). The exact mode of action for these amphiphiles is unknown, though at least two different cytokine expression profiles were observed. The

lipopeptoids C16OH-*N*Lys*N*Lys*N*Lys (**16**) and C16OH-*N*Har*N*Har*N*Har (**20**) were of particular interest, as they were moderate inducers of Groα and IL-8 but did not induce either IL-1β or TNF-α production. These compounds are naturally protease resistant, and may be appealing leads for further discovery of highly selective immunomodulation-based infectious disease therapeutics.

5.6 **Materials and Methods**

5.6.1 Chemical Synthesis

Lipopeptides and lipopeptoids were prepared according to previously established techniques (26-28). In brief, peptides were synthesized as C-terminal amides on Rink amide MBHA resin, using 9-fluorenylmethoxycarbonyl/t-butylcarbamate (Fmoc/Boc) chemistry. Amino acids were coupled to the resin with O-(Benzotriazol-1-yl)-N,N,N',N'-tetramethyluronium tetrafluoroborate (TBTU) activation in dimethylformamide (DMF), with the lysine R-groups protected via Boc. Lipid tails were also added with TBTU, and the completed peptides were cleaved from the resin with trifluoroacetic acid (TFA). Peptides were purified via passage through C18-functionalized silica at 3 PSI. Lipopeptoids were also prepared on Rink amide MBHA resin. Bromoacetic acid was added to the growing chain after activation with diisopropylcarbodiimide (DIC), and the alkyl bromine atom was then displaced by tert-butyl 4-aminobutylcarbamate in N-methyl-2-pyrrolidinone (NMP). Lipid tails were attached via activation with TBTU in DMF, and cleavage and subsequent purification were effected similar to the lipopeptides. Guanidinylation was the result of treatment of the lipopeptides and lipopeptoids with N,N-diBoc-N-triflylguanidine and subsequent deprotection with TFA (40). For further details on the chemical synthesis please see the Supporting Information.

5.6.2 Cytokine Measurements and Cytotoxicity

Human monocytic THP-1 (ATCC® TIB-202) cells were cultured in RPMI-1640 medium containing 2 mM L-glutamine, 1 mM sodium pyruvate, supplemented with 10% (v/v) FBS and maintained in a humidified incubator at 37°C and 5% CO_2 as previously described (31). The cells were differentiated into plastic adherent macrophage-like cells with phorbol 12-myristate 13-acetate (Sigma-Aldrich) and rested for an additional 24 before stimulations as previously described (31). Macrophage-like THP-1 cells were stimulated with the different compounds for 24 hr. TC supernatants were centrifuged at 1500 X g for 5-7 min to obtain cell-free samples and aliquots were stored at -20°C until further use. Cellular cytotoxicity was evaluated by monitoring the release of lactate dehydrogenase employing a colorimetric detection kit (Roche Diagnostics). Production of chemokines Groα and IL-8 were monitored in the TC supernatants by ELISA employing human DuoSet (R&D Systems Inc.) as per the manufacturer's instructions. Production of pro-inflammatory cytokines TNF-α and IL-1β were monitored in the TC supernatants using specific antibody pairs from eBioscience, Inc., as per the manufacturer's instructions. The concentration of the cytokines or chemokines in the TC supernatants was evaluated by establishing a standard curve with serial dilutions of the recombinant human cytokines or chemokines (31).

Statistical analysis: ELISA results were obtained from two biological replicates with two technical replicates each and statistical analyses were performed using Student paired t-test. Error bars in the graphs represents standard error of the mean, and a p-value of less than 0.05 was considered to be statistically significant.

5.7 **Acknowledgements**

This research was supported by the Natural Sciences and Engineering Research Council of Canada (NSERC) and the Canadian Foundation for Innovation (CFI).

5.8 **Tables**

Table 5.1. Cationic amphiphiles in this study.

	Lipopeptides[a]		Lipopeptoids[a]
1	C16-LysGlyLys-NH_2	12	C11-*N*LysGly*N*Lys-NH_2
2	C16OH-LysGlyLys-NH_2	13	C16-*N*LysGly*N*Lys-NH_2
3	C20-LysGlyLys-NH_2	14	C11-*N*Lys*N*Lys*N*Lys-NH_2
4	C11-LysLysLys-NH_2	15	C16-*N*Lys*N*Lys*N*Lys-NH_2
5	C16-LysLysLys-NH_2	16	C16OH-*N*Lys*N*Lys*N*Lys-NH_2
6	C16OH-LysLysLys-NH_2	17	C20-*N*Lys*N*Lys*N*Lys-NH_2
7	C20-LysLysLys-NH_2	18	C11-*N*Har*N*Har*N*Har-NH_2
8	C11-HarHarHar-NH_2	19	C16-*N*Har*N*Har*N*Har-NH_2
9	C16-HarHarHar-NH_2	20	C16OH-*N*Har*N*Har*N*Har-NH_2
10	C16OH-HarHarHar -NH_2	21	C20-*N*Har*N*Har*N*Har-NH_2
11	C20-HarHarHar-NH_2		LL-37[b]

[a] Trifluoroacetate salt; [b] LLGDFFRKSKEKIGKEFKRIVQRIKDFLRNLVPRTES-OH

5.9 **Supporting Information**

Characterization data for new compounds, detailed chemical experimental methods and other supporting information can be found in Chapter 12 of this thesis.

5.10 **References**

1. Tadesse DA, Zhao S, Tong E, Ayers S, Singh A, Bartholomew MJ, et al. Antimicrobial drug resistance in escherichia coli from humans and food animals, united states, 1950-2002. Emerg Infect Dis. 2012 May;18(5):741-9.

2. Hammerum AM, Heuer OE, Emborg HD, Bagger-Skjot L, Jensen VF, Rogues AM, et al. Danish integrated antimicrobial resistance monitoring and research program. Emerg Infect Dis. 2007 Nov;13(11):1632-9.

3. Payne DJ, Gwynn MN, Holmes DJ, Pompliano DL. Drugs for bad bugs: Confronting the challenges of antibacterial discovery. Nat Rev Drug Discov. 2007 Jan;6(1):29-40.

4. Yeung AT, Gellatly SL, Hancock RE. Multifunctional cationic host defence peptides and their clinical applications. Cell Mol Life Sci. 2011 Jul;68(13):2161-76.

5. Zasloff M. Magainins, a class of antimicrobial peptides from xenopus skin: Isolation, characterization of two active forms, and partial cDNA sequence of a precursor. Proc Natl Acad Sci U S A. 1987 Aug;84(15):5449-53.

6. Khandelia H, Ipsen JH, Mouritsen OG. The impact of peptides on lipid membranes. Biochim Biophys Acta. 2008 Jul-Aug;1778(7-8):1528-36.

7. Yang L, Gordon VD, Trinkle DR, Schmidt NW, Davis MA, DeVries C, et al. Mechanism of a prototypical synthetic membrane-active antimicrobial: Efficient hole-punching via interaction with negative intrinsic curvature lipids. Proc Natl Acad Sci U S A. 2008 Dec 30;105(52):20595-600.

8. Ge Y, MacDonald DL, Holroyd KJ, Thornsberry C, Wexler H, Zasloff M. In vitro antibacterial properties of pexiganan, an analog of magainin. Antimicrob Agents Chemother. 1999 Apr;43(4):782-8.

9. Brogden KA. Antimicrobial peptides: Pore formers or metabolic inhibitors in bacteria? Nat Rev Microbiol. 2005 Mar;3(3):238-50.

10. Srinivas N, Jetter P, Ueberbacher BJ, Werneburg M, Zerbe K, Steinmann J, et al. Peptidomimetic antibiotics target outer-membrane biogenesis in pseudomonas aeruginosa. Science. 2010 Feb 19;327(5968):1010-3.

11. Findlay B, Zhanel GG, Schweizer F. Cationic amphiphiles, a new generation of antimicrobials inspired by the natural antimicrobial peptide scaffold. Antimicrob Agents Chemother. 2010 Oct;54(10):4049-58.

12. Kaoud TS, Mitra S, Lee S, Taliaferro J, Cantrell M, Linse KD, et al. Development of JNK2-selective peptide inhibitors that inhibit breast cancer cell migration. ACS Chem Biol. 2011 Jun 17;6(6):658-66.

13. Czihal P, Knappe D, Fritsche S, Zahn M, Berthold N, Piantavigna S, et al. Api88 is a novel antibacterial designer peptide to treat systemic infections with multidrug-resistant gram-negative pathogens. ACS Chem Biol. 2012 Jul 20;7(7):1281-91.

14. Larrick JW, Hirata M, Balint RF, Lee J, Zhong J, Wright SC. Human CAP18: A novel antimicrobial lipopolysaccharide-binding protein. Infect Immun. 1995 Apr;63(4):1291-7.

15. Bowdish DM, Davidson DJ, Lau YE, Lee K, Scott MG, Hancock RE. Impact of LL-37 on anti-infective immunity. J Leukoc Biol. 2005 Apr;77(4):451-9.

16. Larrick JW, Hirata M, Zhong J, Wright SC. Anti-microbial activity of human CAP18 peptides. Immunotechnology. 1995 May;1(1):65-72.

17. Choi KY, Mookherjee N. Multiple immune-modulatory functions of cathelicidin host defense peptides. Front Immunol. 2012;3:149.

18. Heilborn JD, Nilsson MF, Kratz G, Weber G, Sorensen O, Borregaard N, et al. The cathelicidin anti-microbial peptide LL-37 is involved in re-epithelialization of human skin wounds and is lacking in chronic ulcer epithelium. J Invest Dermatol. 2003 Mar;120(3):379-89.

19. Scott MG, Dullaghan E, Mookherjee N, Glavas N, Waldbrook M, Thompson A, et al. An anti-infective peptide that selectively modulates the innate immune response. Nat Biotechnol. 2007 Apr;25(4):465-72.

20. Nijnik A, Madera L, Ma S, Waldbrook M, Elliott MR, Easton DM, et al. Synthetic cationic peptide IDR-1002 provides protection against bacterial infections through chemokine induction and enhanced leukocyte recruitment. J Immunol. 2010 Mar 1;184(5):2539-50.

21. Hancock RE, Nijnik A, Philpott DJ. Modulating immunity as a therapy for bacterial infections. Nat Rev Microbiol. 2012 Mar 16;10(4):243-54.

22. De Y, Chen Q, Schmidt AP, Anderson GM, Wang JM, Wooters J, et al. LL-37, the neutrophil granule- and epithelial cell-derived cathelicidin, utilizes formyl peptide receptor-like 1 (FPRL1) as a receptor to chemoattract human peripheral blood neutrophils, monocytes, and T cells. J Exp Med. 2000 Oct 2;192(7):1069-74.

23. Mookherjee N, Lippert DN, Hamill P, Falsafi R, Nijnik A, Kindrachuk J, et al. Intracellular receptor for human host defense peptide LL-37 in monocytes. J Immunol. 2009 Aug 15;183(4):2688-96.

24. Thwaite JE, Hibbs S, Titball RW, Atkins TP. Proteolytic degradation of human antimicrobial peptide LL-37 by bacillus anthracis may contribute to virulence. Antimicrob Agents Chemother. 2006 Jul;50(7):2316-22.

25. Thaker HD, Som A, Ayaz F, Lui D, Pan W, Scott RW, et al. Synthetic mimics of antimicrobial peptides with immunomodulatory responses. J Am Chem Soc. 2012 Jul 11;134(27):11088-91.

26. Makovitzki A, Baram J, Shai Y. Antimicrobial lipopolypeptides composed of palmitoyl di- and tricationic peptides: In vitro and in vivo activities, self-assembly to nanostructures, and a plausible mode of action. Biochemistry. 2008 Oct 7;47(40):10630-6.

27. Findlay B, Zhanel GG, Schweizer F. Investigating the antimicrobial peptide “Window of activity” using cationic lipopeptides with hydrocarbon and fluorinated tails. Int J Antimicrob Agents. 2012 In press.;40(1):36--42.

28. Findlay B, Szelemej P, Zhanel GG, Schweizer F. Guanidylation and tail effects in cationic antimicrobial lipopeptoids. PloS one. 2012;7(7):e41141.

29. Henzler-Wildman KA, Martinez GV, Brown MF, Ramamoorthy A. Perturbation of the hydrophobic core of lipid bilayers by the human antimicrobial peptide LL-37. Biochemistry. 2004 Jul 6;43(26):8459-69.

30. Simon RJ, Kania RS, Zuckermann RN, Huebner VD, Jewell DA, Banville S, et al. Peptoids: A modular approach to drug discovery. Proc Natl Acad Sci U S A. 1992 Oct 15;89(20):9367-71.

31. Mookherjee N, Brown KL, Bowdish DM, Doria S, Falsafi R, Hokamp K, et al. Modulation of the TLR-mediated inflammatory response by the endogenous human host defense peptide LL-37. J Immunol. 2006 Feb 15;176(4):2455-64.

32. Mookherjee N, Hamill P, Gardy J, Blimkie D, Falsafi R, Chikatamarla A, et al. Systems biology evaluation of immune responses induced by human host defence peptide LL-37 in mononuclear cells. Mol Biosyst. 2009 May;5(5):483-96.

33. Jin T, Xu X, Hereld D. Chemotaxis, chemokine receptors and human disease. Cytokine. 2008 Oct;44(1):1-8.

34. Turner-Brannen E, Choi KY, Arsenault R, El-Gabalawy H, Napper S, Mookherjee N. Inflammatory cytokines IL-32 and IL-17 have common signaling intermediates despite differential dependence on TNF-receptor 1. J Immunol. 2011 Jun 15;186(12):7127-35.

35. Kumar H, Kawai T, Akira S. Pathogen recognition by the innate immune system. Int Rev Immunol. 2011 Feb;30(1):16-34.

36. Agnihotri G, Crall BM, Lewis TC, Day TP, Balakrishna R, Warshakoon HJ, et al. Structure-activity relationships in toll-like receptor 2-agonists leading to simplified monoacyl lipopeptides. J Med Chem. 2011 Dec 8;54(23):8148-60.

37. Takeuchi O, Kawai T, Muhlradt PF, Morr M, Radolf JD, Zychlinsky A, et al. Discrimination of bacterial lipoproteins by toll-like receptor 6. Int Immunol. 2001 Jul;13(7):933-40.

38. Bradley JR. TNF-mediated inflammatory disease. J Pathol. 2008 Jan;214(2):149-60.

39. Yu J, Mookherjee N, Wee K, Bowdish DM, Pistolic J, Li Y, et al. Host defense peptide LL-37, in synergy with inflammatory mediator IL-1beta, augments immune responses by multiple pathways. J Immunol. 2007 Dec 1;179(11):7684-91.

40. Baker TJ, Luedtke NW, Tor Y, Goodman M. Synthesis and anti-HIV activity of guanidinoglycosides. J Org Chem. 2000 Dec 29;65(26):9054-8.

Chapter 6: Neomycin-Phenolic Conjugates: Polycationic Amphiphiles with Broad-spectrum Antibacterial Activity, Low Hemolytic Activity and Weak Serum Protein Binding

By Brandon Findlay, George G. Zhanel and Frank Schweizer. First published in Bioorganic Medicinal Chemistry Letters, 22, 2012, 1499-1503. Reproduced with permission.

6.1 Authorship Considerations

Brandon Findlay was responsible for designing, synthesizing and characterizing the aminoglycoside conjugates, on the advice of Frank Schweizer. The biological activity of the conjugates was then assessed by Nancy Laing under the supervision of George G. Zhanel (NL did not have a role in experimental design and declined authorship). The preliminary draft of the paper was written by Brandon Findlay, annotated by Frank Schweizer and George G. Zhanel, and then rendered into its final form by Brandon Findlay. Frank Schweizer was the corresponding author.

6.2 Abstract

Here we present a proof-of-concept study, combining two known antimicrobial agents into a hybrid structure in order to develop an emergent cationic detergent-like interaction with the bacterial membrane. Six amphiphilic conjugates were prepared by copper(I)-catalyzed 1,3-dipolar cycloaddition between a neomycin B-derived azide and three alkyne-modified phenolic disinfectants. Three conjugates displayed good activity against a variety of clinically relevant Gram-positive and Gram-negative bacteria, including MRSA, without the high level of hemolysis

or strong binding to serum proteins commonly observed with other cationic antimicrobial peptides and detergents.

6.3 **Main Text**

Over the years, many first-line antibiotics have been relegated to the back benches as an increased presence of drug-resistant bacteria rendered them ineffective. At the same time, a reduced focus on antibiotic research at the major pharmaceutical companies has drastically reduced the rate of drug discovery, leaving us more in need of new antimicrobial agents and scaffolds than ever (1, 2). The need for new scaffolds is especially great, as widespread resistance to most antibiotics appears shortly after the drugs are introduced into clinical use, with a gap of roughly twenty years for penicillins and less than nine years for fluoroquinolones (five years for ciprofloxacin) (3, 4). This resistance may affect many drugs with similar scaffolds, limiting the effectiveness of new drugs before they even enter the clinic. Resistance seems to arise from small numbers of bacteria already present in the population at large. Attempts to determine the age of common resistance mechanisms has found that, like the secondary metabolites many current antibiotics are based upon, the genes which code for antibiotic resistance are ancient (5). The potential for widespread drug resistance is thus latent in every bacterial population, and limiting its emergence will require improved education in the use of antibiotics and the creation of antibiotic classes that have been designed with antimicrobial resistance in mind.

Most commercial antibiotics are molecular inhibitors, binding to enzymes, cellular receptors or nucleic acids within the cell and inhibiting their function. Bacterial resistance arises from mechanisms which disrupt the drug-target complex, either through modification of the

binding site (via DNA mutation or chemical alteration), the drug (via acetylases, phosphates and others) or by simply preventing the drug from entering the cell and encountering its target (efflux pumps) (5, 6). Drug efflux is of particular concern, as the poor selectivity of efflux pumps can easily lead to broad antibiotic resistance, with a single pump effective against whole classes of antibiotics (7). Bacteria which endogenously express a large number of drug efflux pumps, such as *Pseudomonas aeruginosa*, are able to withstand most common antimicrobial agents and are often the cause of multi-drug resistant (MDR) infections.

As a means of circumventing these resistance mechanisms, work in our lab and others has explored the potential for (poly)cationic amphiphiles (CAs) such as antimicrobial peptides, lipids and surfactants to act as antimicrobial agents (8-16). Found throughout nature and long used as antimicrobial detergents, cationic amphiphiles do not act on any single target within the cell, instead they disrupt DNA replication, protein synthesis and bacterial membrane integrity (12). Widely varying in structure and size, all CAs are based on two common features: a hydrophobic face that interacts with the lipid bilayer and a polar, cationic face that is drawn via electrostatic interactions to anionic moieties such as some lipid head groups and nucleic acids. Little *in vitro* resistance to these amphiphiles has been observed, due to their multiple modes of action and ability to form pores in the bacterial membrane, but their clinical use has been severely limited due to issues with selectivity, protease susceptibility and toxicity (17). The therapeutic ratio of these amphiphiles has been improved, reducing their ability to lyse red blood cells and increasing selectivity towards Gram-positive and Gram-negative bacteria (18). Nevertheless, the presence of non-specific binding to human serum proteins remains a major limitation of these agents, resulting in loss of antibacterial activity *in vivo* (19). Starting from the structure of an amphiphilic disinfectant, the quaternary ammonium compound benzethonium chloride, **1** (Figure 6.1), we devised alternatives to the classical CAs, in order to create agents

with similar characteristics but devoid of their limitations (20). This work has cumulated in neomycin-phenolic conjugates presented here (Figure 6.2).

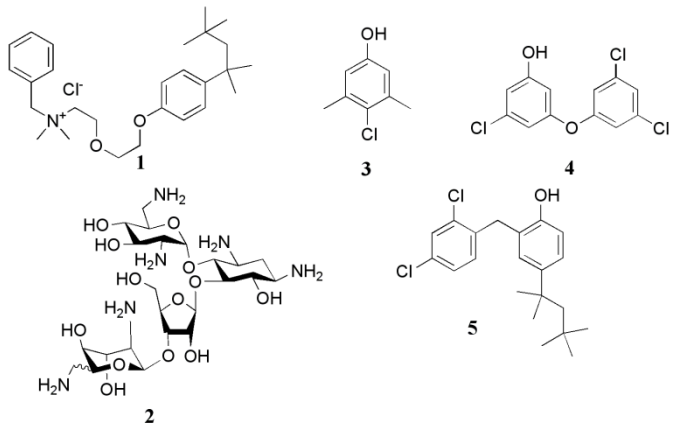

Figure 6.1. Benzethonium chloride, 1, served as the initial template for the hybrids presented in this paper. Neomycin B, 2, was used for its cationic charges, RNA-binding properties and self-promoted uptake, whereas the phenolics chloroxylenol, 3, triclosan, 4, and clofoctol, 5, are expected to induce hydrophobic membrane interactions in the hybrids.

Our conjugates use two known antimicrobial agents to create the cationic and hydrophobic faces required for interaction with bacterial membranes. The hybrid molecules are intended to display three distinct modes of action; one from each participating agent and one from an emergent CA-like behaviour from the superstructure itself. This triple mode-of-action should lead to broad spectrum activity and resilience against bacterial resistance, as resistance to one agent will not alter susceptibility to the other half of the conjugate or to the CA-like mode of action. In optimal cases this will allow the conjugates to retain activity against even MDR bacteria. This strategy has been attempted previously, but has been hampered by the large size of the conjugates, which reduces diffusion across the cellular membrane (21, 22). To maintain permeability we chose phenolic disinfectants as the hydrophobic segment, as phenolics are

known to derive at least part of their activity from moving small cations across the bacterial membrane, which requires rapid diffusion in and out of the cell (20). When combined with the polycationic aminoglycoside neomycin, which is known to self-promote its own uptake into bacterial cells by disrupting polysaccharide-cation interactions (23), we expected our conjugates to display good diffusion kinetics, despite their larger size and high number of hydrogen bond donors and acceptors. Moreover, the RNA-binding motif of neomycin may induce intracellular modes of antibacterial action in the conjugates (24).

Work with other CAs has found that altering the size and shape of the hydrophobic domain can greatly influence antimicrobial activity (12, 25), and so we linked three distinct phenolic disinfectants, **3 – 5**, to neomycin B to create the hybrid compounds **6 – 11** (Figure 6.2). While triclosan, **4**, has been found to inhibit fatty acid synthesis by blocking the key enzyme FabI (26), the targets of chloroxylenol, **3**, and clofoctol, **5**, are unknown. It appears that as a class the phenols, like CAs, have a number of cellular interactions but derive much of their activity from interactions with the bacterial membrane (20). Easily ionized, the phenols seem to ferry small cations across the bacterial membrane, dispersing the membrane polarization. While we expect much of this activity to be inhibited by the ether linkage used to connect these phenols to neomycin B, an analysis of the structure of **1** suggests that interactions with the cellular membrane will be maintained, allowing the hybrids to pass through the membrane and maintain a high intracellular concentration.

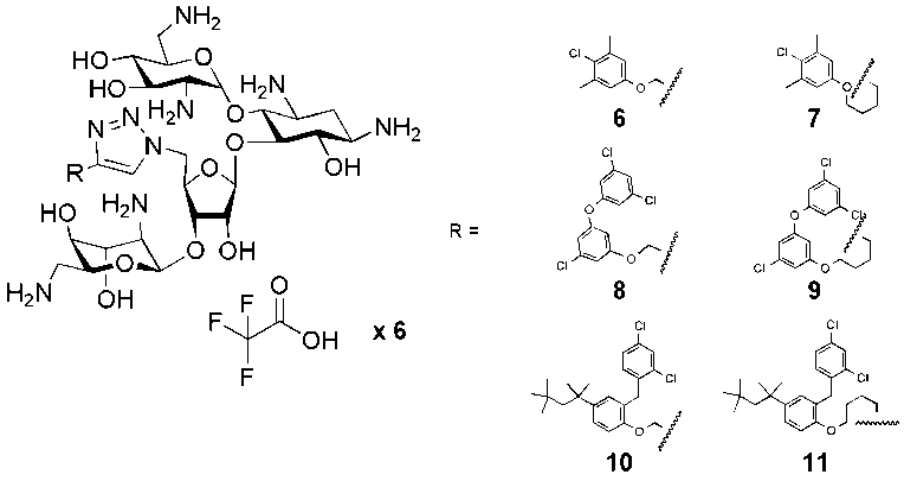

Figure 6.2. Structures of the neomycin-phenol conjugates produced in this study. Conjugates 6 and 7 are based upon chloroxylenol, conjugates 8 and 9 on triclosan and 10 and 11 on clofoctol. All six conjugates use neomycin B to provide the polycationic charge.

To produce the conjugates the two antimicrobials were linked via a copper (I)-catalyzed 1, 3 dipolar cycloaddition reaction between the phenol-modified alkynes (Scheme 1) (27, 28), and the neomycin-based azide **20** (Scheme 2). The length of the phenolic alkyne linker was varied, and attached to the phenols by displacement of the corresponding alkyne sulfonate esters (29). Azide-functionalized neomycin B was prepared as a Boc-protected derivative using previously established methodology (10, 14, 30). The single primary hydroxyl group of neomycin was selected as the point of attachment as previous studies have shown that modifications at this position allow the aminoglycoside to retain antibacterial activity and RNA-binding (14, 31).

Briefly, neomycin sulfate was treated with di-tert-butyl-dicarbonate in a mixture of methanol, water and triethylamine to protect the amino groups. Flash chromatography of crude **18** was then used to separate Boc-protected neomycin B from neomycin C, and the

primary hydroxyl moiety was activated using a large excess of triisopropylsulfonyl chloride (TIPS-Cl) to afford sulfonate ester **19.** Addition of sodium azide in a mixture of DMF and water at 70 °C cleanly produced the required azide **20**. The two halves of the conjugate were then linked through copper (I) catalyzed 1,3-dipolar cycloaddition. Deblocking with trifluoroacetic acid gave the neomycin-phenol conjugates **6 – 11**.

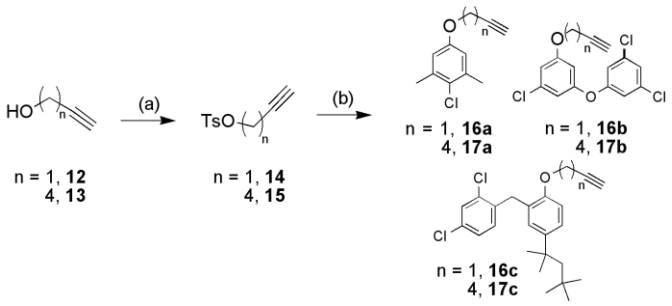

Scheme 1. Synthesis of the alkyne linkers. Conditions: (a) TsCl, KOH, Et_2O (41 – 64%). (b) **3 – 5**, K_2CO_3, DMF (51 – 96%).

Antibacterial activity was assessed using macrobroth dilution assays according to standard CLSI methodology (32). Compound activity was determined against a combination of reference strains of Gram-positive and Gram-negative bacteria and clinically relevant pathogens from the national surveillance CAN-ICU and CANWARD studies (32, 33). The inclusion of clinically relevant bacteria is especially important in light of the rapid increase in antimicrobial resistance with varied resistance mechanisms. Bacteria from current hospital environments are far more likely to be resistant to a variety of antibiotics and disinfectants with different chemical structures and mechanism(s) of action, and testing with only laboratory strains can produce misleadingly effective antimicrobial activities. Full results are summarized in Table 6.1 and Table 6.2 (see section 6.4).

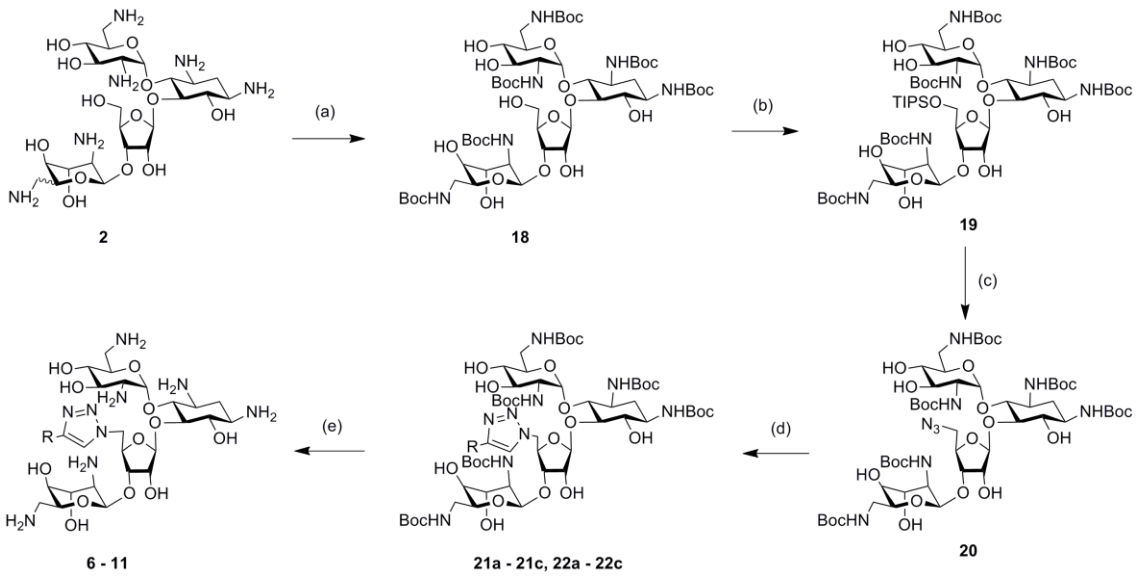

Scheme 2. Synthesis of conjugates **6 - 11**. Conditions: (a) Boc_2O (10 eq), TEA/MeOH/H_2O (61%). (b) TIPS-Cl (31 eq), pyridine (41%). (c) NaN_3 (10 eq), DMF/H_2O (94%). (d) **16a -16c**, **17a – 17c** (1.2 eq), CuI (0.2 eq), DIPEA (3 eq), ACN (50 – 88%). (e) TFA/H_2O (80 – 91%).

The most active hybrids were compounds **9** and **10**, one of which had triclosan as the phenolic with the longer of our two linkers, and the other which had clofoctol and a short linker. Both molecules displayed similar or improved activity against the Gram-positive bacteria in our study, with an improved activity of 64µg/mL observed against the normally highly neomycin B resistant *P. aeruginosa* strain CAN-ICU 62308. Unlike many other CAs, compound **9** was not appreciably hemolytic at near MIC concentrations. The optimal spacing between cationic and hydrophobic domains appears to differ between hydrophobic domains and must be determined on a case-by-case basis.

Inspecting the antimicrobial results as a whole revealed a number of trends. The chloroxylenol conjugates **6** and **7** were broadly ineffective, displaying reduced activities compared to conventional neomycin sulphate. The triclosan conjugate with a short linker, **8**,

was similarly inactive, though the longer triclosan conjugate **9** was more active than neomycin sulphate against MRSA and two *P. aeruginosa* strains. Both conjugates of clofoctol were active, but both displayed increased hemolytic activity, suggesting that the hydrophobic tail of clofoctol mediates non-specific interactions, similar to our standard CA, **1**. The intermediate hemolytic activity of **10** and **11** is likely due to the influence of the cationic aminoglycoside face, which may preferentially target the hybrids to negatively charged bacterial membrane lipids, reducing interactions with zwitterionic eukaryotic cells. In general, it appears that the conjugates are less active against neomycin susceptible bacteria such as MRSE and *Klebsiella pneumoniae*, but more active than neomycin against drug resistant strains such as MRSA and *P. aeruginosa*.

To test the influence of non-specific interactions on conjugate activity antimicrobial testing was repeated in the presence of 4% bovine serum albumin (BSA). Many cationic amphiphiles show greatly reduced activity in the presence of BSA due to protein binding (19), but with the exception of the results for compounds **9** - **11** against *P. aeruginosa*, we observed little difference in activity. Our cationic amphiphile standard, **1**, in contrast had an average 8-fold reduction in efficacy, with the median Gram-positive MIC rising from 2μg/mL to 16μg/mL and the median Gram-negative MIC moving from 32μg/mL to 256μg/mL. This reduction was expected, given the importance of hydrophobicity on nonspecific membrane interactions. As they are not greatly inhibited by BSA, we infer that much of the antimicrobial effect in the conjugates is from the action of either neomycin B or the various phenolics and not directly through disruption of the bacterial membrane. Interestingly, the shorter neomycin-triclosan conjugate **9** retains potent activity in the presence of BSA against two *E. coli* strains (MIC $\leq$ 16) while benzethonium chloride is only weakly active (MIC = 256) under these conditions.

Further characterization of the conjugates' mode of action can be determined by examining the activities of triclosan. Triclosan is known to possess several modes of action, with

much of its activity stemming from inhibition of FabI, a key component of fatty acid synthesis (26). Crystal structures of triclosan bound to FabI suggest that hydrogen bonding between the phenol and enzyme is important to enzyme binding (34). While our unaltered triclosan standard had an MIC against *E. coli* ATCC 25922 of ≤0.25μg/mL, both triclosan conjugates **8** and **9** are less active, suggesting that using the phenol of triclosan to form an ether linkage has removed some of the site specific antimicrobial activity. When this information is combined with the BSA results, it seems likely that for conjugates **8** and **9** improvements in the antibacterial activity over neomycin B must therefore relate to either increased binding to cellular targets, a new resilience to enzymatic inactivation, or an increased concentration of the conjugate in the cell.

Of course, each of these options may come into play. Compounds **9 - 11** remain relatively active against MRSA, while our aminoglycoside control, neomycin sulfate has its activity reduced over 250-fold from *S. aureus* to MRSA. The bacterial strain's resistance is likely due to the presence of neomycin-modifying enzymes that modify the drug, blocking effective binding to RNA or decreasing the drug's intracellular concentration (5). The presence of a large hydrophobic moiety in compounds **9 – 11** likely prevents successful binding to the inactivating enzymes, leading to sustained activity. When we examine the conjugates created with the smaller chloroxylenol moiety we see that they show the expected decrease in activity against MRSA, suggesting the single aromatic ring lacks the bulk required to prevent enzyme interactions.

The increased activity of conjugates **9 - 11** against the two strains of *P. aeruginosa* is somewhat more difficult to explain. All three compounds were roughly four-fold more active than neomycin sulphate, but while *P. aeruginosa* does possess inactivating enzymes, most of its drug resistance stems from the expression of efflux pumps (5, 7). A triclosan-specific interaction is unlikely, due to the presence of a non-susceptible analogue of FabI, Fab V (26), and the

inferences made by examining the activity of conjugates **8** and **9** against *E. coli* (*vide supra)*. One possible explanation is that attaching the hydrophobic phenolics to neomycin has increased the drug's diffusion into the cell, partially overcoming the effect of the efflux pumps. This hypothesis fits well with the reduced efficacy of conjugates **9 - 11** against *P. aeruginosa* in the presence of BSA, as we would expect the hydrophobic protein to reduce the concentration of free conjugate outside of the cell, slowing diffusion and aiding efflux. The effect of efflux pumps and permeability could be further characterized using strains of *P. aeruginosa* with reduced efflux, but the relatively low activity of the conjugates may complicate matters.

In conclusion, we have produced six novel aminoglycoside-phenolic conjugates, in order to test the viability of combining known hydrophobic drugs and aminoglycosides to create compounds with an emergent activity similar to that of the cationic antibacterial peptides and cationic detergents. In general the conjugates displayed improved activity against neomycin sulfate resistant bacteria and slightly reduced activity against neomycin susceptible strains. For several conjugates activity against MRSA was found comparable to that against *S. aureus*, while activity against *P. aeruginosa* was moderately improved. Unlike previous work with analogues of CAs like cationic detergents and amphiphilic aminoglycosides (8, 11, 11, 12), our most active compounds were not appreciably hemolytic, and activity was retained in the presence of BSA. Work is currently in progress to optimize the antimicrobial activity of non-hemolytic neomycin phenol conjugates and to explore the likelihood of resistance development.

6.4 **Acknowledgements**

We are indebted to Dr. E. Lattová for her assistance with high resolution mass spectrometry, to N. Liang for aid in hemolytic and microbial testing and to L.K. Freeman for

helpful discussions. This research was supported by the Canadian Institutes of Health Research (CIHR), Manitoba Health Research Council (MHRC), Natural Sciences and Engineering Research Council of Canada (NSERC) and the Canadian Foundation for Innovation (CFI)

6.5 **Tables**

Table 6.1. Antimicrobial activity[a] and hemolysis of the conjugates and drug standards.

Organism	**Compound**										
	1	**2**[r]	**3**	**4**	**5**[s]	**6**	**7**	**8**	**9**	**10**	**11**
S.aureus[b]	2	1	32	0.5	-	16	16	32	4	8	16
MRSA[c]	2	256	64	≤0.25	-	256	128	128	8	8	16
MSSE[d]	2	0.5	32	1	-	8	8	16	4	4	8
MRSE[e]	8	≤0.25	16	≤0.25	-	8	8	16	2	1	8
E. faecalis[f]	4	16	256	8	-	64	128	64	16	8	64
E. faecium[g]	4	4	256	16	-	128	16	16	8	8	8
S. pneumoniae[h]	2	32	128	128	-	64	64	256	64	64	64
E.coli[i]	32	4	256	≤0.25	-	16	32	64	16	16	64
E.coli[j]	32	1	256	1	-	16	16	64	16	64	64
E.coli[k]	32	8	256	1	-	128	128	128	64	64	128
P.aeruginosa[l]	64	512	512	>512	-	512	512	512	128	128	128
P.aeruginosa[m]	64	256	256	64	-	256	256	256	64	64	64

S. maltophilia[n]	32	>512	128	512	-	>512	>512	>512	>512	512	512
A. baumannii[o]	32	64	128	8	-	>512	512	>512	128	64	256
K. pneumoniae[p]	32	0.25	256	1	-	8	4	32	4	64	32
Hemolysis[q]	77.3	0.69	-	-		0.75	0.75	0.99	1.62	27.5	22.5

[a] MIC_{90}, reported in μg/mL.

[b] ATCC 29213.

[c] ATCC 33592.

[d] 81388 CANWARD 2008.

[e] CAN-ICU 61589.

[f] ATCC 29212.

[g] ATCC 27270.

[h] ATCC 49619.

[i] ATCC 25922.

[j] CAN-ICU 61714.

[k] CAN-ICU 63074.

[l] ATCC 27853.

[m] CAN-ICU 62308.

[n] CAN-ICU 62584.

[o] CAN-ICU 63169.

[p] ATCC 13883.

[q] Percent hemolysis at 100μg/mL of compound.

[r] Neomycin trisulfate hydrate.

[s] Compound 5 was poorly soluble in water and its activity could not be accurately assessed.

Table 6.2. Antimicrobial activity[a] of conjugates and drug standards in the presence of bovine serum albumin (BSA).

Organism	**Compound**										
	1	**2**[q]	**3**	**4**	**5**[r]	**6**	**7**	**8**	**9**	**10**	**11**
S.aureus[b]	16	0.5	512	0.5	-	32	32	64	16	8	16
MRSA[c]	32	128	512	1	-	512	256	256	32	16	32
MSSE[d]	128	0.5	512	1	-	8	8	16	4	2	4
MRSE[e]	128	≤0.25	512	1	-	8	8	16	2	4	4
E. faecalis[f]	32	16	>512	512	-	128	128	128	32	16	64
E. faecium[g]	32	4	>512	512	-	64	32	64	32	8	16
S.pneumoniae[h]	16	8	>512	256	-	128	256	512	128	128	64
E.coli[i]	256	0.25	>512	16	-	32	32	64	16	64	64
E.coli[j]	256	1	>512	16	-	16	16	64	8	128	128
E.coli[k]	256	16	>512	64	-	128	128	256	128	256	256
P.aeruginosa[l]	512	256	>512	>512	-	512	>512	512	512	512	512
P.aeruginosa[m]	512	256	>512	>512	-	256	256	256	256	128	256
S. maltophilia[n]	256	>512	>512	>512	-	>512	>512	>512	>512	>512	>512

***A. baumannii*[o]**	256	32	>512	128	-	>512	512	>512	256	256	>512
***K.pneumoniae*[p]**	256	≤0.25	>512	32	-	4	4	32	2	64	32

[a] MIC_{90}, reported in µg/mL.

[b] ATCC 29213.

[c] ATCC 33592.

[d] 81388 CANWARD 2008.

[e] CAN-ICU 61589.

[f] ATCC 29212.

[g] ATCC 27270.

[h] ATCC 49619.

[i] ATCC 25922.

[j] CAN-ICU 61714.

[k] CAN-ICU 63074.

[l] ATCC 27853.

[m] CAN-ICU 62308.

[n] CAN-ICU 62584.

[o] CAN-ICU 63169.

[p] ATCC 13883.

[q] Neomycin trisulfate hydrate.

[r] Compound 5 was poorly soluble in water and its activity could not be accurately assessed.

6.6 **Supporting Information**

Characterization data for new compounds, detailed experimental methods and other supporting information can be found in Chapter 13 of this thesis.

6.7 **References**

1. Arias CA, Murray BE. Antibiotic-resistant bugs in the 21st century--a clinical super-challenge. N Engl J Med. 2009 Jan 29;360(5):439-43.

2. Payne DJ, Gwynn MN, Holmes DJ, Pompliano DL. Drugs for bad bugs: Confronting the challenges of antibacterial discovery. Nat Rev Drug Discov. 2007 Jan;6(1):29-40.

3. Vatopoulos AC, Kalapothaki V, Legakis NJ. Bacterial resistance to ciprofloxacin in greece: Results from the national electronic surveillance system. greek network for the surveillance of antimicrobial resistance. Emerg Infect Dis. 1999 May-Jun;5(3):471-6.

4. Lowy FD. Antimicrobial resistance: The example of staphylococcus aureus. J Clin Invest. 2003 May;111(9):1265-73.

5. Wright GD. The antibiotic resistome: The nexus of chemical and genetic diversity. Nat Rev Microbiol. 2007 Mar;5(3):175-86.

6. Mulvey MR, Simor AE. Antimicrobial resistance in hospitals: How concerned should we be? CMAJ. 2009 Feb 17;180(4):408-15.

7. Li XZ, Nikaido H. Efflux-mediated drug resistance in bacteria. Drugs. 2004;64(2):159-204.

8. Bera S, Zhanel GG, Schweizer F. Antibacterial activity of guanidinylated neomycin B- and kanamycin A-derived amphiphilic lipid conjugates. J Antimicrob Chemother. 2010 Mar 23(6):1224-7.

9. Bera S, Zhanel GG, Schweizer F. Antibacterial activities of aminoglycoside antibiotics-derived cationic amphiphiles. polyol-modified neomycin B-, kanamycin A-, amikacin-, and neamine-based amphiphiles with potent broad spectrum antibacterial activity. J Med Chem. 2010 Apr 7;53(9):3626-31.

10. Bera S, Zhanel GG, Schweizer F. Evaluation of amphiphilic aminoglycoside-peptide triazole conjugates as antibacterial agents. Bioorg Med Chem Lett. 2010 May 15;20(10):3031-5.

11. Bera S, Zhanel GG, Schweizer F. Design, synthesis, and antibacterial activities of neomycin-lipid conjugates: Polycationic lipids with potent gram-positive activity. J Med Chem. 2008 Oct 9;51(19):6160-4.

12. Findlay B, Zhanel GG, Schweizer F. Cationic amphiphiles, a new generation of antimicrobials inspired by the natural antimicrobial peptide scaffold. Antimicrob Agents Chemother. 2010 Oct;54(10):4049-58.

13. Hanessian S, Pachamuthu K, Szychowski J, Giguere A, Swayze EE, Migawa MT, et al. Structure-based design, synthesis and A-site rRNA co-crystal complexes of novel amphiphilic aminoglycoside antibiotics with new binding modes: A synergistic hydrophobic effect against resistant bacteria. Bioorg Med Chem Lett. 2010 Dec 1;20(23):7097-101.

14. Zhang J, Chiang FI, Wu L, Czyryca PG, Li D, Chang CW. Surprising alteration of antibacterial activity of 5"-modified neomycin against resistant bacteria. J Med Chem. 2008 Dec 11;51(23):7563-73.

15. Ouberai M, El Garch F, Bussiere A, Riou M, Alsteens D, Lins L, et al. The pseudomonas aeruginosa membranes: A target for a new amphiphilic aminoglycoside derivative? Biochim Biophys Acta. 2011 Jun;1808(6):1716-27.

16. Baussanne I, Bussiere A, Halder S, Ganem-Elbaz C, Ouberai M, Riou M, et al. Synthesis and antimicrobial evaluation of amphiphilic neamine derivatives. J Med Chem. 2010 Jan 14;53(1):119-27.

17. Marr AK, Gooderham WJ, Hancock RE. Antibacterial peptides for therapeutic use: Obstacles and realistic outlook. Curr Opin Pharmacol. 2006 Oct;6(5):468-72.

18. Rotem S, Mor A. Antimicrobial peptide mimics for improved therapeutic properties. Biochim Biophys Acta. 2008 Nov 5;1788(8):1582-92.

19. Svenson J, Brandsdal BO, Stensen W, Svendsen JS. Albumin binding of short cationic antimicrobial micropeptides and its influence on the in vitro bactericidal effect. J Med Chem. 2007 Jul 12;50(14):3334-9.

20. McDonnell G, Russell AD. Antiseptics and disinfectants: Activity, action, and resistance. Clin Microbiol Rev. 1999 Jan;12(1):147-79.

21. Pokrovskaya V, Belakhov V, Hainrichson M, Yaron S, Baasov T. Design, synthesis, and evaluation of novel fluoroquinolone-aminoglycoside hybrid antibiotics. J Med Chem. 2009 Apr 23;52(8):2243-54.

22. Waring MJ. Defining optimum lipophilicity and molecular weight ranges for drug candidates-molecular weight dependent lower logD limits based on permeability. Bioorg Med Chem Lett. 2009 May 15;19(10):2844-51.

23. Hancock RE, Bellido F. Antibiotic uptake: Unusual results for unusual molecules. J Antimicrob Chemother. 1992 Mar;29(3):235-9.

24. Schroeder R, Waldsich C, Wank H. Modulation of RNA function by aminoglycoside antibiotics. EMBO J. 2000 Jan 4;19(1):1-9.

25. Chen Y, Guarnieri MT, Vasil AI, Vasil ML, Mant CT, Hodges RS. Role of peptide hydrophobicity in the mechanism of action of alpha-helical antimicrobial peptides. Antimicrob Agents Chemother. 2007 Apr;51(4):1398-406.

26. Zhu L, Lin J, Ma J, Cronan JE, Wang H. Triclosan resistance of pseudomonas aeruginosa PAO1 is due to FabV, a triclosan-resistant enoyl-acyl carrier protein reductase. Antimicrob Agents Chemother. 2010 Feb;54(2):689-98.

27. Meldal M, Tornoe CW. Cu-catalyzed azide-alkyne cycloaddition. Chem Rev. 2008 Aug;108(8):2952-3015.

28. Kolb HC, Finn MG, Sharpless KB. Click chemistry: Diverse chemical function from a few good reactions. Angew Chem Int Ed Engl. 2001 Jun 1;40(11):2004-21.

29. Dickschat JS, Reichenbach H, Wagner-Döbler I, Schulz S. Novel pyrazines from the myxobacterium chondromyces crocatus and marine bacteria. Eur J Org Chem. 2005;2005(19):4141-53.

30. Boer J, Blount KF, Luedtke NW, Elson-Schwab L, Tor Y. RNA-selective modification by a platinum(II) complex conjugated to amino- and guanidinoglycosides. Angew Chem Int Ed Engl. 2005 Jan 28;44(6):927-32.

31. Hanessian S, Masse R, Capmeau ML. Aminoglycoside antibiotics: Synthesis of 5''-amino-5''-deoxyneomycin and 5''-amino-5''-deoxyparomomycin. J Antibiot (Tokyo). 1977 Oct;30(10):893-6.

32. Zhanel GG, DeCorby M, Laing N, Weshnoweski B, Vashisht R, Tailor F, et al. Antimicrobial-resistant pathogens in intensive care units in canada: Results of the canadian national intensive care unit (CAN-ICU) study, 2005-2006. Antimicrob Agents Chemother. 2008 Apr;52(4):1430-7.

33. Zhanel GG, Adam HJ, Low DE, Blondeau J, Decorby M, Karlowsky JA, et al. Antimicrobial susceptibility of 15,644 pathogens from canadian hospitals: Results of the CANWARD 2007-2009 study. Diagn Microbiol Infect Dis. 2011 Mar;69(3):291-306.

34. Stewart MJ, Parikh S, Xiao G, Tonge PJ, Kisker C. Structural basis and mechanism of enoyl reductase inhibition by triclosan. J Mol Biol. 1999 Jul 23;290(4):859-65.

Chapter 7: Tobramycin-Derived Amphiphilic Aminoglycoside-Phenolic Conjugates

By Brandon Findlay and Frank Schweizer. Unpublished research.

7.1 Authorship Considerations

Brandon Findlay was responsible for designing, synthesizing and characterizing the conjugates, on the advice of Frank Schweizer. The following manuscript was prepared by Brandon Findlay, on the advice of Frank Schweizer.

7.2 Introduction

Antimicrobial peptides have been investigated for their potential to disrupt the bacterial membrane, as this mode of action has proven difficult for bacteria to develop effective resistance to (1-4). While this approach has had some success, the use of peptidic cationic amphiphiles as antimicrobial agents is complicated by their susceptibility to proteases (2), their lack of activity in the presence of hydrophobic proteins (5), and their significant toxicity. Amphiphiles with reduced hydrophobicity are less toxic, and have been found to exhibit cellular and subcellular localization, preferentially accumulating across negatively charged membranes such as mitochondria and bacterial cells (6, 7). This localization occurs with hydrophobicity well below that required for membrane disruption (8), and as a result these agents are significantly less toxic that other AMP-mimetics.

In a prior report we designed hybrid antibiotics that were inherently amphiphilic (9), with the intent of creating compounds with two distinct modes of action as well as emergent

membrane interacting behaviour. The aminoglycoside neomycin provided the positive charge, and was added to a number of hydrophobic phenolic disinfectants via the Huisgen cycloaddition. The conjugates were found to exhibit improved activity against MRSA and several strains of the efflux-expressing bacterium *Pseudomonas aeruginosa*, but the activity of the phenolic disinfectants was unfortunately lost when the phenol moiety was used to create an alkynyl linker. To circumvent this hurdle we have prepared a number of tobramycin-bisphenol hybrids, taking advantage of the greater antimicrobial activity of tobramycin and the presence of two independent phenolic moieties in our hydrophobic domains.

7.3 **Results and Discussion**

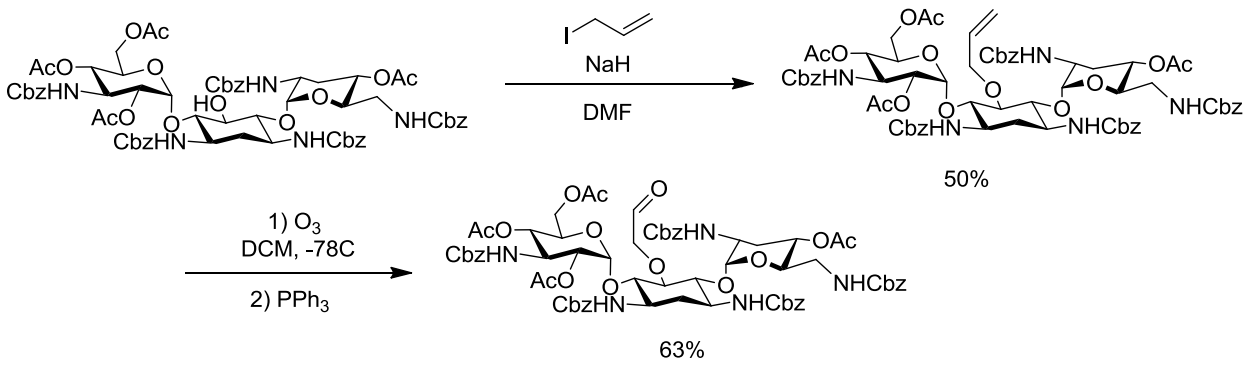

Scheme 1. Previously reported selective modification of the 5-OH position of tobramycin (10).

Like neomycin, tobramycin has a single primary alcohol, which can be modified without prior protection of the secondary alcohols. Unfortunately, alteration of this site was found to significantly reduce tobramycin activity, and so we chose to alter the 5-OH position instead. Both previously published analogue development and a crystal structure of tobramycin bound

to the ribosomal A-site suggested that the 5-OH was not required for antimicrobial activity (10, 11). Unfortunately, in the past alkylation has required the use of sodium hydride and has proven low yielding (Scheme 1) (10), even with the highly reactive electrophile allyl iodide. The resulting alkene must then be cleaved via ozonolysis, requiring equipment that was not available at our institution.

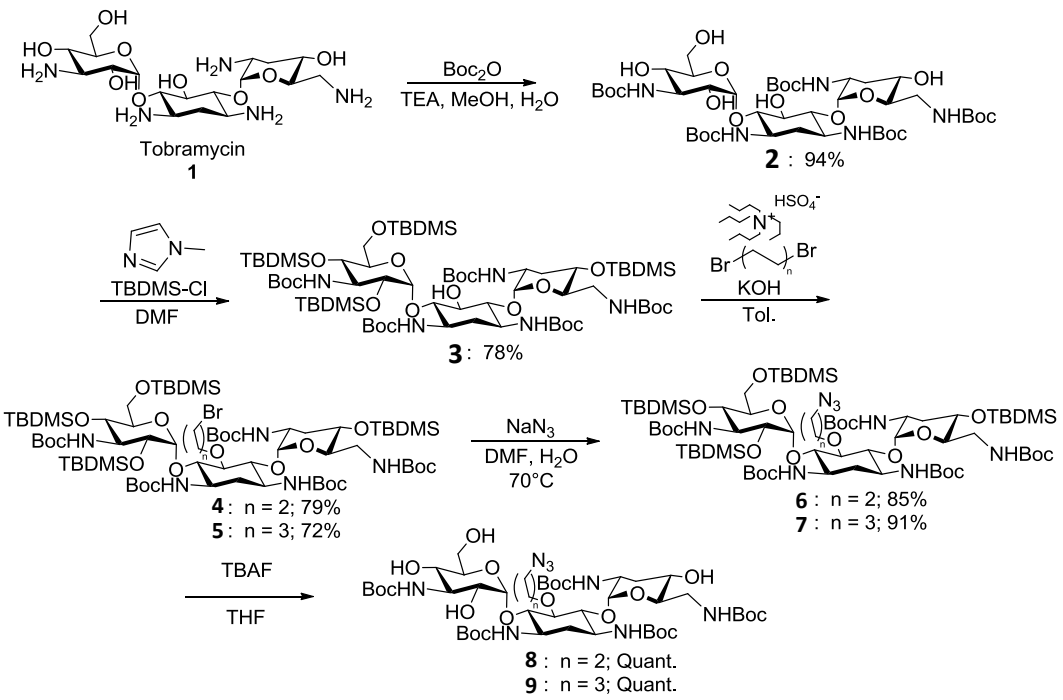

Scheme 2. Preparation of the protected tobramycin azides, **8** and **9**.

To circumvent these hurdles we adopted a different protecting group and alkylation strategy (Scheme 2). For improved solubility the amines of tobramycin were protected with t-butyl carbamates under aqueous conditions (12). The four hydroxyl groups which were not our target were then protected with TBDMS groups to give **3**, with the non-nucleophilic base n-

methylimidazole giving superior yields to the more standard imidazole (13). Alkylation of 5-OH was performed in toluene with the aid of a phase transfer atalyst and potassium iodide. These conditions were derived from a patent procedure for the alkylation of 4-(6-bromohexyloxy)-butylbenzene (14), and similar conditions were independently reported by the Décout group a few months later (15). Under these conditions the yield of the alkylation procedure was improved to approximately 75%, even though the amines were now protected as more labile t-butyl carbamates and the highly active allyl iodide was replaced with 1,4-dibromobutane or 1,6-dibromohexane (compounds, **4** and **5**, respectively). Nucleophilic substitution of the second bromine was effected with sodium azide in a mixture of DMF and water at 70 °C gave **6** and **7** in good yields (16), and the TBDMS groups were then removed via treatment with TBAF in THF to furnish **8** and **9** quantitatively (13).

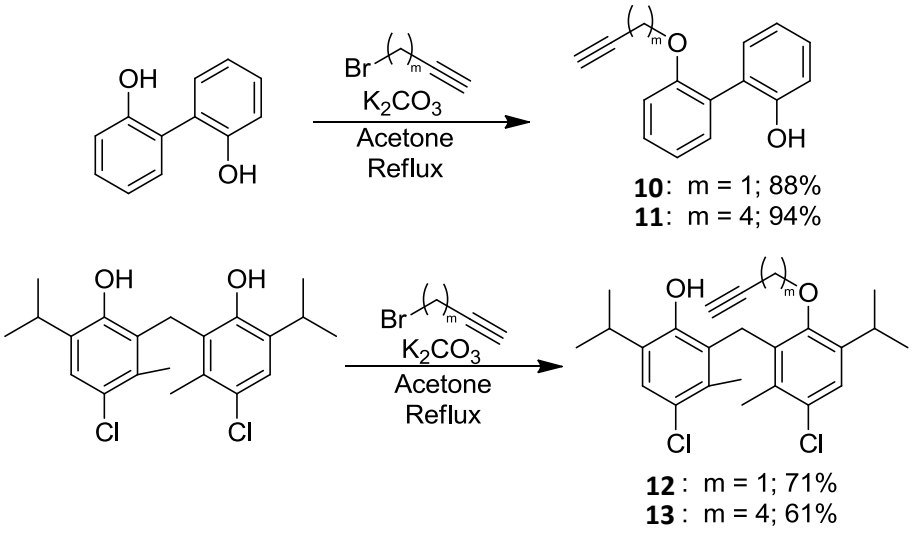

Scheme 3. Preparation of the phenolic alkyne linkers.

The phenolic-alkynes **10 – 13** were prepared from either biphenol or biclotymol, via alkylation with 3-bromo-prop-1-yne or 6-bromo-hex-1-yne in refluxing acetone, with potassium

carbonate serving as a base (17). Attempts to prepare analogues of the electron deficient phenolics hexachlorophene and bromophene were unsuccessful, with either no product observed or a mix of unreacted starting material and di-alkylated phenol recovered. NMR analysis suggested that the two phenols of these compounds formed strong hydrogen bonds to a bridged water molecule, indicating that the monoalkylated product was far more reactive than the starting material. We suspect that this discrepancy led to the observed balance of doubly alkylated products and unreacted starting material.

The azido-tobramycins **8** and **9** and alkynyl-phenolics **10 – 13** were linked via treatment with copper iodide, acetic acid and diisopropylethylamine in dichloromethane, following a published Huisgen cycloaddition procedure (18). Following purification via flash column chromatography the NBoc groups were cleaved in a mixture of TFA and water. Residual hydrophobic impurities were then removed via trituration in diethyl ether, to give hybrids **21 – 29**.

7.4 **Conclusion**

We have prepared a number of new aminoglycoside-phenolic conjugates, for the first time creating amphiphilic aminoglycoside hybrids through the addition of an active hydrophobic antimicrobial. This required the refinement of a gentle alkylation technique, which allowed us to use poorly active electrophiles in the presence of protecting groups susceptible to strong bases such as sodium hydride. Yields from the alkylation are significantly higher than those reported for allyl iodide, and do not require subsequent treatment with specialized ozonolysis equipment. It is our hope that these hybrids will exhibit improved activity against efflux-pump

expressing bacteria, as they are hypothesized to exhibit both membrane localization and pore forming activities.

7.5 **Experimental Procedures**

General methods.

See the Supporting Information for details. Compounds were not produced under anoxic or anhydrous conditions unless specifically noted. Reagents and solvents were purchased from commercially available sources and used without purification, unless otherwise noted. Flash chromatography was performed using silica gel (Silicycle 23 -60 um) using standard techniques. ^{1}H and ^{13}C NMR were recorded on a Bruker AMX-500 or Bruker AMX-300 spectrometer in the noted solvents. Chemical shifts (δ) are reported in parts per million with $CHCl_3$ (7.26 ppm) and CD_2HOH (3.31 ppm) used as internal standards. Thin layer chromatography was performed on pre-coated silica gel glass plates, treated to fluoresce at 254nm. Compounds were visualized with either ultraviolet light or with a mix of ninhydrin and acetic acid in ethanol. Low-resolution mass spectra (ESI+) were obtained on a Varian 500-MS IT Mass Spectrometer. High-resolution mass spectra (MALDI) were obtained on a Bruker UltraPleXtreme, with dihydroxybenzoic acid (DHB) support. Intermediate compounds were determined to be ≥90% pure by NMR, and the purity of compounds used in biological testing was ≥95% as determined by HPLC. Yields are given following purification, unless otherwise stated.

7.6 **Supporting Information**

Characterization data for new compounds, detailed experimental methods and other supporting information can be found in Chapter 14 of this thesis.

7.7 **References**

1. Findlay B, Zhanel GG, Schweizer F. Cationic amphiphiles, a new generation of antimicrobials inspired by the natural antimicrobial peptide scaffold. Antimicrob Agents Chemother. 2010 Oct;54(10):4049-58.

2. Koprivnjak T, Peschel A. Bacterial resistance mechanisms against host defense peptides. Cell Mol Life Sci. 2011 Jul;68(13):2243-54.

3. Arias CA, Murray BE. Antibiotic-resistant bugs in the 21st century--a clinical super-challenge. N Engl J Med. 2009 Jan 29;360(5):439-43.

4. Yeung AT, Gellatly SL, Hancock RE. Multifunctional cationic host defence peptides and their clinical applications. Cell Mol Life Sci. 2011 Jul;68(13):2161-76.

5. Svenson J, Brandsdal BO, Stensen W, Svendsen JS. Albumin binding of short cationic antimicrobial micropeptides and its influence on the in vitro bactericidal effect. J Med Chem. 2007 Jul 12;50(14):3334-9.

6. Pereira MP, Kelley SO. Maximizing the therapeutic window of an antimicrobial drug by imparting mitochondrial sequestration in human cells. J Am Chem Soc. 2011 Mar 16;133(10):3260-3.

7. Kelley SO, Stewart KM, Mourtada R. Development of novel peptides for mitochondrial drug delivery: Amino acids featuring delocalized lipophilic cations. Pharm Res. 2011 Nov;28(11):2808-19.

8. Horton KL, Pereira MP, Stewart KM, Fonseca SB, Kelley SO. Tuning the activity of mitochondria-penetrating peptides for delivery or disruption. Chembiochem. 2012 Feb 13;13(3):476-85.

9. Findlay B, Zhanel GG, Schweizer F. Neomycin-phenolic conjugates: Polycationic amphiphiles with broad-spectrum antibacterial activity, low hemolytic activity and weak serum protein binding. Bioorg Med Chem Lett. 2012 Feb 15;22(4):1499-503.

10. Hanessian S, Tremblay M, Swayze EE. Tobramycin analogues with C-5aminoalkylether chains intended to mimic rings III and IV of paromomycin. Tetrahedron. 2003 Tetrahedron;59(7):983.

11. Francois B, Russell RJ, Murray JB, Aboul-ela F, Masquida B, Vicens Q, et al. Crystal structures of complexes between aminoglycosides and decoding A site oligonucleotides: Role of the number of rings and positive charges in the specific binding leading to miscoding. Nucleic Acids Res. 2005 Oct 7;33(17):5677-90.

12. Quader S, Boyd SE, Jenkins ID, Houston TA. Multisite modification of neomycin B: Combined mitsunobu and click chemistry approach. J Org Chem. 2007 Mar 16;72(6):1962-79.

13. Corey PJ, Venkateswarlu A. Protection of hydroxyl groups as tert-butyldimethylsilyl derivatives. J Am Chem Soc. 1972;94(11/2/2012):6190.

14. Meyer O, Heitger H, inventors; Boehringer, assignee. Process for the manufacture of 4-(6-bromohexyloxy)-butylbenzene. USA patent US 2003/171620 A1. 2003 September 11, 2003.

15. Jackowski O, Bussière A, Vanhaverbeke C, Baussanne I, Peyrin E, Mingeot-Leclercq M, et al. Major increases of the reactivity and selectivity in aminoglycoside O-alkylation due to the presence of fluoride ions. Tetrahedron. 2012 1/14;68(2):737-46.

16. Boer J, Blount KF, Luedtke NW, Elson-Schwab L, Tor Y. RNA-selective modification by a platinum(II) complex conjugated to amino- and guanidinoglycosides. Angew Chem Int Ed Engl. 2005 Jan 28;44(6):927-32.

17. Bremner JB, Keller PA, Pyne SG, Robertson MJ, Sakthivel K, Somphol K, et al. Binaphthyl-anchored antibacterial tripeptide derivatives with hydrophobic C-terminal amino acid variations. Beilstein J Org Chem. 2012;8:1265-70.

18. Shao C, Wang X, Zhang Q, Luo S, Zhao J, Hu Y. Acid-base jointly promoted copper(I)-catalyzed azide-alkyne cycloaddition. J Org Chem. 2011 08/19; 2012/12;76(16):6832-6.

Chapter 8: Summary and Conclusions

By Brandon Findlay.

The work presented in this thesis did not occur in isolation, and to be properly understood it must be viewed in the context of other researchers, both those who set the stage and those who will come after.

One of the first cationic antimicrobial peptides to be extensively characterized was discovered by Michael Zasloff and colleagues in the tissue of the frog *Xenopus laevis* (1). These peptides were found to reduce amphibian mortality post-surgery, and when applied to bacteria *in vitro* were highly antimicrobial, depolarizing and lysing Gram-positive and Gram-negative cells in a matter of minutes. Further studies by Zasloff and others discovered that these first peptides, termed magainins (2), were but one family in a broad class of host defence peptides, produced by plants, animals and bacteria (3). A little over two thousand peptides have been discovered to date, and structures range from simple α-helices to complex cysteine-stabilized β-sheets, disordered strands, and every mix in between. The common thread linking these peptides is their amphiphilic nature, with cationic amino acid residues and a spatially distinct hydrophobic membrane binding domain (4).

Ultimately, it is the hydrophobic domain which imparted the magainins with their *in vitro* activity, and the cationic lysines and histidines that imparted selectivity (5, 6). The cellular membranes of bacteria are rich in negatively charged phospholipids, which draw the cationic peptides to the surface of the cellular envelope. Once close the hydrophobic residues trigger insertion into the membrane, thinning the bilayer. At high peptide concentrations pores begin to form, first transiently and then with some stability. Small ions then freely diffuse across the

bilayer, depolarizing the cell and blocking energy production. The bacterium dies soon after, if not from the depolarization then surely by the lytic effect of high concentrations of the CAMPs acting akin to detergent.

This early view of CAMP action was complicated somewhat by disagreement over the precise mechanism of peptide insertion into the membrane, with the Carpet and Barrel-Stave models gaining popularity, among others (4). During these investigations and early analogue synthesis it was discovered that some peptides did not depolarize the cell at all, instead using their amphiphilic character to translocate into the cytoplasm (7). One such peptide, the bovine lactoferrin based buforin II, binds strongly to DNA and RNA. As with membrane depolarization the bacteria die in a matter of minutes, suggesting broad spectrum inhibition of cellular processes. The key divider between these distinct modes of action was the size and shape of the hydrophobic domain, with smaller groups leading to translocation across the membrane and larger ones permanent binding (8, 9). The exact mechanism for peptide insertion was similarly dependent on structure, and both the Carpet and Barrel-Stave models are viable.

Larger hydrophobic domains were also linked to damage of zwitterionic mammalian membranes, which limited the applicability of CAMPs as therapeutics. (10) Reducing the hydrophobicity may limit antibacterial activity, which is often only moderate *in vitro* (10). To further complicate the issue, CAMPs were found to be inactivated by hydrophobic serum proteins and degraded by bacterial proteases (11, 12).

Investigations into the human CAMP LL-37 discovered that its concentration *in vivo* was significantly below the MIC *in vitro* (13), suggesting that the peptide would offer a poor barrier to bacterial colonization, the original hypothesis for its function. Only in inflamed or infected

tissue is the concentration of CAMPs elevated, with active secretion by lymphocytes responding to injury and infection (14, 15).

If bactericidal effects alone could not explain the role of LL-37, it was unclear why the peptide was expressed at low levels throughout human tissues. Research by the Hancock group and others discovered numerous secondary roles for LL-37, from innate immunity to inflammation and wound healing (14, 16, 17). Exposure of LL-37 may result in the release of a host of cytokines and growth factors, and the peptide is now known to play a key role in the body's response to infection (18). The membrane interacting behaviour typical of CAMPs is but one piece of the picture.

However, in the context of drug discovery, the *in vitro* antibacterial behaviour remains important. Because CAMPs kill through membrane interactions driven by a combination of electrostatics and the hydrophobic effect they are exceedingly broad spectrum, and it is difficult for bacteria to evolve resistance (19). Mutations which reduce peptide binding to the membrane and the resulting uptake are the most effective, but often interfere with bacterial membrane proteins, resulting in strains that are less fit in the absence of peptide.

My first forays into creating improved CAMP mimetics were with ultrashort lipopeptides. Built from three amino acid residues and a long lipid tail, these amphiphiles had been previously shown to have potent antimicrobial activity, though they were unacceptably toxic. By replacing the hydrocarbon tail with fluorocarbons, we sought to reduce the membrane-peptide interactions in the absence of a strong electrostatic interaction, effectively limiting lytic activity against mammalian cells. Conversely, once inserted into the membrane the hydrophobic fluorocarbon tails might preferentially associate, reducing the overall concentration of peptide required for pore formation and increasing bactericidal activity.

A total of twenty-two peptides were prepared, with fluorocarbon tails between seven and eleven carbons and hydrocarbon tails up to sixteen carbons in length (to match the molecular weight of the longest fluorocarbon tails). During synthesis it was discovered that the fully fluorinated tails were too acidic for effective coupling, so only tails with two carbon spacer atoms were included in the series. Two different peptide sequences were tested, LysLysLys and LysGlyLys, to model the effect of both varied positive charge and improved flexibility on activity.

The peptides were tested in the lab of Dr. Zhanel on a number of bacterial strains, drawn from samples collected in intensive care units throughout Canada (20, 21). Peptides with fluorocarbon tails were more effective on a molar basis, but demonstrated reduced activity by mass – a result of the increased molecular weight of their lipid tails. However, both types of lipopeptide were highly toxic to mammalian red blood cells, and both lost the majority of their activity in the presence of the hydrophobic protein BSA. One attempt to reduce membrane interactions by disrupting the hydrophobicity of the lipid tail with a terminal hydroxyl group was partially successful, eliminating both hemolytic activity and the activity against bacteria.

An interesting observation in this work was the difference in activity between the two peptide sequences. The LysGlyLys sequence was found to be the more active of the two, suggesting that the orientation of the cationic groups was more important than their overall number. With the assistance of an undergraduate student, Paul Szelemej, I set out to create a mirroring series of lipopeptoids. Peptoids are similar in structure to natural peptides, but the R-group is shifted to the amide nitrogen, eliminating the potential for back bone hydrogen bonding. As tertiary amides peptoids are also more conformationally restricted than equivalent peptides, but are largely resistant to degradation by proteases (22, 23). The preparation of antimicrobial peptoids had been recently reported, with bulky aryl R-groups used to enforce an

amphiphilic helical conformation. However, no direct comparison between the antimicrobial activity of peptoids and peptides was available.

Once again the cationic amphiphiles were prepared on solid support, and their biological activity was assessed in collaboration with the Zhanel lab against a panel of clinically relevant bacteria. Like the lipopeptides, the lipopeptoids were effective against a majority of bacterial strains, with reduced activity against Gram-negative bacteria, due to the presence of a second cellular membrane. The peptoid sequence was not as crucial to antibacterial activity, and unlike the peptides the 3+ *N*Lys*N*Lys*N*Lys sequence was the most active. Regardless, the majority of activities lay within two- to four-fold that of the equivalent peptides and the hemolytic data was similar, suggesting functional equivalence between the two scaffolds. Unfortunately, this followed to the lipopeptoids' lack of activity in the presence of BSA, and it appeared that amphiphiles with a long lipid tail were unlikely to advance forward as antibacterial agents.

Drawing back to what had been observed with the human CAMP LL-37, we sought to discover if our lipopeptides or lipopeptoids had the ability to modulate the immune response. A number of the previously prepared amphiphiles were selected, and tested in the Mookherjee lab for their ability to induce cytokine production in macrophage-like THP-1 cells. We found that a number of lipopeptides and lipopeptoids weakly induced production of IL-8, with one lipopeptoid, C20-NLysNLysNLys, quite effective at Groα induction. A second screen was planned, and new lipopeptides and lipopeptoids were synthesized to determine a loose SAR.

Similar to earlier results with the antibacterial activity, a long lipid tail was required for inducing production of Groα or IL-8. But, that appeared to be the only unifying trend, with cytokine production exhibiting a sequence and structure dependence absent from the earlier

antibacterial tests. Lipopeptides and lipopeptoids with a central glycine residue were inactive, and there was little difference in activity between the lipid tails sixteen carbons in length that had a terminal polar alcohol and those that did not. In contrast, cytotoxicity of the amphiphiles against the same cell lines was proportional to the previously measured hemolytic and antibacterial activity, suggesting that the increase in cytokine production was not linked to interactions with the cellular membrane.

Several of the lipopeptides were more effective than LL-37 at inducing IL-8 production on both a mass and molar basis, and we grew concerned that the unknown mode of action could be through binding to TLR heterodimers. Many bacteria produce lipopeptides of their own, and these are detected by TLRs and used to trigger inflammation via cytokines like TNF-α (24). Synthetic peptides and peptoids which use this pathway are unlikely to serve as anti-infection therapeutics, due to the harmful effects of systemic TNF-α induction, though they could act as vaccine adjuvants.

When the pro-inflammatory cytokines TNF-α and IL-1β were measured following amphiphile treatment, no significant increase in TNF-α concentration was found, indicating that neither the lipopeptides nor the lipopeptoids activate TLRs. However, a significant portion of the amphiphiles induced production of IL-1β at 50 μM or 100 μM, and several of the most active lipopeptides induced low-level IL-1β production at 10 μM. The varied expression patterns suggest more than one mode of action, with targets distinct from LL-37. As these amphiphiles are also significantly shorter than LL-37 and synthetically accessible, they may form lead structures in future anti-infective drug discovery.

Unfortunately, in the presence of BSA none of the above amphiphiles possess significant antibacterial activity. The large hydrophobic tail required for activity *in vitro* simply binds too

strongly to hydrophobic serum proteins to maintain activity under physiological conditions. To off-set this binding, we devised a series of amphiphilic neomycin B drug conjugates. The intrinsic antimicrobial activity of the aminoglycoside would then ensure activity against relevant bacteria, while the hydrophobic domain could improve interactions with the bacterial membrane, increasing influx. The phenolic disinfectants triclosan, clofoctol and para-chloro-meta-xylenol were selected as hydrophobic domains, due to their rapid diffusion across the bacterial membrane and their low toxicity towards eukaryotic cells (25). The two halves were to be brought together with a Huisgen cycloaddition, allowing a variable linker to be attached to the free hydroxyl of the phenolics.

Following a previously established procedure neomycin sulfate was protected as a t-butyl carbamate and the sole primary alcohol was activated with 2,4,6-trimethylbenzenesulfonyl chloride (26, 27). Nucleophilic substitution with sodium azide then provided the necessary azido-aminoglycoside (28). For the alkyne moiety, propargyl alcohol and 6-hydroxyl-hex-1-yne were activated with tosyl chloride (29), then used to alkylate the phenolic disinfectants. Treatment of the alkyne and azide with copper (I) iodide and diisopropylethylamine brought the two together (30).

The antimicrobial activity of the conjugates was promising, with moderate (2- to 4fold reduction) activity against neomycin-sensitive bacteria and a rescue of activity against a neomycin-resistant MRSA strain. Activity against *Pseudomonas aeruginosa* was improved two to four fold, and this bacterium derives much of its antibiotic resistance from a non-porous bacterial membrane and efflux pumps. And while a reduction against the two *Pseudomonas* strains was observed in the presence of BSA, the activity was only brought down to levels achieved with unmodified neomycin, with no significant reduction in activity against the other

bacterial strains. Similarly, only a small increase in hemolytic activity was observed, indicating that moderate amphiphilic character could be used to improve existing antibiotics.

As expected, alkylation of the phenol moiety eliminated the activity of triclosan, clofoctol, and para-chloro-meta-xylenol, and the conjugates were no more effective than neomycin against phenolic sensitive bacteria. So, we decided to create a new series of drug conjugates, with the anti-*Pseudomonas* antibiotic tobramycin. To retain activity in the hydrophobic domain only bivalent phenolics would be used, so that one phenol could be alkylated and the other left free to act.

While tobramycin also has a primary alcohol which could be selectively modified, previous research in the Schweizer lab suggested that this site was required for strong antimicrobial activity (31). So, the 5-OH was selected instead, as it was known to be non-essential and could be selectively modified (31, 32). However, the previously reported approach was both low yielding and required equipment not readily available in our department (31).

To circumvent these hurdles a new synthetic scheme was devised. The amino groups of tobramycin were first protected as t-butyl carbamates, as before with neomycin (26), and then all alcohols save the 5-OH were protected with t-butyldimethylsilyl chloride (33). The 5-OH was then alkylated with dibromo-alkanes, using potassium hydroxide as a base and tetrabutylammonium hydrogen sulfate as a catalyst (34). The second bromo group could then be substituted with sodium azide to furnish the required azido-tobramycin (28).

Preparation of the phenolic alkynes was complicated by a stable hydrogen bond network between the two phenols of electron deficient bis- and bi-phenols, and at least one water molecule. This network deactivated the starting phenolic, causing the small population of monoalkylated product that formed to proceed rapidly to dialkylation. As two of the most

active phenolics were electron deficient, numerous attempts were made to improve the poor yields, to no avail. However the electron rich biclotymol and neutral biphenol were alkylated without issue.

Initial attempts to bring together the azido-tobramycin and phenolic alkynes were low yielding, even after a full twenty-four hour reaction period and enhancement of the Huisgen conditions. A test reaction with propargyl alcohol suggested that steric hindrance was the culprit, and so the TBDMS groups were removed with TBAF. The cycloaddition then proceeded without issue, and biological assays are ongoing.

8.1 **References**

1. Zasloff M. Magainins, a class of antimicrobial peptides from xenopus skin: Isolation, characterization of two active forms, and partial cDNA sequence of a precursor. Proc Natl Acad Sci U S A. 1987 Aug;84(15):5449-53.

2. Ge Y, MacDonald DL, Holroyd KJ, Thornsberry C, Wexler H, Zasloff M. In vitro antibacterial properties of pexiganan, an analog of magainin. Antimicrob Agents Chemother. 1999 Apr;43(4):782-8.

3. Wang G, Li X, Wang Z. APD2: The updated antimicrobial peptide database and its application in peptide design. Nucleic Acids Res. 2009 Jan;37(Database issue):D933-7.

4. Melo MN, Ferre R, Castanho MA. Antimicrobial peptides: Linking partition, activity and high membrane-bound concentrations. Nat Rev Microbiol. 2009 Mar;7(3):245-50.

5. Giuliani A, Pirri G, Bozzi A, Di Giulio A, Aschi M, Rinaldi AC. Antimicrobial peptides: Natural templates for synthetic membrane-active compounds. Cell Mol Life Sci. 2008 Aug;65(16):2450-60.

6. Khandelia H, Ipsen JH, Mouritsen OG. The impact of peptides on lipid membranes. Biochim Biophys Acta. 2008 Jul-Aug;1778(7-8):1528-36.

7. Park CB, Kim HS, Kim SC. Mechanism of action of the antimicrobial peptide buforin II: Buforin II kills microorganisms by penetrating the cell membrane and inhibiting cellular functions. Biochem Biophys Res Commun. 1998 Mar 6;244(1):253-7.

8. Park CB, Yi KS, Matsuzaki K, Kim MS, Kim SC. Structure-activity analysis of buforin II, a histone H2A-derived antimicrobial peptide: The proline hinge is responsible for the cell-penetrating ability of buforin II. Proc Natl Acad Sci U S A. 2000 Jul 18;97(15):8245-50.

9. Gabriel GJ, Madkour AE, Dabkowski JM, Nelson CF, Nusslein K, Tew GN. Synthetic mimic of antimicrobial peptide with nonmembrane-disrupting antibacterial properties. Biomacromolecules. 2008 Nov;9(11):2980-3.

10. Chen Y, Guarnieri MT, Vasil AI, Vasil ML, Mant CT, Hodges RS. Role of peptide hydrophobicity in the mechanism of action of alpha-helical antimicrobial peptides. Antimicrob Agents Chemother. 2007 Apr;51(4):1398-406.

11. Thwaite JE, Hibbs S, Titball RW, Atkins TP. Proteolytic degradation of human antimicrobial peptide LL-37 by bacillus anthracis may contribute to virulence. Antimicrob Agents Chemother. 2006 Jul;50(7):2316-22.

12. Svenson J, Brandsdal BO, Stensen W, Svendsen JS. Albumin binding of short cationic antimicrobial micropeptides and its influence on the in vitro bactericidal effect. J Med Chem. 2007 Jul 12;50(14):3334-9.

13. Ong PY, Ohtake T, Brandt C, Strickland I, Boguniewicz M, Ganz T, et al. Endogenous antimicrobial peptides and skin infections in atopic dermatitis. N Engl J Med. 2002 Oct 10;347(15):1151-60.

14. Heilborn JD, Nilsson MF, Kratz G, Weber G, Sorensen O, Borregaard N, et al. The cathelicidin anti-microbial peptide LL-37 is involved in re-epithelialization of human skin wounds and is lacking in chronic ulcer epithelium. J Invest Dermatol. 2003 Mar;120(3):379-89.

15. Nijnik A, Hancock RE. The roles of cathelicidin LL-37 in immune defences and novel clinical applications. Curr Opin Hematol. 2009 Jan;16(1):41-7.

16. Bowdish DM, Davidson DJ, Lau YE, Lee K, Scott MG, Hancock RE. Impact of LL-37 on anti-infective immunity. J Leukoc Biol. 2005 Apr;77(4):451-9.

17. Yu J, Mookherjee N, Wee K, Bowdish DM, Pistolic J, Li Y, et al. Host defense peptide LL-37, in synergy with inflammatory mediator IL-1beta, augments immune responses by multiple pathways. J Immunol. 2007 Dec 1;179(11):7684-91.

18. Mookherjee N, Hamill P, Gardy J, Blimkie D, Falsafi R, Chikatamarla A, et al. Systems biology evaluation of immune responses induced by human host defence peptide LL-37 in mononuclear cells. Mol Biosyst. 2009 May;5(5):483-96.

19. Koprivnjak T, Peschel A. Bacterial resistance mechanisms against host defense peptides. Cell Mol Life Sci. 2011 Jul;68(13):2243-54.

20. Zhanel GG, Adam HJ, Low DE, Blondeau J, Decorby M, Karlowsky JA, et al. Antimicrobial susceptibility of 15,644 pathogens from canadian hospitals: Results of the CANWARD 2007-2009 study. Diagn Microbiol Infect Dis. 2011 Mar;69(3):291-306.

21. Zhanel GG, DeCorby M, Laing N, Weshnoweski B, Vashisht R, Tailor F, et al. Antimicrobial-resistant pathogens in intensive care units in canada: Results of the canadian national intensive care unit (CAN-ICU) study, 2005-2006. Antimicrob Agents Chemother. 2008 Apr;52(4):1430-7.

22. Simon RJ, Kania RS, Zuckermann RN, Huebner VD, Jewell DA, Banville S, et al. Peptoids: A modular approach to drug discovery. Proc Natl Acad Sci U S A. 1992 Oct 15;89(20):9367-71.

23. Sanborn TJ, Wu CW, Zuckermann RN, Barron AE. Extreme stability of helices formed by water-soluble poly-N-substituted glycines (polypeptoids) with alpha-chiral side chains. Biopolymers. 2002 Jan;63(1):12-20.

24. Agnihotri G, Crall BM, Lewis TC, Day TP, Balakrishna R, Warshakoon HJ, et al. Structure-activity relationships in toll-like receptor 2-agonists leading to simplified monoacyl lipopeptides. J Med Chem. 2011 Dec 8;54(23):8148-60.

25. McDonnell G, Russell AD. Antiseptics and disinfectants: Activity, action, and resistance. Clin Microbiol Rev. 1999 Jan;12(1):147-79.

26. Quader S, Boyd SE, Jenkins ID, Houston TA. Multisite modification of neomycin B: Combined mitsunobu and click chemistry approach. J Org Chem. 2007 Mar 16;72(6):1962-79.

27. Michael K, Wang H, Tor Y. Enhanced RNA binding of dimerized aminoglycosides. Bioorg Med Chem. 1999 Jul;7(7):1361-71.

28. Boer J, Blount KF, Luedtke NW, Elson-Schwab L, Tor Y. RNA-selective modification by a platinum(II) complex conjugated to amino- and guanidinoglycosides. Angew Chem Int Ed Engl. 2005 Jan 28;44(6):927-32.

29. Dickschat JS, Reichenbach H, Wagner-Döbler I, Schulz S. Novel pyrazines from the myxobacterium chondromyces crocatus and marine bacteria. Eur J Org Chem. 2005;2005(19):4141-53.

30. Bera S, Zhanel GG, Schweizer F. Evaluation of amphiphilic aminoglycoside-peptide triazole conjugates as antibacterial agents. Bioorg Med Chem Lett. 2010 May 15;20(10):3031-5.

31. Hanessian S, Tremblay M, Swayze EE. Tobramycin analogues with C-5aminoalkylether chains intended to mimic rings III and IV of paromomycin. Tetrahedron. 2003 Tetrahedron;59(7):983.

32. Francois B, Russell RJ, Murray JB, Aboul-ela F, Masquida B, Vicens Q, et al. Crystal structures of complexes between aminoglycosides and decoding A site oligonucleotides: Role of the number of rings and positive charges in the specific binding leading to miscoding. Nucleic Acids Res. 2005 Oct 7;33(17):5677-90.

33. Corey PJ, Venkateswarlu A. Protection of hydroxyl groups as tert-butyldimethylsilyl derivatives. J Am Chem Soc. 1972;94(11/2/2012):6190.

34. Meyer O, Heitger H, inventors; Boehringer, assignee. Process for the manufacture of 4-(6-bromohexyloxy)-butylbenzene. USA patent US 2003/171620 A1. 2003 September 11, 2003.

Chapter 9: Future Work

By Brandon Findlay.

This work has settled several questions about the biological properties of cationic amphiphiles, and raised many more. Most pressing is the newly discovered immunomodulatory properties of the lipopeptides and lipopeptoids, of which little is known. These compounds exert their activity without significant cytotoxicity, but from the chemist's perspective only a limited SAR has been established, with only two peptide and two peptoid sequences and a small number of lipid tails. Given the stark difference in activity between the LysLysLys and LysGlyLys sequences it is unlikely that we have discovered the most active peptide or peptide sequence, and so an expanded SAR analysis should be a priority. Arginine, ornithine, diaminobutyric acid and histidine are all readily available cationic amino acids, and any compound with a primary amine could be conceivably attached to the peptoid back bone. Peptides and peptoids between one and five residues in length are of particular interest, and could be directly compared to current immumodulatory peptides such as IDR-1002. The current body of results suggests that carbon tails at least sixteen carbons in length are required for immunomodulation, but to date only single tails and simple alkyl chains have been investigated. Di- and tri-lipid bacterial lipopeptides are known to strongly induce TNF-α though binding to toll-like receptors (TLRs), and analogues based on our sequences should be investigated for similar activity.

Strong binding to hydrophobic serum proteins is a significant drawback for lipopeptide based amphiphiles, but studies have demonstrated that serum albumin contains only a single hydrophobic binding pocket. Amphiphiles with multiple small tails may therefore show reduced

binding to serum albumin, but due to synergy in tail-membrane interactions are unlikely to have reduced antimicrobial activity. Several scaffolds with multiple tails can be readily established through the use of carboxylic acid tails and low generation PAMAM or POPAM dendrimers. As an early test, ethylenediaminetetraacetic acid (EDTA) could be reacted with a short chain amine such as octylamine to create an amphiphile with two positive charges and four lipid tails.

The alkylation reaction that has led to the creation of amphiphilic tobramycin analogues appears to have a wide scope, and may be useful for the creation of further aminoglycoside derivatives. Other drug-drug conjugates could include the hydrophobic antibiotic ciprofloxacin or the poorly permeable rifampicin. Both compounds are likely to benefit from a direct linkage to the cationic aminoglycoside, by increased binding (such as to ciprofloxacin's target DNA gyrase) or by improved antibiotic uptake. Bis-aminoglycosides could also be constructed, by using half an equivalent of a long dibromoalkane in the alkylation reaction. Restricted aminoglycosides could also be produced, and a linkage between the 6''-OH and 5-OH would force the aminoglycoside into a conformation similar to published crystal structures, potentially increasing activity.

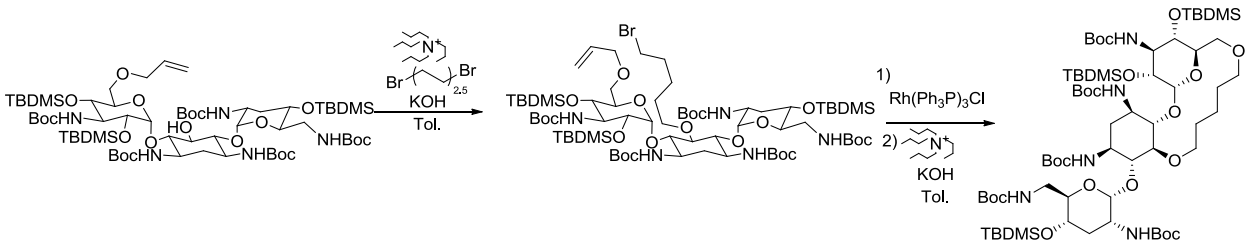

Scheme 1. Potential restricted tobramycin synthesis.

Chapter 10: Supporting Information for Chapter 3

By Brandon Findlay, George G. Zhanel and Frank Schweizer.

First Published as a supplement to the Chapter 3, an article in the International Journal of Antimicrobial Agents, 40, 2012, 36-42. Reproduced with permission.

10.1 In vitro tests:

10.1.1 Bacterial Isolates

Pathogenic bacteria were obtained during either the Canadian National Intensive Care Unit (CAN-ICU) study(1) or as part of the later CANWARD Canadian national surveillance study.(2) The CAN-ICU study included 19 medical centres from across Canada with active ICUs. From September 2005 to June 2006, inclusive, each centre was asked to collect a maximium of 300 consecutive isolates obtained from clinical specimens such as blood, urine, wounds/tissues and respiratory samples (one pathogen per cultured site per patient) originating from their ICU patients. The 4180 isolates obtained corresponded to 2580 patients (1.62 isolates/patient). Study sites were requested to provide only "clinically significant" specimens, originating from patients with a presumed infectious disease. Isolates were delivered to the reference library (Health Sciences Centre, Winnipeg, Canada) on Amies charcoal swabs, then subcultured onto appropriate media and stocked in skim milk at -80 °C until the minimum inhibitory concentration (MIC) testing was carried out.

10.1.2 Antimicrobial Susceptibilities

After subculturing the relevant bacteria twice from frozen stock, *in vitro* activities of the antimicrobials were determined by macrobroth dilution methodology in accordance with the Clinical and Laboratory Standards Institute (CLSI) guidelines (3). The MICs were determined using glass test tubes (2 mL/tube) containing doubling antimicrobial dilutions of cation adjusted Mueller-Hinton broth inoculated to achieve a final concentration of approximately 5 x 10^5 CFU/mL, incubated in ambient air for 24 h prior to reading. Colony counts were performed periodically to confirm inocula. The ATCC organisms *Staphylococcus pneumoniae* ATCC 49619, *Staphylococcus aureus* ATCC 29213, *Enterococcus faecalis* ATCC 29212, *Escherichia coli* ATCC 25922, and *Pseudomonas aeruginosa* ATCC 27853 were used as quality control and to allow easy comparison to previously tested antimicrobials.

10.1.3 Haemolytic Assays

Toxicity to mammalian cells was determined using a sheep red blood cell (erythrocyte) haemolytic assay (4). Erythrocytes were washed and resuspended in Tris buffered saline prior to use. The cell suspension was combined with varying concentrations of antimicrobials, from 50 µg/mL to 1 mg/mL and incubated for thirty minutes. The samples were centrifuged following treatment and the absorbance of the supernatant was measured at 540 nm. A solution of 0.5% ammonium chloride was used as a positive control, with normal buffered solution as the negative control. The toxicity was assessed as a function of percent hemolysis.

10.2 **General Procedures**

Reagents and solvents were purchased from commercially available sources and used without purification, unless otherwise noted. Fluorinated carboxylic acids were purchased from Fluorous Technologies Incorporated. Flash chromatography was performed using silica gel (Silicycle 23 - 60 μm) using standard techniques. ^{1}H and ^{13}C NMR were recorded on a Bruker AMX-500 or Bruker AMX-300 spectrometer in the noted solvents. Chemical shifts (δ) are reported in parts per million relative to tetramethylsilane. Compounds were visualized with either a mix of ninhydrin and acetic acid in ethanol, after spotting onto glass-backed TLC plates. Low-resolution mass spectra (ESI+) were obtained on a Varian 500-MS IT Mass Spectrometer. All compounds were determined to be ≥90% pure by NMR prior to bacterial testing. Rink Amide MBHA resin was used to prepare each peptide and was swelled in DMF for a minimum of thirty minutes prior to initial deprotection.

10.2.1 Fmoc Deprotection

Following established peptide synthesis procedures (5), to remove the Fmoc protecting group, DMF:Piperidine (4:1) was added to pre-swelled resin, until it reached a level approximately three times the height of the bead bed, and the beads were gently agitated by a steady stream of air for forty minutes. The DMF:Piperidine mixture was then drained and the deprotecting process was repeated. The beads were then washed successively three times with DMF, then DCM, then DMF again, and a small sample of the beads was removed. This sample was treated with equal volumes of 2% chloranil and 2% acetaldehyde in DMF and successful deprotection was observed by the beads turning bright red.

10.2.2 Amino Acid Coupling

To freshly deprotected beads was added a solution containing the Fmoc protected amino acid derivative (3 equivalents), TBTU (3 equivalents) and Hunig's Base (8 equivalents) in DMF. The mixtures were premixed at least three minutes prior to addition to ensure effective activation of the carboxylic acids. The solution was then gently agitated for at least three hours, after which time the solvent was drained and the beads were successively washed with 3x DMF, DCM and DMF. Completion of the reaction was verified through the chloranil test, as successfully reacted beads would not change colour in the presence of equal quantities of 2% chloranil and 2% acetaldehyde in DMF.

10.2.3 Carboxylic Acid Coupling

As in the elongation of the amino acid chain, hydrophobic tails were attached to the resin through the use of a mixture containing the carboxylic acid (3 equivalents), TBTU (3 equivalents) and Hunig's Base (8 equivalents) in DMF. Over the course of the syntheses it was found that activated, fluorous carboxylic acids have extremely poor solubility in DMF, leading to the formation of a thick gel. As a result, these compounds were instead premixed in DCM, and Pybop (3 equivalents) was used as the activating agent. The quantity of Hunig's base was unchanged (8 equivalents). Once the coupling mix was added the beads were gently agitated for approximately three hours, after which the chloranil test demonstrated that the coupling was complete.

10.2.4 Cleavage from Rink Amide MBHA Resin

Resin containing the fully protected, complete amino acids was rinsed three times with DCM to remove any residual DMF and dried. Residual DMF was found to interact with the TFA, forming a liquid which could not be removed even under low pressure (>0.001 Torr) using a dry-ice equipped rotary evaporator. An acidic solution of TFA:Water:TIPS (95:2.5:2.5) was then added and the beads were agitated for a minimum of two hours. The TFA was then filtered off and concentrated via evaporation under reduced pressure to yield the crude lipopeptides.

10.2.5 Purification of Lipopeptides

Peptides were taken up in a minimum quantity of water and loaded onto a column containing reverse phase flash silica. The peptides were then eluted by washing the column successively with distilled water (2.5 CV), 50% MeOH in water (2 CV), 75% MeOH in water (2 CV) and MeOH (3 CV). All solvents were stored in glass bottles, and acidified to a concentration of 0.1% TFA. After three or more peptides had been purified with the column the column was washed with DCM and 1% TFA in MeOH. Fractions containing the peptides of interest were collected and the solvent was removed via the steady passage of air at atmospheric pressure. Residual solvents were removed by prolonged (>3 days) exposure to high vacuum.

10.3 **Lipopeptide Spectral Data**

C7-LysGlyLys

^{1}H NMR (300 MHz, MeOD) δ 4.44 – 4.15 (m, 2H), 4.02 – 3.80 (m, 2H), 3.07 – 2.83 (m, 4H), 2.40 – 2.16 (m, 2H), 2.04 – 1.22 (m, 20H), 0.92 (t, J = 6.6, 3H). ^{13}C NMR (75 MHz, MeOD) δ 177.0, 176.9,

175.5, 171.8, 55.4, 54.4, 43.9, 40.6, 40.6, 36.8, 32.8, 32.4, 32.0, 30.2, 28.2, 28.0, 26.9, 23.9, 23.9, 23.7, 14.5. MS (ES) Calc. for $C_{21}H_{43}N_6O_4$ $(M+H)^+$: 443.3. Found 443.4.

C9-LysGlyLys

^{1}H NMR (300 MHz, MeOD) δ 4.47 – 4.16 (m, 2H), 4.02 – 3.80 (m, 2H), 3.09 – 2.83 (m, 4H), 2.44 – 2.16 (m, 2H), 2.05 – 1.19 (m, 24H), 0.91 (t, J = 6.6, 3H). ^{13}C NMR (75 MHz, MeOD) δ 176.9, 176.9, 175.5, 171.8, 55.4, 54.4, 43.9, 40.6, 40.6, 36.8, 33.1, 32.4, 32.0, 30.6, 30.5, 30.4, 28.2, 28.0, 26.9, 23.9, 23.9, 23.8, 14.6. MS (ES) Calc. for $C_{20}H_{48}N_6O_4$ $(M+H)^+$: 471.4. Found 471.4.

C9B-LysGlyLys

^{1}H NMR (300 MHz, MeOD) δ 4.37 (dd, J = 9.4, 4.8, 1H), 4.24 (dd, J = 7.9, 6.3, 1H), 3.98 – 3.82 (m, 2H), 3.07 – 2.84 (m, 4H), 2.28 (t, J = 7.3, 2H), 2.04 – 1.06 (m, 23H), 0.90 (d, J = 6.6, 6H). ^{13}C NMR (75 MHz, MeOD) δ 176.8, 176.6, 174.9, 174.2, 55.1, 54.8, 54.3, 40.6, 40.6, 36.9, 32.8, 32.3, 32.3, 30.9, 30.6, 29.3, 28.6, 28.2, 28.2, 28.1, 27.1, 24.0, 23.9, 23.8, 23.2. MS (ES) Calc. for $C_{21}H_{49}N_6O_4$ $(M+H)^+$: 485.4. Found 485.4.

C11-LysGlyLys

^{1}H NMR (300 MHz, MeOD) δ 4.29 (ddd, *J* = 14.0, 10.6, 5.4, 2H), 4.00 – 3.79 (m, 2H), 3.05 – 2.82 (m, 4H), 2.26 (t, *J* = 7.2, 2H), 1.98 – 1.15 (m, 29H), 0.90 (t, *J* = 6.6, 3H). ^{13}C NMR (75 MHz, MeOD) δ 176.9, 176.9, 175.5, 171.8, 55.4, 54.4, 43.9, 40.6, 40.6, 36.8, 33.2, 32.4, 32.0, 30.8, 30.8, 30.6, 30.6, 30.5, 28.2, 28.0, 26.9, 24.0, 23.9, 23.9, 14.6. MS (ES) Calc. for $C_{22}H_{51}N_6O_4$ $(M+H)^+$: 499.4. Found 499.5.

C14-LysGlyLys

^{1}H NMR (500 MHz, MeOD) δ 4.34 (dd, J = 9.6, 4.7, 1H), 4.22 (dd, J = 8.1, 6.2, 1H), 3.95 – 3.82 (m, 2H), 2.99 – 2.86 (m, 4H), 2.34 – 2.18 (m, 2H), 1.98 – 1.38 (m, 14H), 1.38 – 1.18 (m, 20H), 0.90 (t, J = 7.0, 3H). ^{13}C NMR (126 MHz, MeOD) δ 176.8, 176.8, 175.4, 171.7, 55.3, 54.2, 43.7, 40.5, 40.5, 36.7, 33.1, 32.3, 31.9, 30.8, 30.8, 30.8, 30.8, 30.7, 30.5, 30.5, 30.4, 28.1, 27.9, 26.8, 23.8, 23.8, 23.7, 14.4. MS (ES) Calc. for $C_{28}H_{57}N_6O_4$ $(M+H)^+$: 541.4. Found 541.7.

C16-LysGlyLys

^{1}H NMR (500 MHz, MeOD) δ 4.34 (dd, J = 9.6, 4.7, 1H), 4.22 (dd, J = 8.1, 6.2, 1H), 3.96 – 3.81 (m, 2H), 3.01 – 2.84 (m, 4H), 2.33 – 2.17 (m, 2H), 1.97 – 1.38 (m, 14H), 1.38 – 1.21 (m, 24H), 0.90 (t, J = 7.0, 3H). ^{13}C NMR (126 MHz, MeOD) δ 176.9, 176.8, 175.4, 171.7, 55.3, 54.3, 43.8, 40.5, 40.5, 36.7, 33.1, 32.2, 31.9, 30.8, 30.8, 30.7, 30.5, 30.5, 30.4, 28.1, 27.9, 26.8, 23.8, 23.8, 23.7, 14.5. MS (ES) Calc. for $C_{30}H_{61}N_6O_4$ $(M+H)^+$: 569.5. Found 569.7.

C20-LysGlyLys

^{1}H NMR (500 MHz, MeOD) δ 4.42 – 4.30 (m, 1H), 4.22 (dd, J = 8.2, 6.1, 1H), 3.89 (q, J = 16.7, 2H), 3.00 – 2.86 (m, 4H), 2.26 (td, J = 7.4, 3.2, 2H), 1.97 – 1.38 (m, 14H), 1.38 – 1.21 (m, 32H), 0.95 – 0.84 (m, 3H), 0.00 (dd, J = 8.2, 6.1, 1H), 4.39 – 4.29 (m, 1H), 3.97 – 3.81 (m, 2H), 2.34 – 2.19 (m, 2H), 3.02 – 2.83 (m, 4H). ^{13}C NMR (126 MHz, MeOD) δ 176.8, 176.8, 175.3, 171.7, 55.2, 54.2, 43.7, 40.5, 40.5, 36.7, 33.1, 32.3, 31.9 – 30.4 (m, aliphatic carbons), 28.1, 27.9, 26.8, 23.8, 23.8, 23.7, 14.5. MS (ES) Calc. for $C_{34}H_{69}N_6O_4$ $(M+H)^+$: 625.5. Found 625.8.

C16OH-LysGlyLys

^{1}H NMR (500 MHz, MeOD, mixture of rotamers) δ 4.38 – 4.27 (m, 2H), 4.19 (dd, J = 8.1, 6.2, 1H), 3.93 – 3.79 (m, 2H), 3.50 (t, J = 6.7, 1H), 2.95 – 2.83 (m, 4H), 2.29 – 2.17 (m, 2H), 1.93 – 1.18 (m, 38H). ^{13}C NMR (126 MHz, MeOD) δ 177.0, 176.9, 175.5, 171.8, 63.2, 55.4, 54.4, 43.9, 40.6, 40.6, 36.8, 33.8, 32.4, 32.0, 31 – 30.5 m, aliphatic carbons), 30.3, 29.3, 28.2, 28.0, 27.1, 26.9, 26.8, 23.9, 23.9. MS (ES) Calc. for $C_{30}H_{61}N_6O_5$ $(M+H)^+$: 585.5. Found 585.7.

F7-LysGlyLys

^{1}H NMR (300 MHz, MeOD) δ 4.44 – 4.18 (m, 1H), 4.06 – 3.81 (m, 1H), 3.08 – 2.83 (m, 1H), 2.72 – 2.40 (m, 0H), 2.01 – 1.34 (m, 6H). ^{13}C NMR (75 MHz, MeOD) δ 176.9, 175.2, 173.4, 171.8, 55.5, 54.2, 43.9, 40.6, 40.6, 32.4, 32.0, 28.2, 28.0, 27.6, 27.4 – 27.2 (m, adjacent to CF bonds), 23.9, 23.8. MS (ES) Calc. for $C_{21}H_{34}F_9N_6O_4$ $(M+H)^+$: 605.2. Found 605.2.

F9-LysGlyLys

^{1}H NMR (300 MHz, MeOD) δ 4.38 (dd, J = 9.5, 4.7, 1H), 4.28 (dd, J = 8.0, 6.0, 1H), 4.01 – 3.83 (m, 2H), 3.04 – 2.86 (m, 4H), 2.72 – 2.41 (m, 4H), 2.02 – 1.37 (m, 12H). ^{13}C NMR (75 MHz, MeOD) δ 176.8, 175.1, 173.2, 171.7, 55.4, 54.1, 43.7, 43.7, 40.5, 40.4, 32.3, 31.9, 28.1, 27.9, 27.4 - 27.2 (m, adjacent to CF bonds), 23.7, 23.7. MS (ES) Calc. for $C_{23}H_{34}F_{13}N_6O_4$ $(M+H)^+$: 705.2. Found 705.1.

F9B-LysGlyLys

^{1}H NMR (300 MHz, MeOD) δ 4.37 (dd, J = 9.4, 4.7, 1H), 4.27 (dd, J = 7.9, 6.2, 1H), 4.01 – 3.83 (m, 2H), 3.03 – 2.84 (m, 4H), 2.75 – 2.38 (m, 4H), 2.00 – 1.33 (m, 12H). ^{13}C NMR (75 MHz, MeOD) δ 176.9, 175.2, 173.4, 171.8, 55.5, 54.2, 43.9, 40.6, 40.6, 32.4, 32.1, 28.3, 28.0, 27.8, 27.5 - 27.3 (m, adjacent to CF bonds), 23.9. MS (ES) Calc. for $C_{24}H_{34}F_{15}N_6O_4$ $(M+H)^+$: 755.2. Found 755.2.

F11-LysGlyLys

^{1}H NMR (300 MHz, MeOD) δ 4.49 – 4.21 (m, 2H), 4.09 – 3.82 (m, 2H), 3.14 – 2.86 (m, 4H), 2.82 – 2.41 (m, 4H), 2.08 – 1.27 (m, 12H). ^{13}C NMR (75 MHz, MeOD) δ 176.9, 175.2, 173.4, 171.8, 55.5, 54.2, 43.9, 40.7, 40.6, 32.4, 32.1, 28.3, 28.0, 27.8, 27.5 - 27.4 (m, adjacent to CF bonds), 23.9, 23.9, 23.8. MS (ES) Calc. for $C_{25}H_{34}F_{17}N_6O_4$ $(M+H)^+$: 805.2. Found 805.2.

C7-LysLysLys

^{1}H NMR (300 MHz, MeOD) δ 4.48 – 4.18 (m, 3H), 3.05 – 2.83 (m, 6H), 2.27 (t, J = 7.6, 2H), 2.01 – 1.21 (m, 26H), 0.92 (t, J = 6.6, 3H). ^{13}C NMR (75 MHz, MeOD) δ 176.8, 176.7, 174.9, 174.2, 55.1, 54.8, 54.3, 40.6, 40.6, 40.6, 36.9, 32.8, 32.7, 32.3, 32.3, 30.2, 28.2, 28.1, 28.0, 27.0, 24.0, 23.9, 23.8, 23.7, 14.5. MS (ES) Calc. for $C_{25}H_{52}N_7O_4$ $(M+H)^+$: 514.4. Found 514.1.

C9-LysLysLys

^{1}H NMR (300 MHz, MeOD) δ 4.48 – 4.14 (m, 3H), 3.01 – 2.84 (m, 6H), 2.35 – 2.15 (m, 2H), 1.99 – 1.17 (m, 30H), 0.91 (t, J = 6.7, 3H). ^{13}C NMR (75 MHz, MeOD) δ 176.8, 176.7, 174.9, 174.2, 55.1,

54.8, 54.2, 40.6, 40.6, 40.6, 36.9, 33.1, 32.7, 32.3, 32.3, 30.6, 30.5, 30.4, 28.2, 28.1, 28.0, 27.0, 24.0, 23.9, 23.8, 23.8, 14.6. MS (ES) Calc. for $C_{27}H_{56}N_7O_4$ $(M+H)^+$: 542.4. Found 542.1.

C9B-LysLysLys

1H NMR (300 MHz, MeOD) δ 4.44 – 4.18 (m, 3H), 3.05 – 2.86 (m, 6H), 2.26 (t, J = 7.5, 2H), 1.98 – 1.10 (m, 29H), 0.89 (d, J = 6.6, 6H). ^{13}C NMR (75 MHz, MeOD) δ 176.8, 176.6, 174.9, 174.2, 55.1, 54.8, 54.3, 40.6, 40.6, 40.3, 36.9, 32.8, 32.3, 32.3, 30.9, 30.6, 29.3, 28.6, 28.2, 28.2, 28.2, 28.1, 27.1, 24.0, 23.9, 23.8, 23.2, 23.2. MS (ES) Calc. for $C_{28}H_{58}N_7O_4$ $(M+H)^+$: 556.4. Found 555.9.

C11-LysLysLys

^{1}H NMR (300 MHz, MeOD) δ 4.35 – 4.07 (m, 3H), 2.85 (dd, J = 8.8, 4.2, 6H), 2.15 (t, J = 7.4, 2H), 1.89 – 1.10 (m, 34H), 0.81 (t, J = 6.7, 3H). ^{13}C NMR (75 MHz, MeOD) δ 176.8, 176.7, 174.9, 174.3, 55.1, 54.8, 54.2, 40.6, 40.6, 40.6, 36.9, 33.2, 32.7, 32.3, 32.3, 30.9, 30.9, 30.8, 30.6, 30.6, 30.5, 28.3, 28.2, 28.1, 27.1, 24.0, 23.9, 23.8, 14.6. MS (ES) Calc. for $C_{29}H_{60}N_7O_4$ $(M+H)^+$: 570.5. Found 570.2.

C14-LysLysLys

^{1}H NMR (500 MHz, MeOD) δ 4.39 – 4.30 (m, 2H), 4.27 (dd, J = 8.4, 6.1, 1H), 3.01 – 2.88 (m, 6H), 2.26 (td, J = 7.2, 1.5, 2H), 1.96 – 1.40 (m, 20H), 1.41 – 1.27 (m, 20H), 0.91 (t, J = 6.9, 3H). ^{13}C NMR (126 MHz, MeOD) δ 176.8, 176.6, 174.9, 174.2, 55.1, 54.8, 54.2, 40.6, 40.6, 40.6, 36.9,

33.2, 32.8, 32.3, 32.3, 30.9, 30.9, 30.9, 30.9, 30.8, 30.6, 30.6, 30.5, 28.2, 28.2, 28.1, 27.1, 24.0, 23.9, 23.9, 23.8, 14.6. MS (ES) Calc. for $C_{32}H_{66}N_7O_4$ $(M+H)^+$: 612.5. Found 612.8.

C16-LysLysLys

^{1}H NMR (500 MHz, MeOD) δ 4.38 – 4.19 (m, 3H), 3.04 – 2.84 (m, 6H), 2.33 – 2.16 (m, 2H), 1.98 – 1.38 (m, 20H), 1.38 – 1.19 (m, 24H), 0.90 (t, J = 6.9, 3H). ^{13}C NMR (126 MHz, MeOD) δ 176.8, 176.7, 174.9, 174.2, 55.1, 54.8, 54.2, 40.6, 40.6, 40.6, 36.9, 33.2, 32.7, 32.3, 32.3, 30.9 – 30.5 (m, aliphatic peaks), 28.2, 28.1, 28.0, 27.1, 24.0, 23.9, 23.9, 23.8, 14.6. MS (ES) Calc. for $C_{34}H_{70}N_7O_4$ $(M+H)^+$: 640.5. Found 640.8.

C20-LysLysLys

^{1}H NMR (500 MHz, MeOD) δ 4.38 – 4.31 (m, 2H), 4.31 – 4.22 (m, 1H), 3.03 – 2.91 (m, 6H), 2.32 – 2.21 (m, 2H), 1.94 – 1.41 (m, 20H), 1.41 – 1.22 (m, 32H), 0.92 (t, J = 6.9, 3H). ^{13}C NMR (126 MHz, MeOD) δ 176.8, 176.6, 174.9, 174.2, 55.0, 54.7, 54.2, 40.6, 40.6, 40.6, 36.9, 33.2, 32.8, 32.4, 32.3, 30.9 – 30.6 (m, aliphatic peaks), 28.2, 28.2, 28.1, 27.1, 24.0, 23.9, 23.9, 23.8, 14.6. MS (ES) Calc. for $C_{36}H_{78}N_7O_4$ $(M+H)^+$: 696.6. Found 696.9.

C16OH-LysLysLys

^{1}H NMR (500 MHz, MeOD, mixture of rotamers) δ 4.41 – 4.27 (m, 3H), 4.23 (dd, J = 8.2, 6.2, 1H), 3.52 (t, J = 6.7, 1H), 2.93 (dd, J = 8.8, 5.0, 6H), 2.23 (dd, J = 8.1, 6.0, 2H), 1.98 – 1.14 (m, 44H). ^{13}C NMR (126 MHz, MeOD) δ 176.8, 176.7, 174.9, 174.2, 63.2, 55.1, 54.8, 54.2, 40.6, 40.6, 40.6,

36.9, 33.8, 32.8, 32.3, 32.3, 30.9 – 30.3 (m, aliphatic carbons), 28.2, 28.2, 28.1, 27.1, 26.8, 24.0, 23.9, 23.8. MS (ES) Calc. for $C_{34}H_{70}N_7O_5$ $(M+H)^+$: 656.5. Found 656.8.

F7-LysLysLys

^{1}H NMR (300 MHz, MeOD) δ 4.41 – 4.20 (m, 3H), 2.95 (ddd, J = 18.1, 13.4, 10.8, 6H), 2.71 – 2.40 (m, 4H), 1.99 – 1.33 (m, 18H). ^{13}C NMR (75 MHz, MeOD) δ 176.6, 174.6, 174.1, 173.1, 55.1, 54.8, 54.1, 40.6, 40.5, 40.5, 32.6, 32.2, 32.1, 28.1, 28.0, 28.0, 27.6, 27.3 – 27.2 (m, adjacent to CF bonds), 23.8, 23.8, 23.7. MS (ES) Calc. for $C_{25}H_{43}F_9N_7O_4$ $(M+H)^+$: 676.3. Found 675.7.

F9-LysLysLys

^{1}H NMR (300 MHz, MeOD) δ 4.48 – 4.20 (m, 3H), 2.94 (dd, J = 8.4, 4.6, 6H), 2.68 – 2.37 (m, 4H), 2.02 – 1.29 (m, 18H). ^{13}C NMR (75 MHz, MeOD) δ 176.7, 174.8, 174.3, 173.3, 55.3, 54.9, 54.2, 40.6, 40.6, 40.6, 32.7, 32.3, 32.2, 28.2, 28.1, 28.1, 27.8, 27.5 – 27.4 (m, adjacent to CF bonds), 23.9, 23.9, 23.8. MS (ES) Calc. for $C_{27}H_{43}F_{13}N_7O_4$ $(M+H)^+$: 776.3. Found 775.6.

F9B-LysLysLys

^{1}H NMR (300 MHz, D2O) δ 4.41 – 4.18 (m, 3H), 3.12 – 2.85 (m, 6H), 2.77 – 2.43 (m, 4H), 2.02 – 1.22 (m, 18H). ^{13}C NMR (75 MHz, D2O) δ 181.3, 179.0, 179.0, 178.6, 58.7, 58.4, 58.4, 44.1, 44.1, 44.1, 35.4, 35.3, 35.3, 31.5 (m, weak, adjacent to CF bonds), 31.2, 27.1, 27.1, 27.0. MS (ES) Calc. for $C_{26}H_{43}F_{15}N_7O_4$ $(M+H)^+$: 826.3. Found 825.8.

F11-LysLysLys

^{1}H NMR (300 MHz, MeOD) δ 4.43 – 4.18 (m, 3H), 3.06 – 2.84 (m, 6H), 2.67 – 2.37 (m, 4H), 1.99 – 1.15 (m, 18H). ^{13}C Signal was too weak for full characterization. MS (ES) Calc. for $C_{29}H_{43}F_{17}N_7O_4$ $(M+H)^+$: 876.3. Found 876.2.

10.4 **References**

1. Zhanel GG, DeCorby M, Laing N, Weshnoweski B, Vashisht R, Tailor F, et al. Antimicrobial-resistant pathogens in intensive care units in canada: Results of the canadian national intensive care unit (CAN-ICU) study, 2005-2006. Antimicrob Agents Chemother. 2008 Apr;52(4):1430-7.

2. Zhanel GG, Adam HJ, Low DE, Blondeau J, Decorby M, Karlowsky JA, et al. Antimicrobial susceptibility of 15,644 pathogens from canadian hospitals: Results of the CANWARD 2007-2009 study. Diagn Microbiol Infect Dis. 2011 Mar;69(3):291-306.

3. Rennie RP, Callihan DR, Barry AL, Krisher K, Munro SD, Sei K, et al. Protocols for evaluating dehydrated mueller-hinton agar; approved standard-second edition. In: CLSI; 2006. p. 1-29.

4. Dathe M, Schumann M, Wieprecht T, Winkler A, Beyermann M, Krause E, et al. Peptide helicity and membrane surface charge modulate the balance of electrostatic and hydrophobic interactions with lipid bilayers and biological membranes. Biochemistry. 1996 Sep 24;35(38):12612-22.

5. Chan WC, White PD. Fmoc solid phase peptide synthesis: A practical approach. 1st ed. New York, United States: Oxford University Press; 2000.

Chapter 11: Supporting Information for Chapter 4

By Brandon Findlay, George G. Zhanel and Frank Schweizer. First published as supplementary information to Chapter 4, PLOS ONE, 2012, e41141. Reproduced with permission.

11.1 In vitro tests:

11.1.1 Bacterial Isolates

Pathogenic bacteria were obtained during either the Canadian National Intensive Care Unit (CAN-ICU) study (1) or as part of the later CANWARD Canadian national surveillance study (2). The CAN-ICU study included 19 medical centres from across Canada with active ICUs. From September 2005 to June 2006, inclusive, each centre was asked to collect a maximium of 300 consecutive isolates obtained from clinical specimens such as blood, urine, wounds/tissues and respiratory samples (one pathogen per cultured site per patient) originating from their ICU patients. The 4180 isolates obtained corresponded to 2580 patients (1.62 isolates/patient). Study sites were requested to provide only "clinically significant" specimens, originating from patients with a presumed infectious disease. Isolates were delivered to the reference library (Health Sciences Centre, Winnipeg, Canada) on Amies charcoal swabs, then subcultured onto appropriate media and stocked in skim milk at -80°C until the minimum inhibitory concentration (MIC) testing was carried out.

11.1.2 Antimicrobial Susceptibilities

After subculturing the relevant bacteria twice from frozen stock, *in vitro* activities of the antimicrobials were determined by macrobroth dilution methodology in accordance with the Clinical and Laboratory Standards Institute (CLSI) guidelines (3). The MICs were determined using glass test tubes (2 mL/tube) containing doubling antimicrobial dilutions of cation adjusted Mueller-Hinton broth inoculated to achieve a final concentration of approximately 5 x 10^5 CFU/mL, incubated in ambient air for 24 hr prior to reading. Colony counts were performed periodically to confirm inocula. The ATCC organisms *Staphylococcus pneumoniae* ATCC 49619, *Staphylococcus aureus* ATCC 29213, *Enterococcus faecalis* ATCC 29212, *Escherichia coli* ATCC 25922, and *Pseudomonas aeruginosa* ATCC 27853 were used as quality control and to allow easy comparison to previously tested antimicrobials. Each test in this series was performed without replication. In our experience with cationic amphiphiles the results are accurate to within a single doubling.

11.1.3 Haemolytic Assays

Toxicity to mammalian cells was determined using a sheep red blood cell (erythrocyte) haemolytic assay (4). Erythrocytes were washed and resuspended in Tris buffered saline prior to use, at a concentration of 1.46 - 4.5 x 10^9 cells/mL (on average 3.08 x 10^9 cells/mL). The cell suspension was diluted with varying concentrations of antimicrobials, from 50 µg/mL to 1 mg/mL and incubated for thirty minutes (final erythrocyte concentration 4.08 x 10^8 cells/mL). The samples were centrifuged following treatment and the absorbance of the supernatant was measured at 540 nm. A solution of 0.5% ammonium chloride was used as a positive control,

with normal buffered solution as the negative control. The toxicity was assessed as a function of percent hemolysis.

11.2 **General Procedures**

Reagents and solvents were purchased from commercially available sources and used without purification, unless otherwise noted. Fluorinated carboxylic acids were purchased from Fluorous Technologies Incorporated. Flash chromatography was performed using silica gel (Silicycle 23 -60 um) using standard techniques. ^{1}H and ^{13}C NMR were recorded on a Bruker AMX-500 or Bruker AMX-300 spectrometer in the noted solvents. Chemical shifts (δ) are reported in parts per million relative to tetramethylsilane. Compounds were visualized with either a mix of ninhydrin and acetic acid in ethanol, after spotting onto glass backed TLC plates. Low-resolution mass spectra (ESI+) were obtained on a Varian 500-MS IT Mass Spectrometer. All compounds were determined to be ≥90% pure by NMR prior to bacterial testing. Rink Amide MBHA resin was used to prepare each peptide and was swelled in DMF for a minimum of thirty minutes prior to initial deprotection.

11.2.1 t-Butyl (4-aminobutyl)carbamate Synthesis

To a rapidly stirring solution of 1,4-diaminobutane (34.0 mL, 3 eq) and triethylamine (25.0 mL) in ice cold methanol (225 mL) was added a solution of Boc anhydride (24.9 g, 1 eq) in methanol (50 mL) over a period of 1 hr. The solution was allowed to gradually warm to room

temperature and stir overnight. The methanol and triethylamine was then removed, and water added. Acetic acid was added (6.5 mL, 1.1 eq), and the solution extracted twice with diethyl ether. The aqueous layer was then basified with sodium carbonate and extracted twice with DCM. The DCM layers were combined, washed with 10% $NaCO_3$, and concentrated. t-Butyl (4-aminobutyl)carbamate was obtained as a light yellow oil and used without further purification (10.4g, 49%).

11.2.2 Fmoc Deprotection

To deblock the Rink amide resin prior to functionalization and to remove the Fmoc protecting group of the glycine residue following attachment to the growing peptoid chain, DMF:Piperidine (4:1) was added to pre-swelled resin, until it reached a level approximately three times the height of the bead bed, and the beads were gently agitated by a steady stream of air for forty minutes. The DMF:Piperidine mixture was then drained and the deprotecting process was repeated. The beads were then washed successively three times with DMF, then DCM, then DMF again, and a small sample of the beads was removed. This sample was treated with equal volumes of 2% chloranil and 2% acetaldehyde in DMF and successful deprotection was observed by the beads turning bright red.

11.2.3 Peptoid Residue Synthesis

Following an established procedure (5), to beads containing unprotected amine moieties were added diisopropylcarbodiimide (DIC) (16.6 equivalents) and 2-bromoacetic acid (20 equivalents) in DMF. The mixture was agitated with a steady stream of nitrogen gas for thirty minutes, during which time a light yellow foam developed. The reactants were then

drained off, and the resin was washed three times with DMF, three times with DCM and three times with NMP. A solution of tert-butyl (4-aminobutyl)carbamate (20 equivalents) in NMP was then added and agitated for ninety minutes. Once again the reaction mixture was drained and the beads were washed three times successively with NMP, DCM and DMF. At this point the chloranil test registered positive, with blue-green beads. Addition of bromoacetic acid could then be repeated for the NLysNLysNLys based residues, or Fmoc-Gly-OH added, as appropriate.

11.2.4 Amino Acid Coupling

To the growing peptoid residues was added Fmoc-protected glycine (3 equivalents), TBTU (3 equivalents) and Hunig's Base (8 equivalents) in DMF. The mixtures were premixed at least three minutes prior to addition to ensure effective activation of the carboxylic acids. The solution was then gently agitated for at least three hours, after which time the solvent was drained and the beads were successively washed with 3x DMF, DCM and DMF. Completion of the reaction was verified through the chloranil test, as successfully reacted beads would not change colour in the presence of equal quantities of 2% chloranil and 2% acetaldehyde in DMF.

11.2.5 Carboxylic Acid Coupling

As in the coupling of the glycine residues, hydrophobic tails were attached to the resin through the use of a mixture containing the carboxylic acid (3 equivalents), TBTU (3 equivalents) and Hunig's Base (8 equivalents) in DMF. Because the activated fluorous carboxylic acids had extremely poor solubility in DMF they were instead premixed in DCM, with Pybop (3 equivalents) used as the activator. The quantity of Hunig's base was unchanged (8 equivalents).

Once the coupling mix was added the beads were gently agitated for approximately three hours, after which the chloranil test demonstrated that the coupling was complete.

11.2.6 Cleavage from Rink Amide MBHA Resin

Resin containing the fully protected, complete peptoids was rinsed three times with DCM to remove any residual DMF, then dried under a steady vacuum. An acidic solution of TFA:Water:TIPS (95:2.5:2.5) was then added and the beads were agitated for a minimum of two hours. The TFA was filtered off and concentrated via evaporation under reduced pressure to yield crude lipopeptoids.

11.2.7 Purification of Lipopeptoids

Peptoids were taken up in a minimum quantity of water and loaded onto a column containing C18 functionalized silica gel. The peptoids were then eluted by washing the column successively with distilled water (2.5 CV), 50% MeOH in water (2 CV), 75% MeOH in water (2 CV) and MeOH (3 CV). All solvents were stored in glass bottles, and acidified with 0.1% TFA. After three or more compounds had been purified with the column the column was washed with DCM and 1% TFA in MeOH. Fractions containing the peptoids of interest were collected and the solvent was removed via the steady passage of air at atmospheric pressure. Residual solvents were removed by prolonged (>3 days) exposure to high vacuum.

11.3 **Lipopeptoid Rotameric States**

C14-NLysNLysNLys: ^{1}H NMR (500 Mhz, D2O). Shifts were normalized by adjusting the HDO peak according to previously reported values (6). Glycine hydrogens are found from 4.0 – 4.5ppm and α-hydrogens of the lipid carbonyl are visible from 2.1 – 2.5ppm.

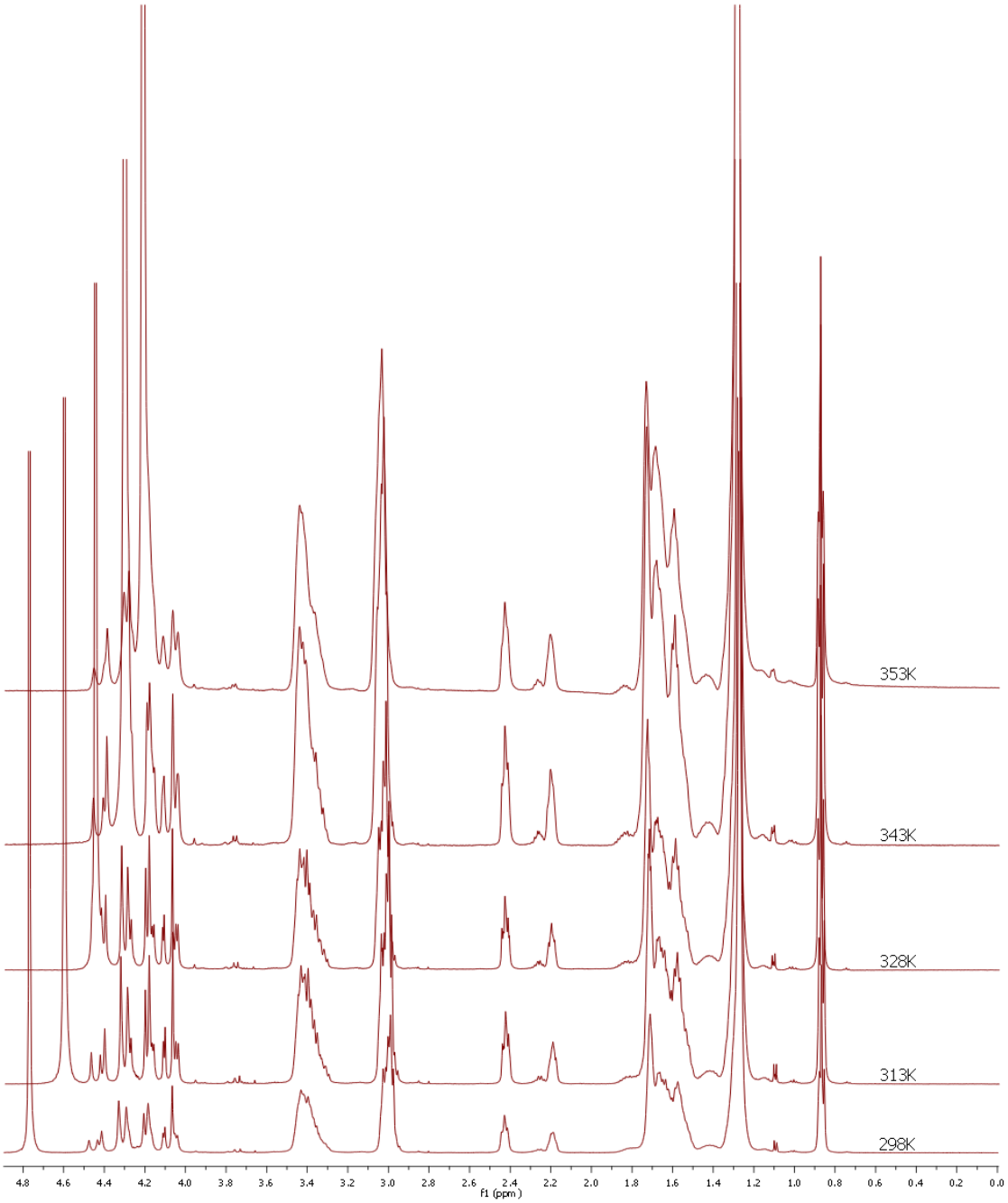

11.4 **Lipopeptoid Spectral Data**

C11-*N*LysGly*N*Lys

^{1}H NMR (500 MHz, MeOD, mixture of rotamers) δ 4.27 – 3.95 (m, 6H), 3.51 – 3.34 (m, 4H), 3.04 – 2.88 (m, 4H), 2.50 – 2.40 (m, 1H), 2.37 – 2.27 (m, 1H), 1.79 – 1.52 (m, 10H), 1.45 – 1.21 (m, 14H), 0.90 (t, J = 6.9, 3H). ^{13}C NMR (126 MHz, MeOD, mixture of rotamers) δ 176.9, 176.4, 176.4, 173.8, 173.7, 173.0, 172.0, 171.8, 171.8, 171.8, 171.6, 171.6, 171.2, 171.1, 51.9, 50.7, 50.4, 50.2, 48.4, 48.3, 47.9, 47.9, 42.2, 42.2, 42.0, 40.6, 40.5, 34.3, 34.3, 33.9, 33.2, 30.8, 30.8, 30.8, 30.7, 30.6, 30.6, 30.6, 30.6, 26.7, 26.5, 26.4, 25.9, 25.9, 25.8, 25.5, 25.4, 23.9, 14.6. MS (ES) Calc. for $C_{25}H_{51}N_6O_4$ $(M+H)^+$: 499.4. Found 499.6.

C14-*N*LysGly*N*Lys

^{1}H NMR (500 MHz, MeOD, mixture of rotamers) δ 4.23 – 3.99 (m, 6H), 3.50 – 3.36 (m, 4H), 3.03 – 2.88 (m, 4H), 2.49 – 2.40 (m, 1H), 2.37 – 2.29 (m, 1H), 1.78 – 1.51 (m, 10H), 1.44 – 1.19 (m, 20H), 0.90 (t, J = 6.9, 3H). ^{13}C NMR (126 MHz, MeOD, mixture of rotamers) δ 176.9, 176.4, 173.8, 173.7, 173.0, 172.0, 171.8, 171.8, 171.8, 171.6, 171.5, 171.2, 171.1, 51.9, 50.7, 50.4, 50.2, 48.4, 48.2, 47.9, 47.8, 42.2, 42.2, 42.0, 40.6, 40.5, 40.5, 34.3, 34.3, 33.9, 33.2, 30.9, 30.9, 30.8, 30.8, 30.6, 30.6, 26.7, 26.5, 26.5, 26.4, 25.9, 25.9, 25.8, 25.5, 25.4, 23.9, 21.6, 14.6. MS (ES) Calc. for $C_{28}H_{57}N_6O_4$ $(M+H)^+$: 541.4. Found 541.7.

C16-*N*LysGly*N*Lys

^{1}H NMR (500 MHz, MeOD, mixture of rotamers) δ 4.25 – 3.96 (m, 6H), 3.51 – 3.34 (m, 4H), 3.05 – 2.85 (m, 4H), 2.45 (t, J = 7.3, 1H), 2.33 (t, J = 7.3, 1H), 1.77 – 1.54 (m, 10H), 1.29 (s, 24H), 0.90 (t, J = 6.8, 3H). ^{13}C NMR (126 MHz, MeOD, mixture of rotamers) δ 176.9, 176.4, 176.3, 173.8, 173.8, 173.0, 172.0, 171.8, 171.8, 171.8, 171.6, 171.6, 171.2, 171.1, 51.9, 50.7, 50.4, 50.2, 48.4, 48.2, 47.9, 47.9, 42.2, 42.2, 42.0, 40.6, 40.5, 40.5, 34.3, 34.3, 33.9, 33.2, 30.9, 30.9, 30.8, 30.8, 30.6, 30.6, 26.7, 26.5, 26.5, 26.4, 25.9, 25.9, 25.8, 25.5, 25.4, 23.9, 14.6. MS (ES) Calc. for $C_{30}H_{61}N_6O_4$ $(M+H)^+$: 569.5. Found 569.7.

C20-*N*LysGly*N*Lys

^{1}H NMR (500 MHz, MeOD, mixture of rotamers) δ 4.22 – 3.97 (m, 6H), 3.45 (dd, J = 13.5, 6.6, 4H), 3.02 – 2.87 (m, 4H), 2.47 – 2.43 (m, 1H), 2.35 – 2.24 (m, 1H), 1.77 – 1.52 (m, 10H), 1.42 – 1.21 (m, 32H), 0.90 (t, J = 6.9, 3H). ^{13}C NMR (126 MHz, MeOD, mixture of rotamers) δ 177.0, 176.4, 174.0, 173.8, 173.8, 173.8, 173.0, 172.0, 54.4, 51.9, 50.7, 50.4, 50.2, 48.4, 48.3, 47.9, 47.9, 47.9, 42.2, 42.2, 42.0, 40.6, 40.5, 40.5, 34.3, 34.3, 33.9, 33.9, 33.2, 30.9, 30.9, 30.8, 30.8, 30.6, 30.6, 26.8, 26.5, 26.5, 25.9, 25.9, 25.5, 25.4, 23.9, 14.6. MS (ES) Calc. for $C_{34}H_{69}N_6O_4$ $(M+H)^+$: 625.5. Found 625.7.

F11-*N*LysGly*N*Lys

^{1}H NMR (500 MHz, MeOD, mixture of rotamers) δ 4.28 – 3.95 (m, 6H), 3.55 – 3.35 (m, 4H), 3.07 – 2.90 (m, 4H), 2.87 – 2.77 (m, 1H), 2.77 – 2.67 (m, 1H), 2.65 – 2.45 (m, 2H), 1.80 – 1.56 (m, 8H).

^{13}C NMR (126 MHz, MeOD, mixture of rotamers) δ 173.8, 173.8, 173.6, 173.0, 172.9, 172.9, 171.9, 171.8, 171.7, 171.6, 171.4, 171.3, 171.1, 51.8, 51.8, 50.7, 50.6, 50.5, 50.3, 50.2, 50.0,

50.0, 48.4, 48.3, 48.2, 42.3, 42.2, 42.1, 42.0, 40.6, 40.5, 33.2, 30.9, 27.8, 26.5, 26.4, 25.9, 25.9, 25.8, 25.5, 25.4, 25.3, 25.1. MS (ES) Calc. for $C_{25}H_{34}F_{17}N_6O_4$ $(M+H)^+$: 805.2. Found 805.5.

C11-*N*HarGly*N*Har NBoc

^{1}H NMR (500 MHz, CDCl3, mixture of rotamers) δ 11.47 (d, J = 10.2, 2H), 8.42 – 8.24 (m, 2H), 7.23 – 5.54 (m, 3H), 4.22 – 3.91 (m, 6H), 3.39 (dd, J = 14.9, 8.4, 8H), 2.30 (dt, J = 58.1, 7.4, 2H), 1.90 (s, 0H), 1.74 – 1.38 (m, 46H), 1.24 (s, 14H), 0.86 (t, J = 6.8, 3H). ^{13}C NMR (126 MHz, CDCl3, mixture of rotamers) δ 174.4, 171.0, 170.0, 169.8, 169.1, 163.7, 163.7, 156.5, 156.4, 153.5, 153.5, 83.4, 79.6, 50.6, 50.5, 49.5, 48.4, 41.2, 40.5, 40.3, 33.1, 32.1, 29.8, 29.7, 29.7, 29.6, 29.5, 28.5, 28.3, 26.6, 26.6, 26.3, 26.2, 25.9, 25.4, 22.9, 14.3.

C11-*N*HarGly*N*Har

^{1}H NMR (500 MHz, MeOD, mixture of rotamers) δ 4.24 – 3.98 (m, 6H), 3.53 – 3.37 (m, 4H), 3.26 – 3.11 (m, 4H), 2.46 (t, J = 7.5, 1H), 2.34 (t, J = 7.5, 1H), 1.79 – 1.50 (m, 10H), 1.40 – 1.23 (m, 14H), 0.90 (t, J = 6.8, 3H). ^{13}C NMR (126 MHz, MeOD, mixture of rotamers) δ 177.0, 177.0, 176.4, 173.8, 173.1, 173.0, 172.0, 171.9, 171.8, 171.7, 171.7, 171.6, 171.2, 171.0, 158.8, 158.8, 51.8, 50.8, 50.7, 50.4, 50.3, 50.3, 48.4, 47.9, 42.3, 42.3, 42.2, 42.2, 42.0, 34.3, 33.9, 33.2, 30.9, 30.8, 30.8, 30.8, 30.6, 30.6, 28.3, 27.2, 27.2, 27.1, 26.9, 26.7, 26.6, 26.5, 26.5, 25.7, 25.7, 25.6, 24.4, 23.9, 14.6. MS (ES) Calc. for $C_{27}H_{55}N_{10}O_4$ $(M+H)^+$: 583.4. Found 583.8.

C14-*N*HarGly*N*Har NBoc

^{1}H NMR (500 MHz, CDCl3, mixture of rotamers) δ 11.55 – 11.35 (m, 2H), 8.45 – 8.22 (m, 2H), 7.22 – 5.57 (m, 3H), 4.21 – 3.86 (m, 6H), 3.52 – 3.27 (m, 8H), 2.42 – 2.12 (m, 2H), 1.76 – 1.38 (m, 46H), 1.38 – 1.14 (m, 20H), 0.86 (t, J = 6.9, 3H). ^{13}C NMR (126 MHz, CDCl3, mixture of rotamers) δ 174.3, 171.0, 169.8, 169.6, 169.1, 163.7, 163.6, 156.4, 156.4, 153.5, 153.5, 153.4, 83.4, 79.6, 50.5, 50.4, 49.4, 48.4, 47.1, 47.0, 47.0, 41.4, 41.2, 40.4, 40.3, 33.1, 32.1, 29.9, 29.8, 29.7, 29.7, 29.6, 29.5, 28.5, 28.3, 26.6, 26.6, 26.3, 25.9, 25.4, 22.9, 14.3.

C14-*N*HarGly*N*Har

^{1}H NMR (500 MHz, MeOD, mixture of rotamers) δ 4.27 – 3.97 (m, 6H), 3.51 – 3.38 (m, 4H), 3.24 – 3.11 (m, 4H), 2.45 (t, J = 7.4, 1H), 2.33 (t, J = 7.4, 1H), 1.75 – 1.49 (m, 10H), 1.29 (s, 20H), 0.90 (t, J = 6.7, 3H). ^{13}C NMR (126 MHz, MeOD, mixture of rotamers) δ 177.0, 177.0, 176.4, 173.8, 173.1, 173.0, 172.0, 171.9, 171.8, 171.7, 171.7, 171.6, 171.2, 171.0, 158.8, 158.8, 51.8, 50.7, 50.7, 50.4, 50.4, 50.3, 50.3, 50.0, 48.6, 48.4, 47.9, 42.3, 42.3, 42.2, 42.2, 42.0, 34.3, 33.9, 33.2, 30.9, 30.9, 30.8, 30.8, 30.8, 30.6, 30.6, 27.2, 27.2, 27.2, 27.1, 26.9, 26.7, 26.6, 26.5, 26.5, 25.7, 25.7, 25.6, 23.9, 14.6. MS (ES) Calc. for $C_{30}H_{61}N_{10}O_4$ $(M+H)^+$: 625.5. Found 625.9.

C16-*N*HarGly*N*Har NBoc

^{1}H NMR (500 MHz, MeOD, mixture of rotamers) δ 4.26 – 3.97 (m, 6H), 3.52 – 3.33 (m, 8H), 2.39 (dt, J = 57.7, 7.5, 2H), 1.76 – 1.40 (m, 46H), 1.40 – 1.20 (m, 24H), 0.90 (t, J = 6.9, 3H). ^{13}C NMR (126 MHz, MeOD, mixture of rotamers) δ 176.4, 173.9, 171.9, 171.6, 171.3, 171.1, 171.0, 164.7, 157.8, 157.7, 154.3, 84.6, 84.5, 80.5, 80.4, 50.3, 50.3, 50.2, 50.1, 48.2, 42.2, 42.1, 41.7, 41.7,

41.4, 41.4, 34.3, 33.8, 33.2, 31.0, 30.9, 30.8, 30.7, 30.6, 30.6, 28.8, 28.4, 27.7, 27.7, 27.6, 27.5, 27.5, 27.0, 26.9, 26.7, 26.6, 26.5, 25.9, 25.8, 23.9, 14.6.

C16-*N*HarGly*N*Har

^{1}H NMR (300 MHz, MeOD, mixture of rotamers) δ 4.27 – 3.98 (m, 6H), 3.54 – 3.38 (m, 4H), 3.29 – 3.13 (m, 4H), 2.48 (t, J = 7.5, 1H), 2.36 (t, J = 7.4, 1H), 1.80 – 1.51 (m, 10H), 1.31 (s, 24H), 0.93 (t, J = 6.7, 3H). ^{13}C NMR (126 MHz, MeOD, mixture of rotamers) δ 177.1, 177.0, 176.4, 173.8, 173.1, 173.0, 172.0, 171.9, 171.8, 171.7, 171.7, 171.6, 171.2, 171.0, 158.8, 158.8, 51.8, 51.8, 50.8, 50.7, 50.4, 50.4, 50.3, 50.3, 48.4, 47.9, 42.3, 42.3, 42.3, 42.2, 42.0, 34.3, 33.9, 33.2, 30.9, 30.9, 30.8, 30.8, 30.8, 30.6, 30.6, 27.2, 27.2, 27.1, 26.9, 26.7, 26.6, 26.5, 26.5, 25.7, 25.7, 25.6, 23.9, 14.6. MS (ES) Calc. for $C_{32}H_{65}N_{10}O_4$ $(M+H)^+$: 653.5. Found 653.8.

C20-*N*HarGly*N*Har r NBoc

^{1}H NMR (500 MHz, CDCl3, mixture of rotamers) δ 11.48 (d, J = 10.3, 2H), 8.58 – 8.15 (m, 2H), 7.22 – 5.51 (m, 3H), 4.28 – 3.85 (m, 6H), 3.57 – 3.17 (m, 8H), 2.46 – 2.26 (m, 2H), 1.72 – 1.40 (m, 46H), 1.40 – 1.07 (m, 32H), 0.87 (t, J = 6.9, 3H). ^{13}C NMR (126 MHz, CDCl3, mixture of rotamers) δ 174.4, 174.3, 173.9, 171.0, 170.7, 170.0, 169.9, 169.7, 169.1, 168.7, 168.6, 163.7, 163.7, 156.5, 156.4, 153.5, 153.5, 153.5, 83.4, 79.6, 51.8, 50.6, 50.6, 50.4, 50.2, 49.5, 49.2, 48.5, 48.3, 47.1, 47.0, 41.5, 41.2, 40.8, 40.5, 40.4, 40.3, 40.2, 33.5, 33.2, 32.1, 31.4, 29.9, 29.9, 29.9, 29.8, 29.7, 29.7, 29.6, 29.6, 28.5, 28.3, 26.8, 26.6, 26.3, 26.2, 25.9, 25.5, 25.3, 25.2, 24.9, 22.9, 14.3. MS (ES) Calc. for $C_{56}H_{104}N_{10}NaO_{12}$ $(M+Na)^+$: 1131.8. Found 1132.4.

C20-*N*HarGly*N*Har

^{1}H NMR (500 MHz, MeOD, mixture of rotamers) δ 4.26 – 3.95 (m, 6H), 3.53 – 3.38 (m, 4H), 3.26 – 3.11 (m, 4H), 2.45 (t, J = 7.5, 1H), 2.33 (t, J = 7.5, 1H), 1.76 – 1.48 (m, 10H), 1.48 – 1.11 (m, 32H), 0.90 (t, J = 6.8, 3H). ^{13}C NMR (126 MHz, MeOD, mixture of rotamers) δ 177.1, 177.0, 176.4, 173.8, 173.1, 172.0, 171.9, 171.8, 171.7, 171.7, 171.6, 171.2, 171.0, 158.8, 158.8, 51.8, 51.8, 50.8, 50.8, 50.7, 50.4, 50.4, 50.3, 50.3, 50.3, 47.9, 42.3, 42.3, 42.3, 42.0, 34.3, 33.9, 33.2, 30.9, 30.9, 30.8, 30.8, 30.8, 30.6, 30.6, 30.6, 27.3, 27.2, 27.2, 27.2, 27.1, 26.9, 26.7, 26.6, 26.5, 26.5, 25.7, 25.7, 25.7, 23.9, 14.6. MS (ES) Calc. for $C_{36}H_{73}N_{10}O_4$ $(M+H)^+$: 709.6. Found 710.0.

F11-*N*HarGly*N*Har Nboc

^{1}H NMR (500 MHz, CDCl3, mixture of rotamers) δ 11.65 – 11.34 (m, 2H), 8.37 (s, 2H), 7.18 – 5.50 (m, 3H), 4.24 – 3.90 (m, 6H), 3.54 – 3.29 (m, 8H), 2.75 – 2.64 (m, 2H), 2.64 – 2.43 (m, 2H), 1.79 – 1.35 (m, 44H). ^{13}C NMR (126 MHz, CDCl3, mixture of rotamers) δ 171.0, 171.0, 170.9, 170.9, 170.7, 170.0, 169.2, 169.1, 168.8, 168.7, 168.5, 163.7, 163.7, 156.5, 156.5, 156.4, 153.6, 153.5, 153.5, 83.5, 79.7, 79.6, 51.4, 50.5, 50.4, 50.3, 50.2, 49.3, 49.0, 48.4, 48.3, 47.5, 47.3, 46.9, 41.5, 41.2, 40.7, 40.4, 40.2, 40.2, 29.9, 29.8, 28.5, 28.5, 28.5, 28.3, 28.2, 28.2, 28.1, 27.1, 26.9, 26.6, 26.6, 26.1, 26.0, 25.9, 25.1, 25.0, 24.8, 24.5, 24.2. MS (ES) Calc. for $C_{47}H_{69}F_{17}N_{10}NaO_{12}$ $(M+Na)^+$: 1311.5. Found 1312.3.

F11-*N*HarGly*N*Har

^{1}H NMR (500 MHz, MeOD, mixture of rotamers) δ 4.27 – 3.94 (m, 6H), 3.53 – 3.39 (m, 4H), 3.26 – 3.12 (m, 4H), 2.86 – 2.78 (m, 1H), 2.71 (d, J = 6.4, 1H), 2.55 (dd, J = 16.8, 9.9, 2H), 1.65 (dd, J =

33.6, 19.8, 8H). ^{13}C NMR (126 MHz, MeOD, mixture of rotamers) δ 173.8, 173.8, 173.7, 173.7, 173.1, 173.0, 172.9, 171.9, 171.9, 171.7, 171.7, 171.5, 171.4, 171.2, 171.0, 158.8, 158.8, 51.7, 50.8, 50.7, 50.5, 50.5, 50.3, 50.3, 50.1, 50.0, 48.5, 48.4, 48.4, 42.3, 42.3, 42.2, 42.1, 42.0, 27.8, 27.7, 27.3, 27.2, 27.2, 27.1, 26.7, 26.7, 26.7, 25.7, 25.7, 25.3, 25.1. MS (ES) Calc. for $C_{77}H_{39}F_{17}N_{10}O_{12}$ $(M+2H)^{2+}$: 445.3. Found 445.5.

C11-*N*Lys*N*Lys*N*Lys

^{1}H NMR (500 MHz, MeOD, mixture of rotamers) δ 4.52 – 3.99 (m, 6H), 3.55 – 3.33 (m, 6H), 3.05 – 2.87 (m, 6H), 2.50 – 2.39 (m, 1H), 2.30 – 2.16 (m, 1H), 1.80 – 1.48 (m, 14H), 1.41 – 1.22 (m, 14H), 0.90 (t, J = 6.9, 3H).^{13}C NMR (126 MHz, MeOD, mixture of rotamers) δ 177.5, 177.5, 177.2, 176.3, 173.0, 172.1, 172.1, 171.6, 171.4, 51.0, 50.3, 47.8, 40.5, 40.2, 34.3, 33.9, 33.2, 30.8, 30.8, 30.6, 27.0, 26.6, 26.6, 26.5, 26.4, 26.0, 25.9, 25.9, 25.8, 25.8, 25.7, 25.6, 25.4, 25.3, 23.9, 14.6. MS (ES) Calc. for $C_{29}H_{60}N_7O_4$ $(M+H)^{+}$: 570.5. Found 570.6.

C14-*N*Lys*N*Lys*N*Lys

^{1}H NMR (500 MHz, MeOD, mixture of rotamers) δ 4.51 – 3.98 (m, 6H), 3.51 – 3.32 (m, 6H), 3.06 – 2.85 (m, 6H), 2.51 – 2.37 (m, 1H), 2.28 – 2.15 (m, 1H), 1.78 – 1.45 (m, 14H), 1.45 – 1.19 (m, 20H), 0.90 (t, J = 6.9, 3H). ^{13}C NMR (126 MHz, MeOD, mixture of rotamers) δ 177.5, 176.2, 173.7, 173.0, 173.0, 172.1, 172.1, 171.6, 171.4, 171.1, 171.0, 170.6, 51.1, 50.3, 47.8, 40.6, 40.5, 40.5, 40.4, 34.3, 34.2, 33.9, 33.2, 30.9, 30.9, 30.8, 30.6, 26.6, 26.6, 26.5, 26.5, 26.5, 26.4, 26.0, 25.9, 25.9, 25.9, 25.8, 25.8, 25.6, 25.5, 23.9, 14.6. MS (ES) Calc. for $C_{32}H_{66}N_7O_4$ $(M+H)^{+}$: 612.5. Found 612.7.

C16-*N*Lys*N*Lys*N*Lys

^{1}H NMR (500 MHz, MeOD, mixture of rotamers) δ 4.51 – 3.97 (m, 6H), 3.50 – 3.33 (m, 6H), 3.07 – 2.89 (m, 6H), 2.49 – 2.37 (m, 1H), 2.29 – 2.14 (m, 1H), 1.81 – 1.49 (m, 14H), 1.28 (s, 24H), 0.90 (t, J = 6.9, 3H). ^{13}C NMR (126 MHz, MeOD, mixture of rotamers) δ 177.5, 177.5, 177.2, 176.2, 173.4, 173.3, 173.0, 172.1, 172.1, 171.6, 171.6, 171.4, 170.9, 170.7, 170.6, 51.0, 50.4, 50.3, 50.2, 47.8, 40.6, 40.6, 40.5, 40.5, 40.4, 34.3, 34.2, 33.9, 33.8, 33.2, 30.9, 30.9, 30.8, 30.6, 29.1, 26.6, 26.6, 26.5, 26.4, 26.4, 26.0, 25.9, 25.9, 25.8, 25.8, 25.6, 25.6, 25.4, 25.4, 25.3, 23.9, 14.6. MS (ES) Calc. for $C_{34}H_{70}N_7O_4$ $(M+H)^+$: 640.5. Found 640.8.

C20-*N*Lys*N*Lys*N*Lys

^{1}H NMR (500 MHz, MeOD, mixture of rotamers) δ 4.53 – 3.97 (m, 6H), 3.51 – 3.33 (m, 6H), 3.06 – 2.87 (m, 6H), 2.48 – 2.39 (m, 1H), 2.27 – 2.17 (m, 1H), 1.80 – 1.47 (m, 14H), 1.31 (s, J = 25.5, 32H), 0.90 (t, J = 7.0, 3H). ^{13}C NMR (126 MHz, MeOD, mixture of rotamers) δ 177.5, 177.4, 177.2, 176.2, 176.2, 176.2, 176.1, 172.1, 172.1, 171.6, 171.4, 51.0, 50.8, 50.8, 50.7, 50.3, 47.8, 40.6, 40.6, 40.5, 40.5, 40.4, 34.3, 34.2, 34.2, 33.9, 33.9, 33.8, 33.2, 30.9, 30.9, 30.8, 30.8, 30.6, 26.6, 26.6, 26.6, 26.5, 26.5, 26.4, 26.0, 25.9, 25.9, 25.9, 25.8, 25.8, 25.6, 25.4, 23.9, 14.6. MS (ES) Calc. for $C_{38}H_{78}N_7O_4$ $(M+H)^+$: 696.6. Found 696.9.

F11-*N*Lys*N*Lys*N*Lys

^{1}H NMR (500 MHz, MeOD, mixture of rotamers) δ 4.55 – 3.93 (m, 6H), 3.54 – 3.34 (m, 6H), 3.06 – 2.89 (m, 6H), 2.86 – 2.76 (m, 1H), 2.70 – 2.37 (m, 3H), 1.85 – 1.51 (m, 12H). MS (ES) Calc. for $C_{29}H_{43}F_{17}N_7O_4$ $(M+H)^+$: 876.3. Found 876.6.

C11-*N*Har*N*Har*N*Har NBoc

^{1}H NMR (500 MHz, CDCl3, mixture of rotamers) δ 11.49 (s, 3H), 8.35 (s, 3H), 4.53 – 3.86 (m, 6H), 3.44 (s, 12H), 2.46 – 2.18 (m, 2H), 1.80 – 1.01 (m, 82H), 0.95 – 0.78 (m, 3H). ^{13}C NMR (126 MHz, CDCl3, mixture of rotamers) δ 163.8, 156.4, 156.4, 153.6, 153.5, 148.9, 83.6, 83.4, 83.4, 79.6, 79.6, 79.5, 50.9, 49.5, 49.3, 48.8, 47.9, 47.4, 46.9, 40.5, 40.5, 40.3, 40.2, 33.0, 32.1, 31.5, 29.8, 29.7, 29.5, 28.5, 28.3, 28.2, 26.8, 26.7, 26.6, 26.2, 26.1, 25.4, 24.9, 22.9, 14.3.

C11-*N*Har*N*Har*N*Har

^{1}H NMR (500 MHz, MeOD, mixture of rotamers) δ 4.52 – 3.96 (m, 6H), 3.51 – 3.33 (m, 6H), 3.27 – 3.08 (m, 6H), 2.43 (t, J = 7.4, 1H), 2.28 – 2.17 (m, 1H), 1.78 – 1.45 (m, 14H), 1.45 – 1.10 (m, 14H), 0.90 (t, J = 6.8, 3H). ^{13}C NMR (126 MHz, MeOD, mixture of rotamers) δ 177.6, 176.2, 173.8, 173.1, 172.1, 171.7, 171.6, 171.4, 171.1, 170.7, 170.6, 158.9, 158.8, 158.8, 51.0, 50.7, 50.5, 50.4, 47.9, 47.9, 42.4, 42.3, 42.1, 34.3, 34.3, 33.9, 33.2, 33.2, 27.2, 26.8, 26.7, 26.6, 25.9, 25.7, 25.7, 25.6, 23.9, 14.6. MS (ES) Calc. for $C_{32}H_{63}N_{13}O_4$ $(M+H)^+$: 696.5. Found 696.9.

C14-*N*Har*N*Har*N*Har NBoc

^{1}H NMR (500 MHz, CDCl3, mixture of rotamers) δ 11.47 (s, 2H), 8.84 (s, 1H), 8.33 (d, J = 4.0, 3H), 4.43 – 3.86 (m, 6H), 3.50 – 3.25 (m, 12H), 2.31 (d, J = 7.7, 2H), 1.78 – 1.31 (m, 68H), 1.31 – 1.10 (m, 20H), 0.85 (t, J = 6.9, 3H). ^{13}C NMR (126 MHz, CDCl3, mixture of rotamers) δ 173.7, 171.6, 169.4, 163.7, 163.7, 156.4, 153.5, 153.5, 153.4, 83.5, 83.3, 83.3, 79.5, 79.5, 50.8, 48.7, 40.5, 32.9, 32.1, 29.8, 29.8, 29.7, 29.7, 29.6, 29.5, 28.4, 28.2, 28.1, 28.0, 26.6, 25.3, 22.8, 14.3.

C14-*N*Har*N*Har*N*Har

^{1}H NMR (500 MHz, MeOD, mixture of isomers) δ 4.52 – 4.00 (m, 6H), 3.51 – 3.33 (m, 6H), 3.26 – 3.11 (m, 6H), 2.52 – 2.35 (m, 1H), 2.30 – 2.14 (m, 1H), 1.88 – 1.47 (m, 14H), 1.29 (s, 20H), 0.90 (t, J = 6.8, 3H). ^{13}C NMR (126 MHz, MeOD, mixture of rotamers) δ 177.6, 177.6, 177.3, 177.3, 176.9, 176.3, 176.2, 176.2, 173.9, 173.8, 173.4, 173.4, 173.1, 172.2, 172.2, 172.1, 172.1, 171.7, 171.6, 171.5, 171.1, 171.1, 171.0, 170.9, 170.9, 170.8, 170.7, 170.6, 158.9, 158.8, 51.0, 50.8, 50.7, 50.5, 50.4, 50.3, 50.1, 48.5, 48.1, 47.9, 42.4, 42.3, 42.3, 42.3, 41.9, 34.3, 34.3, 33.9, 33.2, 30.9, 30.8, 30.6, 29.4, 27.4, 27.3, 27.2, 27.2, 27.1, 27.1, 27.0, 26.9, 26.8, 26.8, 26.7, 26.6, 26.5, 26.4, 25.9, 25.9, 25.8, 25.7, 25.7, 25.7, 25.6, 23.9, 14.6. MS (ES) Calc. for $C_{35}H_{72}N_{13}O_4$ $(M+H)^+$: 738.6. Found 739.0.

C16-*N*Har*N*Har*N*Har Nboc

^{1}H NMR (500 MHz, CDCl3, mixture of isomers) δ 11.48 (s, 3H), 8.34 (s, 3H), 4.08 (d, J = 71.3, 6H), 3.41 (d, J = 22.4, 12H), 2.32 (s, 2H), 1.53 (d, J = 50.1, 92H), 0.87 (s, 3H). ^{13}C NMR (126 MHz, CDCl3, mixture of isomers) δ 163.7, 156.5, 156.4, 156.4, 156.3, 153.5, 153.5, 153.4, 83.4, 83.3,

79.6, 79.5, 50.8, 49.5, 49.2, 48.8, 40.5, 33.0, 32.1, 29.9, 29.7, 29.7, 29.6, 28.5, 28.3, 28.2, 28.1, 26.7, 26.6, 26.1, 25.4, 22.9, 14.3.

C16-*N*Har*N*Har*N*Har

^{1}H NMR (500 MHz, MeOD, mixture of rotamers) δ 4.50 – 3.96 (m, 6H), 3.51 – 3.34 (m, 6H), 3.25 – 3.13 (m, 6H), 2.50 – 2.36 (m, 1H), 2.30 – 2.18 (m, 1H), 1.82 – 1.46 (m, 14H), 1.46 – 1.21 (m, 24H), 0.90 (t, J = 6.9, 3H). ^{13}C NMR (126 MHz, MeOD, mixture of rotamers) δ 177.6, 177.6, 176.3, 176.2, 176.2, 173.4, 173.4, 173.1, 172.2, 172.1, 172.1, 171.6, 171.5, 171.1, 171.1, 171.0, 170.9, 170.9, 170.8, 170.7, 170.6, 158.8, 158.8, 67.0, 51.0, 50.7, 50.5, 50.4, 50.3, 48.1, 47.9, 42.4, 42.4, 42.3, 42.3, 34.3, 34.3, 33.9, 33.2, 31.0, 30.9, 30.8, 30.8, 30.6, 27.4, 27.3, 27.2, 27.1, 26.9, 26.8, 26.7, 26.7, 26.6, 26.5, 26.4, 25.9, 25.7, 25.7, 25.6, 23.9, 14.6. MS (ES) Calc. for $C_{37}H_{76}N_{13}O_4$ $(M+H)^+$: 766.6. Found 767.0.

C20-*N*Har*N*Har*N*Har Nboc

^{1}H NMR (500 MHz, CDCl3, mixture of rotamers) δ 11.47 (s, 3H), 8.53 – 8.05 (m, 3H), 4.31 – 3.86 (m, 6H), 3.54 – 3.24 (m, 12H), 2.26 (dd, J = 62.9, 55.2, 2H), 1.85 – 1.04 (m, 100H), 0.86 (t, J = 6.8, 3H). ^{13}C NMR (126 MHz, CDCl3, mixture of rotamers) δ 173.5, 169.4, 169.2, 163.5, 156.2, 153.3, 153.3, 83.2, 83.1, 79.4, 79.3, 51.1, 50.7, 49.3, 49.1, 49.1, 48.6, 48.6, 47.7, 47.2, 46.8, 40.4, 40.4, 40.3, 40.3, 40.3, 40.1, 40.1, 40.0, 32.8, 32.8, 31.9, 31.9, 29.8, 29.8, 29.7, 29.7, 29.7, 29.7, 29.6, 29.6, 29.6, 29.6, 29.5, 29.5, 29.4, 29.4, 28.3, 28.3, 28.1, 28.1, 28.0, 28.0, 26.6, 26.5, 26.5, 26.4, 25.9, 25.9, 25.2, 25.2, 22.7, 22.7, 14.1, 14.1.

C20-*N*Har*N*Har*N*Har

^{1}H NMR (500 MHz, MeOD, mixture of rotamers) δ 4.51 – 4.00 (m, 6H), 3.48 – 3.34 (m, 6H), 3.27 – 3.15 (m, 6H), 2.48 – 2.37 (m, 1H), 2.27 – 2.18 (m, 1H), 1.80 – 1.46 (m, 14H), 1.42 – 1.21 (m, 32H), 0.90 (t, J = 6.9, 3H). ^{13}C NMR (126 MHz, MeOD, mixture of rotamers) δ 177.6, 176.3, 176.2, 176.2, 173.4, 173.4, 173.1, 172.1, 171.6, 171.5, 171.1, 171.1, 158.8, 158.8, 67.1, 51.0, 50.5, 50.3, 47.9, 42.4, 42.3, 42.3, 34.3, 34.3, 33.9, 33.2, 30.9, 30.9, 30.8, 30.8, 30.6, 30.6, 27.4, 27.3, 27.2, 26.8, 26.7, 26.6, 26.4, 25.9, 25.8, 25.7, 25.6, 23.9, 14.6. MS (ES) Calc. for $C_{41}H_{85}N_{13}O_4$ - $(M+H)^{2+}$: 411.9. Found 412.1.

11.5 References

1. Zhanel GG, DeCorby M, Laing N, Weshnoweski B, Vashisht R, Tailor F, et al. Antimicrobial-resistant pathogens in intensive care units in canada: Results of the canadian national intensive care unit (CAN-ICU) study, 2005-2006. Antimicrob Agents Chemother. 2008 Apr;52(4):1430-7.

2. Zhanel GG, Adam HJ, Low DE, Blondeau J, Decorby M, Karlowsky JA, et al. Antimicrobial susceptibility of 15,644 pathogens from canadian hospitals: Results of the CANWARD 2007-2009 study. Diagn Microbiol Infect Dis. 2011 Mar;69(3):291-306.

3. Rennie RP, Callihan DR, Barry AL, Krisher K, Munro SD, Sei K, et al. Protocols for evaluating dehydrated mueller-hinton agar; approved standard-second edition. In: CLSI; 2006. p. 1-29.

4. Dathe M, Schumann M, Wieprecht T, Winkler A, Beyermann M, Krause E, et al. Peptide helicity and membrane surface charge modulate the balance of electrostatic and hydrophobic

interactions with lipid bilayers and biological membranes. Biochemistry. 1996 Sep 24;35(38):12612-22.

5. Chongsiriwatana NP, Patch JA, Czyzewski AM, Dohm MT, Ivankin A, Gidalevitz D, et al. Peptoids that mimic the structure, function, and mechanism of helical antimicrobial peptides. Proc Natl Acad Sci U S A. 2008 Feb 26;105(8):2794-9.

6. Gottlieb HE, Kotlyar V, Nudelman A. NMR chemical shifts of common laboratory solvents as trace impurities. J Org Chem. 1997 Oct 17;62(21):7512-5.

Chapter 12: Supporting Information for Chapter 5

By Brandon Findlay, Neeloffer Mookherjee and Frank Schweizer. First published as a supplement to Chapter 5; PLOS ONE, 2013, e54280. Reproduced with permission.

12.1 General Chemical Procedures

Reagents and solvents were purchased from commercially available sources and used without purification, unless otherwise noted. Fluorinated carboxylic acids were purchased from Fluorous Technologies Incorporated. Flash chromatography was performed using silica gel (Silicycle 23 -60 um) using standard techniques. ^{1}H and ^{13}C NMR were recorded on a Bruker AMX-500 or Bruker AMX-300 spectrometer in the noted solvents. Chemical shifts (δ) are reported in parts per million relative to tetramethylsilane. Peptides were prepared according to standard techniques (1), with modifications from procedure as documented below. Compounds were visualized with either a mix of ninhydrin and acetic acid in ethanol, after spotting onto glass backed TLC plates. Low-resolution mass spectra (ESI+) were obtained on a Varian 500-MS IT Mass Spectrometer. All compounds were determined to be ≥90% pure by NMR prior to bacterial testing. Rink Amide MBHA resin was used to prepare each peptide and was swelled in DMF for a minimum of thirty minutes prior to initial deprotection.

12.2 t-Butyl (4-aminobutyl)carbamate Synthesis

To a rapidly stirring solution of 1,4-diaminobutane (34.0 mL, 3 eq) and triethylamine (25.0 mL) in ice cold methanol (225 mL) was added a solution of Boc anhydride (24.9 g, 1 eq) in

methanol (50 mL) over a period of 1 hr. The solution was allowed to gradually warm to room temperature and stir overnight. The methanol and triethylamine was then removed, and water added. Acetic acid was added (6.5 mL, 1.1 eq), and the solution extracted twice with diethyl ether. The aqueous layer was then basified with sodium carbonate and extracted twice with DCM. The DCM layers were combined, washed with 10% $NaCO_3$, and concentrated. t-Butyl (4-aminobutyl)carbamate was obtained as a light yellow oil and used without further purification (10.4g, 49%).

12.2.1 Fmoc Deprotection

To remove the Fmoc protecting group, DMF:Piperidine (4:1) was added to pre-swelled resin, until it reached a level approximately three times the height of the bead bed, and the beads were gently agitated by a steady stream of air for forty minutes. The DMF:Piperidine mixture was then drained and the deprotecting process was repeated. The beads were then washed successively three times with DMF, then DCM, then DMF again, and a small sample of the beads was removed. This sample was treated with equal volumes of 2% chloranil and 2% acetaldehyde in DMF and successful deprotection was observed by the beads turning bright red.

12.2.2 Amino Acid Coupling

To freshly deprotected beads was added a solution containing the Fmoc protected amino acid derivative (3 equivalents), TBTU (3 equivalents) and Hunig's Base (8 equivalents) in DMF. The mixtures were premixed at least three minutes prior to addition to ensure effective activation of the carboxylic acids. The solution was then gently agitated for at least three hours, after which time the solvent was drained and the beads were successively washed with 3x DMF,

DCM and DMF. Completion of the reaction was verified through the chloranil test, as successfully reacted beads would not change colour in the presence of equal quantities of 2% chloranil and 2% acetaldehyde in DMF.

12.2.3 Peptoid Residue Synthesis

Following established procedure,(2) to the Rink Amide peptoid containing resin was added diisopropylcarbodiimide (DIC) (16.6 equivalents) and 2-bromoacetic acid (20 equivalents) in DMF. The mixture was agitated with a constant flow of N_2 gas for thirty minutes, during which time a light yellow foam developed. The reaction mixture was then removed via filtration, and the resin washed three times successively with DMF, DCM and DMF. A solution of tert-butyl (4-aminobutyl)carbamate (20 equivalents) in NMP was then added and the beads once more agitated by nitrogen gas, now for ninety minutes. Once again the reaction mixture was filtered away and the beads were washed three times successively with NMP, DCM and DMF. Complete reaction of free amines was verified through a chloranil test, and the synthesis was carried forward with new residues as appropriate.

12.2.4 Carboxylic Acid Coupling

As in the elongation of the amino acid chain, hydrophobic tails were attached to the resin through the use of a mixture containing the carboxylic acid (3 equivalents), TBTU (3 equivalents) and Hunig's Base (8 equivalents) in DMF. Over the course of the syntheses it was found that activated, fluorous carboxylic acids have extremely poor solubility in DMF, leading to the formation of a thick gel. As a result, these compounds were instead premixed in DCM, and Pybop (3 equivalents) was used as the activating agent. The quantity of Hunig's base was

unchanged (8 equivalents). Once the coupling mix was added the beads were gently agitated for approximately three hours, after which the chloranil test demonstrated that the coupling was complete.

12.2.5 Cleavage from Rink Amide MBHA Resin

Resin containing the fully protected, complete amino acids was rinsed three times with DCM to remove any residual DMF and dried. Residual DMF was found to interact with the TFA, forming a liquid which could not be removed even under low pressure (>0.001 Torr) using a dry-ice equipped rotary evaporator. An acidic solution of TFA:Water:TIPS (95:2.5:2.5) was then added and the beads were agitated for a minimum of two hours. The TFA was then filtered off and concentrated via evaporation under reduced pressure to yield the crude lipopeptides.

12.2.6 Purification of Lipopeptides and Lipopeptoids

Peptides were taken up in a minimum quantity of water and loaded onto a column containing reverse phase flash silica. The peptides were then eluted by washing the column successively with distilled water (2.5 CV), 50% MeOH in water (2 CV), 75% MeOH in water (2 CV) and MeOH (3 CV). All solvents were stored in glass bottles, and acidified to a concentration of 0.1% TFA. After three or more peptides had been purified with the column the column was washed with DCM and 1% TFA in MeOH. Fractions containing the peptides of interest were collected and the solvent was removed via the steady passage of air at atmospheric pressure. Residual solvents were removed by prolonged (>3 days) exposure to high vacuum.

12.2.7 Guanidinylation Reaction

Following established procedure,(3) full length peptides and peptoids of interest were dissolved in a mixture of 1,4-dioxane and water. N′,N′′-diboc-N-triflylguanidine (3 eq per amine) and triethylamine (1.5 eq per amine) were then added, and the mixture was stirred at room temperature for 3-4 days. The dioxane was then removed under reduced pressure and the mixture was extracted three times with $CHCl_3$. The organic layer was washed once with brine and dried over anhydrous sodium sulfate to yield the crude NBoc protected peptides and peptoids. Flash chromatography in 9:1 DCM:MeOH provided the pure Nboc protected amphiphiles as white solids.

Cleavage of the Boc protecting groups was effected by stirring the compounds in 9:1 TFA:H_2O for one hour. Residual polar functionalities were removed via trituration in 49:1 Et_2O:MeOH to give the desired compounds as clear oils, following prolonged exposure to high vacuum.

12.3 **Spectral Data for Newly Synthesized Compounds.**

C16-LysGlyLys (1)

^{1}H NMR (500 MHz, MeOD) δ 4.34 (dd, J = 9.6, 4.7, 1H), 4.22 (dd, J = 8.1, 6.2, 1H), 3.96 – 3.81 (m, 2H), 3.01 – 2.84 (m, 4H), 2.33 – 2.17 (m, 2H), 1.97 – 1.38 (m, 14H), 1.38 – 1.21 (m, 24H), 0.90 (t, J = 7.0, 3H). ^{13}C NMR (126 MHz, MeOD) δ 176.9, 176.8, 175.4, 171.7, 55.3, 54.3, 43.8, 40.5, 40.5, 36.7, 33.1, 32.2, 31.9, 30.8, 30.8, 30.7, 30.5, 30.5, 30.4, 28.1, 27.9, 26.8, 23.8, 23.8, 23.7, 14.5. MS (ES) Calc. for $C_{30}H_{61}N_6O_4$ $(M+H)^+$: 569.5. Found 569.7.

C16OH-LysGlyLys (2)

^{1}H NMR (500 MHz, MeOD, mixture of rotamers) δ 4.38 – 4.27 (m, 2H), 4.19 (dd, J = 8.1, 6.2, 1H), 3.93 – 3.79 (m, 2H), 3.50 (t, J = 6.7, 1H), 2.95 – 2.83 (m, 4H), 2.29 – 2.17 (m, 2H), 1.93 – 1.18 (m, 38H). ^{13}C NMR (126 MHz, MeOD) δ 177.0, 176.9, 175.5, 171.8, 63.2, 55.4, 54.4, 43.9, 40.6, 40.6, 36.8, 33.8, 32.4, 32.0, 31 – 30.5 m, aliphatic carbons), 30.3, 29.3, 28.2, 28.0, 27.1, 26.9, 26.8, 23.9, 23.9. MS (ES) Calc. for $C_{30}H_{61}N_6O_5$ $(M+H)^+$: 585.5. Found 585.7.

C20-LysGlyLys (3)

^{1}H NMR (500 MHz, MeOD) δ 4.42 – 4.30 (m, 1H), 4.22 (dd, J = 8.2, 6.1, 1H), 3.89 (q, J = 16.7, 2H), 3.00 – 2.86 (m, 4H), 2.26 (td, J = 7.4, 3.2, 2H), 1.97 – 1.38 (m, 14H), 1.38 – 1.21 (m, 32H), 0.95 – 0.84 (m, 3H), 0.00 (dd, J = 8.2, 6.1, 1H), 4.39 – 4.29 (m, 1H), 3.97 – 3.81 (m, 2H), 2.34 – 2.19 (m, 2H), 3.02 – 2.83 (m, 4H). ^{13}C NMR (126 MHz, MeOD) δ 176.8, 176.8, 175.3, 171.7, 55.2, 54.2, 43.7, 40.5, 40.5, 36.7, 33.1, 32.3, 31.9 – 30.4 (m, aliphatic carbons), 28.1, 27.9, 26.8, 23.8, 23.8, 23.7, 14.5. MS (ES) Calc. for $C_{34}H_{69}N_6O_4$ $(M+H)^+$: 625.5. Found 625.8.

C11-HarHarHar NBoc

^{1}H NMR (500 MHz, CDCl3) δ 11.46 (s, 3H), 8.33 (d, J = 4.1, 3H), 4.47 – 4.19 (m, 3H), 3.54 – 3.24 (m, 6H), 2.23 (t, J = 7.7, 2H), 2.01 – 1.15 (m, 88H), 0.86 (t, J = 7.0, 3H). ^{13}C NMR (75 MHz, CDCl3) δ 174.6, 173.9, 173.2, 172.7, 171.6, 156.2, 156.1, 156.1, 153.3, 153.2, 83.6, 83.4, 83.3, 54.2,

53.0, 41.1, 40.8, 40.8, 40.7, 36.5, 32.0, 29.7 – 29.4 (m, aliphatic peaks), 28.6, 28.6, 28.3, 28.1, 28.0, 25.6, 23.1, 22.7, 14.1.

C11-HarHarHar (8)

^{1}H NMR (500 MHz, D2O) δ 4.33 – 4.14 (m, 3H), 3.17 – 3.04 (m, 6H), 2.23 (t, J = 6.9, 2H), 1.86 – 1.27 (m, 20H), 1.27 – 1.13 (m, 14H), 0.79 (t, J = 6.8, 3H). ^{13}C NMR (126 MHz, D2O) δ 177.5, 176.4, 174.3, 173.7, 156.7, 156.7, 156.7, 53.6, 53.4, 53.4, 40.9, 40.9, 40.8, 35.3, 31.2, 30.5, 30.4, 30.3, 28.7, 28.5, 28.4, 28.1, 27.3, 25.3, 22.3, 22.2, 22.1, 22.1, 13.4. MS (ES) Calc. for $C_{32}H_{66}N_{13}O_4$ $(M+H)^+$: 696.5. Found 696.7.

C16-HarHarHar NBoc

^{1}H NMR (500 MHz, CDCl3) δ 11.45 (s, 3H), 8.37 (s, 3H), 4.48 – 4.21 (m, 3H), 3.50 – 3.29 (m, 6H), 2.25 (t, J = 7.6, 2H), 2.02 – 1.15 (m, 98H), 0.87 (t, J = 6.9, 3H). ^{13}C NMR (75 MHz, CDCl3) δ 174.3, 173.8, 171.5, 156.1, 156.1, 156.1, 153.2, 83.4, 83.3, 83.2, 55.7, 54.0, 52.9, 40.7, 36.4, 31.9, 31.5, 31.4, 31.4, 29.7 – 27.9 (m, aliphatic peaks), 25.6, 23.1, 22.7, 14.1.

C16-HarHarHar (9)

^{1}H NMR (500 MHz, D2O) δ 4.42 – 4.20 (m, 3H), 3.32 – 3.08 (m, 6H), 2.36 – 2.21 (m, 2H), 1.98 – 1.36 (m, 20H), 1.29 (s, 24H), 0.89 (t, J = 6.6, 3H). ^{13}C NMR (126 MHz, D2O) δ 176.3, 174.2, 173.6, 156.7, 156.7, 156.7, 53.8, 53.5, 53.4, 40.9, 40.8, 35.4, 31.5, 30.6, 30.5, 29.4 - 28.7 (m, aliphatic

peaks), 27.5, 27.4, 27.4, 25.4, 22.4, 22.3, 22.3, 22.2, 13.6. MS (ES) Calc. for $C_{37}H_{76}N_{13}O_4$ $(M+H)^+$: 766.6. Found 766.7.

C16OH-HarHarHar NBoc

^{1}H NMR (300 MHz, CDCl3) δ 11.44 (s, 3H), 8.30 (s, 3H), 4.59 – 4.22 (m, 3H), 3.61 (t, J = 6.6, 2H), 3.36 (s, 6H), 2.35 – 2.08 (m, 2H), 2.02 – 1.09 (m, 100H). ^{13}C NMR (75 MHz, CDCl3) δ 174.3, 173.9, 172.5, 171.5, 163.5, 163.4, 163.3, 156.2, 156.2, 156.1, 153.3, 83.3, 83.3, 83.2, 79.6, 79.5, 79.4, 63.1, 53.9, 53.8, 52.9, 40.8, 40.7, 40.7, 36.5, 32.9, 31.9, 31.6, 29.6, 29.5, 29.5, 29.4, 28.8, 28.7, 28.6, 28.4, 28.3, 28.2, 28.1, 25.8, 25.7, 23.1, 23.1.

C16OH-HarHarHar (10)

^{1}H NMR (500 MHz, D2O) δ 4.43 – 4.24 (m, 3H), 3.61 (t, J = 6.7, 2H), 3.26 – 3.09 (m, 6H), 2.39 – 2.17 (m, 2H), 1.95 – 1.17 (m, 44H). ^{13}C NMR (126 MHz, D2O) δ 177.0, 174.8, 174.3, 157.4, 157.4, 157.4, 62.5, 54.4, 54.2, 54.0, 41.5, 41.5, 36.1, 32.3, 31.2, 31.2, 31.1, 31.1, 30.2, 30.2, 29.9 – 29.6 (m, aliphatic peaks), 29.4, 29.2, 28.1, 28.1, 28.0, 28.0, 26.1, 26.0, 26.0, 23.0, 23.0, 22.9, 22.9, 22.8, 22.8. MS (ES) Calc. for $C_{37}H_{76}N_{13}O_5$ $(M+H)^+$: 782.6. Found 782.9.

C20-HarHarHar (11)

^{1}H NMR (500 MHz, D2O) δ 4.43 – 4.19 (m, 3H), 3.30 – 3.07 (m, 6H), 2.44 – 2.15 (m, 2H), 1.98 – 1.51 (m, 14H), 1.51 – 1.09 (m, 32H), 0.90 (t, J = 6.2, 3H). ^{13}C NMR (126 MHz, D2O) δ 176.2, 175.9, 174.1, 173.5, 156.7, 156.7, 156.7, 53.8, 53.6, 53.5, 40.8, 35.6, 31.9, 30.7, 29.8 – 29.6 (m, aliphatic

peaks), 29.4, 29.2, 27.7, 27.5, 25.6, 22.6, 22.3, 13.8. MS (ES) Calc. for $C_{41}H_{85}N_{13}O_4$ $(M+2H)^{2+}$: 411.8. Found 412.1.

C16OH-NLysNLysNLys (16)

^{1}H NMR (500 MHz, D2O, mixture of rotamers) δ 4.54 – 3.92 (m, 6H), 3.55 (t, J = 6.9, 2H), 3.50 – 3.21 (m, 6H), 3.08 – 2.90 (m, 6H), 2.48 – 2.33 (m, 1H), 2.27 – 2.10 (m, 1H), 1.89 – 1.46 (m, 16H), 1.28 (s, 22H). ^{13}C NMR (126 MHz, D2O) δ 177.1, 177.1, 176.8, 176.7, 176.1, 173.5, 173.4, 173.0, 172.8, 172.5, 172.4, 172.1, 170.9, 170.9, 170.6, 170.4, 170.3, 170.2, 170.1, 170.0, 170.0, 169.9, 169.8, 169.7, 169.3, 61.9, 49.8, 49.5, 49.4, 49.4, 49.2, 49.2, 49.0, 48.8, 48.8, 48.7, 48.3, 48.2, 48.2, 48.1, 48.0, 47.9, 47.7, 47.7, 47.6, 47.5, 47.3, 47.3, 47.1, 47.0, 46.9, 46.8, 46.8, 39.1, 39.0, 33.0, 32.9, 32.5, 32.4, 31.9, 31.8, 29.5, 29.4, 29.4, 29.3, 29.2, 29.0, 28.9, 28.8, 25.6, 25.5, 25.2, 25.1, 25.0, 25.0, 24.9, 24.9, 24.8, 24.8, 24.7, 24.6, 24.5, 24.1, 24.1, 23.8, 23.8, 23.7, 23.6, 23.5. MS (ES) Calc. for $C_{38}H_{78}N_7O_4$ $(M+H)^+$: 656.5. Found 656.7.

C16OH-$N_{Har}N_{Har}N_{Har}$ NBoc

^{1}H NMR (300 MHz, CDCl3) δ 11.50 (s, 3H), 8.38 (s, 3H), 4.08 (d, J = 42.6, 6H), 3.62 (dd, J = 7.0, 6.2, 2H), 3.44 (s, 12H), 2.32 (t, J = 7.3, 2H), 1.83 – 1.04 (m, 92H). ^{13}C NMR (75 MHz, CDCl3) δ 173.6, 171.2, 169.7, 169.1, 156.3, 156.3, 156.3, 153.4, 153.3, 83.4, 83.4, 83.3, 79.6, 79.6, 79.5, 63.1, 40.5, 32.9, 29.7, 29.6, 29.6, 29.5, 28.4, 28.2, 26.6, 26.6, 26.6, 26.5, 26.1, 25.9, 25.3.

C16OH-*N*Har*N*Har*N*Har (20)

^{1}H NMR (500 MHz, D2O, mixture of rotamers) δ 4.57 – 4.02 (m, 6H), 3.64 – 3.51 (m, 2H), 3.51 – 3.28 (m, 6H), 3.28 – 2.98 (m, 6H), 2.55 – 2.35 (m, 1H), 2.27 – 2.12 (m, 1H), 1.89 – 1.49 (m, 16H), 1.49 – 1.14 (m, 22H). ^{13}C NMR (126 MHz, D2O, mixture of rotamers) δ 176.0, 173.5, 173.4, 171.1, 170.9, 170.3, 170.1, 156.8, 156.8, 156.8, 61.9, 49.2, 48.4, 47.5, 40.8, 40.8, 32.8, 32.4, 31.8, 31.7, 29.8 – 28.6 (m, aliphatic peaks), 29.4, 29.2, 29.2, 29.0, 25.5 – 25.1 (m, aliphatic peaks), 23.9.

C7-LysGlyLys (S1)

^{1}H NMR (300 MHz, MeOD) δ 4.44 – 4.15 (m, 2H), 4.02 – 3.80 (m, 2H), 3.07 – 2.83 (m, 4H), 2.40 – 2.16 (m, 2H), 2.04 – 1.22 (m, 20H), 0.92 (t, J = 6.6, 3H). ^{13}C NMR (75 MHz, MeOD) δ 177.0, 176.9, 175.5, 171.8, 55.4, 54.4, 43.9, 40.6, 40.6, 36.8, 32.8, 32.4, 32.0, 30.2, 28.2, 28.0, 26.9, 23.9, 23.9, 23.7, 14.5. MS (ES) Calc. for $C_{21}H_{43}N_6O_4$ $(M+H)^+$: 443.3. Found 443.4.

C9B-LysGlyLys (S2)

^{1}H NMR (300 MHz, MeOD) δ 4.37 (dd, J = 9.4, 4.8, 1H), 4.24 (dd, J = 7.9, 6.3, 1H), 3.98 – 3.82 (m, 2H), 3.07 – 2.84 (m, 4H), 2.28 (t, J = 7.3, 2H), 2.04 – 1.06 (m, 23H), 0.90 (d, J = 6.6, 6H). ^{13}C NMR (75 MHz, MeOD) δ 176.8, 176.6, 174.9, 174.2, 55.1, 54.8, 54.3, 40.6, 40.6, 36.9, 32.8, 32.3, 32.3, 30.9, 30.6, 29.3, 28.6, 28.2, 28.2, 28.1, 27.1, 24.0, 23.9, 23.8, 23.2. MS (ES) Calc. for $C_{21}H_{49}N_6O_4$ $(M+H)^+$: 485.4. Found 485.4.

F9B-LysGlyLys (S3)

^{1}H NMR (300 MHz, MeOD) δ 4.37 (dd, J = 9.4, 4.7, 1H), 4.27 (dd, J = 7.9, 6.2, 1H), 4.01 – 3.83 (m, 2H), 3.03 – 2.84 (m, 4H), 2.75 – 2.38 (m, 4H), 2.00 – 1.33 (m, 12H). ^{13}C NMR (75 MHz, MeOD) δ 176.9, 175.2, 173.4, 171.8, 55.5, 54.2, 43.9, 40.6, 40.6, 32.4, 32.1, 28.3, 28.0, 27.8, 27.5 - 27.3 (m, adjacent to CF bonds), 23.9. MS (ES) Calc. for $C_{24}H_{34}F_{15}N_6O_4$ $(M+H)^+$: 755.2. Found 755.2.

F9-LysLysLys (S4)

^{1}H NMR (300 MHz, MeOD) δ 4.48 – 4.20 (m, 3H), 2.94 (dd, J = 8.4, 4.6, 6H), 2.68 – 2.37 (m, 4H), 2.02 – 1.29 (m, 18H). ^{13}C NMR (75 MHz, MeOD) δ 176.7, 174.8, 174.3, 173.3, 55.3, 54.9, 54.2, 40.6, 40.6, 40.6, 32.7, 32.3, 32.2, 28.2, 28.1, 28.1, 27.8, 27.5 – 27.4 (m, adjacent to CF bonds), 23.9, 23.9, 23.8. MS (ES) Calc. for $C_{27}H_{43}F_{13}N_7O_4$ $(M+H)^+$: 776.3. Found 775.6.

F7-HarGHar (S5)

^{1}H NMR (500 MHz, MeOD) δ 4.43 – 4.30 (m, 1H), 4.30 – 4.15 (m, 1H), 3.98 – 3.78 (m, 2H), 3.27 – 3.07 (m, 4H), 2.69 – 2.42 (m, 4H), 1.98 – 1.80 (m, 2H), 1.80 – 1.67 (m, 2H), 1.67 – 1.26 (m, 8H). ^{13}C NMR (126 MHz, MeOD) δ 176.9, 175.2, 173.2, 171.7, 158.7, 158.5, 66.9, 55.5, 54.2, 49.9, 43.7, 42.2, 32.4, 32.0, 29.4, 29.2, 27.5 (t, J=21.8), 27.1 (t, J=5.7), 23.9, 23.9, 15.4. MS (ES) Calc. for $C_{23}H_{38}F_9N_{10}O_4$ $(M+H)^+$: 689.29. Found 689.6.

12.4 **Figures and Tables**

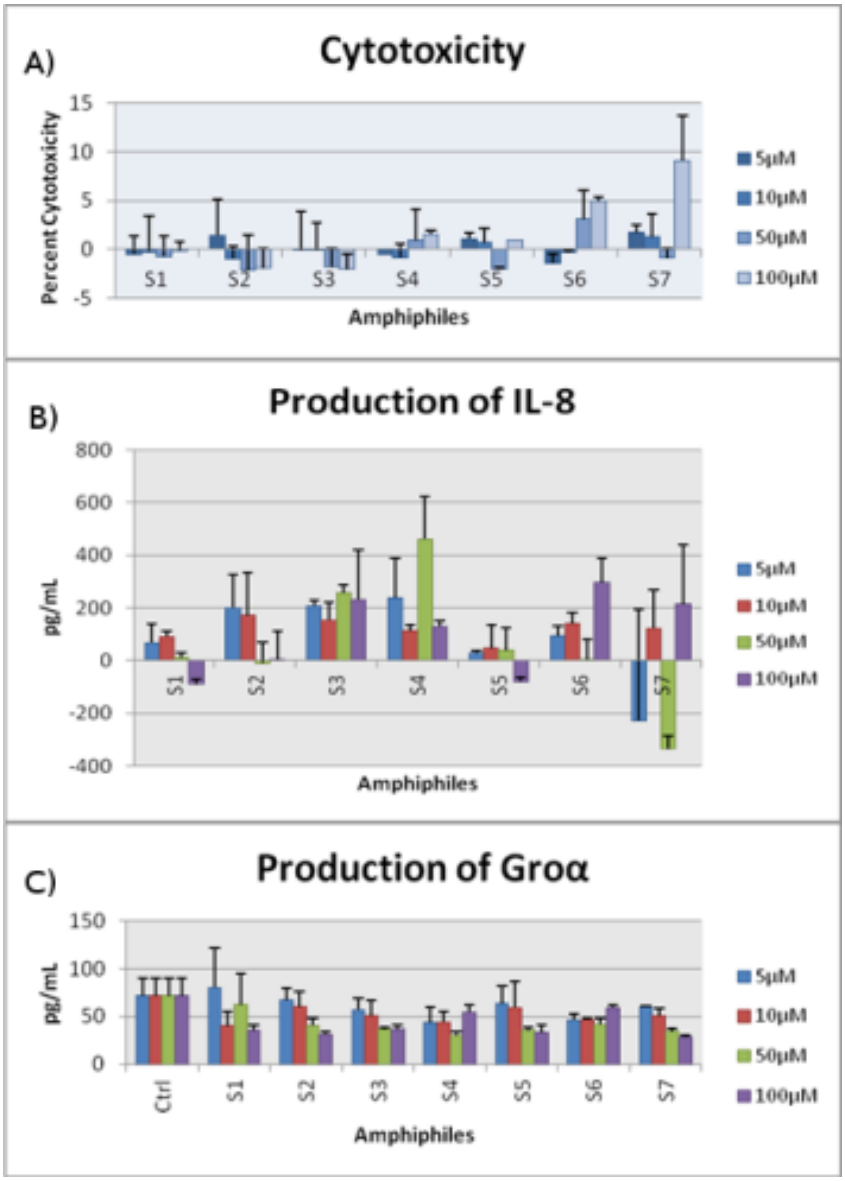

Figure 12.1 Immunological properties of the compounds presented in Table 12.1.

Table 12.1. Compound sequences.

	Amphiphile	Molecular Mass
	Lipopeptides[a]	
S1	**C7-LysGlyLys-NH_2**	670.64
S2	**$(CH_3)_2(CH_2)_6COO$-LysGlyLys-NH_2**	712.72
S3	**$(CF_3)_2(CF_2)_4(CH_2)_2COO$-LysGlyLys-$NH_2$**	982.57
S4	**$CF_3(CF_2)_5(CH_2)_2COO$-LysLysLys-NH_2**	117.72
S5	**$CF_3(CF_2)_3(CH_2)_2COO$ -HarGHar-NH_2**	916.64
	Lipopeptoids[a]	
S6	**$CF_3(CF_2)_7(CH_2)_2COO$-NLysGlyNLys-NH_2**	1032.59
S7	**C14-NLysNLysNLys-NH_2**	953.97

[a] Trifluroacetate salt

Table 12.2. Antimicrobial activity of select amphiphiles, derived from previous research.

Sample:	**4**	**5**	**6**	**7**	**21**
S.aureus ATCC 29213	561[a]	8.1	128	7.7	6.9
MRSA ATCC 33592	>561	4.1	128	7.7	14
MSSE 81388 CANWARD 2008	281	<0.25	128	7.7	6.9
MRSE (CZ >32) CAN-ICU	281	<0.25	128	7.7	6.9

61589					

[a] Values are given in µM.

12.5 **References**

1. Chan WC, White PD. Fmoc solid phase peptide synthesis: A practical approach. 1st ed. New York, United States: Oxford University Press; 2000.

2. Chongsiriwatana NP, Patch JA, Czyzewski AM, Dohm MT, Ivankin A, Gidalevitz D, et al. Peptoids that mimic the structure, function, and mechanism of helical antimicrobial peptides. Proc Natl Acad Sci U S A. 2008 Feb 26;105(8):2794-9.

3. Baker TJ, Luedtke NW, Tor Y, Goodman M. Synthesis and anti-HIV activity of guanidinoglycosides. J Org Chem. 2000 Dec 29;65(26):9054-8.

Chapter 13: Supporting Information for Chapter 6

By Brandon Findlay, George G. Zhanel and Frank Schweizer. First published as supplementary material in support of Chapter 6; Bioorganic Medicinal Chemistry Letters, 22, 2012, 1499-1503. Reproduced with permission.

13.1 Experimental Procedures

Reagents and solvents were purchased from commercially available sources and used without purification, unless otherwise noted. Flash chromatography was performed using silica gel (Silicycle 23 -60 um) using standard techniques. ^{1}H and ^{13}C NMR were recorded on a Bruker AMX-500 or Bruker AMX-300 spectrometer in the noted solvents. Chemical shifts (δ) are reported in parts per million relative to tetramethylsilane. Thin layer chromatography was performed on pre-coated silica gel glass plates, treated to fluoresce at 254nm. Compounds were visualized with either ultraviolet light or with a mix of ninhydrin and acetic acid in ethanol. Low-resolution mass spectra (ESI+) were obtained on a Varian 500-MS IT Mass Spectrometer. High-resolution mass spectra were obtained on the Manitoba/Sciex prototype quadrupole quadrupole-TOF mass spectrometer (positive ion MALDI-qQ-TOF). All compounds were determined to be ≥90% pure by NMR, following at least three days under high vacuum. Yields are given following purification, unless otherwise stated.

13.2 **In vitro tests:**

13.2.1 Bacterial Isolates

Clinically relevant bacteria were obtained as part of the Canadian National Intensive Care Unit (CAN-ICU) study(1) or as part of the later CANWARD Canadian national surveillance study.(2) The CAN-ICU study included 19 medical centres from across Canada with active ICUs. From September 2005 to June(3) 2006, inclusive, each centre was asked to collect a maximium of 300 consecutive isolates recovered from clinical specimens such as blood, urine, wounds/tissues and respiratory samples (one pathogen per cultured site per patient) originating from their ICU patients. The 4180 isolates obtained represented 2580 patients (for 1.62 isolates/patient). The study sites were requested to obtain only "clinically significant" specimens, originating from patients with a presumed infectious disease. Isolates were shipped to the reference library (Health Sciences Centre, Winnipeg, Canada) on Amies charcoal swabs, then subcultured onto appropriate media and stocked in skim milk at -80°C until minimum inhibitory concentration (MIC) testing was carried out.

13.2.2 Antimicrobial Susceptibilities

Following two subcultures from frozen stock, *in vitro* activities of the antimicrobials were determined by macrobroth dilution methodology, in accordance with the Clinical and Laboratory Standards Institute (CLSI) guidelines(3) The MICs were determined using glass test tubes (2 mL/tube) containing doubling antimicrobial dilutions of cation adjusted Mueller-Hinton broth inoculated to achieve a final concentration of approximately 5 x 10^5 CFU/mL, incubated in ambient air for 24 hr prior to reading. Colony counts were performed periodically to confirm inocula. The ATCC organisms *Staphylococcus pneumoniae* ATCC 49619, *Staphylococcus aureus*

ATCC 29213, *Enterococcus faecalis* ATCC 29212, *Escherichia coli* ATCC 25922, and *Pseudomonas aeruginosa* ATCC 27853 were used as standards to ensure adequate quality control.

13.2.3 Hemolytic Assays

Toxicity to mammalian cells was determined using a human red blood cell (erythrocyte) hemolytic assay. Erythrocytes were washed and resuspended in Tris buffered saline prior to use. The cell suspension was combined with varying concentrations of antimicrobials, from 50 µg/mL to 1 mg/mL. The samples were centrifuged following treatment and the absorbance of the supernatant was measured at 540 nm. Triton X-100 was used as a positive control, with Tris buffered saline as a negative control. The toxicity was assessed as a function of percent hemolysis.

13.3 **Chemical Syntheses:**

13.3.1 Procedure for the Preparation of Alkyne Linkers 14 and 15:

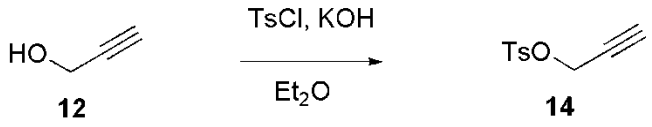

12 **14**

Based upon the preparation by Dickshats et al.,(4) to an ice-cold solution of propargyl alcohol **15** (1.00g, 1 eq) and tosyl chloride (4.09g, 1.2 eq) in ether was added potassium hydroxide (12.0g, 10 eq). The solution stirred at room temperature for thirty minutes, then

poured into ice water. The organic layer was removed and the aqueous layer was extracted twice with ethyl acetate. The organic layers were combined and dried with sodium sulfate, and the crude product purified by flash chromatography (hexanes/DCM, 1/1) to produce **14** as a clear oil (1.53g, 41%). ^{1}H NMR (300 MHz, CDCl3) δ 7.82 (d, J = 8.3, 2H), 7.35 (d, J = 8.0, 2H), 4.78 – 4.65 (m, 2H), 2.47 (dd, J = 3.9, 3.3, 4H). ^{13}C NMR (75 MHz, CDCl3) δ 145.4, 133.1, 130.1, 128.3, 77.5, 75.6, 57.5, 21.9.

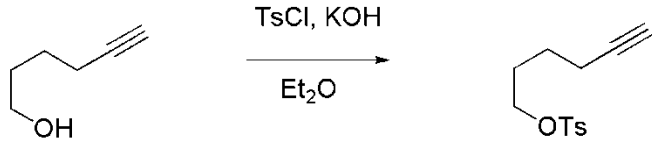

13 **15**

As in the synthesis of **14**, the alkynyl alcohol **13** (0.231g, 1 eq) and tosyl chloride (0.571g, 1.2 eq) were dissolved in diethyl ether and cooled to 0 °C. Potassium hydroxide (1.68g, 10 eq) was added in portions and the mixture was allowed to slowly warm to room temperature and stirred until the starting material was no longer visible by TLC, approximately 20 hr after addition. Water was added, the ether removed and the aqueous layer extracted twice with ethyl acetate. The organic layers were combined and dried, and the crude product purified by flash chromatography (hexanes/DCM, 1/1), to produce compound **15** as a clear oil (0.381g, 64%). ^{1}H NMR (300 MHz, CDCl3) δ 7.79 (d, J = 8.2, 2H), 7.35 (d, J = 7.9, 2H), 4.06 (t, J = 6.2, 2H), 2.45 (s, 3H), 2.16 (td, J = 6.9, 2.6, 2H), 1.92 (dd, J = 3.3, 2.0, 1H), 1.90 – 1.71 (m, 2H), 1.65 – 1.45 (m, 2H). ^{13}C NMR (75 MHz, CDCl3) δ 144.9, 133.2, 130.0, 128.0, 83.5, 70.0, 69.1, 27.9, 24.3, 21.7, 17.8.

13.3.2 General Procedure for the Production of Ethers 16a - 16c, 17a - 17c:

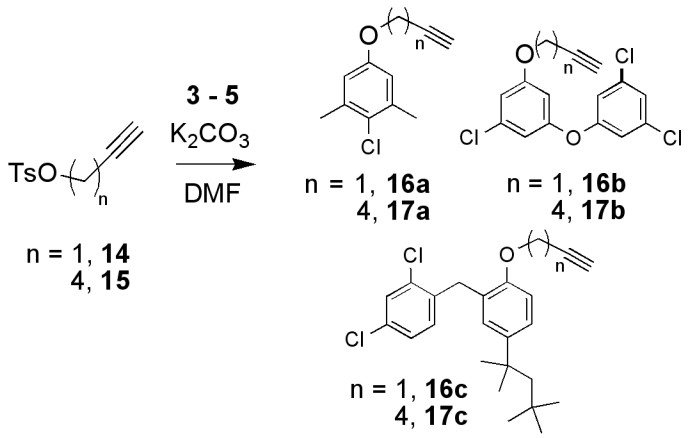

To a solution of one of the phenols **3 - 5** (1 eq) and tosyl ester (1.2 eq) dissolved in dry DMF was added potassium carbonate (2.5 eq). The mixture was stirred at room temperature for either 20 hours (compounds C to E) or two days (F to H), at which point the starting material was no longer visible by TLC. The solvent was then removed under reduced pressure and the crude mixture was purified by flash chromatography (hexanes/ethyl acetate, 1/9), to afford the phenol-alkynes **16a - 16c**, **17a – 17c** as white solids (51 – 96%, 69 – 92%).

16a

^{1}H NMR (300 MHz, $CDCl_3$, 298K) δ 6.71 (s, 2H), 4.65 (d, *J* = 2.3, 2H), 2.51 (t, *J* = 2.3, 1H), 2.36 (s, 6H). ^{13}C NMR (75 MHz, $CDCl_3$, 298K) δ 155.5, 137.4, 127.4, 115.1, 78.7, 75.7, 56.1, 21.2.

16b

^{1}H NMR (300 MHz, $CDCl_3$, 298K) δ 7.44 (dd, *J* = 2.4, 0.8, 1H), 7.22 – 7.06 (m, 2H), 6.97 (ddd, *J* = 8.6, 2.3, 0.9, 1H), 6.86 (dd, *J* = 8.6, 0.7, 1H), 6.71 (dd, *J* = 8.8, 0.7, 1H), 4.79 – 4.65 (m, 2H), 2.60 –

2.49 (m, 1H). ^{13}C NMR (75 MHz, $CDCl_3$, 298K) δ 152., 149.4, 144.1, 130.5, 130.2, 128.7, 128.0, 125.2, 122.6, 121.5, 119.0, 116.6, 77.7, 76.8, 57.3.

16c

^{1}H NMR (300 MHz, $CDCl_3$, 298K) δ 7.38 (d, *J* = 2.1, 1H), 7.21 (dd, *J* = 8.6, 2.5, 1H), 7.13 – 7.06 (m, 2H), 7.00 (d, *J* = 8.3, 1H), 6.90 (d, *J* = 8.6, 1H), 4.65 (d, *J* = 2.4, 2H), 4.04 (s, 2H), 2.48 (s, 1H), 1.65 (s, 2H), 1.31 (s, 6H), 0.68 (s, 9H). ^{13}C NMR (75 MHz, $CDCl_3$, 298K) δ 153.6, 143.3, 137.5, 135.0, 132.3, 131.8, 129.3, 129.1, 127.0, 126.9, 125.4, 111.6, 79.1, 75.4, 57.2, 56.3, 38.2, 33.6, 32.5, 32.0, 31.8.

17a

^{1}H NMR (500 MHz, $CDCl_3$, 298K) δ 6.63 (s, 2H), 3.93 (t, *J* = 6.3, 2H), 2.34 (s, 6H), 2.27 (td, *J* = 7.0, 2.6, 2H), 1.97 (t, *J* = 2.6, 1H), 1.94 – 1.84 (m, 2H), 1.76 – 1.65 (m, 2H). ^{13}C NMR (126 MHz, $CDCl_3$, 298K) δ 157.0, 137.2, 126.3, 114.7, 84.3, 68.9, 67.6, 28.5, 25.2, 21.1, 18.3.

17b

^{1}H NMR (500 MHz, $CDCl_3$, 298K) δ 7.43 (d, *J* = 2.5, 1H), 7.08 (dd, *J* = 8.8, 2.5, 1H), 7.00 – 6.89 (m, 3H), 6.62 (d, *J* = 8.8, 1H), 3.94 (t, *J* = 6.1, 2H), 2.13 (td, *J* = 7.0, 2.6, 2H), 1.94 (t, *J* = 2.6, 1H), 1.80 – 1.70 (m, 2H), 1.43 (q, *J* = 9.2, 7.1, 2H). ^{13}C NMR (126 MHz, $CDCl_3$, 298K) δ 152.8, 151.1, 143.1, 130.9, 130.4, 127.9, 127.7, 124.5, 122.5, 121.2, 117.8, 114.9, 84.0, 68.9, 68.6, 28.0, 24.8, 18.1.

17c

^{1}H NMR (300 MHz, $CDCl_3$, 298K) δ 7.38 (d, *J* = 2.1, 1H), 7.19 (dd, *J* = 8.5, 2.4, 1H), 7.14 – 7.04 (m, 2H), 6.94 (d, *J* = 8.3, 1H), 6.76 (d, *J* = 8.5, 1H), 4.02 (s, 2H), 3.93 (t, *J* = 6.1, 2H), 2.19 (td, *J* = 7.0, 2.6, 2H), 1.96 (t, *J* = 2.6, 1H), 1.91 – 1.74 (m, 2H), 1.67 (s, 2H), 1.63 – 1.49 (m, 2H), 1.31 (s, 6H), 0.70 (s, 9H). ^{13}C NMR (75 MHz, $CDCl_3$, 298K) δ 154.6, 141.9, 137.7, 134.8, 132.0, 131.3, 129.0, 128.9, 126.7, 126.2, 125.3, 110.4, 84.1, 68.6, 67.1, 57.0, 37.9, 33.7, 32.3, 31.8, 31.7, 28.3, 25.1, 18.1.

13.3.3 Preparation of Neomycin Azide 18:

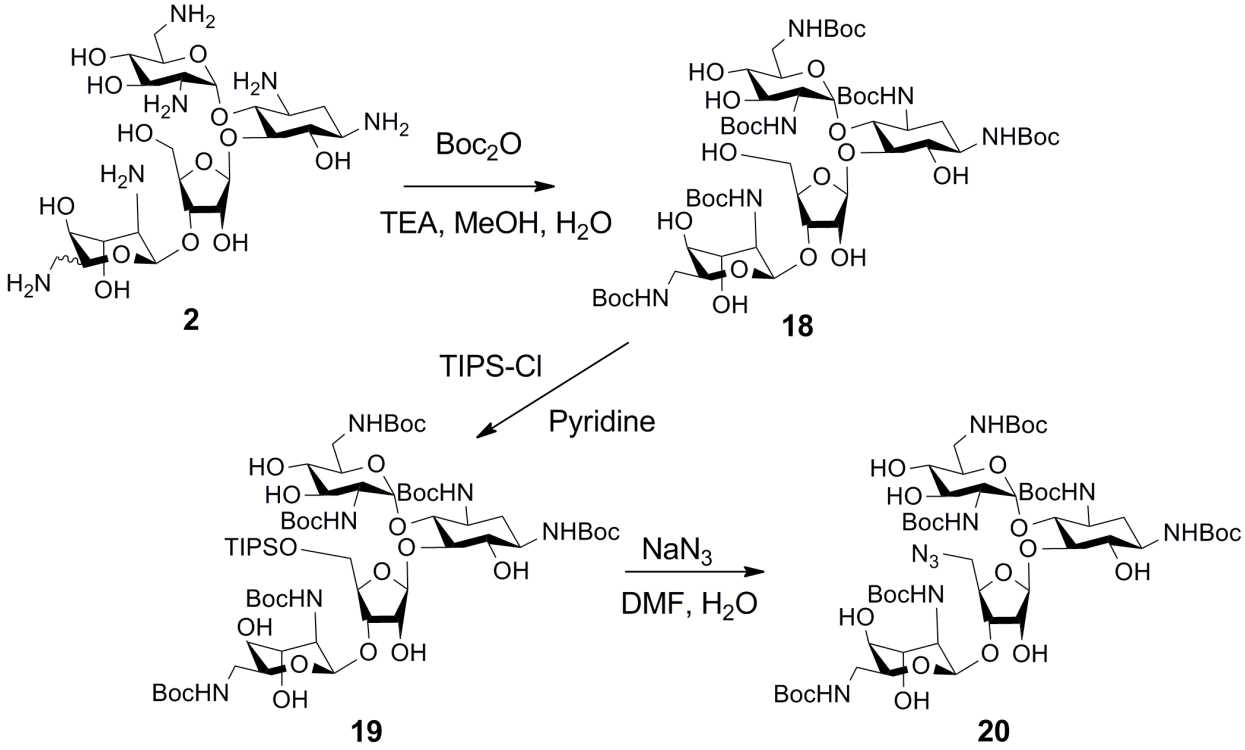

To a solution of neomycin sulfate (3.00 g, 1 eq) in methanol (10 mL), water (10 mL) and triethylamine (7 mL) was added Boc anhydride (5.02 g, 10 eq). The temperature was raised to 55 °C and the solution refluxed for 20 hours, at which point the mixture was concentrated to a white solid. Flash chromatography (DCM/acetone, 3/2) provided the known Boc-protected neomycin B derivative **18** as a white solid (1.31g, 61%).(5)

Based upon a procedure by Michael et al.,(6) the Boc-protected aminoglycoside (1.020 g, 1 eq) was then dissolved in pyridine (20 mL) and a large excess of triisopropylbenzenesulfonyl chloride added (7.98 4g, 31 eq). After two days the reaction was quenched with sodium bicarbonate and the pyridine and water were removed under reduced pressure. The mixture was then dissolved in water and extracted twice with ethyl acetate. The mixture was purified via flash chromatography (DCM/methanol, 50/2) to furnish **19** as a pure compound (0.510 g, 41%).

Compound **19** (0.241 g, 1 eq) was dissolved in DMF/water (9/1, 2.0 mL), and sodium azide added (0.107g, 10 eq). The mixture was stirred at 70 °C for three days then concentrated under reduced pressure. Flash chromatography (DCM/MeOH, 9/1) provided **20** as a single component(7) (0.190 g, 94%). ^{1}H NMR (300 MHz, MeOD) δ 6.80 – 6.58 (m, 2H), 6.58 – 6.36 (m, 2H), 6.18 (d, J = 10.1, 1H), 5.48 (s, 1H), 5.18 (d, J = 1.4, 1H), 4.94 (d, J = 1.5, 1H), 4.43 – 4.24 (m, 2H), 4.05 (d, J = 3.3, 1H), 3.96 – 3.43 (m, 12H), 3.41 – 3.13 (m, 8H), 2.07 – 1.86 (m, 1H), 1.61 – 1.31 (m, 54H). MS (ES) Calc. for $C_{53}H_{93}N_9O_{24}$ (M): 1239.6. Found 1263.3 (M+Na).

13.3.4 General Procedure for the 1,3-dipolar cycloaddition

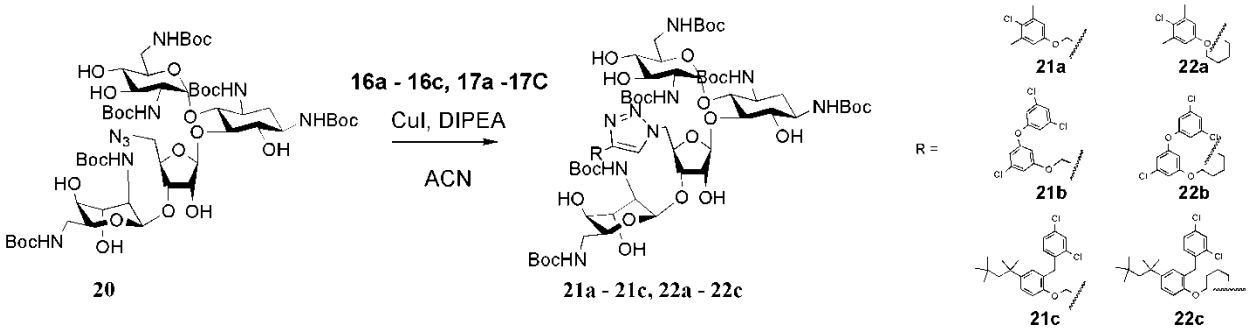

To a solution of the Neomycin Azide and Copper Iodide in Acetonitrile was added each of the phenol alkynes (1.5 eq), dissolved in a minimum of THF. Hunig's base was then added and the reaction was stirred for one hour at room temperature, until the azide starting material was no longer visible by TLC. The solvent was then removed under reduced pressure and the mixture purified by flash chromatography (DCM/methanol, 10/1) to produce the Boc-protected conjugates **21a – 21c, 22a – 22c** (50 - 88%).

21a

^{1}H NMR (500 MHz, MeOD) δ 8.33 – 8.14 (m, 1H), 6.85 (s, 2H), 5.39 (s, 1H), 5.15 (d, J = 27.0, 3H), 4.96 (s, 1H), 4.84 – 4.81 (m, 1H), 4.77 – 4.67 (m, 1H), 4.46 – 4.23 (m, 2H), 4.23 – 4.13 (m, 1H), 3.91 (s, 2H), 3.77 (s, 2H), 3.38 (dt, J = 63.5, 37.5, 14H), 2.34 (s, 6H), 2.02 – 1.89 (m, 1H), 1.63 – 1.22 (m, 54H). MS (ES) Calc. for $C_{64}H_{104}ClN_9NaO_{25}$ $(M+Na)^+$: 1456.7. Found 1457.6.

21b

^{1}H NMR (500 MHz, MeOD) δ 8.11 (s, 1H), 7.43 (dd, J = 36.3, 2.2, 2H), 7.19 (dd, J = 8.8, 2.5, 1H), 7.04 – 6.91 (m, 2H), 6.73 (d, J = 8.8, 1H), 5.36 (s, 1H), 5.25 (q, J = 12.0, 2H), 5.14 (s, 1H), 4.94 (s, 1H), 4.85 – 4.79 (m, 1H), 4.67 (dd, J = 14.2, 5.3, 1H), 4.40 – 4.09 (m, 3H), 4.00 – 3.83 (m, 2H), 3.84 – 3.69 (m, 2H), 3.64 – 3.32 (m, 10H), 3.26 – 3.11 (m, 2H), 1.94 (d, J = 12.2, 1H), 1.52 – 1.23 (m, 56H). MS (ES) Calc. for $C_{68}H_{102}Cl_3N_9NaO_{26}$ $(M+Na)^+$: 1588.6. Found 1589.7.

21c

^{1}H NMR (500 MHz, MeOD) δ 8.21 (s, 1H), 7.39 (d, J = 2.1, 1H), 7.24 (dd, J = 8.5, 2.1, 1H), 7.16 (dd, J = 8.3, 2.1, 1H), 7.09 (t, J = 7.9, 2H), 7.03 (d, J = 2.0, 1H), 5.39 (s, 1H), 5.28 – 5.08 (m, 3H), 4.96 (d, J = 1.2, 1H), 4.90 – 4.85 (m, 1H), 4.76 – 4.63 (m, 1H), 4.44 – 4.12 (m, 3H), 4.08 – 3.86 (m, 4H), 3.81 – 3.71 (m, 2H), 3.67 – 3.32 (m, 11H), 3.26 – 3.08 (m, 2H), 2.02 – 1.88 (m, 1H), 1.66 (s, 2H), 1.58 – 1.13 (m, 61H), 0.72 – 0.60 (m, 9H). MS (ES) Calc. for $C_{77}H_{121}Cl_2N_9NaO_{25}$ $(M+Na)^+$: 1664.8. Found 1665.7.

22a

^{1}H NMR (500 MHz, MeOD) δ 7.98 (s, 1H), 6.69 (s, 2H), 5.41 (s, 1H), 5.16 (s, 1H), 4.94 (d, J = 1.2, 1H), 4.82 (s, 1H), 4.69 – 4.51 (m, 2H), 4.27 (dd, J = 60.0, 31.4, 3H), 4.08 – 3.85 (m, 4H), 3.77 (d, J = 8.3, 2H), 3.68 – 3.32 (m, 12H), 3.21 (d, J = 9.3, 2H), 2.83 (t, J = 7.1, 2H), 2.31 (s, 6H), 1.86 (dd, J = 28.7, 7.1, 4H), 1.52 – 1.31 (m, 54H). MS (ES) Calc. for $C_{67}H_{110}ClN_9NaO_{25}$ $(M+Na)^+$: 1498.7. Found 1499.5.

22b

^{1}H NMR (500 MHz, MeOD) δ 7.92 (s, 1H), 7.46 (d, J = 2.5, 1H), 7.15 (dd, J = 9.2, 2.4, 2H), 7.04 (d, J = 8.5, 1H), 6.98 (dd, J = 8.5, 2.3, 1H), 6.67 (d, J = 8.8, 1H), 5.40 (s, 1H), 5.18 (s, 1H), 4.94 (s, 1H), 4.84 – 4.77 (m, 1H), 4.61 (dd, J = 14.2, 6.1, 1H), 4.37 – 4.12 (m, 3H), 4.04 – 3.86 (m, 4H), 3.81 – 3.70 (m, 2H), 3.66 – 3.32 (m, 11H), 3.21 (t, J = 9.3, 2H), 2.68 (t, J = 7.0, 2H), 1.95 (d, J = 12.2, 1H), 1.72 – 1.54 (m, 4H), 1.54 – 1.22 (m, 55H). MS (ES) Calc. for $C_{71}H_{108}Cl_3N_9NaO_{26}$ $(M+Na)^+$: 1630.6. Found 1631.5.

22c

^{1}H NMR (500 MHz, MeOD) δ 7.94 (s, 1H), 7.39 (d, J = 1.7, 1H), 7.20 (dd, J = 8.5, 1.8, 1H), 7.14 (dd, J = 8.3, 1.7, 1H), 7.10 – 6.97 (m, 2H), 6.86 (d, J = 8.6, 1H), 5.46 – 5.33 (m, 1H), 5.17 (s, 1H), 4.94 (s, 1H), 4.84 – 4.79 (m, 1H), 4.66 – 4.55 (m, 1H), 4.49 – 4.09 (m, 3H), 4.05 – 3.83 (m, 6H), 3.83 – 3.70 (m, 2H), 3.68 – 3.29 (m, 11H), 3.21 (t, J = 9.3, 2H), 2.86 – 2.64 (m, 2H), 2.02 – 1.89 (m, 1H), 1.80 (s, 4H), 1.67 (s, 2H), 1.53 – 1.20 (m, 61H), 0.67 (s, 9H). MS (ES) Calc. for $C_{80}H_{128}Cl_2N_9Na_2O_{25}$ $(M+H+2Na)^{3+}$: 576.9. Found 579.5.

13.3.5 General Deprotection Procedure

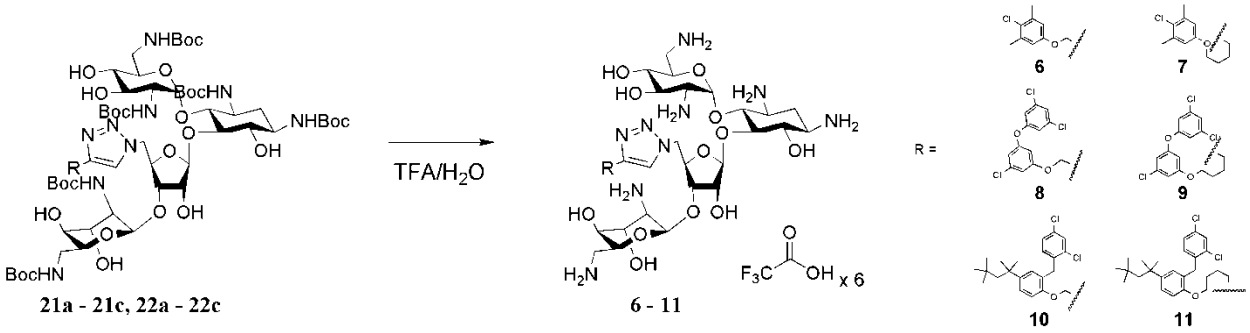

The Boc-protected conjugates were cooled to 0 °C and a solution of TFA/water (19/1) was added. After three minutes of mixing at 0 °C the acid was removed under reduced pressure. The residue was then triturated three times with Et_2O/MeOH (49/1), to produce the conjugates **6 - 11** as TFA salts, (80 - 91%).(8)

6

^{1}H NMR (500 MHz, MeOD) δ 8.27 (s, 1H), 6.81 (s, 2H), 6.00 (d, *J* = 3.8, 1H), 5.45 (d, *J* = 4.1, 1H), 5.34 (d, *J* = 1.4, 1H), 5.15 (s, 2H), 4.94 – 4.87 (m, 1H), 4.87 – 4.76 (m, 1H), 4.55 – 4.43 (m, 2H),

4.37 – 4.27 (m, 1H), 4.17 – 3.95 (m, 4H), 3.86 (t, *J* = 9.0, 1H), 3.72 – 3.62 (m, 2H), 3.62 – 3.53 (m, 2H), 3.53 – 3.36 (m, 5H), 3.29 – 3.19 (m, 3H), 2.52 – 2.39 (m, 1H), 2.34 (d, *J* = 3.2, 6H), 2.05 (q, *J* = 12.6, 1H). ^{13}C NMR (126 MHz, MeOD) δ 157.8, 145.6, 138.6, 138.6, 127.9, 126.7, 116.1, 116.1, 111.3, 97.1, 96.9, 86.8, 82.0, 78.0, 76.7, 75.0, 74.2, 73.0, 72.3, 71.9, 69.6, 69.3, 69.3, 62.6, 55.2, 53.2, 53.1, 51.3, 50.3, 41.8, 41.7, 29.7, 21.1, 21.1. MS (HRMS) Calc. for $C_{34}H_{57}ClN_9O_{13}$ $(M+H)^+$: 834.378. Found 834.375.

7

^{1}H NMR (500 MHz, MeOD) δ 7.97 (s, 1H), 6.68 (s, 2H), 5.97 (s, 1H), 5.45 (d, *J* = 4.2, 1H), 5.36 (s, 1H), 4.89 – 4.83 (m, 1H), 4.74 (dd, *J* = 14.9, 4.5, 1H), 4.52 (d, *J* = 4.3, 2H), 4.36 – 4.24 (m, 1H), 4.19 – 3.92 (m, 6H), 3.84 (t, *J* = 8.7, 1H), 3.69 (s, 1H), 3.63 – 3.34 (m, 7H), 3.31 – 3.19 (m, 4H), 2.80 (d, *J* = 7.4, 2H), 2.45 (d, *J* = 8.2, 1H), 2.31 (s, 6H), 2.01 (d, *J* = 11.5, 1H), 1.85 (dd, *J* = 13.0, 6.9, 4H). ^{13}C NMR (126 MHz, MeOD) δ 158.6, 149.9, 138.2, 138.2, 127.0, 124.7, 115.7, 115.7, 111.0, 97.2, 97.1, 86.9, 82.3, 78.1, 76.9, 75.1, 74.3, 73.0, 72.3, 71.7, 69.6, 69.4, 69.3, 68.8, 68.8, 55.3, 53.1, 53.1, 51.3, 50.3, 41.8, 41.6, 30.1, 27.4, 26.2, 21.1, 21.1. MS (HRMS) Calc. for $C_{37}H_{63}ClN_9O_{13}$ $(M+H)^+$: 876.424. Found 876.416.

8

^{1}H NMR (500 MHz, MeOD, 298K) δ 8.19 (s, 1H), 7.48 (d, *J* = 2.5, 1H), 7.34 (d, *J* = 2.3, 1H), 7.21 (dd, *J* = 8.8, 2.5, 1H), 7.03 (dd, *J* = 8.6, 2.3, 1H), 6.94 (d, *J* = 8.6, 1H), 6.76 (d, *J* = 8.8, 1H), 6.00 (d, *J* = 3.8, 1H), 5.44 (d, *J* = 4.0, 1H), 5.34 (d, *J* = 1.4, 1H), 5.23 (s, 2H), 4.93 – 4.88 (m, 1H), 4.76 (dd, *J* = 14.9, 5.4, 1H), 4.54 – 4.44 (m, 2H), 4.35 – 4.27 (m, 1H), 4.19 – 4.09 (m, 2H), 4.05 (dd, *J* = 10.4, 8.6, 1H), 4.01 – 3.96 (m, 1H), 3.86 (t, *J* = 9.0, 1H), 3.73 – 3.64 (m, 2H), 3.62 – 3.53 (m, 2H), 3.53 – 3.45 (m, 1H), 3.46 – 3.33 (m, 4H), 3.30 – 3.19 (m, 3H), 2.46 (dt, *J* = 12.3, 4.1, 1H), 2.12 – 1.98 (m,

1H). ^{13}C NMR (126 MHz, MeOD) δ 153.6, 151.7, 145.4, 144.8, 131.6, 131.3, 129.6, 129.4, 127.0, 126.0, 123.4, 122.9, 120.3, 117.4, 111.3, 97.1, 96.9, 86.8, 82.0, 78.0, 76.6, 75.0, 74.2, 73.1, 72.3, 71.8, 69.6, 69.4, 69.3, 63.8, 55.3, 53.3, 53.1, 51.3, 50.3, 41.9, 41.7, 29.7. MS (HRMS) Calc. for $C_{38}H_{55}Cl_3N_9O_{14}$ $(M+H)^+$: 966.294. Found 966.278.

9

^{1}H NMR (500 MHz, MeOD) δ 7.91 (s, 1H), 7.44 (d, *J* = 2.5, 1H), 7.19 – 7.09 (m, 2H), 7.06 (d, *J* = 8.5, 1H), 6.99 (dd, *J* = 8.5, 2.3, 1H), 6.66 (d, *J* = 8.8, 1H), 5.99 (d, *J* = 3.5, 1H), 5.45 (d, *J* = 4.4, 1H), 5.36 (s, 1H), 4.86 – 4.81 (m, 1H), 4.73 (dd, *J* = 14.9, 4.8, 1H), 4.58 – 4.42 (m, 2H), 4.36 – 4.23 (m, 1H), 4.20 – 3.90 (m, 6H), 3.85 (t, *J* = 9.0, 1H), 3.69 (d, *J* = 2.8, 1H), 3.61 – 3.53 (m, 2H), 3.53 – 3.37 (m, 6H), 3.30 – 3.12 (m, 3H), 2.65 (t, *J* = 7.4, 2H), 2.45 (d, *J* = 12.0, 1H), 2.04 (q, *J* = 24.0, 12.2, 1H), 1.73 – 1.51 (m, 4H). ^{13}C NMR (126 MHz, MeOD) δ 154.4, 152.6, 149.7, 144.2, 132.3, 131.1, 129.1, 128.7, 125.2, 124.6, 123.9, 122.3, 118.9, 116.0, 111.0, 97.2, 97.1, 86.8, 82.3, 78.1, 75.1, 74.3, 73.1, 72.3, 71.7, 69.8, 69.6, 69.4, 69.3, 55.3, 53.2, 53.1, 51.2, 50.3, 50.0, 41.8, 41.6, 29.7, 29.7, 27.0, 26.1. MS (HRMS) Calc. for $C_{41}H_{61}Cl_3N_9O_{14}$ $(M+H)^+$: 1008.341. Found 1008.313.

10

^{1}H NMR (500 MHz, MeOD) δ 8.25 (s, 1H), 7.40 (d, *J* = 2.1, 1H), 7.25 (dd, *J* = 8.6, 2.3, 1H), 7.16 (dd, *J* = 8.3, 2.1, 1H), 7.08 – 7.00 (m, 3H), 6.03 (d, *J* = 3.8, 1H), 5.46 (d, *J* = 4.2, 1H), 5.36 (d, *J* = 1.3, 1H), 5.18 (s, 2H), 4.99 – 4.87 (m, 1H), 4.79 (dd, *J* = 14.8, 5.0, 1H), 4.52 (d, *J* = 2.8, 2H), 4.36 – 4.27 (m, 1H), 4.19 – 4.09 (m, 2H), 4.09 – 3.94 (m, 4H), 3.87 (t, *J* = 9.0, 1H), 3.73 – 3.64 (m, 2H), 3.63 – 3.53 (m, 2H), 3.54 – 3.47 (m, 1H), 3.46 – 3.36 (m, 4H), 3.30 – 3.17 (m, 3H), 2.53 – 2.42 (m, 1H), 2.06 (q, *J* = 12.6, 1H), 1.67 (s, 2H), 1.28 (s, 6H), 0.66 (s, 9H). ^{13}C NMR (126 MHz, MeOD) δ 155.5, 145.9, 144.0, 139.0, 136.1, 133.6, 133.4, 130.0, 130.0, 128.2, 128.0, 126.7, 126.7, 112.5, 111.3,

97.1, 97.0, 86.9, 82.1, 78.0, 76.6, 75.0, 74.3, 73.1, 72.4, 71.7, 69.6, 69.4, 62.7, 58.0, 55.3, 53.3, 53.1, 51.3, 50.3, 50.0, 41.8, 41.7, 39.0, 34.1, 33.2, 32.5, 32.4, 32.4, 32.4, 32.4, 29.7. MS (ES) Calc. for $C_{47}H_{74}Cl_2N_9O_{13}$ $(M+H)^+$: 1042.478. Found 1042.476.

11

^{1}H NMR (500 MHz, MeOD) δ 7.93 (s, 1H), 7.38 (d, *J* = 2.1, 1H), 7.21 (dd, *J* = 8.6, 2.4, 1H), 7.13 (dd, *J* = 8.3, 2.1, 1H), 7.07 (d, *J* = 2.4, 1H), 7.00 (d, *J* = 8.3, 1H), 6.85 (d, *J* = 8.6, 1H), 5.99 (d, *J* = 3.8, 1H), 5.45 (d, *J* = 4.5, 1H), 5.36 (d, *J* = 1.4, 1H), 4.86 – 4.83 (m, 1H), 4.78 – 4.68 (m, 1H), 4.57 – 4.47 (m, 2H), 4.35 – 4.27 (m, 1H), 4.19 – 3.91 (m, 8H), 3.85 (t, *J* = 9.0, 1H), 3.72 – 3.67 (m, 1H), 3.62 – 3.36 (m, 8H), 3.31 – 3.19 (m, 3H), 2.73 (t, *J* = 7.3, 2H), 2.53 – 2.42 (m, 1H), 2.11 – 1.99 (m, 1H), 1.84 – 1.70 (m, 4H), 1.68 (s, 2H), 1.30 (s, 6H), 0.68 (s, 9H). ^{13}C NMR (126 MHz, MeOD) δ 156.1, 149.8, 143.0, 139.5, 136.0, 133.35, 133.9, 130.0, 129.9, 128.0, 127.5, 126.7, 124.6, 111.9, 111.0, 97.1, 97.1, 86.8, 82.3, 78.1, 76.6, 75.1, 74.3, 73.1, 72.3, 71.7, 69.6, 69.4, 69.3, 68.7, 61.7, 58.1, 55.3, 53.2, 53.0, 51.2, 50.3, 50.0, 41.8, 41.6, 38.9, 34.5, 33.2, 32.5, 32.5, 32.4, 32.4, 32.4, 27.4, 26.2. MS (HRMS) Calc. for $C_{49}H_{78}Cl_2N_9O_{13}$ $(M+H)^+$: 1084.525. Found 1084.512.

Peaks from the trifluoroacetate counterions appeared from δ 163.8 – 162.2 (CF_3-$\underline{C}OO^-$) and 121.9 – 114.8 ($\underline{C}F_3$-COO^-), and varied in intensity between samples.

13.4 References

1. Zhanel GG, DeCorby M, Laing N, Weshnoweski B, Vashisht R, Tailor F, et al. Antimicrobial-resistant pathogens in intensive care units in canada: Results of the canadian national intensive care unit (CAN-ICU) study, 2005-2006. Antimicrob Agents Chemother. 2008 Apr;52(4):1430-7.

2. Zhanel GG, Adam HJ, Low DE, Blondeau J, Decorby M, Karlowsky JA, et al. Antimicrobial susceptibility of 15,644 pathogens from canadian hospitals: Results of the CANWARD 2007-2009 study. Diagn Microbiol Infect Dis. 2011 Mar;69(3):291-306.

3. Rennie RP, Callihan DR, Barry AL, Krisher K, Munro SD, Sei K, et al. Protocols for evaluating dehydrated mueller-hinton agar; approved standard-second edition. In: CLSI; 2006. p. 1-29.

4. Dickschat JS, Reichenbach H, Wagner-Döbler I, Schulz S. Novel pyrazines from the myxobacterium chondromyces crocatus and marine bacteria. Eur J Org Chem. 2005;2005(19):4141-53.

5. Quader S, Boyd SE, Jenkins ID, Houston TA. Multisite modification of neomycin B: Combined mitsunobu and click chemistry approach. J Org Chem. 2007 Mar 16;72(6):1962-79.

6. Michael K, Wang H, Tor Y. Enhanced RNA binding of dimerized aminoglycosides. Bioorg Med Chem. 1999 Jul;7(7):1361-71.

7. Boer J, Blount KF, Luedtke NW, Elson-Schwab L, Tor Y. RNA-selective modification by a platinum(II) complex conjugated to amino- and guanidinoglycosides. Angew Chem Int Ed Engl. 2005 Jan 28;44(6):927-32.

8. Bera S, Zhanel GG, Schweizer F. Evaluation of amphiphilic aminoglycoside-peptide triazole conjugates as antibacterial agents. Bioorg Med Chem Lett. 2010 May 15;20(10):3031-5.

Chapter 14: Supporting Information for Chapter 7

By Brandon Findlay and Frank Schweizer. Unpublishd work.

14.1 Experimental Procedures

Compounds were not produced under anoxic or anhydrous conditions unless specifically noted. Reagents and solvents were purchased from commercially available sources and used without purification, unless otherwise noted. Flash chromatography was performed using silica gel (Silicycle 23 -60 um) using standard techniques. ^{1}H and ^{13}C NMR were recorded on a Bruker AMX-500 or Bruker AMX-300 spectrometer in the noted solvents. Chemical shifts (δ) are reported in parts per million with $CHCl_3$ (7.26 ppm) and CD_2HOH (3.31 ppm) used as internal standards. Thin layer chromatography was performed on pre-coated silica gel glass plates, treated to fluoresce at 254nm. Compounds were visualized with either ultraviolet light or with a mix of ninhydrin and acetic acid in ethanol. Low-resolution mass spectra (ESI+) were obtained on a Varian 500-MS IT Mass Spectrometer. High-resolution mass spectra (MALDI) were obtained on a Bruker UltraPleXtreme, with dihydroxybenzoic acid (DHB) support. Intermediate compounds were determined to be ≥90% pure by NMR following prolonged (>72 hr) exposure to high vacuum, and the purity of compounds used in biological testing was ≥95% as determined by HPLC. Yields are given following purification, unless otherwise stated.

14.2 Chemistry

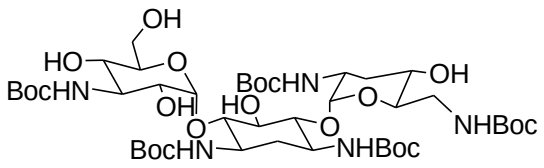

2

N-Boc Tobramycin (2)

Tobramycin (2.0 g, 1 eq.) was dissolved in a mixture of TEA, MeOH and H_2O (14 mL : 20 mL : 20 mL) and an excess of di-tert-butyl-dicarbonate was added (10 g, 10.7 eq.). The mixture was warmed to 55 °C and stirred overnight, after which the solvents and excess di-tert-butyl-dicarbonate were removed under reduced pressure to give the target compound as a white solid (3.89 g, 94%). ^{1}H NMR (500 MHz, MeOD) δ 5.13 (m, 1H), 5.09 (m, 1H), 3.95 (s, 1H), 3.92 – 3.24 (m, 15H), 2.09 (m, 2H), 1.52 (m, 47H). ^{13}C NMR (75 MHz, MeOD) δ 159.7, 159.5, 158.1, 157.9, 157.8, 99.8, 99.6, 83.8, 82.7, 80.9, 80.6, 80.6, 80.5, 80.3, 77.1, 74.9, 73.6, 72.2, 69.8, 66.6, 62.4, 57.3, 51.7, 51.3, 51.1, 42.1, 36.0, 34.4, 29.1 – 28.8 (m, butyl peaks). MS (ES) Calc. for $C_{43}H_{77}N_5NaO_{19}$ $(M+Na)^+$: 990.5. Found 991.0.

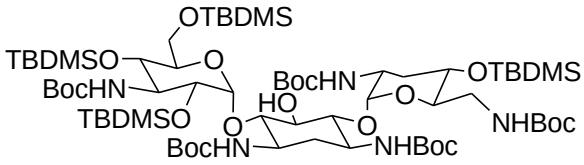

3

N-Boc-4',2",4",6"-tetra-TBDMS Tobramycin (3)

Boc protected Tobramycin (0.25g, 1 eq) was dissolved in dry DMF (1.0 mL) and TBDMS-Cl (0.18 g, 4.4 eq) was added, followed by methylimidazole (0.22mL, 10 eq). The reaction was stirred at room temperature for four days, further TBDMS-Cl (0.17g, 4.4eq) was added, and the reaction was continued for a further three days. The solution was then poured into water and extracted three times with dichloromethane, washed with brine and dried with sodium sulfate. This crude mixture was then purified though flash chromatography (4:1 Hex:EtOAc) to give the desired product as a white solid (0.25 g, 68%). ^{1}H NMR (500 MHz, CDCl3) δ 4.94 (s, 1H), 4.89 (s, 1H), 3.97 – 3.04 (m, 15H), 2.84 – 2.56 (m, 2H), 2.01 (s, 1H), 1.73 – 1.18 (m, 47H), 0.96 – 0.67 (m, 36H), 0.23 – 0.13 (m, 24H). ^{13}C 13C NMR (126 MHz, CDCl3) δ 156.2, 155.7, 155.2, 154.9, 154.9, 99.5, 98.5, 82.1, 80.0, 79.7, 79.6, 78.9, 76.1, 75.4, 73.0, 67.6, 63.3, 51.0, 51.0, 50.5, 49.7, 41.5, 34.8, 28.7 – 28.4 (m, butyl peaks), 26.4 – 25.7 (m, butyl peaks), 18.6, 18.3., 18.2, 18.0, -3.4, -3.7, -4.0, -4.1, -4.5, -4.6, -4.8, -4.9, -5.1. MS (ES) Calc. for $C_{67}H_{133}N_5NaO_{19}Si_4$ $(M+Na)^+$: 1446.9. Found 1447.3.

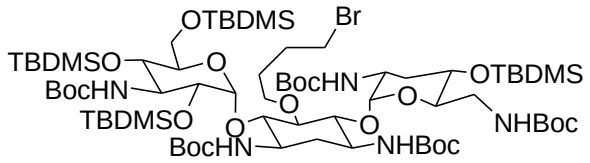

4

5-(4-Bromobutyl)- N-Boc-4',2",4",6"-tetra-TBDMS Tobramycin (4).

To compound 3 (0.39 g, 1 eq) dissolved in toluene (1.0 mL) was added potassium hydroxide (0.083 g, 5.5 eq), an excess of 1,4-dibromobutane (0.18 mL, 5 eq) and a catalytic amount of tetrabutylammonium hydrogen sulfate (.0011 g, 0.1 eq). This mixture was stirred at room temperature overnight and then water was added. The aqueous layer was extracted twice with toluene and once with EtOAC and the organic layers combined, washed with brine and dried with sodium sulfate. The crude organic layer was then purified via flash chromatography (9:1 Hex:EtOAc) to give the desired product as a tan solid (0.34 g, 79%). ^{1}H NMR (500 MHz, CDCl3) δ 5.15 (d, J = 30.3, 2H), 4.29 – 4.03 (m, 3H), 3.89 – 3.08 (m, 17H), 2.46 (s, 1H), 1.92 (ddd, J = 65.7, 34.9, 29.4, 4H), 1.62 (s, 2H), 1.58 – 1.21 (m, 46H), 0.89 (dd, J = 26.0, 17.6, 36H), 0.23 – -0.05 (m, 24H). ^{13}C NMR (75 MHz, MeOD) δ 158.5, 158.2, 157.7, 157.3, 157.1, 97.0, 86.9, 80.9, 80.7, 79.7, 78.4, 75.2, 74.3, 73.7, 72.8, 71.0, 68.8, 65.2, 57.6, 53.0, 42.2, 36.7, 34.6, 31.3, 30.6, 29.5 – 28.9 (m, butyl peaks), 27.1, 27.0, 26.9 – 26.6 (m, butyl peaks), 19.6, 19.2, 19.1, 19.1, -3.0 – -4.8 (m, methyl peaks). MS (ES) Calc. for $C_{71}H_{140}BrN_5NaO_{19}Si_4$ $(M+Na)^+$: 1580.8. Found 1581.3.

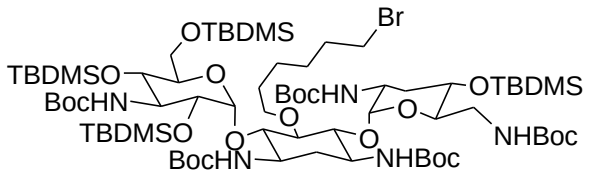

5

5-(6-Bromohexyl)- N-Boc-4',2",4",6"-tetra-TBDMS Tobramycin (5).

Similar to the synthesis of compound 4, N-Boc-2',2",4",6"-tetra-TBDMS Tobramycin (0.25 g, 1 eq) was mixed with potassium hydroxide (0.044 g, 4 eq), an excess of 1,6-dibromohexane (0.14 mL, 5.4 eq) and catalytic tetrabutylammonium hydrogen sulfate (.0057 g, 0.1 eq). After stirring

overnight water was added and the aqueous layer was extracted twice with toluene and once with EtOAc. The organic layers were combined, washed with brine and dried with sodium sulfate. Flash chromatography (4:1 Hex:EtOAc) furnished the target compound as a tan solid (0.19 g, 72%). ^{1}H NMR (500 MHz, CDCl3) δ 5.29 – 5.09 (m, 2H), 4.25 – 3.97 (m, 2H), 3.88 – 3.30 (m, 14H), 3.30 – 3.07 (m, 3H), 2.46 (s, 1H), 2.03 – 1.73 (m, 4H), 1.61 – 1.19 (m, 53H), 1.16 – 0.65 (m, 36H), 0.23 – -0.16 (m, 24H). ^{13}C NMR (75 MHz, MeOD) δ 158.5, 158.3, 157.8, 157.3, 157.2, 96.9, 86.8, 80.9, 80.8, 80.6, 80.4, 80.4, 79.7, 78.3, 75.2, 75.0, 73.7, 72.8, 71.1, 68.9, 65.3, 57.9, 55.2, 53.2, 50.2, 42.3, 36.9, 34.5, 34.4, 34.4, 34.3, 34.2, 33.9, 31.8, 29.9, 29.5 – 28.9 (m, butyl peaks), 27.2 – 26.6 (m, butyl peaks), 19.7, 19.2, 19.1, 19.1, -3.0 – -4.8 (m, methyl peaks). MS (ES) Calc. for $C_{73}H_{144}BrN_5NaO_{19}Si_4$ $(M+Na)^+$: 1608.9. Found 1609.5.

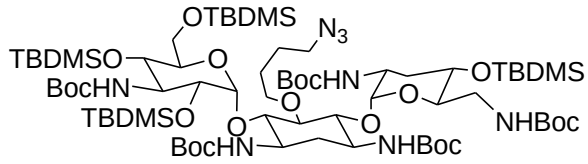

6

5-(6-Azidobutyl)- N-Boc-4',2",4",6"-tetra-TBDMS Tobramycin (6).

To a mixture of compound 4 (0.29 g, 1 eq) in DMF and H_2O (9:1) was added an excess of sodium azide (0.12 g, 10 eq). The mixture was heated to 70 °C overnight and then the solvent was removed under reduced pressure. Trituration three times with Et_2O furnished the 5-azido-N-Boc-2',2",4",6"-tetra-TBDMS Tobramycin as a pure white solid (0.23 g, 85%). ^{1}H NMR (500 MHz, CDCl3) δ 5.33 – 4.96 (m, 2H), 4.13 (s, 3H), 3.96 – 2.96 (m, 17H), 2.47 (s, 1H), 2.16 – 1.97 (m, 1H), 1.75 – 1.19 (m, 51H), 1.19 – 0.63 (m, 36H), 0.39 – 0.20 (m, 24H). ^{13}C NMR (75 MHz, MeOD) δ

158.3, 158.1, 157.6, 157.2, 157.0, 96.8, 86.7, 80.7, 80.6, 80.2, 79.6, 78.1, 75.0, 74.4, 73.6, 72.7, 71.0, 68.7, 65.2, 57.6, 53.0, 52.7, 42.1, 36.6, 29.3 – 28.7(m, butyl peaks), 27.0 – 26.5 (m, butyl peaks), 19.5, 19.1, 19.0, 19.0, -3.1 – -5.0 (m, methyl peaks). MS (ES) Calc. for $C_{73}H_{144}BrN_5Na_2O_{19}Si_4$ $(M+2Na)^{2+}$: 815.9. Found 815.2.

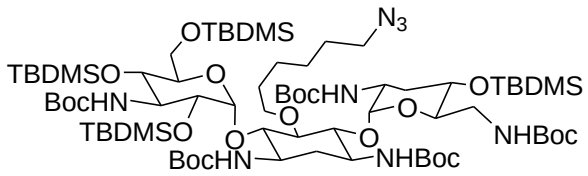

7

5-(6-Azidohexyl)- N-Boc-4',2",4",6"-tetra-TBDMS Tobramycin (7).

Compound 7 was synthesized from compound 5 (0.070 g, 1 eq), using the same procedure as in the production of compound 6 (0.062 g, 91%). ^{1}H NMR (500 MHz, CDCl3) δ 5.34 – 4.96 (m, 2H), 4.28 – 3.95 (m, 3H), 3.95 – 3.06 (m, 17H), 2.45 (s, 1H), 2.08 – 1.87 (m, 1H), 1.70 – 1.09 (m, 55H), 1.09 – 0.58 (m, 36H), 0.08 (dt, J = 23.8, 6.4, 24H). ^{13}C NMR (126 MHz, CDCl3) δ 155.6, 155.6, 154.9, 154.9, 154.7, 96.6, 85.9, 80.1, 79.6, 79.4, 75.4, 73.2, 72.8, 71.7, 68.2, 67.2, 63.3, 57.4, 51.6, 50.6, 49.0, 48.5, 41.8, 36.1, 35.8, 30.6, 29.0 – 28.5 (m, butyl peaks), 27.1, 26.3 – 25.8 (m, butyl peaks), 18.6, 18.4, 18.2, 18.0, -3.3 – -5.1 (m, methyl peaks). MS (ES) Calc. for $C_{73}H_{144}N_8NaO_{19}Si_4$ $(M+Na)^{+}$: 1572.0. Found 1572.4.

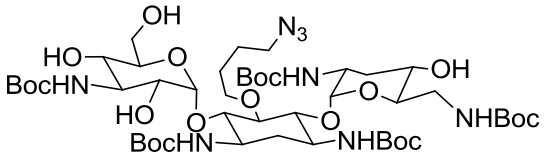

8

5-(6-Azidobutyl)-N-Boc Tobramycin (8).

Compound 8 was synthesized from 6 (0.5086 g, 1 eq), via treatment with TBAF (3.4 mL, 1M in THF, 10eq) in THF (7.5 mL) for two hours. The crude material was purified by column chromatography as a white solid (0.3557 g, Quantitative yield). ^{1}H NMR (500 MHz, MeOD) δ 5.38 – 5.27 (m, 1H), 5.25 (d, J = 2.5, 1H), 4.04 – 3.91 (m, 1H), 3.91 – 3.81 (m, 1H), 3.77 (dd, J = 11.6, 2.1, 1H), 3.74 – 3.51 (m, 7H), 3.48 (t, J = 9.8, 1H), 3.44 – 3.32 (m, 4H), 3.27 – 3.20 (m, 2H), 3.15 – 3.05 (m, 2H), 2.05 – 1.91 (m, 1H), 1.91 – 1.83 (m, 1H), 1.71 – 1.49 (m, 6H), 1.52 – 1.26 (m, 46H). ^{13}C NMR (126 MHz, MeOD) δ 159.5, 159.3, 158.1, 157.7, 157.6, 98.9, 97.0, 86.4, 80.9, 80.5, 80.2, 79.0, 78.4, 74.3, 74.0, 73.3, 72.1, 70.5, 67.3, 62.7, 57.2, 54.1, 52.7, 52.5, 50.5, 50.3, 50.3, 42.3, 36.1, 35.0, 29.0 – 28.7 (m, butyl peaks), 26.5, 26.2, 20.9, 18.9. MS (ES) Calc. for $C_{47}H_{84}N_8NaO_{19}$ $(M+Na)^+$: 1088.2. Found 1088.0.

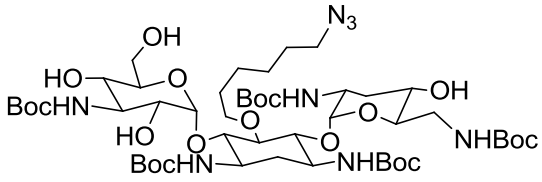

9

5-(6-Azidohexyl)-N-Boc Tobramycin (9).

Compound 9 was synthesized from 7 (0.7222 g, 1 eq), via treatment with TBAF (5.0 mL, 1M in THF, 11 eq) in THF (10.0 mL) for two hours. The crude material was purified by column chromatography as a white solid (0.4996 g, Quantitative yield). ^{1}H NMR (500 MHz, MeOD) δ 5.32 (s, 1H), 5.29 (d, J = 2.0, 1H), 3.97 (dd, J = 14.1, 7.0, 1H), 3.94 – 3.86 (m, 1H), 3.82 – 3.54 (m, 8H), 3.50 (t, J = 9.5, 1H), 3.47 – 3.34 (m, 6H), 3.26 (t, J = 7.0, 2H), 3.18 – 3.08 (m, 1H), 1.98 (s, 1H),

1.94 – 1.85 (m, 1H), 1.72 – 1.52 (m, 6H), 1.52 – 1.27 (m, 49H). ^{13}C NMR (126 MHz, MeOD) δ 159.6, 159.3, 158.1, 157.7, 157.6, 98.8, 97.0, 86.2, 80.9, 80.4, 80.4, 80.2, 79.0, 78.4, 74.6, 74.1, 73.3, 72.0, 70.5, 67.3, 62.6, 57.3, 54.1, 52.4, 50.5, 50.4, 42.4, 36.1, 35.0, 31.2, 29.8, 29.0 – 28.6 (m, butyl peaks), 28.0, 26.9, 26.2, 20.9, 13.9. MS (ES) Calc. for $C_{49}H_{88}N_8NaO_{19}$ $(M+Na)^+$: 1116.3. Found 1116.1.

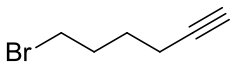

6-bromohex-1-yne was prepared by treatment of 6-hydroxy-1-yne (1.0 mL, 1 eq) with carbon tetrabromide (3.1 g, 1.1 eq) and triphenylphosphine (2.4 g, 1.1 eq) in dichloromethane (10 mL). The reagents were mixed at 0°C, then allowed to warm to room temperature. After 2 hours at room temperature the dichloromethane was removed under reduced pressure, and the mixture was slowly added to hexanes. The precipitated triphenylphosphine oxide was removed via vacuum filtration and the hexanes was then removed under reduced pressure to furnish the title compound as an impure mixture (2.3 g, approx. 64%). A crude NMR was used to confirm completion of the reaction by comparison to previously published spectra,(1) and this mixture was used without further purification. ^{1}H NMR (500 MHz, CDCl3) δ 3.44 (t, J = 6.7, 2H), 2.24 (td, J = 7.0, 2.6, 2H), 2.03 – 1.93 (m, 3H), 1.69 (dt, J = 14.3, 7.1, 2H).

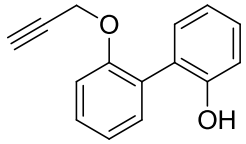

10

1-Propynyl-1'-hydroxy-biphenyl (10).

Compound **10** was synthesized from 1,1'-dihydroxybiphenyl (0.2007 g, 1 eq), via treatment with propargyl bromide (0.13 mL, 80% in toluene, 1.1 eq) and potassium carbonate (0.2295 g, 1.5 eq) in refluxing acetone (5.0 mL) for 16 hr. The crude mixture was filtered and the title compound was obtained as a clear oil (0.243 g, 88%) after column chromatography (24:1 Hex:EtOAC). ^{1}H NMR (500 MHz, CDCl3) δ 7.52 – 7.06 (m, 6H), 6.98 (dd, J = 14.5, 7.7, 2H), 5.83 (s, 1H), 4.69 (d, J = 1.2, 2H), 2.48 (s, 1H). ^{13}C NMR (126 MHz, CDCl3) δ 153.9, 153.6, 132.8, 131.5, 129.6, 129.5, 127.8, 125.9, 123.3, 121.1, 117.4, 114.1, 78.1, 76.7, 57.0. MS(ES) Calc. for $C_{15}H_{13}O_2$ $(M+H)^+$: 225.1. Found 225.2.

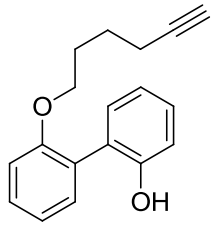

11

1-Hexynyl-1'-hydroxy-biphenyl (11).

Compound **11** was synthesized from 1,1'-dihydroxybiphenyl (0.3014 g, 1 eq), via treatment with bromohexyne (0.5431 g, ~50% 1.1 eq) and potassium carbonate (0.3374 g, 1.5 eq) in refluxing acetone (3.0 mL) for 16 hr. The crude mixture was filtered and the title compound was obtained as a clear oil (0.402 g, 94%) after column chromatography (24:1 Hex:EtOAC). ^{1}H NMR (500 MHz, CDCl3) δ 7.40 – 7.34 (m, 2H), 7.31 – 7.27 (m, 1H), 7.26 (dd, J = 7.6, 1.5, 1H), 7.12 (td, J = 7.5, 0.9, 1H), 7.07 – 6.99 (m, 3H), 6.41 (s, 1H), 4.08 (t, J = 6.4, 2H), 2.17 (td, J = 6.9, 2.6, 2H), 1.93 (t, J = 2.6, 1H), 1.87 (tt, J = 12.5, 6.4, 2H), 1.63 – 1.57 (m, 2H). ^{13}C NMR (126 MHz, CDCl3) δ 155.1, 154.0, 132.8, 131.5, 129.4, 129.4, 128.0, 126.6, 122.7, 121.1, 117.7, 113.7, 84.1, 69.4, 68.9, 28.2, 24.9, 18.1. MS(ES) Calc. for $C_{18}H_{18}NaO_2$ $(M+Na)^+$: 289.1. Found. 289.3.

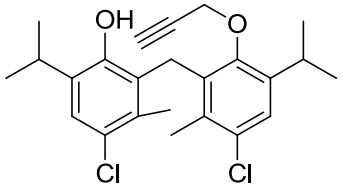

12

1-Propynyl-Biclotymol (12).

Compound **12** was synthesized from biclotymol (0.2076 g, 1 eq), via treatment with propargyl bromide (0.065 mL, 80% in toluene, 1.1 eq) and potassium carbonate (0.1130 g, 1.5 eq) in refluxing acetone (1.5 mL) for 16 hr. The crude mixture was filtered and the title compound was obtained as a yellow solid (0.169 g, 71%) after column chromatography (24:1 Hex:EtOAC). ^{1}H NMR (500 MHz, CDCl3) δ 7.12 (s, 2H), 5.59 (s, 2H), 4.09 (s, 2H), 3.06 (dt, J = 13.7, 6.8, 2H), 2.37 (s, 6H), 1.21 (d, J = 6.9, 12H). ^{13}C NMR (126 MHz, CDCl3) δ 152.1, 151.1, 141.1, 134.6, 134.3, 133.3, 132.4, 132.3, 126.5, 126.4, 125.3, 125.1, 78.2, 76.7, 62.8, 27.4, 27.1, 27.0, 24.0, 24.0, 22.7, 22.7, 17.4, 16.8. MS(ES) Calc. for $C_{24}H_{28}Cl_2NaO_2$ $(M+Na)^+$: 441.1. Found 441.4.

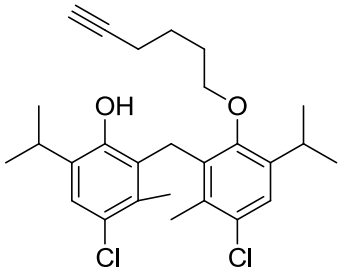

13

1-Hexynyl-Biclotymol (13).

Compound **13** was synthesized from biclotymol (0.1492g, 1 eq), via treatment with bromohexyne (0.1424 g, ~50%, 1.1 eq) and potassium carbonate (0.0884 g, 1.5 eq) in refluxing acetone (1.5 mL) for 16 hr. The crude mixture was filtered and the title compound was obtained as a white solid (0.112 g, 61%) after column chromatography (24:1 Hex:EtOAC). ^{1}H NMR (500 MHz, CDCl3) δ 7.20 (s, 1H), 7.08 (s, 1H), 6.60 (s, 1H), 4.05 (s, 2H), 3.87 (t, J = 6.5, 2H), 3.31 – 3.20 (m, 1H), 3.20 – 3.09 (m, 1H), 2.47 (s, 3H), 2.30 (td, J = 6.9, 2.6, 2H), 2.17 (s, 3H), 2.04 – 1.96 (m, 3H), 1.83 – 1.70 (m, 2H), 1.25 (d, J = 6.9, 6H), 1.15 (d, J = 6.9, 6H). ^{13}C NMR (126 MHz, CDCl3) δ 152.4, 151.6, 140.8, 134.8, 134.3, 132.5, 131.9, 131.8, 126.4, 126.1, 125.1, 124.5, 83.9, 75.6, 69.2, 29.3, 27.0, 26.9, 26.7, 25.1, 23.9, 23.9, 22.7, 22.7, 18.5, 17.6, 16.7. MS(ES) Calc. for $C_{27}H_{34}Cl_2NaO_2$ $(M+Na)^+$: 483.2. Found 483.4.

14.2.1 General procedure for the Huisgen cycloaddition.

To a mixture of the aminoglycoside derivative (1 eq) and alkyne phenolic (1.2 eq) in dichloromethane was added diisopropylethylamine (2 eq) and acetic acid (2 eq) and copper (I) iodide (0.1 eq). The mixture was allowed to stir for 16 hr, at which point the solvent was

removed under reduced pressure. The crude material was then purified via column chromatography (1:0 DCM:MeOH -> 9:1 DCM:MeOH).

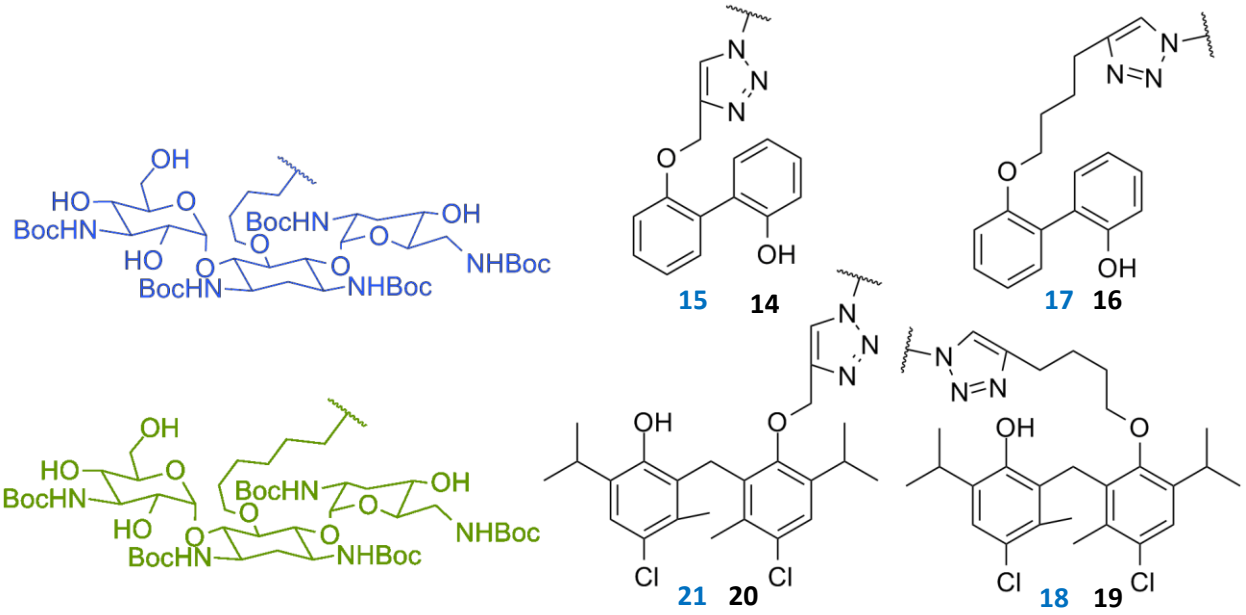

Methyl-Biphenol-NBoc-Butyl-Tobramycin Adduct (15).

Compound **8** (0.034 g) was coupled to alkyne **10** to give the title compound as a white solid (0.025 g, 60%). ^{1}H NMR (300 MHz, MeOD) δ 7.77 (s, 1H), 7.36 – 7.20 (m, 2H), 7.20 – 7.09 (m, 3H), 7.09 – 6.96 (m, 1H), 6.90 – 6.83 (m, 2H), 5.33 (s, 1H), 5.24 (d, J = 3.0, 1H), 5.14 (s, 2H), 4.34 (t, J = 6.7, 2H), 4.15 – 3.97 (m, 1H), 3.97 – 3.80 (m, 1H), 3.80 – 3.34 (m, 16H), 2.06 – 1.77 (m, 4H), 1.73 – 1.52 (m, 3H), 1.52 – 1.26 (m, 46H).

Methyl-Biphenol-NBoc-Hexyl-Tobramycin Adduct (14).

Compound 9 (0.040 g) was coupled to alkyne **10** to give the title compound as a white solid (0.046 g, 90%). ^{1}H NMR (300 MHz, MeOD) δ 7.63 (s, 1H), 7.31 – 7.13 (m, 2H), 7.13 – 7.02 (m,

3H), 6.98 (t, J = 7.4, 1H), 6.80 (dd, J = 7.3, 3.7, 2H), 5.27 (s, 1H), 5.24 (d, J = 3.5, 1H), 5.09 (s, 2H), 4.26 (t, J = 6.9, 2H), 4.02 – 3.78 (m, 2H), 3.78 – 3.42 (m, 10H), 3.33 (s, 5H), 3.14 – 2.99 (m, 1H), 2.05 – 1.68 (m, 4H), 1.68 – 1.45 (m, 4H), 1.45 – 1.08 (m, 49H).

Butyl-Biphenol-NBoc-Butyl-Tobramycin Adduct (17).

Compound 8 (0.041 g) was coupled to alkyne **11** to give the title compound as a white solid (0.046 g, 90%). ^{1}H NMR (300 MHz, MeOD) δ 7.57 (s, 1H), 7.34 – 7.24 (m, 1H), 7.20 (td, J = 7.8, 1.7, 1H), 7.17 – 7.10 (m, 2H), 7.06 – 6.95 (m, 2H), 6.85 (ddd, J = 6.0, 3.5, 1.1, 2H), 5.38 – 5.29 (m, 1H), 5.26 (d, J = 2.8, 1H), 4.32 (t, J = 7.1, 2H), 4.15 – 3.93 (m, 3H), 3.88 (s, 1H), 3.84 – 3.33 (m, 15H), 3.29 – 3.20 (m, 1H), 2.61 (t, J = 6.6, 2H), 2.05 – 1.79 (m, 4H), 1.77 – 1.54 (m, 6H), 1.50 – 1.33 (m, 47H). MS(ES) Calc. for $C_{65}H_{102}N_8NaO_{21}$ $(M+Na)^+$: 1353.7. Found 1354.2.

Butyl-Biphenol-NBoc-Hexyl-Tobramycin Adduct (16).

Compound 9 (0.042 g) was coupled to alkyne **11** to give the title compound as a white solid (0.050 g, 95%). ^{1}H NMR (500 MHz, MeOD) δ 7.51 (s, 1H), 7.32 – 7.24 (m, 1H), 7.21 (dd, J = 7.4, 1.2, 1H), 7.18 – 7.08 (m, 2H), 7.05 – 6.95 (m, 2H), 6.85 (dd, J = 7.6, 5.0, 2H), 5.33 (s, 1H), 5.29 (s, 1H), 4.30 (t, J = 7.1, 2H), 3.99 (t, J = 5.3, 3H), 3.94 – 3.87 (m, 1H), 3.81 – 3.33 (m, 15H), 3.16 – 3.09 (m, 1H), 2.63 (t, J = 6.6, 2H), 2.03 – 1.93 (m, 1H), 1.86 (dd, J = 14.6, 7.3, 3H), 1.75 – 1.52 (m, 6H), 1.52 – 1.21 (m, 51H).

Methyl-Biclotymol-NBoc-Butyl-Tobramycin Adduct (21).

Compound 8 (0.038 g) was coupled to alkyne **12** to give the title compound as a yellow solid (0.045 g, 86%). ^{1}H NMR (300 MHz, MeOD) δ 8.02 (s, 1H), 7.10 (s, 1H), 6.95 (s, 1H), 5.29 (s, 1H), 5.20 (s, 1H), 4.84 (s, 2H), 4.38 (t, J = 7.3, 2H), 4.25 (s, 2H), 4.08 – 3.93 (m, 1H), 3.93 – 3.81 (m, 1H), 3.81 – 3.28 (m, 16H), 3.22 – 3.02 (m, 2H), 1.93 (s, 6H), 1.84 (s, 4H), 1.73 – 1.46 (m, 3H), 1.46 – 1.20 (m, 46H), 1.18 – 1.02 (m, 12H).

Methyl-Biclotymol-NBoc-Hexyl-Tobramycin Adduct (20).

Compound 9 (0.043 g) was coupled to alkyne **12** to give the title compound as a yellow solid (0.047 g, 79%). ^{1}H NMR (500 MHz, MeOD) δ 7.98 (s, 1H), 7.11 (s, 1H), 6.97 (s, 1H), 5.29 (s, 1H), 5.25 (s, 1H), 4.85 (s, 2H), 4.37 (t, J = 7.2, 2H), 4.23 (s, 2H), 3.95 (d, J = 7.0, 1H), 3.87 (s, 1H), 3.78 – 3.50 (m, 10H), 3.45 (dd, J = 10.9, 7.9, 1H), 3.38 (d, J = 15.6, 4H), 3.23 – 3.13 (m, 2H), 3.13 – 3.03 (m, 1H), 1.97 (s, 4H), 1.87 (s, 5H), 1.67 – 1.61 (m, 2H), 1.61 – 1.50 (m, 2H), 1.50 – 1.28 (m, 50H), 1.21 – 1.04 (m, 12H). MS(ES) Calc. for $C_{73}H_{116}Cl_2N_8NaO_{21}$ $(M+Na)^+$: 1533.8. Found 1534.1.

Butyl-Biclotymol-NBoc-Butyl-Tobramycin Adduct (18).

Compound 8 (0.038 g) was coupled to alkyne **13** to give the title compound as a yellow solid (0.047 g, 79%). ^{1}H NMR (500 MHz, MeOD) δ 7.76 (s, 1H), 7.12 (s, 1H), 7.01 (s, 1H), 5.40 – 5.30 (m, 1H), 5.31 – 5.20 (m, 1H), 4.34 (t, J = 6.7, 2H), 4.23 (s, 2H), 4.13 – 4.01 (m, 1H), 3.95 – 3.85 (m, 1H), 3.82 – 3.52 (m, 11H), 3.52 – 3.45 (m, 1H), 3.45 – 3.33 (m, 5H), 3.28 – 3.10 (m, 3H), 2.78 (d, J = 6.5, 2H), 2.08 – 1.82 (m, 14H), 1.72 – 1.56 (m, 4H), 1.53 – 1.32 (m, 45H), 1.25 – 1.08 (m, 12H). MS(ES) Calc. for $C_{74}H_{118}Cl_2N_8NaO_{21}$ $(M+Na)^+$: 1547.8. Found 1547.8.

Butyl-Biclotymol-NBoc-Hexyl-Tobramycin Adduct (19).

Compound 9 (0.042 g) was coupled to alkyne **13** to give the title compound as a yellow solid (0.054 g, 91%). ^{1}H NMR (500 MHz, MeOD) δ 7.95 – 7.65 (m, 1H), 7.15 – 6.94 (m, 2H), 5.33 (s, 1H), 5.24 (s, 1H), 4.35 (s, 2H), 4.12 – 3.93 (m, 2H), 3.88 (s, 1H), 3.82 – 3.31 (m, 19H), 3.26 – 3.05 (m, 2H), 1.97 (dt, J = 39.0, 15.0, 12H), 1.65 (dd, J = 22.1, 10.3, 6H), 1.40 (dd, J = 29.4, 19.0, 45H), 1.20 – 0.67 (m, 18H). MS(ES) Calc. for $C_{76}H_{122}Cl_2N_8NaO_{21}$ $(M+Na)^+$: 1577.8. Found 1578.2.

14.2.2 General deprotection procedure.

The adduct of interest was cooled to 0°C and trifluoroacetic acid was added (90% in water, 1.5 mL). The mixture was mixed for five minutes, at which point the trifluoroacetic acid was removed under reduced pressure. The crude material was then purified via trituration in 98:2 ether:methanol to give the final compound. Purity was then evaluated via HPLC analysis, and if necessary compounds were then further purified via HPLC.

HPLC analysis method: Atlantis dC_{18} column, 5µm, 4.6 x 50mm. Flow 1.0 mL/min; buffer A, water 0.1% TFA; buffer B, acetonitrile. Gradient 15% B to 85% B over 20 minutes. Injection 10 µL of 1 mg/mL; detection at 212nm.

HPLC purification method: Atlantis dC_{18} column, 5µm, 19 x 100mm. Flow 16 mL/min; buffer A, water 0.1% TFA; buffer B, acetonitrile. Gradient 15% B to 85% B over 20 minutes. Detection at 212nm.

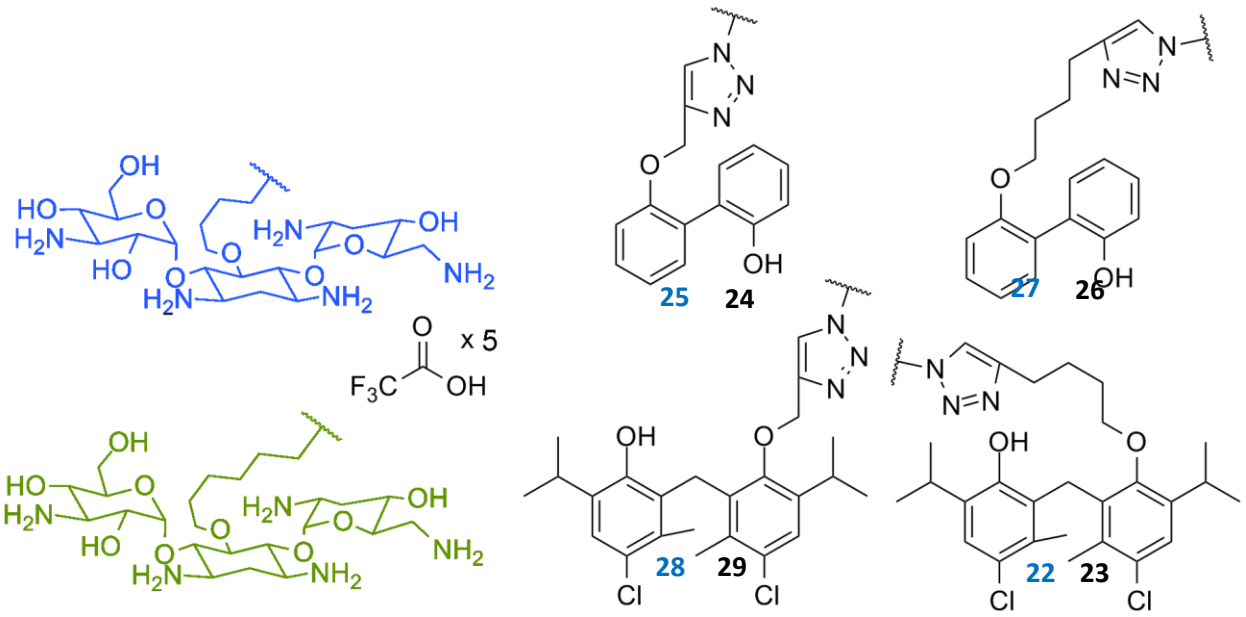

Peaks from the trifluoroacetate counterions appeared from δ 163.8 – 162.2 (CF_3-$\underline{C}OO^-$) and 121.9 – 114.8 ($\underline{C}F_3$-COO^-), and varied in intensity between samples.

Methyl-Biphenol-Butyl-Tobramycin Adduct (25).

Compound **15** (0.027 g) was cleaved to produce the title compound as a white solid (0.028 g, Quantitative yield). ^{1}H NMR (500 MHz, MeOD) δ 7.79 (s, 1H), 7.37 – 7.30 (m, 1H), 7.25 (dd, J = 7.5, 1.7, 1H), 7.22 – 7.16 (m, 2H), 7.16 – 7.10 (m, 1H), 7.05 (td, J = 7.4, 1.0, 1H), 6.90 – 6.82 (m, 2H), 5.39 (d, J = 2.4, 1H), 5.17 (s, 2H), 5.11 (d, J = 3.4, 1H), 4.50 – 4.34 (m, 2H), 4.25 – 4.15 (m, 2H), 4.00 – 3.86 (m, 3H), 3.86 – 3.70 (m, 5H), 3.70 – 3.58 (m, 2H), 3.58 – 3.36 (m, 5H), 3.16 (dd, J

= 13.9, 3.2, 1H), 2.49 (dt, J = 12.3, 4.2, 1H), 2.21 – 2.14 (m, 2H), 2.06 (q, J = 12.6, 1H), 1.98 (q, J = 7.4, 2H), 1.65 – 1.52 (m, 2H). ^{13}C NMR (126 MHz, MeOD) δ 157.0, 155.6, 145.8, 133.0, 132.6, 130.3, 129.7, 129.6, 127.4, 125.3, 122.8, 120.6, 116.9, 115.1, 102.7, 94.2, 84.0, 83.3, 78.4, 78.0, 75.6, 73.7, 70.5, 66.8, 64.8, 63.6, 61.3, 56.4, 55.1, 51.1, 51.1, 49.9, 39.7, 29.7, 29.2, 28.0, 27.2. HRMS(MALDI) Calc. for $C_{37}H_{56}N_8NaO_{11}$ $(M+Na)^+$: 811.3960. Found 811.3958.

Methyl-Biphenol-Hexyl-Tobramycin Adduct (24).

Compound **14**(0.037 g) was cleaved to produce the title compound as a white solid (0.037 g, 95%). ^{1}H NMR (500 MHz, MeOD) δ 7.73 (s, 1H), 7.31 (td, J = 8.3, 1.7, 1H), 7.25 (dd, J = 7.5, 1.7, 1H), 7.20 – 7.13 (m, 2H), 7.11 (dd, J = 7.9, 1.7, 1H), 7.05 (td, J = 7.5, 0.9, 1H), 6.88 – 6.82 (m, 2H), 5.41 (d, J = 2.5, 1H), 5.15 (s, 2H), 5.11 (d, J = 3.4, 1H), 5.06 (d, J = 4.4, 0H), 4.36 (td, J = 6.8, 2.2, 2H), 4.26 – 4.13 (m, 2H), 3.98 (s, 1H), 3.96 – 3.53 (m, 11H), 3.53 – 3.41 (m, 3H), 3.19 (dd, J = 13.8, 3.3, 1H), 2.49 (dt, J = 12.3, 4.2, 1H), 2.25 – 2.15 (m, 2H), 2.07 (q, J = 12.6, 1H), 1.94 – 1.81 (m, 2H), 1.67 – 1.56 (m, 2H), 1.48 – 1.37 (m, 1H), 1.37 – 1.23 (m, 3H). ^{13}C NMR (126 MHz, MeOD) δ 157.1, 155.6, 145.7, 132.9, 132.6, 130.3, 129.7, 129.6, 127.3, 125.1, 122.7, 120.6, 116.8, 115.1, 102.5, 94.1, 83.7, 83.1, 78.0, 77.3, 75.4, 73.9, 70.5, 66.7, 65.0, 63.7, 61.3, 56.4, 55.1, 54.0, 51.2, 51.1, 49.9, 39.9, 30.9, 30.8, 30.0, 29.1, 27.3, 26.1. HRMS(MALDI) Calc. for $C_{39}H_{60}N_8NaO_{11}$ $(M+Na)^+$: 839.4273. Found 839.4279.

Butyl-Biphenol-Butyl-Tobramycin Adduct (27).

Compound **17** (0.043 g) was cleaved to produce the title compound as a white solid (0.028 g, 62%). ^{1}H NMR (500 MHz, MeOD) δ 7.56 (s, 1H), 7.37 – 7.24 (m, 1H), 7.22 (dd, J = 7.4, 1.5, 1H),

7.17 – 7.09 (m, 2H), 7.05 – 6.95 (m, 2H), 6.91 – 6.81 (m, 2H), 5.42 (d, J = 2.1, 1H), 5.12 (d, J = 3.3, 1H), 4.46 – 4.30 (m, 2H), 4.25 – 4.16 (m, 2H), 4.02 – 3.86 (m, 4H), 3.85 – 3.70 (m, 6H), 3.66 (t, J = 9.8, 2H), 3.62 – 3.35 (m, 5H), 3.19 (dd, J = 13.8, 3.1, 1H), 2.64 (t, J = 6.8, 2H), 2.49 (dt, J = 8.3, 3.9, 1H), 2.33 – 2.13 (m, 2H), 2.07 (q, J = 12.6, 1H), 2.02 – 1.91 (m, 2H), 1.75 – 1.56 (m, 6H). ^{13}C NMR (126 MHz, MeOD) δ 157.9, 155.9, 149.6, 132.9, 132.8, 129.9, 129.8, 129.6, 127.8, 123.7, 122.0, 120.6, 116.9, 114.1, 102.7, 94.4, 84.2, 83.4, 78.6, 78.1, 75.7, 73.8, 70.7, 69.4, 67.0, 65.0, 61.5, 56.5, 51.2, 51.2, 50.0, 49.1, 39.8, 29.9, 29.7, 29.4, 28.2, 27.6, 27.1, 25.9. HRMS(MALDI) Calc. for $C_{40}H_{62}N_8NaO_{11}$ $(M+Na)^+$: 853.4430. Found 853.4425.

Butyl-Biphenol-Hexyl-Tobramycin Adduct (26).

Compound **16** (0.050 g) was cleaved to produce the title compound as a white solid (0.047 g, 89%). ^{1}H NMR (500 MHz, MeOD) δ 7.54 (s, 1H), 7.34 – 7.25 (m, 1H), 7.21 (dd, J = 7.4, 1.5, 1H), 7.18 – 7.07 (m, 2H), 7.07 – 6.95 (m, 2H), 6.85 (dd, J = 7.5, 4.8, 2H), 5.42 (d, J = 2.4, 1H), 5.12 (d, J = 3.3, 1H), 4.34 (t, J = 6.4, 2H), 4.25 – 4.13 (m, 2H), 4.00 (t, J = 5.3, 2H), 3.93 – 3.62 (m, 9H), 3.58 (t, J = 8.8, 2H), 3.53 – 3.40 (m, 3H), 3.35 (s, 1H), 3.19 (dd, J = 13.7, 3.1, 1H), 2.64 (t, J = 6.6, 2H), 2.49 (dt, J = 12.2, 4.1, 1H), 2.20 (d, J = 4.3, 2H), 2.07 (q, J = 12.6, 1H), 1.89 (d, J = 5.9, 2H), 1.75 – 1.58 (m, 6H), 1.48 – 1.38 (m, 2H), 1.38 – 1.25 (m, 2H). ^{13}C NMR (126 MHz, MeOD) δ 157.9, 155.9, 149.3, 132.8, 132.8, 129.9, 129.8, 129.6, 127.8, 123.5, 122.0, 120.6, 116.9, 114.0, 102.7, 94.3, 83.9, 83.2, 78.1, 77.4, 75.5, 74.0, 70.7, 69.4, 66.9, 65.2, 61.4, 56.6, 51.3, 51.2, 50.0, 50.0, 40.1, 31.2, 31.0, 30.1, 29.7, 29.3, 27.5, 27.0, 26.3, 25.9. HRMS(MALDI) Calc. for $C_{42}H_{66}N_8NaO_{11}$ $(M+Na)^+$: 881.4743. Found 881.4742.

Methyl-Biclotymol-Butyl-Tobramycin Adduct (28).

Compound **21** (0.045 g) was cleaved to produce the title compound as a yellow solid (0.043 g, 91%). ^{1}H NMR (500 MHz, MeOD) δ 8.07 (s, 1H), 7.16 (s, 1H), 7.02 (s, 1H), 5.46 (d, J = 2.1, 1H), 5.13 (d, J = 3.2, 1H), 4.89 (s, 2H), 4.59 – 4.37 (m, 3H), 4.32 (s, 2H), 4.23 (t, J = 9.5, 2H), 4.01 – 3.88 (m, 2H), 3.88 – 3.38 (m, 13H), 3.27 – 3.08 (m, 2H), 2.49 (dd, J = 8.3, 4.2, 1H), 2.34 – 2.13 (m, 2H), 2.13 – 1.96 (m, 5H), 1.96 – 1.82 (m, 3H), 1.77 – 1.56 (m, 2H), 1.26 – 1.08 (m, 13H). ^{13}C NMR (126 MHz, MeOD) δ 154.3, 151.9, 149.3, 145.3, 141.9, 136.8, 136.0, 135.1, 134.0, 132.5, 130.2, 127.7, 126.1, 125.8, 125.2, 102.7, 94.4, 84.2, 83.4, 78.6, 78.1, 75.7, 73.9, 70.7, 68.6, 67.0, 66.9, 65.0, 61.5, 56.5, 51.4, 51.2, 50.0, 39.8, 29.9, 29.3, 28.3, 28.1, 28.0, 27.5, 27.3, 24.1, 23.3, 16.8, 16.7, 15.6. HRMS(MALDI) Calc. for $C_{46}H_{72}Cl_2N_8NaO_{11}$ $(M+Na)^+$: 1005.4589. Found 1005.4576.

Methyl-Biclotymol-Hexyl-Tobramycin Adduct (29).

Compound **20** (0.043 g) was cleaved to produce the title compound as a yellow solid (0.034 g, 76%). ^{1}H NMR (500 MHz, MeOD) δ 8.03 (s, 1H), 7.16 (s, 1H), 7.01 (s, 1H), 5.43 (d, J = 2.4, 1H), 5.12 (d, J = 3.1, 1H), 4.88 (s, 2H), 4.44 (t, J = 6.3, 2H), 4.30 (s, 2H), 4.25 – 4.15 (m, 2H), 3.96 – 3.83 (m, 2H), 3.83 – 3.72 (m, 4H), 3.72 – 3.63 (m, 2H), 3.63 – 3.53 (m, 2H), 3.53 – 3.39 (m, 3H), 3.38 – 3.32 (m, 2H), 3.26 – 3.16 (m, 3H), 2.57 – 2.41 (m, 1H), 2.22 (s, 2H), 2.12 – 1.98 (m, 4H), 1.98 – 1.86 (m, 5H), 1.72 – 1.59 (m, 2H), 1.51 – 1.28 (m, 4H), 1.24 – 1.06 (m, 12H). ^{13}C NMR (126 MHz, MeOD) δ 154.3, 151.9, 145.1, 142.0, 136.8, 136.0, 135.1, 133.9, 132.5, 130.2, 127.7, 126.1, 125.6, 125.2, 102.7, 94.3, 83.9, 83.2, 78.2, 77.4, 75.6, 74.1, 70.7, 68.5, 66.9, 65.2, 61.4, 56.6, 51.3, 51.3, 50.1, 49.1, 40.1, 31.3, 31.0, 30.2, 29.3, 28.1, 28.0, 27.5, 27.3, 26.3, 24.1, 23.3, 16.8, 16.7. HRMS(MALDI) Calc. for $C_{48}H_{76}Cl_2NaN_8O_{11}$ $(M+Na)^+$: 1033.4903 Found 1033.4901.

Butyl-Biclotymol-Butyl-Tobramycin Adduct (22).

Compound **18** (0.040 g) was cleaved to produce the title compound as a yellow solid (0.036 g, 86%). ^{1}H NMR (500 MHz, MeOD) δ 7.76 (s, 1H), 7.12 (s, 1H), 7.02 (s, 1H), 5.43 (d, J = 2.3, 1H), 5.11 (d, J = 3.3, 1H), 4.47 – 4.32 (m, 2H), 4.25 – 4.17 (m, 4H), 3.96 – 3.85 (m, 2H), 3.84 – 3.70 (m, 8H), 3.70 – 3.62 (m, 2H), 3.55 (t, J = 9.0, 1H), 3.51 – 3.39 (m, 4H), 3.28 – 3.16 (m, 3H), 2.80 (t, J = 6.8, 2H), 2.49 (dt, J = 12.1, 4.1, 1H), 2.31 – 2.17 (m, 2H), 2.12 – 2.04 (m, 1H), 1.98 (d, J = 17.3, 8H), 1.95 – 1.81 (m, 4H), 1.64 (dd, J = 13.5, 6.7, 2H), 1.20 (d, J = 6.9, 6H), 1.18 (d, J = 6.9, 6H). ^{13}C NMR (126 MHz, MeOD) δ 154.8, 152.0, 149.3, 141.7, 136.4, 135.9, 134.9, 133.9, 132.0, 130.0, 127.6, 126.0, 125.2, 123.7, 102.7, 94.4, 84.2, 83.4, 78.6, 78.1, 75.8, 75.7, 73.8, 70.7, 66.9, 65.0, 61.5, 56.5, 51.2, 51.2, 50.0, 50.0, 39.8, 30.9, 29.9, 29.3, 28.2, 28.0, 28.0, 27.6, 27.5, 27.0, 26.4, 24.1, 23.3, 16.8, 16.6. HRMS(MALDI) Calc. for $C_{49}H_{78}Cl_2N_8NaO_{11}$ $(M+Na)^+$: 1047.5059. Found 1047.5060.

Butyl-Biclotymol-Hexyl-Tobramycin Adduct (23).

Compound **19**(0.042 g) was cleaved to produce the title compound as a yellow solid (0.040 g, 91%). ^{1}H NMR (500 MHz, MeOD) δ 7.70 (s, 1H), 7.10 (s, 1H), 7.00 (s, 1H), 5.41 (d, J = 2.1, 1H), 5.10 (d, J = 3.1, 1H), 4.77 – 4.70 (m, 1H), 4.37 – 4.26 (m, 2H), 4.26 – 4.11 (m, 4H), 3.92 – 3.53 (m, 10H), 3.53 – 3.38 (m, 5H), 3.35 – 3.31 (m, 1H), 3.27 – 3.11 (m, 3H), 2.78 (t, J = 6.9, 2H), 2.51 – 2.40 (m, 1H), 2.20 (s, 2H), 2.12 – 2.00 (m, 1H), 1.98 (s, 3H), 1.95 (s, 3H), 1.92 – 1.76 (m, 6H), 1.69 – 1.49 (m, 2H), 1.49 – 1.35 (m, 1H), 1.35 – 1.23 (m, 3H), 1.21 – 1.12 (m, 12H). ^{13}C NMR (126 MHz, MeOD) δ 163.0, 154.8, 152.0, 149.2, 141.7, 136.4, 136.0, 134.9, 133.9, 131.9, 130.0, 127.6,

126.0, 125.2, 123.4, 102.7, 94.3, 83.9, 83.2, 78.1, 77.4, 75.7, 75.5, 74.0, 70.7, 67.0, 66.9, 65.2, 61.4, 56.6, 51.3, 51.2, 50.1, 40.1, 31.2, 31.0, 30.9, 30.2, 29.3, 28.0, 27.5, 27.4, 27.0, 26.3, 24.1, 23.3, 16.8, 16.6, 15.6. HRMS(MALDI) Calc. for $C_{51}H_{82}Cl_2N_8NaO_{11}$ $(M+Na)^+$: 1075.5372. Found 1075.5362.

14.3 References

1. Sharma S, Oehlschlager AC. Scope and mechanism of stannylalumination of 1-alkynes. J Org Chem. 1989 10/01; 2012/11;54(21):5064-73.

Chapter 15: Copyrighted Works for which Permission Was Obtained

Chapter 2 (Pages 5-39)**:** Cationic amphiphiles, a new generation of antimicrobials inspired by the natural antimicrobial peptide scaffold

Brandon Findlay, George G Zhanel, Frank Schweizer.

Chapter 3 (Pages 40-64)**:** Investigating the antimicrobial peptide 'window of activity' using cationic lipopeptides with hydrocarbon and fluorinated tails

Brandon Findlay, George G Zhanel, Frank Schweizer.

Chapter 4 (Pages 65-90)**:** Guanidinylation and Tail Effects in Cationic Antimicrobial Lipopeptoids

Brandon Findlay, Paul Szelemej, George G Zhanel, Frank Schweizer.

Chapter 5 (Pages 91-111)**:** Ultrashort Cationic Lipopeptides and Lipopeptoids Selectively Induce Cytokine Production in Blood-Derived Mononuclear Immune Cells.

Brandon Findlay, Neeloffer Mookherjee, Frank Schweizer.

Chapter 6 (Pages 112-133)**:** Neomycin-phenolic conjugates: Polycationic amphiphiles with broad-spectrum antibacterial activity, low hemolytic activity and weak serum protein binding

Brandon Findlay, George G. Zhanel, Frank Schweizer.